Bio-oil production via catalytic fast pyrolysis of woody biomass

Ville Paasikallio

Aalto University

Bio-oil production via catalytic fast pyrolysis of woody biomass

Ville Paasikallio

A doctoral dissertation completed for the degree of Doctor of Science (Technology) to be defended, with the permission of the Aalto University School of Chemical Technology, at a public examination held at the lecture hall Ke2 of the school on November 11th 2016 at 12:00.

Aalto University
School of Chemical Technology
Department of Biotechnology and Chemical Technology
Industrial Chemistry

Supervising professor

Professor Jukka Seppälä, Aalto University, Finland

Thesis advisors

Dr. Jani Lehto, VTT Technical Research Centre of Finland Ltd, Finland
Dr. Juha Lehtonen, VTT Technical Research Centre of Finland Ltd, Finland

Preliminary examiners

Dr. Dietrich Meier, thermophil international, Germany
Dr. Robbie Venderbosch, BTG Biomass Technology Group B.V., The Netherlands

Opponent

Professor Wolter Prins, Ghent University, Belgium

NORDIC ECOLABEL

441   697
Printed matter

Abstract

Fast pyrolysis of biomass is a thermochemical conversion process where solid biomass such as wood is thermally converted under a non-oxidative atmosphere at a temperature of approximately 500°C. The main product from this process is bio-oil, a highly oxygenated liquid with very challenging fuel properties. The quality of the bio-oil can be improved using a variety of catalytic processes. One such technology is catalytic fast pyrolysis (CFP), which integrates a catalytic vapor-phase upgrading step directly into a fast pyrolysis process itself. The overall purpose of this is to improve the quality of the bio-oil that is produced in the fast pyrolysis process. This, in turn, can facilitate easier utilization of the bio-oil in demanding applications such as upgrading to transportation fuels. CFP is most often carried out using acidic zeolite catalysts, which are capable of removing oxygen from the pyrolysis vapors in the form of carbon oxides and water. Because both carbon and hydrogen are lost together with the oxygen, the quality of bio-oil improves at the expense of the yield.

Acidic catalysts and highly oxygenated pyrolysis vapors are a combination which results in rapid catalyst deactivation due to coke formation. In order to maintain an adequate level of catalyst activity, the catalyst must be regenerated on a frequent basis. From the perspective of continuous operation, this sets certain requirements on the reactor technology for CFP. The results of this thesis show that bubbling fluidized bed reactors, which are commonly used for research purposes and do not normally include the possibility of continuous catalyst addition and removal, have clear operational limitations for CFP. Such reactors can, nevertheless, be used for catalyst testing and parametric studies as long as the effect of short-term catalyst deactivation is taken into account.

Circulating fluidized bed reactors with continuous catalyst regeneration provide a much more convenient technological platform for CFP. The effect of coke-induced reversible deactivation is effectively negated, and the focus can be shifted to process performance and catalyst long-term stability. The latter factor is considered to be one of the key questions for CFP. It was shown in this thesis that the combination of biomass-derived inorganic contaminants and severe reaction/regeneration conditions cause irreversible changes in the catalyst structure and properties, which in turn reflects in the quality of the bio-oil. The results of this thesis also highlight the diverse overall character of the CFP products. The partially upgraded bio-oil product is accompanied by a separate aqueous liquid with varying amounts of dissolved organics. Thus, efficient utilization of the CFP products would very likely entail more than one valorization approach.

Tiivistelmä

Nopea pyrolyysi on termokemiallinen konversioprosessi missä kiinteä biomassa kuten puu-aines konvertoidaan termisesti hapettomissa olosuhteissa noin 500 °C lämpötilassa. Prosessin päätuote on runsaasti happipitoisia yhdisteitä sisältävä bioöljy, jolla on erittäin haastavat polttoaineominaisuudet. Bioöljyn laatua voidaan parantaa erilaisilla katalyyttisillä prosesseilla. Yksi näistä on katalyyttinen nopea pyrolyysi (KNP), missä pyrolyysiprosessiin itseensä sisällytetään katalyyttinen höyryfaasijalostusvaihe. Tämän tarkoitus on parantaa nopeassa pyrolyysissä tuotettavan bioöljyn laatua, joka voi osaltaan parantaa bioöljyn käytettävyyttä haastavissa sovelluksissa kuten jalostuksessa liikennepolttoaineiksi. KNP:ssä käytetään tyypillisesti happamia zeoliittikatalyyttejä, jotka voivat poistaa happea hiilen oksideina ja vetenä. Koska hapen mukana menetetään sekä hiiltä että vetyä, bioöljyn laadunparannus tapahtuu öljysaannon kustannuksella.

Happokatalyytit ja happirikkaat pyrolyysihöyryt ovat yhdistelmä joka johtaa nopeaan kata-lyytin deaktivoitumiseen katalyytin koksaantumisen vuoksi. Riittävän aktiivisuustason ylläpitäminen vaatii katalyytin regeneroimista lyhyin aikavälein. Tämä taasen asettaa tiettyjä vaatimuksia KNP:ssä käytettävälle reaktoriteknologialle erityisesti jatkuvan käytettävyyden näkökulmasta. Tämän väitöskirjan tulokset näyttävät selvästi että yleisesti tutkimuskäytössä olevilla kuplaleijupetireaktoreilla, joista tyypillisesti puuttuu mahdollisuus katalyytin jatkuvalle poistolle ja lisäämiselle, on selkeitä käyttöteknisiä rajoituksia KNP:n kohdalla. Tällaisia reaktoreita voidaan silti käyttää katalyyttitestaukseen ja prosessimuuttujien tutkimukseen, kunhan katalyytin deaktivoituminen otetaan huomioon.

Jatkuvatoimiseen katalyytin regenerointiin pystyvät kiertoleijupetireaktorit soveltuvat huomattavasti paremmin KNP:lle. Koksaantumisen aiheuttaman reversiibelin deaktivaation sijaan fokusalueiksi muodostuvat prosessin suorituskyky ja katalyytin elinikä, joista jälkim-mäinen on yksi olennainen epävarmuustekijä KNP:n tapauksessa. Tässä väitöskirjassa on osoitettu, että biomassaperäisten epäorgaanisten epäpuhtauksien ja vaativien reaktio- ja regenerointiolosuhteiden yhdistelmä aiheuttaa muutoksia katalyytin rakenteessa ja omi-naisuuksissa, joka myös heijastuu bioöljyn laadussa. Tämän väitöskirjan tulokset myös korostavat KNP:n tuotteiden monitahoisuutta. Pääasiallisen öljytuotteen lisäksi prosessissa muodostuu erillinen vesifaasi joka sisältää vaihtelevan määrän liuennutta orgaanista ainesta. KNP:n koko tuotespektrin tehokas hyödyntäminen tulee täten todennäköisesti vaatimaan useamman kuin yhden jatkojalostusmenetelmän käyttöä.

Preface

The experimental work that is reported in this thesis was mainly carried out at VTT Technical Research Centre of Finland between 2011 and 2016. Certain parts of the experimental work were carried out during visits to Utah State University in 2012-2013, and to CERTH - The Centre for Research & Technology, Hellas in 2015. This work was carried out in two projects funded by Tekes - the Finnish Funding Agency for Innovation: 'Pilot-scale development of new 2G BTL technologies based on gasification and pyrolysis' and 'High value bio-oils for transportation and diesel power plants'.

I am grateful to my original thesis supervisor Professor Juha Lehtonen for his guidance and interest towards my work, and to Professor Jukka Seppälä who agreed to become the official supervisor in 2016. I also want to express my gratitude to my thesis advisor Dr. Jani Lehto who helped shape the work that is presented in this thesis. I would also like to thank Dr. Yrjö Solantausta and Dr. Anja Oasmaa for providing me the opportunity to work in this interesting field, and for helping me develop further as a researcher during the years I spent at VTT. Mr. Christian Lindfors and Ms. Eeva Kuoppala also deserve special thanks for their valuable contributions to this work.

I also want offer my thanks to the group of technicians at VTT. Without the hard work and expertise of Jaana Korhonen, Sirpa Lehtinen, Elina Paasonen, Sampo Ratinen, Pekka Saarimäki and Jouko Kukkonen, this thesis would not have been possible.

In addition to the people mentioned here, I want to express my sincere thanks to all my other co-authors both in Finland and abroad, and to everyone else who has in some way contributed towards the work presented in this thesis.

Finally, I would like to thank my family and friends for helping me find

the right balance between work and free time. I especially want to thank my wife Shan for her support and encouragement during this lengthy project, and my parents for always supporting my studies.

Espoo, October 16, 2016,

Ville Paasikallio

Contents

List of Publications

This thesis consists of an overview and of the following publications which are referred to in the text by their Roman numerals.

I Ville Paasikallio, Christian Lindfors, Jani Lehto, Anja Oasmaa, Matti Reinikainen. Short Vapour Residence Time Catalytic Pyrolysis of Spruce Sawdust in a Bubbling Fluidized-Bed Reactor with HZSM-5 Catalysts. *Topics in Catalysis*, Volume 56, issue 9, pages 800-812, DOI: 10.1007/s11244-013-0037-y, June 2013.

II Ville Paasikallio, Foster Agblevor, Anja Oasmaa, Jani Lehto, Juha Lehtonen. Catalytic Pyrolysis of Forest Thinnings with ZSM-5 Catalysts: Effect of Reaction Temperature on Bio-oil Physical Properties and Chemical Compositions. *Energy & Fuels*, Volume 27, issue 12, pages 7587-7601, DOI: 10.1021/ef401947f, November 2013.

III Ville Paasikallio, Christian Lindfors, Eeva Kuoppala, Yrjö Solantausta, Anja Oasmaa, Jani Lehto, Juha Lehtonen. Product quality and catalyst deactivation in a four day catalytic fast pyrolysis production run. *Green Chemistry*, Volume 16, pages 3549-3559, DOI: 10.1039/c4gc00571f, June 2014.

IV Ville Paasikallio, Konstantinos Kalogiannis, Angelos Lappas, Jani Lehto, Juha Lehtonen. Catalytic fast pyrolysis: Influencing bio-oil quality with the catalyst-to-biomass ratio. *Energy Technology*, Early View Article, DOI: 10.1002/ente.201600094, July 2016.

V Christian Lindfors, Ville Paasikallio, Eeva Kuoppala, Matti Reinikainen, Anja Oasmaa, Yrjö Solantausta. Co-processing of Dry Bio-oil, Catalytic Pyrolysis Oil, and Hydrotreated Bio-oil in a Micro Activity

Test Unit. *Energy & Fuels*, Volume 29, issue 6, pages 3707-3714, DOI: 10.1021/acs.energyfuels.5b00339, June 2015.

Author's Contribution

Publication I: "Short Vapour Residence Time Catalytic Pyrolysis of Spruce Sawdust in a Bubbling Fluidized-Bed Reactor with HZSM-5 Catalysts"

V. Paasikallio planned and carried out the pyrolysis experiments and was the main contributor in the interpretation of the results and writing of the manuscript. C. Lindfors instructed the work and took part in planning the experiments. J. Lehto and A. Oasmaa reviewed and commented on the manuscript. M. Reinikainen was responsible for the NH_3-TPD (temperature programmed desorption of ammonia) analyses.

Publication II: "Catalytic Pyrolysis of Forest Thinnings with ZSM-5 Catalysts: Effect of Reaction Temperature on Bio-oil Physical Properties and Chemical Compositions"

V. Paasikallio planned and carried out the pyrolysis experiments and most of the bio-oil characterization. V. Paasikallio was the main contributor in the interpretation of the results and writing of the manuscript. F. Agblevor oversaw the experimental work, and contributed towards experimental planning, interpretation of results and manuscript preparation. J. Lehto and A. Oasmaa reviewed and commented on the manuscript. J. Lehtonen reviewed and commented on the manuscript and supervised V. Paasikallio's doctoral studies.

Publication III: "Product quality and catalyst deactivation in a four day catalytic fast pyrolysis production run"

V. Paasikallio, C. Lindfors and E. Kuoppala planned the pyrolysis experiment and the bio-oil analyses, and interpreted the results. V. Paasikallio planned and interpreted the catalyst analyses. V. Paasikallio was the main contributor in writing of the manuscript. Y. Solantausta, A. Oasmaa and J. Lehto reviewed and commented on the manuscript. J. Lehtonen reviewed and commented on the manuscript and supervised V. Paasikallio's doctoral studies.

Publication IV: "Catalytic fast pyrolysis: Influencing bio-oil quality with the catalyst-to-biomass ratio"

V. Paasikallio and K. Kalogiannis planned and oversaw the pyrolysis experiments. V. Paasikallio was the main contributor in the interpretation of the results and writing of the manuscript. A. Lappas and J. Lehto reviewed and commented on the manuscript. J. Lehtonen reviewed and commented on the manuscript and supervised V. Paasikallio's doctoral studies.

Publication V: "Co-processing of Dry Bio-oil, Catalytic Pyrolysis Oil, and Hydrotreated Bio-oil in a Micro Activity Test Unit"

C. Lindfors and E. Kuoppala planned the experiments and were the main contributors for interpreting the results. C. Lindfors was the main contributor for writing the manuscript. V. Paasikallio took part in the interpretation of the results and writing of the manuscript, particularly concerning the effect of different bio-oil qualities on the process. M. Reinikainen designed the reactor system. A. Oasmaa and Y. Solantausta reviewed and commented on the manuscript.

List of abbreviations

BFB	Bubbling fluidized bed
C/B	Catalyst-to-biomass
C/O	Catalyst-to-oil
CFB	Circulating fluidized bed
CFP	Catalytic fast pyrolysis
DAB	Dry ash-free basis
DB	Dry basis
ESP	Electrostatic precipitator
FCC	Fluid catalytic cracking
GC-FID	Gas chromatography - flame ionization detector
GC-MS	Gas chromatography - mass spectrometry
H/C_{eff}	Effective hydrogen-to-carbon ratio
HCO	Heavy cycle oil
HDO	Hydrodeoxygenation
HHV	Higher heating value
HMW	High molecular weight
HVF	Hot vapor filter
LHV	Lower heating value
LMW	Low molecular weight
LCO	Light cycle oil
LPG	Liquid petroleum gas
MAT	Microactivity test
MCR	Micro carbon residue
MTG	Methanol-to-gasoline
NMR	Nuclear magnetic resonance
PAH	Polyaromatic hydrocarbon
SAR	Silica-to-alumina ratio
TAN	Total acid number

TFP	Thermal fast pyrolysis
VGO	Vacuum gas oil
WHSV	Weight hourly space velocity
WT	Weight

1. Introduction

1.1 Background

The general motivation to develop production technologies for liquid bio-fuels stems from a number of economic, environmental, and political drivers. Dwindling petroleum reserves and their particular geographical distribution are two of the underlying reasons behind the interest to convert other natural resources such as biomass, coal, and natural gas into liquid fuels. In addition to the availability questions and geopolitical issues that surround the existing global fuel production chains, the environmental aspects of biofuel production and utilization have grown to become ever more important in the recent years. Although other forms of renewable energy can at least partially offset stationary power generation that is based on fossil fuels, biomass remains as the sole source of readily available renewable carbon [1]. Therefore, for energy applications which rely on the utilization of liquid fuels, e.g. transportation, biofuels are expected to play an important role on the path towards decarbonization. While hybrid and electric technologies have been steadily gaining ground in normal passenger cars, liquid fuels are expected to maintain their essential role in the near-term future. The utilization of liquid fuels is even more deeply rooted in the fields of aviation, marine transport, and heavy duty road vehicles, and thus demand for fuels which fulfill the requirements of these sectors is expected to remain strong. Although biofuels by themselves will not offer a singular all-encompassing solution for addressing the energy needs of the future, they can, nevertheless, be a part of a larger shift towards cleaner technologies.

While the need to develop technologies for producing cleaner fuels has been globally recognized, the cyclic nature of the overall world economy

Thousands of Barrels Produced, by Year (US)

■ Petroleum   ■ Biofuels
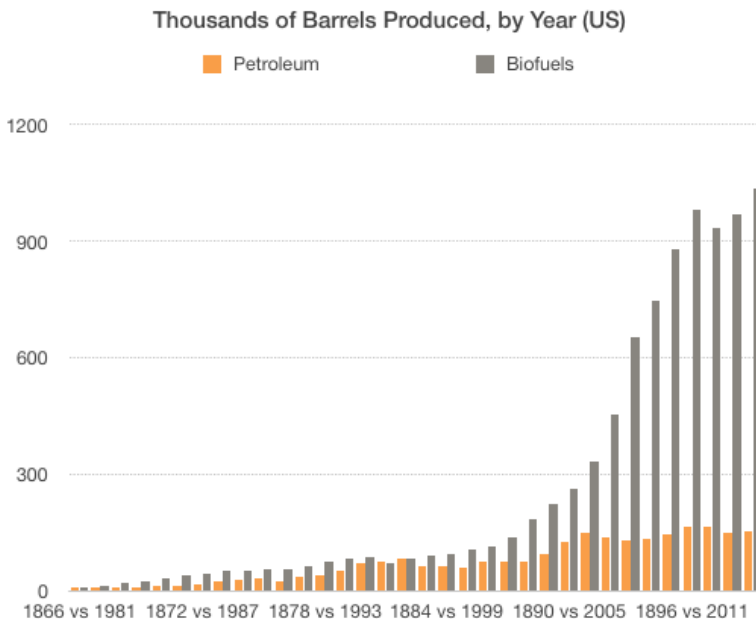
Figure 1.1. Comparison of petroleum and biofuels production in the United States start-
ing from a point in time when the annual production corresponded to a rate
10 000 barrels per day [4].

and the recent decrease in the crude oil prices has naturally affected the
economic incentives for carrying this out in practice. Nevertheless, with
the support of suitable subsidy schemes and investment aids, and policy-
driven demand in general, several industrial demonstration plants which
produce liquid biofuels from lignocellulosic biomass have been constructed
and commissioned in the recent years [2, 3]. Although progress may at
times appear slow, one should bear in mind that production of petroleum-
based fuels did grow to its current magnitude overnight either. In fact,
as it can be seen in Figure 1.1, production of liquid biofuels in the United
States has increased substantially more rapidly than petroleum produc-
tion did during its infancy. The overall consumption base for oil products
was, of course, entirely different in the latter half of the 19th century. In
addition to this, liquid biofuels are typically blended together with fos-
sil fuels in the form of e.g. ethanol. Thus, their demand is tied to the
demand of fossil fuels, and therefore liquid biofuels do not constitute an
independent product category of their own.

The path from small-scale laboratory experiments towards industrial
demonstration is typically an arduous process, which entails many poten-
tial pitfalls. Therefore, in order to facilitate a smooth scale-up process, cer-

tain critical information has to be obtained during each intermediate step. This also serves to increase the overall knowledge of the target process, thus giving a more thorough understanding of the potential challenges that may arise during the course of process development. One technology which has already undergone this scale-up process is fast pyrolysis of biomass. In fast pyrolysis, solid biomass is thermally decomposed in the absence of oxygen [5, 6]. This process, which takes place within a matter of a few seconds, is typically carried out under atmospheric pressure at a temperature of approximately 500 °C. At these conditions, the volatile part of lignocellulosic biomass decomposes into vapors and gases, whereas the non-volatile part is recovered in the form of a solid product, biochar. The vapors are subsequently condensed to form a liquid product, which is commonly referred to as bio-oil or pyrolysis oil. Fast pyrolysis bio-oil itself is a highly complex mixture, which contains hundreds of individual compounds originating from the thermal decomposition of the three main constituents of lignocellulosic biomass: cellulose, hemicellulose, and lignin. Although more than half of the energy and carbon in the original biomass feedstock can be recovered in the bio-oil, this primary fuel product bears little resemblance to the petroleum-derived fuels that are one of the backbones of modern society.

Many of the particular fuel properties of pyrolysis oil, which are shown in Table 1.1, fundamentally arise from the fact that pyrolysis oil has an elemental composition which is very similar to the original biomass feedstock. In contrast to the hydrocarbon fuels which are routinely consumed in both stationary and mobile applications, pyrolysis oil contains up to 40 wt% of oxygen on dry basis. This oxygen is present in the form of various organic compound types, e.g. acids, aldehydes, ketones, alcohols, anhydrosugars, and phenols [8]. In addition to low molecular weight molecules which can be individually identified, a large part of these bio-oils consists of heavier holocellulose and lignin fragments, which have been only partially depolymerized during the pyrolysis process. This multitude of organic molecules is typically supplemented by 20-30 wt% of water, which is the single-most abundant compound in fast pyrolysis bio-oils. Ultimately, individual compounds with varying organic functionalities, and potential interactions between the different compounds imparts pyrolysis oil with its distinct complexity and character. Nevertheless, even with this array of challenging physicochemical properties, fast pyrolysis bio-oil can be used as a fuel in district heating boilers and stationary energy applica-

Table 1.1. Fuel properties of a typical thermal fast pyrolysis bio-oil and petroleum-derived light fuel oil [7].

Property	Typical bio-oil	Light fuel oil
Water (wt%)	20-30	0
Solids (wt%)	< 0.5	-
Ash (wt%)	0.01-0.1	0.01 max
Nitrogen (wt%)	< 0.4	0.02
Sulfur (wt%)	< 0.05	0.001 max
Viscosity (40 °C, cSt)	15-35	2.0-4.5
Density (15 °C, kg/dm^3)	1.10-1.30	0.845 max
Flash point (°C)	40-110	60
Pour point (°C)	-9-36	-5 min
Lower heating value (MJ/kg)	13-18	42.6
pH	2-3	-

tions [9, 7].

If pyrolysis oil is to be used in demanding applications such as the transportation sector, it must first undergo a certain degree of upgrading. Most of the suggested upgrading processes have their technological foundations in the oil refining industry. Because the key differentiating factor between petroleum distillates and pyrolysis oil is the high oxygen content of the latter, technologies which are capable of heteroatom removal have always featured prominently in pyrolysis oil upgrading research. Catalytic hydrotreating, which can be used for removing oxygen via hydrodeoxygenation (HDO) reactions, has long been considered as the technology of choice for converting pyrolysis oil into hydrocarbons [10, 11]. This technology was originally developed for removing sulfur and nitrogen impurities in petroleum. In addition to oxygen removal and hydrogenation reactions, this process is also capable of lowering the molecular weight of the final products via cracking reactions. However, because of the complex character of the feedstock, catalytic hydrotreating of pyrolysis oils has proven to be substantially more challenging than its closest counterparts in oil refining, i.e. hydrodesulphurization and hydrocracking. Another oil refining process which has been adapted for pyrolysis oil upgrading is fluid catalytic cracking (FCC), in which heavy hydrocarbon fractions are converted into lighter products over solid acid catalysts without any external hydrogen [12, 13]. Although the process conditions and the underlying chemistry is completely different compared to the hydrotreating alterna-

tive, both of these processes can ultimately be used for converting pyrolysis oils into higher value hydrocarbon products [14, 15]. However, because of the challenges that are associated with upgrading crude pyrolysis oils, altering the pyrolysis process itself to yield more readily upgradeable oils is another avenue of research that is being actively pursued.

In addition to previously described post-pyrolysis upgrading strategies, it is possible to incorporate the first upgrading step directly into the pyrolysis process itself. One particular way of achieving this is to introduce a catalyst into the pyrolysis process. With this approach, which is referred to as catalytic fast pyrolysis (CFP), the primary thermal decomposition reactions are followed by a secondary set of catalytic reactions. During these catalytic reactions, the pyrolysis vapors are further transformed via a multitude of reactions, many of which include the rejection of oxygen in the form of water, carbon monoxide (CO), and carbon dioxide (CO_2). This type of transformation results in a trade-off between the quantity of bio-oil that is obtained and its quality, i.e. less bio-oil is produced but it presents more favorable quality characteristics. Studying this quantity versus quality relationship is still a primary concern for developing a more profound understanding of the CFP process. However, the bio-oil from CFP is still ultimately an intermediate product, and thus any changes in product quality will also reflect directly in the subsequent upgrading processes. Although the bio-oil yield from CFP is lower compared to the purely thermal conversion pathway, the envisioned attractiveness of the CFP concept is based on the improved processability of the intermediate product.

The different technologies that have been introduced in the previous paragraphs offer several pathways leading to transportation fuels. The ones which are considered most relevant within the framework of this thesis are presented in Figure 1.2. In order for any industrial scale CFP-based biofuel production concept to be realized, a more intricate knowledge of the process itself and its products needs to be developed. The overall outcome of a CFP process is determined by a wide array of different factors. Just as in any other chemical transformation process, some variables play a pivotal role, whereas others may only have a minute effect. Identifying the parameters which exert the most influence on the CFP process is, therefore, a topic of central importance. When considering the overall conversion process, the events taking place within the CFP reactor can be divided into two distinct phenomena: pyrolysis and catal-
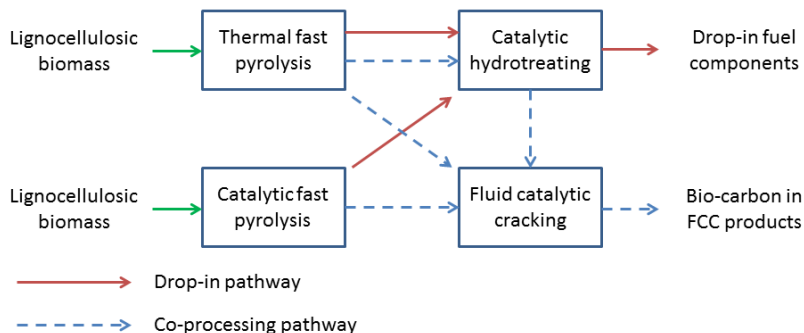
Figure 1.2. Process concepts for producing transportation fuels via thermal and catalytic fast pyrolysis of lignocellulosic biomass.

ysis. It is already widely established that temperature is a key variable in any thermochemical conversion process, including pyrolysis [16, 17]. The first requirement for any catalytic process is a catalyst that is able to convert the reactants to the desired products with high activity and selectivity. One thing that practically all catalytic processes, however, have in common is catalyst deactivation [18]. The rate at which the activity of the catalyst decreases depends on factors such as feedstock, catalyst, and process conditions, and it reflects directly on what type of reactor configuration is best suited for a given process [19]. Although these aforementioned three factors, i.e. temperature, catalyst deactivation and reactor configuration, are by no means the only relevant variables as far as CFP is concerned, all of them can be expected to influence product quality. Attempting to delve deeper into the character of CFP bio-oils may not at first glance appear to be such a daunting endeavor, but one should bear in mind that considerable efforts have been taken just to determine the composition and properties of bio-oils from conventional fast pyrolysis processes [8, 20]. Introducing a completely new variable, i.e. the catalyst, into the process, also causes the character of the bio-oils to undergo a drastic change. Understanding this change and the variables that govern it should be one of the foundations upon which the CFP technology can be further developed. One unsuccessful attempt [21] at commercializing this technology already highlights the hazards of undue haste, while simultaneously emphasizing that interest towards the CFP technology is not merely academic.

1.2   Scope of the research

Catalytic fast pyrolysis is a technology which can be used for producing partially upgraded bio-oils, which exhibit improved quality characteristics compared to conventional thermal fast pyrolysis (TFP) bio-oils. The properties and composition of TFP bio-oils depend on a large number of feedstock- and process-related variables. Introducing a catalyst directly into this already otherwise complex process further increases the number of factors that influence bio-oil quality. This shift from a purely thermal process into a thermocatalytic one also presents new challenges, such as how to efficiently address the effect of catalyst deactivation, and understanding how the properties of the catalyst reflect in the properties of the final bio-oil product.

The objective of this thesis was to examine which variables play the most prominent role in determining product quality in CFP of woody biomass, and to develop a thorough understanding of how bio-oil characteristics change in the presence of a solid acid zeolite catalyst under varying process conditions and configurations. Experiments were initially carried out using bench-scale bubbling fluidized bed (BFB) reactors. Bio-oils produced under varying process conditions were extensively characterized in order to understand this thermocatalytic transformation process. Based on experiences and knowledge gained in the experiments that are reported in Publications I and II, it became clear that coke-induced reversible catalyst deactivation significantly limited the usability of typical BFB reactors in the CFP process.

In the latter half of the thesis, which corresponds to Publications III and IV, the experimental work was conducted using circulating fluidized bed (CFB) reactors. The purpose of this work was to assess whether continuous catalyst regeneration makes it possible to maintain constant bio-oil quality, and to identify critical factors which potentially limit the further applicability of the CFP process. The experimental work consisted of a continuous 96 h our pilot-scale experiment (Publication III), and a parametric study concerning the effect of a critical process variable, the catalyst-to-biomass ratio (Publication IV).

The thesis also touched upon the subject of co-processing bio-oils in an oil refinery FCC unit in Publication V. The purpose of this study was to compare the co-processability of two partially upgraded bio-oils derived from two different processes: CFP and HDO. Comparing the behavior of

two bio-oils with a similar degree of upgrading can also provide new insights concerning the quality and characteristics of the oils themselves.

Based on this, the primary research questions of this thesis can be formulated as follows:

1. How does the presence of a solid acid catalyst affect bio-oil properties and composition?

2. What kind of reactor technology offers the most convenient solution for producing bio-oil with constant quality via CFP?

3. Can constant bio-oil quality be maintained indefinitely under conditions which eliminate the effect of reversible catalyst deactivation?

4. Can bio-oil quality be further improved by supplying an excess of catalyst into the CFP process?

5. Is aromatic CFP bio-oil a suitable feedstock for a subsequent acid-catalyzed upgrading process?

1.3 Dissertation structure

Following the introductory chapter, this dissertation provides a compact literature review concerning CFP of biomass. The purpose of this brief review is to familiarize the reader with the technologies, concepts, and phenomena that are considered pertinent for understanding the results of this dissertation. This is followed by a materials and methods section, which outlines the experimental methodologies and materials that have been utilized during the course of this research.

The results of the dissertation are presented in thematic sections, each of which corresponds to an individual journal publication. In Chapter 4, each section begins with an introductory note, which further explains the context and objectives of the experimental work that was carried out in a given publication. In general, Chapter 4 seeks to highlight the most relevant results from each publication. Because of this, the allotted space is not distributed evenly between the five publications. In particular, Publications III and IV play a more prominent role, as these are deemed to offer the largest overall contributions of this dissertation.

2. Literature review

2.1 Technology for fast pyrolysis of biomass

In order to understand how CFP can be implemented in practice and what kind of challenges it entails, it is first necessary to familiarize oneself with the basic technology that is applied for conventional, i.e. thermal fast pyrolysis. As it was mentioned in Chapter 1.1, fast pyrolysis is a thermochemical conversion process where lignocellulosic biomass is thermally decomposed in the absence of oxygen. This non-oxidative conversion process, which takes place within a matter of seconds, is typically carried out at a temperature of approximately 500 °C. At this temperature, the individual components of biomass, i.e. cellulose, hemicellulose, and lignin decompose via depolymerization and cracking reactions which form organic vapors, water, and non-condensable which consist primarily of carbon oxides and light hydrocarbons. The unreacted fraction of the biomass feedstock remains as a solid carbonaceous residue, char. The organic vapors which are released in the decomposition reactions form the primary product of interest, i.e. bio-oil. In order to maximize the yield of bio-oil, a certain set of conditions must be fulfilled. These include [22]:

1. Carefully controlled reaction temperature
2. Rapid heating of biomass particles
3. Short vapor residence time in the pyrolysis reactor
4. Rapid separation of char from vapors
5. Rapid quenching of pyrolysis vapors

These factors place very strict requirements for the reactor technology that can be used for fast pyrolysis. Fluidized bed reactors have been
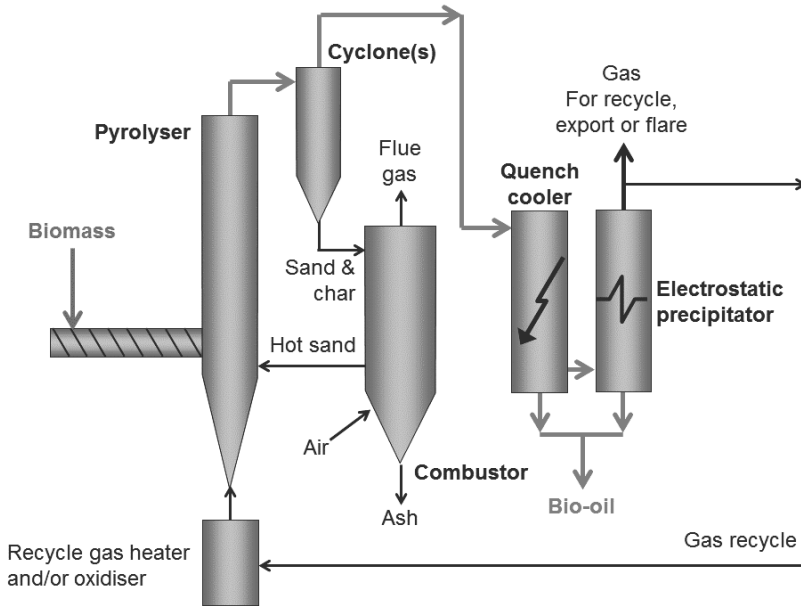
Figure 2.1. Schematic representation of a circulating fluidized bed reactor used for fast pyrolysis of biomass [23].

widely recognized as the technology of choice for carrying out this process. In addition to offering very efficient temperature control and rapid heating rates, fluidized bed reactors are readily scalable to the industrial size range.

The fluidized bed reactors which are most commonly applied for fast pyrolysis of biomass can be divided into two types: bubbling fluidized bed (BFB) and circulating fluidized bed (CFB) reactors. A schematic example of a CFB reactor is provided in Figure 2.1. Both BFB and CFB reactors utilize a solid heat transfer material such as sand to heat up the biomass particles that are introduced into the system. In addition to the solid heat transfer material, fluidized bed reactors require a fluidization gas, which is passed through the reactor at a certain velocity. Figure 2.2 introduces the different states of fluidization which are attained by increasing the velocity of the fluidization gas. For BFB reactors, the desired operational range is found between the minimum fluidization velocity and the onset of pneumatic transport, which is also referred to as the terminal velocity. At the regime of bubbling fluidization where the pressure loss remains constant, small gas bubbles travel upwards through the solid heat transfer material, which in turn behaves in a similar fashion as a boiling fluid. During operation, the heat transfer material remains inside the reactor, whereas the pyrolysis products, which also include the solid char residue,
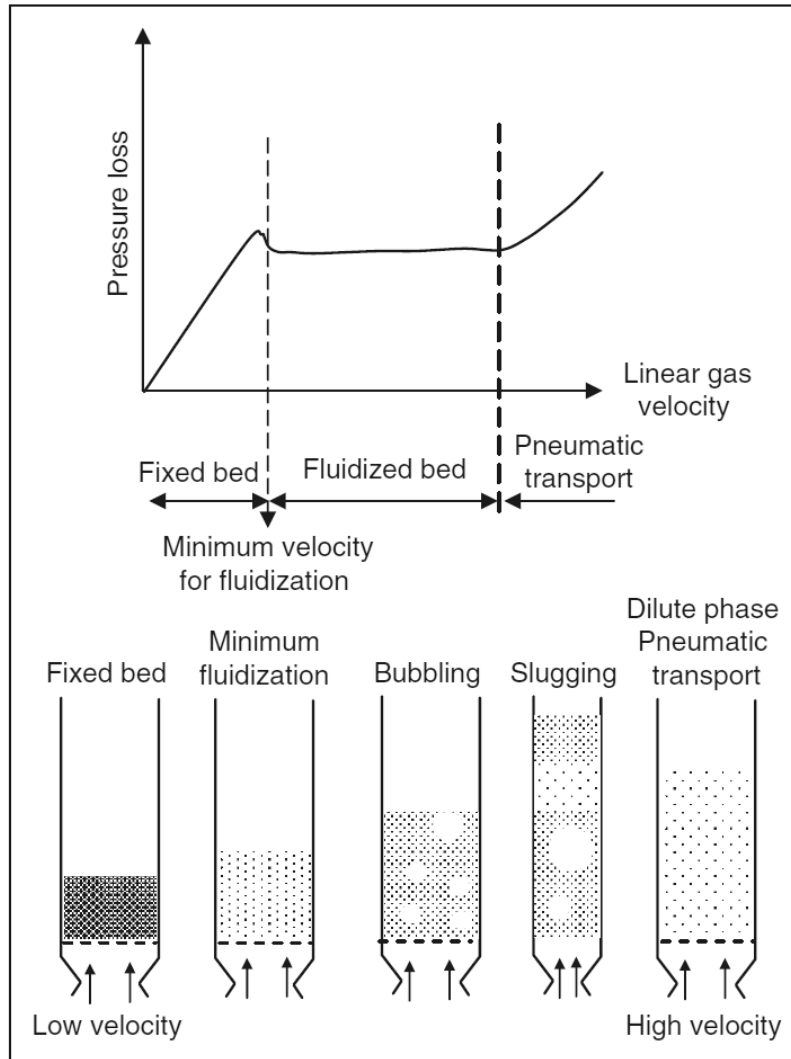
Figure 2.2. Different fluidization regimes within a fluidized bed reactor [24].

are continuously flushed out from the reactor by the fluidization gas flow. For CFB reactors, in order for the pyrolysis products and the heat transfer material itself to be carried upwards through the reactor, the fluidization velocity has to surpass the terminal velocity of the heat transfer material and the char. This state of operation corresponds to the pneumatic transport regime in Figure 2.2. Because the heat transfer material does not remain within the reactor, it has to be continuously supplied into the reactor in order to provide the necessary heat for the pyrolysis process. This difference in the operational characteristics of BFB and CFB reactors is essential to comprehend, as it has direct implications on the CFP process.

After the reactor, the entrained solids, i.e. char for BFB reactors and a mixture of char and heat transfer material for CFB reactors, have to be separated from the vapors and gases. This is typically carried out using either cyclones or alternatively a hot vapor filter (HVF). The HVF is capable of separating practically all the solids from the pyrolysis product stream, but a gradually increasing pressure drop typically limits the long-term usability of this particular technology. Cyclones, on the other hand, are not very effective at removing particles which are smaller than 15-20 μm [25], which can result in some char and heat transfer material carrying over into the bio-oil. For BFB reactors which are utilized for research purposes, such as the ones which have been used in this thesis, the separated char is directed into a suitable collection vessel which can be emptied after the experiment. On the other hand, for CFB reactors, the solids are fed into a separate regeneration unit, which combusts the char in order to reheat the heat transfer material. The reheated heat transfer material is fed back into the reactor to supply the heat for the pyrolysis reactions. The energy that is contained in the char allows autothermal operation of the CFB reactor, whereas small BFB units are typically heated by electricity.

After separating the solids, the pyrolysis vapors, which contain both organic compounds and water, have to be condensed in order to recover the bio-oil. The condensation is typically carried out in multiple stages, which may employ a variety condensation means and temperatures. There are two main philosophies for designing the liquid recovery system and collecting the liquid products. The conventional approach is to implement the liquid recovery using a configuration which allows one to obtain a single homogeneous product bio-oil. Although this bio-oil is still typically collected in more than one stage, the condensation conditions are selected so that post-pyrolysis mixing of liquid products can be readily carried out. The alternative is to collect the bio-oil in several distinct fractions which can, in theory, be utilized in different targeted applications. This fractional condensation approach can be realized by e.g. manipulating the condensation temperatures within the liquid recovery system. In both cases, the actual condensation is carried out using a variety of suitable devices, with heat exchangers, electrostatic precipitators (ESPs) and scrubbers being the most commonly used options. Heat exchangers condense the vapors simply by cooling them down, ESPs utilize a high voltage to charge and condense particularly aerosols, while in scrubbers

a liquid, which is typically a hydrocarbon solvent or recirculated product bio-oil, is sprayed into the pyrolysis vapors in order to quench them. After all the liquid products have been condensed, a part of the product gases can be recirculated back into the pyrolysis process to be used as the fluidization gas. Excess gases can be combusted e.g. in the regenerator. In practice with smaller experimental units, the gases are typically vented rather than recirculated.

2.2 Catalytic fast pyrolysis

2.2.1 Coupling pyrolysis and catalysis in practice

Before delving deeper into the characteristics of the process itself, it is pertinent to examine how the CFP process can be implemented in practice. The overall concept of CFP revolves around introducing a catalyst directly into the pyrolysis process. There are two operational approaches for carrying this out: in situ CFP [26, 27] and ex situ CFP [28, 29]. In the former option, which is also the focus of this thesis, both pyrolysis and catalysis take place within the single pyrolysis reactor, whereas in the latter option the pyrolysis reactor is followed by a dedicated catalytic reactor. Both alternatives have their own benefits and shortcomings, but the in situ option offers the simplicity of carrying out the whole process within a single reactor. When utilizing fluidized bed reactors, which were discussed in Section 2.1, the shift from a purely thermal decomposition process into a thermocatalytic one can be realized simply by replacing the inert solid heat transfer material with a solid catalyst [30, 31]. In this case, the released pyrolysis vapors come into immediate contact with the active sites of the catalyst, thus allowing the upgrading reactions to proceed directly after the thermal decomposition reactions. CFP can be carried out in both BFB and CFB reactors, but as it will be discussed in Section 2.2.3, CFB reactors have a distinct edge over their bubbling counterparts.

2.2.2 Chemistry of catalytic fast pyrolysis

The chemistry of a given heterogeneously catalyzed process largely depends on what type of catalyst is used. Although various catalysts can and have been employed for CFP, an overwhelming number of studies, including this thesis, have focused on the use acidic zeolites, particularly the

HZSM-5 variant. Different zeolites have different pore structures, which in turn directly impact the diffusion of both reactants and products. This characteristic imparts zeolites with so-called shape selectivity; the size of the molecules which can enter, exit, or form inside the zeolite is defined by the pore size. The concept of CFP can be said to have originated from the methanol-to-gasoline (MTG) process [32], where methanol is converted over a HZSM-5 zeolite catalyst into primarily aromatic gasoline. The vapors originating from biomass pyrolysis are far more complicated to process than methanol, but a number of studies [33, 34, 35] have nevertheless shown that the structural characteristics, i.e. pore size and structure, of HZSM-5 allow it to surpass the performance of other zeolite types in CFP. Analogously to the MTG process, in CFP biomass-derived oxygenates can also be ultimately converted into aromatic hydrocarbons. In the MTG process, the formation of aromatic hydrocarbons has been shown to take place via the so-called 'hydrocarbon pool' mechanism [36, 37], and a similar scheme has been suggested for CFP as well [38, 39].

In the hydrocarbon pool concept, the aromatic hydrocarbons are formed from a pool of hydrocarbon intermediates which has formed within the pores of the zeolite. The products form within the pores, after which they are desorbed outside from the zeolite crystals. Before any catalytic reactions take place, the biomass macromolecules are first thermally decomposed into a wide array of monomeric and oligomeric species. These primary pyrolysis vapors can then further react in the gas phase, or interact with the active sites of the catalyst. In order to take part in the hydrocarbon pool, the compounds found in the pyrolysis vapors have to first lose their oxygenate functionalities via a combination of dehydration, decarbonylation, and decarboxylation reactions, which produce, water, CO, and CO_2, respectively [34, 40]. Thus, the overall conversion route typically includes several different steps. One suggested reaction pathway for glucose, i.e. the monomeric constituent of cellulose, is shown in Figure 2.3. The notion of the hydrocarbon pool has been further supported by performing biomass CFP in the presence of isotopically labeled oxygenates. Zhang et al. [41] showed that co-conversion of pine and methanol over HZSM-5 formed aromatic hydrocarbons which contained carbon from both feedstocks. Thus, methanol and oxygenates from pine pyrolysis were able to interact and eventually combine under CFP conditions.

Lignin, on the other hand, already contains the aromatic ring structure that can be created by HZSM-5. This does not, however, mean that
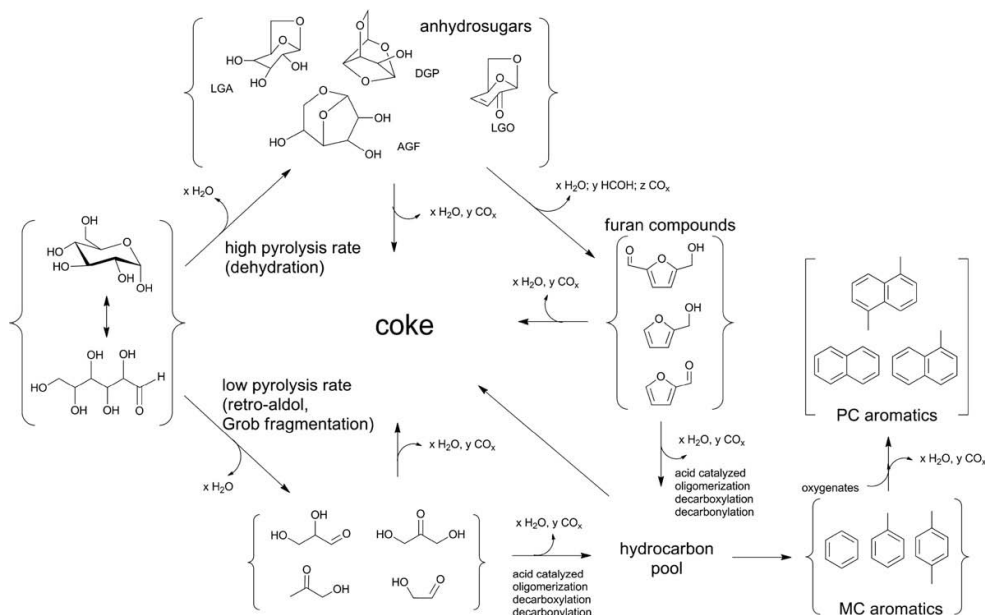
Figure 2.3. Suggested reaction mechanism of glucose over HZSM-5 in CFP [40].

lignin would be an exceptionally suitable feedstock for the production of aromatic hydrocarbons via CFP. Thermal fast pyrolysis of lignin is known to be a challenging process in itself - yields of liquid products are limited while a large amount of char is typically produced [42]. Even the presence of phenol, which is the simplest monomeric compound originating from lignin, can cause rapid deactivation of HZSM-5 zeolites due to its strong interaction with the acid sites coupled with pore blockage [43]. It has been suggested that in the CFP of lignin, simple phenols would be responsible for catalyst deactivation, whereas formation of aromatics would proceed via olefins and methanol which have been liberated from the side chains of the lignin monomers/oligomers [44]. In general, the CFP of isolated lignins has been shown to result in heavy coke formation [45, 46].

In the literature, considerable efforts have been made in order to elucidate the reaction mechanisms that are involved in the CFP of biomass. Usually, this entails examining what are the various steps which are required in the conversion of biomass-derived oxygenates into aromatic hydrocarbons. While this serves to increase the overall knowledge regarding CFP, under realistic process settings, i.e. in fluidized bed reactors, aromatic hydrocarbons typically constitute only a part of the overall liquid products [47, 48]. Thus, they are essentially mixed together with thermal decomposition products which have not undergone full conversion

over the catalyst. Although the reaction mechanisms which have been included in this section may suggest that CFP can be used for producing aromatic hydrocarbons selectively, one should bear in mind that in most cases, the actual product is still a complex bio-oil.

2.2.3 Catalyst deactivation and regeneration

Coke formation and reversible deactivation

When an acidic catalyst such as HZSM-5 is exposed to biomass pyrolysis vapors, a part of these vapors is always converted to coke, a carbonaceous deposit that is retained on the catalyst. Coke lowers the activity of zeolites by directly covering the active sites, or alternatively by blocking access to larger areas of the zeolite micropore structure. The rate at which the catalyst loses its activity due to coking depends on a number of factors, which include e.g. reactant and catalyst type. When carrying out CFP in a reactor which operates with a fixed catalyst batch without continuous regeneration, the extent of catalyst deactivation essentially depends on how much biomass has been processed over the catalyst. This is sometimes described using the biomass-to-catalyst ratio, which should not be confused with the circulation-based catalyst-to-biomass (C/B) ratio that is discussed in Publication IV.

When the HZSM-5 catalyst is at its most active state, it is under suitable conditions able to convert biomass pyrolysis into an oxygenate-free slate of aromatic hydrocarbons [38]. However, as the cumulative amount of processed biomass increases, oxygenate compounds start to break through the catalyst bed. This overall deactivation process is visualized in Figure 2.4, which shows how the distribution of different lumped compound groups changed with increasing biomass-to-catalyst ratio in CFP of pine over HZSM-5. Intermediate products such as phenol, cresols and furans appeared first, and were subsequently followed by primary pyrolysis vapors. As the proportion of oxygenates in the CFP vapors increased, aromatic hydrocarbons exhibited a corresponding decrease until a point of complete deactivation was reached. At this stage, it is possible that the catalyst still influenced the formation phenol and cresols, but aromatic hydrocarbons were no longer detected in the products. The most intense phase of coke formation also occurred at low biomass-to-catalyst ratios, when the catalyst still retained most of its initial activity.

The characteristics of the zeolite itself also have an impact on the de-
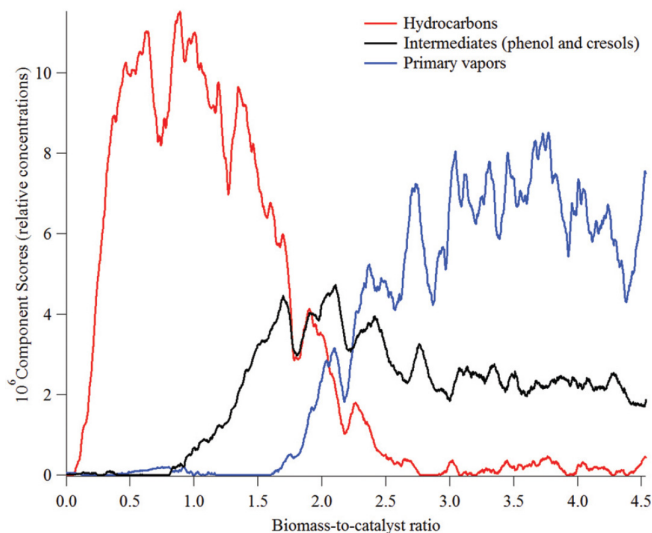
Figure 2.4. Changes in the product distribution of pine CFP as a function of the biomass-to-catalyst ratio [38].

activation process. Coke forming tendency in the CFP process is known to be affected by the pore structure of the zeolite [33, 28, 49]. Large-pore zeolites such as Y zeolite have been shown produce more coke compared HZSM-5. When considering the differences between zeolites of a single structural type, acidity can have a significant effect on the rate of deactivation. The acidity of a given zeolite is determined by its silica-to-alumina ratio (SAR). Aluminum species are responsible for the acidity of zeolites, and thus zeolites with lower SAR values and consequently more Al in their structure are more acidic. In general, a higher number of acid sites can enhance coke formation in two ways. When distance between the individual acid sites decreases, bimolecular reactions involving two acid sites can occur more readily. In addition to this, a higher acidity means that there are more individual acid sites along the diffusion pathways of reactants/products. Therefore, the desired products have an increased likelihood of undergoing further undesirable reactions while diffusing out from the zeolite pores [50].

Wan et al. [51] studied the effect of HZSM-5 acidity in the upgrading oak pyrolysis vapors using a variety of approaches, and reached an overall conclusion that HZSM-5 catalysts with lower SAR values deactivated more rapidly. Over the SAR range of 23-80 that was examined in this study, the initial activity per acid site did not actually vary. However, when the experiments were carried out using a fixed total number of acid

sites, the more acidic catalysts lost their activity more rapidly. When using a fixed catalyst mass rather than a fixed number of acid sites, the most acidic HZSM-5 zeolite exhibited the highest initial activity in terms of alkylbenzenes production. Upon continuous exposure to oak pyrolysis vapors, the less acidic catalysts (SAR 50/80) eventually surpassed the activity of the HZSM-5 with a SAR of 23. Quite often in analytical studies, the effect of catalyst deactivation is mitigated by operating with a large excess of catalyst. The product distribution from experiments such as these can, nevertheless, provide an indication whether e.g. a certain catalyst is prone to rapid deactivation. Engtrakul et al. [52] examined the effect of catalyst acidity in catalytic upgrading of pine pyrolysis vapors, and observed that using HZSM-5 zeolites with lower SAR ratios increased the formation of polyaromatic hydrocarbons. While this in itself is not a sign of catalyst deactivation, the increased presence of polyaromatic coke precursors does suggest a higher potential for coke formation.

The studies which have been discussed in this section so far clearly indicate that HZSM-5 zeolites deactivate already at low biomass-to-catalyst ratios. In practice, this translates to a frequent need for catalyst regeneration. Without regeneration, the bio-oil quality keeps changing as a function of time. This change can be observed as e.g. increasing oxygen content and increasing average molecular weight [53]. The effect of catalyst deactivation can be to a certain extent overcome by employing a cyclical mode of operation, where the catalyst is periodically regenerated in situ. Carrying out the regeneration at frequent enough intervals essentially seeks to mimic the continuous regeneration process that is utilized in FCC units. However, variation in bio-oil properties can still occur even when the regeneration is carried out every five or ten minutes [54]. Based on general applicability rules for different reactor types, a circulating fluidized bed type reactor coupled with continuous catalyst regeneration would be the most suitable option for a process where catalyst deactivation occurs within a matter of seconds or minutes [19].

Contaminants in biomass CFP

While the deactivating effect of coke can be negated with a simple oxidative regeneration treatment, there are other sources of deactivation which are potentially irreversible on the zeolite catalyst. Biomass-derived contaminants, which constitute primarily alkaline and earth-alkaline metals such as Na, K, Mg, and Ca, can deposit on the catalyst. While relatively

little is still known concerning the effects of long-term exposure to these contaminants, the overall situation resembles the contamination of FCC catalysts with metals such V, Ni, Na, and Fe. Coupling metals deposition with severe reaction and regeneration conditions results in permanent changes in catalyst structure and performance [55, 56]. This perpetual decline in the performance of the catalyst makes it necessary to partially replace the overall catalyst inventory on a continuous basis.

When considering the transfer of biomass impurities onto the catalyst during CFP, there are two instances where this can potentially take place. First of all is the pyrolysis reactor itself, where the typically utilized reaction temperature is approximately 500 °C. At this temperature, it is possible for some of the biomass metals to volatilize, thus facilitating their potential transfer onto the catalyst. However, in fast pyrolysis, most of the inorganic matter that is present in the original biomass feedstock tends to accumulate in the solid char residue [57, 58]. The role of char inorganics becomes elevated if CFP is carried out in a CFB (circulating fluidized bed) reactor. In this case, the regeneration of the catalyst takes place in the presence of char at temperatures of 650-700 °C [26]. Thus, the biomass impurities are given an opportunity to deposit themselves on the catalyst at an elevated temperature. Even if the biomass inorganics do not deposit on the catalyst, accumulation of ash could potentially affect the process given a long enough time frame.

Mullen et al. [58] observed that inorganic elements from switchgrass accumulated on HZSM-5 in a linear overall fashion when CFP was carried out in a BFB reactor at 500 °C. The effect of these inorganic contaminants on the properties of the catalyst itself was not examined in this case. However, some changes in the composition of the bio-oil were observed. In particular, the amount of aromatic hydrocarbons in the bio-oil decreased, whereas alkyl phenols displayed the opposite trend. Although it is more challenging to draw definite conclusions from experiments involving kilogram quantities of biomass and catalyst, this change in bio-oil composition matches the observations of Mukarakate et al. [38] concerning coke-induced deactivation during CFP. Although the initial cause of deactivation is different, this suggests that there might be some similarities in these two modes of deactivation.

Yildiz et al. [59] studied the effect of ash in CFP by subjecting a HZSM-5 catalyst to multiple reaction-regeneration cycles in the presence of char, or alternatively by mixing ash directly with the fresh catalyst. Presence of
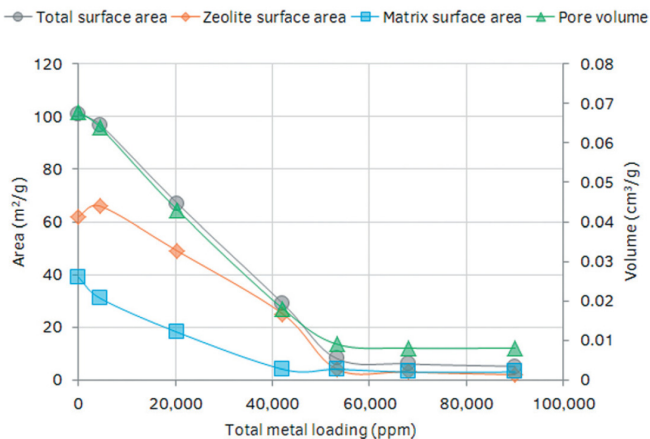
Figure 2.5. Effect of catalyst metal loading on ZSM-5 surface area and pore volume; the spray impregnated catalyst was subjected to steaming at 815 °C for 24 h [61].

ash with the fresh catalyst caused only slight changes in the product distribution and bio-oil composition. The effect of eight successive reaction-regeneration cycles was also limited. The catalyst that the authors used was diluted with sand using a ratio of 1:14. Thus, the overall catalyst amount in the reactor system was limited, which could have in turn hindered any potential interactions between the catalyst and the biomass inorganics. The same authors also followed up their experimental work with a review [60] which examines different process configuration for CFP. Their overall conclusion was that regeneration of the catalyst in the presence of the char should be explicitly avoided, which in turn dictates that ex situ CFP would be the preferred technology.

In a recent paper by Stefanidis et al. [61], the authors examined the effect biomass metals on an ZSM-5 catalyst using two methodologies: spray impregnation of metals (K, Ca, Mg, Na) followed by steaming at 815 °C, and in situ CFP with periodic catalyst regeneration in the presence of the char. Figure 2.5 shows that the combination of spray impregnation and high temperature steaming resulted in severe loss of catalyst surface area and porosity. On the other hand, the catalyst which was first steamed at 788 °C and then exposed to biomass (1500 g biomass processed over 150 g of catalyst) under CFP conditions, retained much more of its original surface area and pore volume. Comparison of this realistically deactivated catalyst to samples which were only steamed revealed that the metals only had a slight effect on catalyst performance. It is likely that the drastic changes in catalyst properties which were presented in Figure 2.5, stemmed from the fact that the contaminant metals were deposited

to the catalyst prior to steaming.

Apart from the long-term effects of biomass contaminants, alkali and alkaline earth metals can also have a more immediate impact on the CFP process. The presence of these metals has been shown to enhance the formation of char and carbon oxides at the expense condensable organic vapors. This in turn lead to a decrease in the yield of aromatic hydrocarbons, as less organic vapors were available for conversion over the HZSM-5 catalyst [62].

2.2.4 Product quality

Although many CFP-related studies focus on the production of aromatic hydrocarbons, the condensable bio-oil product is still a complex mixture containing a variety of compound groups. Because of increased water production and changes in the chemical composition of the organic products, the liquid products from CFP normally separate into two phases: an organic bio-oil phase and an aqueous phase with varying amounts of dissolved organics. When combining the aspect of phase separation with the fact that the overall yield of organic liquids is clearly lower compared to TFP, the actual yield of recoverable bio-oil in CFP can be, to say the least, very limited. The occurrence of phase separation, however, requires that most of the organics and water are either condensed in a single stage, or mixed after condensation. In systems employing fractional condensation, the bio-oil fraction is more often collected from a single source such as the ESP. The bio-oil is the primary product of interest, and therefore this section focuses on discussing its properties. However, as it will be shown in Publications III and IV, the aqueous phase organics can also constitute a very significant product fraction which cannot be overlooked.

One of the main purposes of CFP is to alleviate the challenging characteristics of TFP bio-oils. The changes in the bio-oil physicochemical characteristics result from the chemical transformations that alter the highly polar nature of the pyrolysis vapors. The characteristics of the final bio-oil product stem from these transformations, and the subsequent phase separation that may occur afterwards. During phase separation, highly oxygenated water-soluble compounds preferentially enrich in the aqueous phase. While this represents a decrease in the amount of recoverable bio-oil, it simultaneously decreases the bio-oil oxygen content. Depending on the functionality of these water-soluble oxygenates, other positive changes such as decreased acidity can also result from the phase separation.

In CFP, oxygen is rejected from the pyrolysis vapors in the form of water and carbon oxides. Consequently, bio-oils from CFP contain less oxygen than their thermally produced counterparts. CFP bio-oils are rich in carbon but poor in hydrogen, which can be observed as low molar H/C ratios. The low H/C ratio also indicates that the composition of CFP bio-oils is highly aromatic [63]. This overall change in the elemental composition increases the energy density of the bio-oil, which is also reflected in its heating value. Other positive changes which have been associated with CFP bio-oils include higher pH and lower total acid number (TAN) [64], which correlate with a decreased concentration of carboxylic acids. Use of catalysts can also decrease the viscosity of bio-oils by cracking heavier oligomeric molecules into smaller monomeric units. This change is more evident when comparing low-moisture CFP bio-oils to thermally produced bio-oils with similar water content [65], as typical fast pyrolysis bio-oils with water content of 20-30 wt% already exhibit low viscosities. CFP bio-oils have also been observed to possess better storage stability compared to TFP bio-oils [64, 66].

2.3 Further upgrading of CFP bio-oils

The two main alternatives for further upgrading of CFP bio-oils are catalytic hydrotreating and co-processing in a FCC process, the latter of which was also studied in this thesis. In the FCC process, a heavy petroleum distillate such as vacuum gas oil (VGO) is catalytically cracked in the presence of a solid acid catalyst [67, 55]. The active component of a FCC catalyst is Y zeolite, while ZSM-5 based formulations are used as additives which e.g. boost the production of olefins. The FCC process is carried out in a transported bed reactor system, which comprises a riser-type reactor, a catalyst regenerator, as well as cyclonic separators and a stripper. This configuration is necessary due to the rapid rate of coke formation, which causes reversible deactivation of the catalyst. The coke is burned off in the regenerator at 650-700 °C, which also provides the necessary heat for vaporizing the FCC feedstock and for the endothermic cracking reactions. Overall, CFB reactors which are used in fast pyrolysis resemble FCC units rather closely. In the FCC process, VGO is converted into dry gas, liquid petroleum gas (LPG), gasoline, and heavier liquid products via a wide variety of acid-catalyzed reactions. The various distillate fractions are then further processed in other refinery operations, after which they
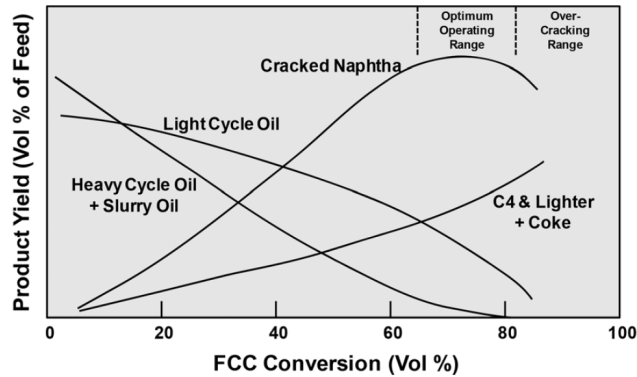
Figure 2.6. FCC product distribution as a function of feedstock conversion [69].

are blended into to the final product streams. FCC units are most commonly operated to maximize the yield of gasoline. LPG is also a valuable product, as is light cycle oil (LCO), which can be used in the production of diesel. Because bio-oils still contain varying amounts of oxygen, oxygen rejection also takes place during FCC co-processing. Both CFP and FCC employ acid catalysts, and thus similar reactions which produce water and carbon oxides occur in both processes.

The motivation behind co-processing bio-oils is two-fold. From a technical perspective, diluting the bio-oil with a conventional hydrocarbon feedstock serves to alleviate the challenges that are encountered in the upgrading of pure bio-oil [68]. Utilizing existing fuel production infrastructure would also decrease the capital expenses associated with building dedicated upgrading facilities for bio-oil. In addition to the technical benefits, co-processing would also allow refiners to introduce biogenic carbon into their fuel products. However, quantification of this bio-carbon is not straightforward, and has to be carried out via radiocarbon analysis [14].

FCC is considered as the single-most important unit in a modern oil refinery. Because of its large throughput, even small changes in the product distribution can have a significant economic impact. Thus, introduction of a bio-oil component into the FCC should not, preferably, induce undesirable changes in the overall product distribution. The FCC product distribution is evaluated in terms of distillate fraction yields, which are tightly linked to the overall conversion of the feedstock. As it can be seen in Figure 2.6, the overall conversion has to be maintained at a certain range in order to maximize the gasoline yield. It has been reported that for co-

processing of hydrotreated bio-oils, gasoline yields which are comparable to the conversion of pure VGO are attainable [70]. However, hydrogen transfer from VGO to the bio-oil increased the overall level of unsaturation, which subsequently resulted in an increased coke yield. Even if the overall product distribution would remain largely undisturbed by the inclusion of bio-oil, other challenges have also been identified. Quantification of biogenic carbon in the cracking products has shown that even under co-processing conditions, bio-oil can preferentially form coke and gases rather than liquid products [14]. Additionally, some of the more refractory bio-oil compounds like phenolics will not be completely converted, and therefore will be present in the final products [71].

3. Materials and methods

3.1 Feedstocks

A number of different woody biomass feedstocks were utilized in the CFP experiments which are reported in this thesis. The main characteristics of the feedstocks are presented in Table 3.1. Although a different biomass type was used in each publication, each feedstock consisted of typical woody biomass with low ash content. Feedstocks such as these are known to give high yields of organic liquids in fast pyrolysis [72], and thus they provide a good point of reference for comparing thermal and catalytic fast pyrolysis.

Table 3.1. Properties of the woody biomass feedstocks which were utilized in the CFP experiments.

Publication	I	II	III	IV
Biomass type	Spruce	Mixed[a]	Pine	Beech[b]
Moisture (wt%)	6.3	6.7	12.0	8.0
Carbon (wt%, db)	50.6	50.6	51.4	48.4
Hydrogen (wt%, db)	6.1	6.1	5.9	5.8
Nitrogen (wt%, db)	0.1	0.2	0.1	n.d.
Oxygen by difference (wt%, db)	43.1	41.9	42.2	45.7
Ash (wt%, db)	0.1	1.2	0.4	0.5
Volatiles (wt%, db)	83.6	81.6	83.9	n.d.
Higher heating value (MJ/kg, db)	20.1	20.3	20.4	n.d.
Particle size (mm)	0.55-0.92	< 1	< 5	0.15-0.50

[a] Forest thinnings which contained both softwood and hardwood material

[b] Commercially available Lignocel HBS 150–500

3.2 Catalysts

Commercially available acidic HZSM-5 zeolites were used in all CFP studies. The zeolites were supplied by Zeolyst International for Publications I, III, and IV. The experiments in Publication II were carried out using zeolites supplied by Süd-Chemie and BASF, but only results obtained with the Süd-Chemie catalyst are included in the summary part of this dissertation. The catalysts were received either in the form of extrudates, or as a spray dried powder. The extrudates were subsequently ground and sieved to obtain a suitable particle size fraction. The equilibrium FCC catalyst which was used in Publication V was provided by Neste, a Finnish oil refining company.

3.3 Experimental systems and procedures

3.3.1 Catalytic fast pyrolysis

The experiments in each publication were carried out using different experimental systems. The pyrolysis experiments, which have been reported in Publications I-IV, were conducted using fluidized bed reactors with varying operational scales and configurations. The main characteristics of each reactor system are given in Table 3.2, whereas the detailed information can be found in the respective publications and the references contained therein. All of the experimental systems that were used for biomass pyrolysis consist of the same primary elements: biomass feeding

Table 3.2. Main characteristics of the fast pyrolysis experimental systems that were utilized in this thesis.

Publication	I	II	III	IV
Reactor type	BFB	BFB	CFB	CFB
Feedstock	Solid	Solid	Solid	Solid
Capacity	0.8 kg/h	0.2 kg/h	20 kg/h	0.5 kg/h
Catalyst inventory	0.3 kg	0.1 kg	90-100 kg	10-15 kg
Catalyst regeneration	Periodic	None	Continuous	Continuous
Solids separation	2 cyclones	HVF	2 cyclones	Stripper, HVF
Liquid recovery	2 condensers, ESP	2 condensers, ESP	2 scrubbers, condenser	2 condensers

system, fluidized bed reactor, solids separation, and liquid recovery. The biomass is fed into the reactor using a screw feeding system. For Publications I and II, the reactor was a BFB (bubbling fluidized bed) type. In BFB reactors, the catalyst remains in the reactor while the pyrolysis products, i.e. pyrolysis vapors, non-condensable gases, and char are flushed out by the fluidization gas. Because the catalyst is in continuous contact with the pyrolysis vapors, it gradually loses its activity due to coke formation. On the other hand, CFB (circulating fluidized bed) reactors were utilized in Publications III and IV. For these reactors, both catalyst and biomass are continuously fed into the reactor. The solids traverse the length of the riser reactor, after which the pyrolysis vapors and the non-condensable gases are separated from the catalyst and the char, which are subsequently directed into a regenerator. The purpose of the regenerator is to continuously combust the char and the coke that are formed in catalytic pyrolysis.

In both BFB and CFB systems, the separation of solids from vapors and gases is carried out using either cyclones or a HFV (hot vapor filter). The HVF is the more efficient solution, and typically results in bio-oils which are practically free of solids. In contrast to this, particulate matter, i.e. char and catalyst, may pass through the cyclones, thus ending up in the product bio-oil. The experimental systems in Publications III and IV included separate regeneration units for combusting the char and catalytic coke. In addition to this, the system in Publication III utilized recirculation of product gases for the purpose of fluidization.

3.3.2 FCC co-processing via microactivity tests

The co-processing experiments of Publication V were carried out in a microactivity test (MAT) reactor. The MAT procedure is a standardized (ASTM D3907) method for testing the activity of FCC catalysts. In this case, certain aspects of the MAT procedure were modified in order to suit the research requirements identified at that time. The reactor itself is a fixed bed type, which in these experiments had a catalyst loading of 10 g. The hydrocarbon/bio-oil blends were introduced into the reactor with a syringe pump. For the experiments that are discussed in this dissertation summary, a total of 10 g of the feedstock was processed in three reaction-regeneration cycles. The liquid products were condensed and collected in cooled liquid traps. The hydrocarbon feedstock for these experiments was VGO supplied by Neste. The co-processed bio-oil samples included a low

water content TFP bio-oil, a CFP bio-oil and a catalytically hydrotreated bio-oil.

3.4 Analysis of bio-oils from CFP

The product bio-oils were analyzed using a variety of methodologies. The analytical tools which were utilized can be divided into two main categories: fuel property analyses and chemical composition analyses. The main fuel property analyses that have been applied for the characterization of CFP bio-oils are listed in Table 3.3. The applicability of these analyses for bio-oils is described in more detail elsewhere [73].

Table 3.3. Standard fuel analyses which have been applied in the characterization of fast pyrolysis bio-oils.

Property	Analysis method	Standard
Water content	Karl Fisher titration	ASTM E203-96
Elemental composition (CHN)	Combustion	ASTM D5291
Solids content	Filtration	ASTM D7579
Heating value	Bomb calorimetry	DIN 51900
Total acid number	Potentiometric titration	ASTM D664
Micro carbon residue	Destructive distillation	ASTM D4530
Kinematic viscosity	Capillary/Stabinger viscometry	ASTM D445
Density	Digital Density Meter	ASTM D4052

The chemical composition of bio-oils was analyzed using several techniques. These included VTT's solvent fractionation method [74] and carbon-13 nuclear magnetic resonance (^{13}C NMR) spectroscopy, both of which can provide an overview of the bio-oil chemical composition. The volatile fraction of bio-oil was examined using different gas chromatographic methods. Qualitative analysis, i.e. compound identification, was carried out using gas chromatography - mass spectrometry (GC-MS). Quantitative analysis of certain compounds was performed using gas chromatography with a flame ionization detector (GC-FID). The details of the applied techniques can be found in the publications and the references contained therein.

4. Results and discussion

4.1 Exploring the limitations of BFB reactors in CFP

A purely thermal process such as fast pyrolysis can be in theory maintained at a stable state indefinitely, as long as an adequate amount of heat is being provided. Shifting from this operational mode into a thermocatalytic one introduces a new and rather significant variable: catalyst deactivation. In BFB reactors, the catalyst is in continuous contact with the pyrolysis vapors. Exposing the catalyst's acid sites to a multitude of oxygenates with varying functionalities and molecular sizes results in severe coke formation, and as a result, the catalyst starts to lose its activity rapidly. One way to examine the rate of the deactivation process is monitoring the composition of the non-condensable product gases. Using HZSM-5 catalysts in CFP typically increases the formation of CO, whereas CO_2 is not influenced to such a large extent. This characteristic makes it possible to use the molar ratio of these two product gases as a metric for catalyst deactivation. Figure 4.1 shows how the CO/CO_2 ratio decreased during three hour CFP experiments in a BFB reactor. Although the CO/CO_2 ratio was higher compared to the non-catalytic experiment even after 3 h, the gradual change in the gas composition was a clear indication of the catalyst continuously losing its activity. Consequently, any bio-oil that was produced during the stage when catalyst still retained most of its initial has been diluted with further products from periods of lower catalytic activity. This limitation could, of course, be circumvented by periodically sampling the bio-oil. Nevertheless, with the current experimental arrangement, the observed changes in the overall physicochemical characteristics of the bio-oils remained limited.

The rate of coke formation also decreased with time. Samples of the
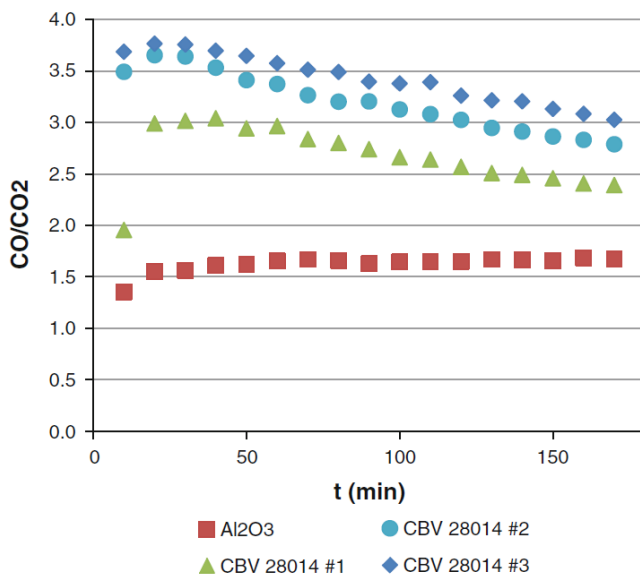
Figure 4.1. Molar CO/CO_2 ratio as a function of time in CFP of spruce sawdust with HZSM-5 (SAR = 280) at 500 °C using different WHSVs. The data series 'Al$_2$O$_3$' refers to a non-catalytic experiment. (I).

HZSM-5 catalyst (SAR = 280) which were collected after 30, 60 ja 180 minute experiments, contained 4.9, 6.2 and 7.6 wt% of carbon, respectively. Under the conditions that were employed in these experiments, the average rate of carbon formation over a given time period correlated with the amount of carbon that had previously deposited on the catalyst. As it can be seen in Figure 4.2, the average rate of carbon formation during the first 30 minutes was approximately four times higher compared to the time period of 30-60 minutes. During the final stage (60-180 min), the average rate of carbon formation had further decreased. These observations also reflect the autoinhibitive character of coke formation on acidic zeolites; the rate of desired reactions decreases on coked zeolites, but so does the rate of coke formation.

In order to observe the effect of the catalyst in a more definite fashion, it was necessary to shorten the duration of the experiments. This made it possible to maintain a higher level of catalytic activity throughout the experiment. One practical challenge was, however, the limited amount of liquid products that is produced during shorter experiments. In order to overcome this limitation, the catalyst had to be regenerated periodically directly in the BFB reactor, and each experiment had to include an adequate number of these reaction-regeneration cycles. This methodology was applied for further studying the deactivation characteristics of

HZSM-5 zeolites with varying degrees of acidity. The mass of the catalyst bed was kept constant, and therefore the number of available acid sites increased with increasing catalyst acidity. The challenging nature of biomass pyrolysis vapors became even more pronounced when the acidity of the catalyst increased. Figure 4.3 displays a linearly increasing trend in coke formation as a function of the zeolite strong acid site concentration. All three catalysts had similar specific surface areas prior to use, but the differences in coke formation also reflected clearly on the amount of surface area that was accessible after the 30 min experiments. Based on these observations, the more acidic catalysts would require more frequent
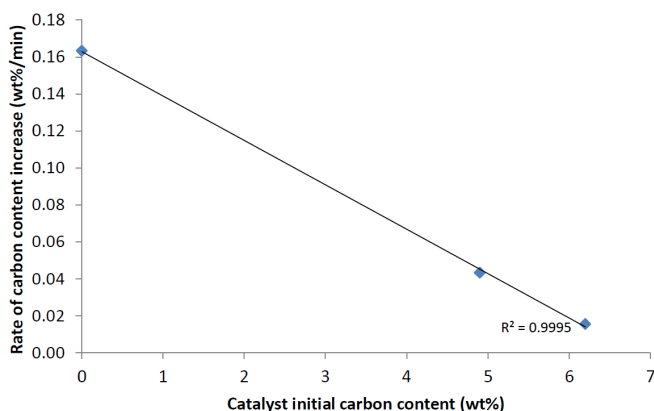
Figure 4.2. Average rate of catalyst carbon content increase over a given time period as a function of the catalyst carbon content in CFP of spruce sawdust with HZSM-5 (SiO_2/Al_2O_3 = 280) at 500 °C. From left to right, the data points correspond to time periods of 0-30, 30-60 and 60-180 min.
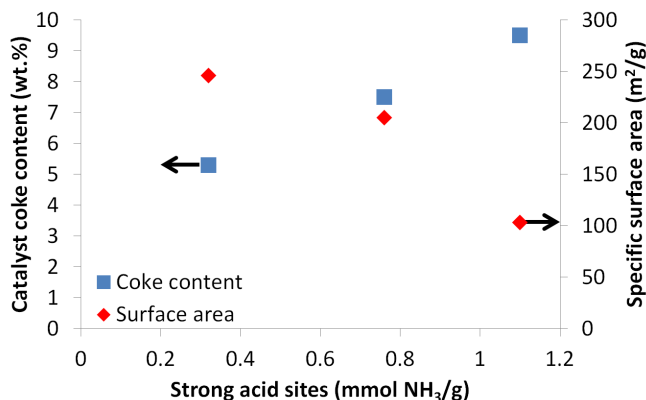
Figure 4.3. Catalyst coke content and specific surface area of the spent catalyst as a function of strong acid site concentration; three HZSM-5 catalysts with SiO_2/Al_2O_3 ratios of 280, 55 and 23 were used in 30 min spruce CFP experiments at 500 °C.

Table 4.1. Product distribution from thermal and catalytic fast pyrolysis of spruce in BFB reactor at 500 °C; HZSM-5 with SAR 280 was regenerated after 30 min.

Operational mode	Thermal	Catalytic
Organic liquids	59	29
Water	11	21
Char/coke	13	18
Gases	10	25

regeneration if a stable level of activity is to be maintained.

Operation with the least acidic HZSM-5 catalyst (SAR 280) and a re-generation interval of 30 min made it possible to observe the effect of the catalyst while it still retained most of its initial activity. As it can be seen in Table 4.1, the yield of organic liquids exhibited a notable decrease compared to the thermal experiment, while more gases, water, and char/coke were produced. A change of this magnitude also reflected in the properties of the bio-oil. The dry basis oxygen content decreased from 36.6 to 23.6 wt%. Based on the TAN values (56 vs. 28 mg KOH/g), the catalytically produced bio-oil was also clearly less acidic.

Overall, the results from Publication I show that partially deoxygenated bio-oils can be produced using mildly acidic HZSM-5 zeolites with a regeneration interval of 30 min. After 30 min of operation, even a mildly acidic HZSM-5 has a considerable amount of coke deposits on it, and thus requires regeneration. Using more acidic HZSM-5 variants increased the rate of coke formation, which in turn suggests that more frequent regeneration would be necessary. Although an approach such as this can still be implemented for research purposes, its practicality can be considered questionable at best. Another alternative for periodic catalyst regeneration would be to continuously withdraw and add catalyst into the reactor, as was demonstrated by Jae et al. [75]. The authors used specially designed ball valves with wells drilled into them to meter the catalyst into and out from the reactor. This approach makes it possible to maintain a stable level of catalyst activity even in a BFB reactor. When using an electrically heated research reactor, the overall heat balance of the system does not play a significant role. However, for an industrial unit, the hot catalyst that is continuously introduced into the reactor would also have to provide the heat that is required by the endothermic pyrolysis process. Thus, the rate of catalyst replacement would ultimately be dictated by the energy needs of the CFP process itself. Although continuous

regeneration and circulation of the catalyst could be arranged for a BFB reactor, there are additional factors which would favor the usage of CFB reactors. These include better scalability of CFB reactors, and enhanced mixing and heat transfer characteristics. Operating a BFB reactor with a spray-dried catalyst that has a minimum fluidization velocity of < 1 cm/s could also prove challenging, especially in a situation where continuous catalyst withdrawal and addition were required.

4.2 Influencing bio-oil quality characteristics with CFP reaction temperature

Typical BFB reactors which have been designed and constructed for research purposes operate with a fixed catalyst batch, which is not continuously renewed during operation. This, coupled with reversible catalyst deactivation, limits the functionality of these reactors for CFP research. Nevertheless, they can still be utilized to explore the effect of different process variables such as the reaction temperature, as long as the effect of catalyst deactivation is not entirely ignored. While the CFP process is expected to behave in a different way in BFB and CFB reactors, comprehensive characterization of the liquid products that have been produced in a BFB system can, nevertheless, yield valuable information concerning the characteristics of these partially upgraded bio-oils. In Publication II, the effect of reaction temperature was evaluated by pyrolyzing forest thinnings at 400, 475, and 550 °C, over a commercial HZSM-5 catalyst in a bench-scale BFB reactor. The duration of a single experiment was 2 h, which, based on the results of Publication I, was expected to lead to significant deactivation of the catalyst. Because of this, separate bio-oil samples were collected at the middle of the experiment, i.e. after 1 h of pyrolysis.

Varying the reaction temperature in the presence of the catalyst had a clear impact on the overall CFP product distribution, which is shown in Table 4.2. When the catalyst was used, operating at 400 °C resulted in the highest yield of organic liquids and char, whereas clearly more gases were produced at higher temperatures. Based on what is known about the effect of temperature in TFP [5, 6, 16], it can be assumed that more organic vapors would have been released at 475 °C than at 400 °C. This notion is also supported by the high char/coke yield which was observed at 400 °C. These factors, together with the product distribution of Table 4.2, would

Table 4.2. Overall product yields (wt%, dry basis) from TFP, and CFP of forest thinnings with HZSM-5 at different reaction temperatures; experiment duration 2 h, WHSV = 2 h^{-1}.

Operational mode	Thermal	Catalytic		
Temperature (°C)	475	400	475	550
Organic liquids	38±0.5	24±0.6	15±0.9	14±0.6
Water	17±1.0	22±0.3	23±0.3	21±0.9
Char/coke	19±1.1	25±0.7	20±0.2	18±0.1
Gases (by difference)	24±0.4	30±1.0	42±0.3	48±0.2
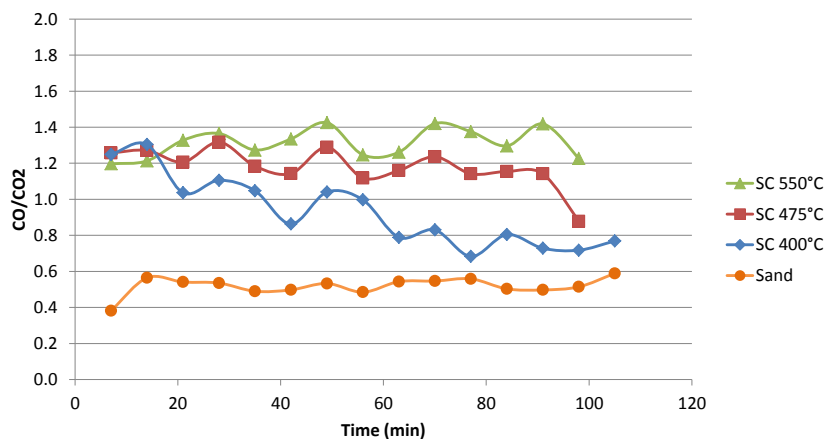
Figure 4.4. Weight-based CO/CO_2 ratio as a function of time for TFP at 475 °C and CFP over HZSM-5 at 400, 475, and 550 °C (II).

indicate that the activity of the catalyst was either clearly lower, or that it was lost more rapidly at 400 °C. Observation of the CO/CO_2 ratio as a function of time in Figure 4.4 shows a clearly decreasing trend for 400 °C, whereas at 475 and 550 °C the ratio remained more stable. This would indicate that at 400 °C, the catalyst was indeed losing its activity more rapidly. Nevertheless, the CO/CO_2 ratio remained constantly higher compared to the non-catalytic reference experiment. Although evaluating the effect of catalyst deactivation was not the primary purpose of this study, it was to a certain extent taken into account by sampling the bio-oil from the ESP at the middle of the experiment, i.e. after 60 min. Comparing the properties and composition of this intermediate bio-oil to the one that was recovered at the end of the experiment reflects the effect of catalyst deactivation, but it also served to increase the overall size of the bio-oil sample matrix.

Table 4.3. Physicochemical properties of ESP bio-oils from thermal and catalytic fast pyrolysis of forest thinnings.

Operational mode	Thermal	Catalytic				
Temperature (°C)	475	400		475		550
Bio-oil sample	0-2 h	0-1 h	1-2 h	0-1 h	1-2 h	0-2 h
Water (wt%)	3.7	1.4	1.6	0.6	0.9	0.9
Carbon (wt%, db)	59.1	64.3	65.4	73.6	68.7	68.3
Hydrogen (wt%, db)	6.5	6.6	6.9	6.8	6.7	6.7
Nitrogen (wt%, db)	0.4	0.8	0.8	0.5	0.6	0.9
Oxygen by difference (wt%, db)	34.0	28.3	27.0	19.1	24.0	24.1
H/C (mol/mol)	1.31	1.22	1.25	1.10	1.16	1.21
O/C (mol/mol)	0.43	0.33	0.31	0.20	0.26	0.30
Higher heating value (MJ/kg, db)	25.6	28.9	27.7	32.8	31.9	30.1
pH	3.0	2.9	2.9	3.2	3.1	3.9
Dynamic viscosity (cP, 40 °C)	560	62	115	-	175	311

4.2.1 Bio-oil physicochemical properties

Varying the reaction temperature had a clear impact on the properties of the bio-oils, which are presented in Table 4.3. It should be emphasized that the values in this table refer only to the bio-oils that were recovered from the ESP (electrostatic precipitator). For the catalytic experiments, the liquids that were collected from the condensers were primarily in the form of aqueous condensates. For the non-catalytic experiment, it would have been possible to combine the liquid products from the ESP and the condensers. This would have resulted in a more typical fast pyrolysis bio-oil with high water content. The TFP bio-oil that is included in Table 4.3 is, in this case, more viscous and somewhat less oxygenated compared to typical bio-oils [72]. Nevertheless, the staged condensation approach that was utilized here made it possible to observe the effect of the catalyst in a less ambiguous fashion, as the positive effects of the catalyst primarily reflect in the bio-oil that was recovered from the ESP. When CFP was carried out at 550 °C, no bio-oil could be recovered after 1 h. Because of this, Table 4.3 only contains results for the overall bio-oil which was collected after the 2 h experiment. At 475 °C, not enough bio-oil was recovered after 1 h to carry out the viscosity determination.

In general, the catalytically produced bio-oils had lower oxygen content and lower viscosities compared to the TFP bio-oil. The lower oxygen content also reflected directly in the HHV (higher heating value) of the bio-oils. In addition to the lower oxygen content, the molar H/C ratio de-

creased when the catalyst was utilized. This coincided with the increased water yield, which signified that substantial amounts of hydrogen were being removed together with the oxygen. These low H/C ratios also signified the increasingly aromatic character of these bio-oils, which was subsequently confirmed in a number of compositional analyses. The effect of catalyst deactivation was also evident when comparing the bio-oil samples which were collected at middle and at the end of the experiment. This reflected in e.g. the oxygen content and the viscosity of the bio-oils, both of which tended to increase with time. When considering the effect of reaction temperature, the most interesting results were obtained at 400 °C. Although the bio-oil oxygen content was higher compared to what was observed at higher temperatures, the viscosity was remarkably low. Use of low reaction temperatures has also been reported to result in low viscosity bio-oils in TFP [17]. In TFP, the change in the bio-oil composition and water content was, however, identified as the primary reason behind the observed differences in viscosity.

4.2.2 Bio-oil chemical composition

In order to better understand the compositional changes that take place during CFP, the bio-oils were characterized using a variety of analytical techniques. This included ^{13}C NMR (nuclear magnetic resonance) spectroscopy, GC-MS (gas chromatography - mass spectrometry), quantitative GC-FID (gas chromatography with flame ionization detector) analysis, and solvent fractionation. Both ^{13}C NMR and solvent fractionation can be used for obtaining an overview of the bio-oil chemical composition. The results of the ^{13}C NMR analysis (see Table 5 in Publication II for details) confirmed that the CFP bio-oils were largely aromatic. Compared to the TFP bio-oil, the CFP bio-oils contained smaller relative amounts of oxygenate functionalities which are associated with carbohydrate decomposition products. The bio-oil produced at 400 °C contained more oxygenated functionalities, which also supported the results of the elemental analysis. The highly aromatic character of the CFP bio-oils also meant that these oils were increasingly hydrophobic. Figure 4.5 shows that more than half of the bio-oils consisted of water-insoluble material, which, in the case of TFP bio-oils, is primarily pyrolytic lignin [74, 8]. For CFP bio-oils, the fraction that is generally classified as LMW lignin can also contain aromatic hydrocarbons (and extractives), as these are insoluble in water but soluble in dichloromethane. The solvent extraction proce-
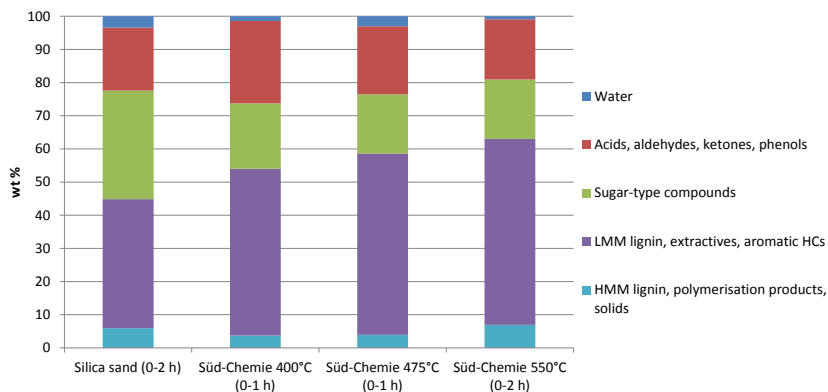
Figure 4.5. Solvent fractionation analysis of ESP bio-oils from TFP at 475 °C, and CFP at varying reaction temperatures (II).

dure could also be modified (see Figure 9 in Publication II) to take into account the presence of volatile water-insoluble compounds, a category under which aromatic hydrocarbons would also fall under. The amount of these water-insoluble volatiles was correlated with a number of other factors, which included the proportion of aromatic carbon in ^{13}C NMR, the molar H/C ratio of the bio-oil, and the amount of single- and two-ring aromatic hydrocarbons as quantified by GC-FID.

In addition to the ^{13}C NMR and solvent fractionation analyses which divide the bio-oil into certain functionality groups or macro-fractions, it is possible to examine the effect of the catalyst on individual compounds. Comparison of the TFP bio-oil and the CFP oil produced at 475 °C in GC-MS (see Figure 13 in Publication II) showed a distinct decrease in the proportion of carbohydrate decomposition such as levoglucosan. Phenolic compounds, which in this case include phenols, catechols and syringols, along with one- and two-ring aromatic hydrocarbons became the dominant compound groups in the total ion chromatogram. The actual concentration of aromatic hydrocarbons in the bio-oils was, however, less than 3.5 wt% in all cases. Quantitative analysis of various water-soluble oxygenates in the bio-oils, the results of which are presented in Figure 4.6, supported the results of the other analyses. The CFP bio-oils contained more lignin monomers, and in general, less carboxylic acids, less aldehydes and ketones, and less furanic compounds compared to the TFP bio-oil.
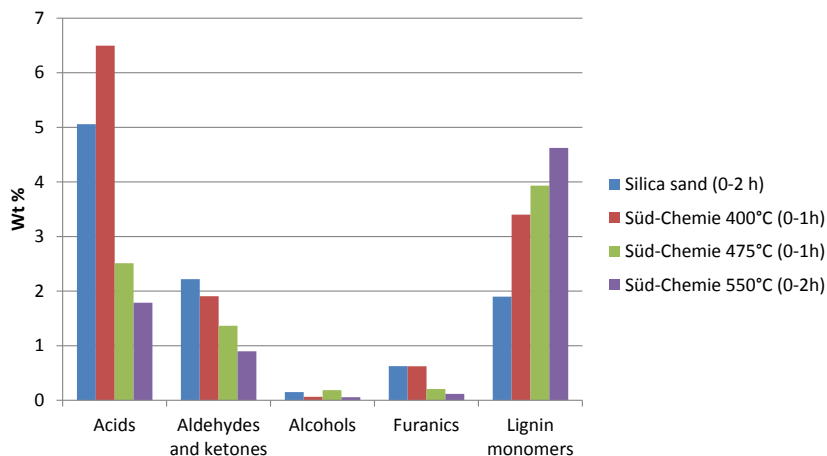
Figure 4.6. Concentration of different organic compound groups in TFP and CFP bio-oils as determined by GC-FID (II).

4.2.3 Summary of findings

The results from Publication II showed that reaction temperature plays an important role in determining CFP bio-oil properties and composition. The CFP bio-oils which were produced at temperatures of 400, 475, and 550 °C exhibited clear differences in their physicochemical properties, which also changed as a function of time due to catalyst deactivation. CFP at 400 °C appeared to be particularly interesting, as it yielded a low viscosity of bio-oil with a moderate degree of deoxygenation. This study also showed that a variety of analytical techniques can be employed to comprehensively characterize these partially upgraded bio-oils. Comprehensive characterization methods such ^{13}C NMR and solvent fractionation can be supported by quantitative gas chromatography to monitor the changes in the concentration of individual key compounds. A combinatorial approach employing multiple analytical techniques can help better understand the transformation process that takes place during CFP.

4.3 Maintaining stable bio-oil quality with continuous catalyst regeneration

4.3.1 Objectives and overview of the experiment

Based on the results presented in Publications I and II, it was abundantly clear that due to catalyst deactivation, it is not practical to attempt to

maintain constant bio-oil quality when performing CFP in a BFB reactor without continuous catalyst addition and removal. The most convenient way of overcoming this hurdle was to switch to a CFB reactor, which allowed continuous regeneration of the catalyst in a much more straightforward manner. Unlike in BFB reactors where the catalyst is exposed to a cumulatively increasing amount of pyrolysis vapors, the catalyst and biomass vapors are in contact with each other for mere seconds in the CFB system. Coke formation does take place, but its effect on catalyst performance is effectively negated as the coked catalyst is immediately subjected to an oxidative treatment in the regenerator. Because of this, the catalyst which is recirculated back into the reactor should have negligible or at least very low coke content, and thus possess most of its original activity. When reversible catalyst deactivation is no longer a prime concern, other factors will become more influential in determining the product quality. The suitability of CFB reactors for TFP has been well established, which is evident in the form of high organic liquid yields [72, 76]. Successful catalytic operation has also been reported previously [26, 47, 77], but only for experiments with limited experimental duration.

In Publication III, a prolonged (96 h) CFP experiment was carried out in pilot-scale pyrolysis unit with a biomass processing capacity of 20 kg/h. In addition to the duration and the scale of the experiment, it should be noted that the pyrolysis unit itself had an industrially relevant configuration. This included practically autothermal operation after reaching a steady state, bio-oil condensation with scrubbers that used the product itself as the quenching liquid, and recirculation of product gases for fluidization. The purpose of this experiment was threefold:

1. Determine the overall product distribution and product quality from the 96 h time period

2. Determine if there are clear changes in bio-oil properties as a function of time-on-stream

3. Determine if changes in catalyst properties and characteristics can account for the variation of bio-oil quality

Items 2 and 3 in the previous list were considered to be of essential importance, because observations such as these could indicate whether there is a clear decrease in catalyst activity due to reasons other than coking. Information such as this could be used to evaluate the overall lifetime of the catalyst, and subsequently the rate of catalyst replacement.
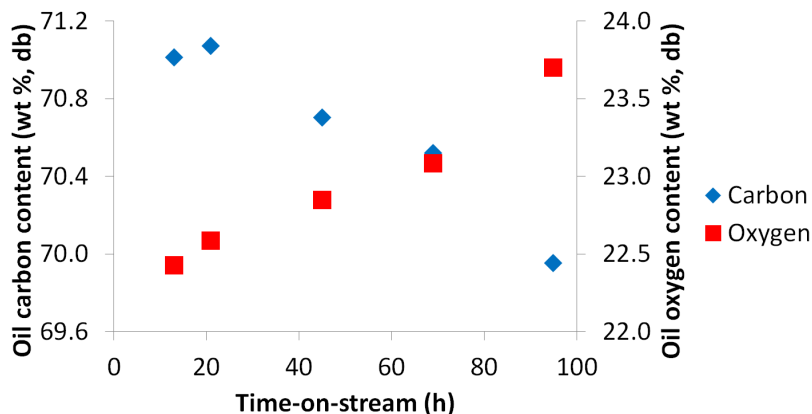
Figure 4.7. Bio-oil carbon and oxygen content (wt%, dry basis) as a function of time-on-stream in pilot-scale CFP of pine sawdust over HZSM-5 at 520 °C.

At this stage, one factor which should be further explored is the form that the CFP liquid products are recovered in. Increased water production due to acid-catalyzed dehydration reactions coupled with chemical transformation of the bio-oil organics lead to the formation of a two-phase product, which contained a hydrophobic organic phase, i.e. bio-oil, and a separate aqueous phase with dissolved organics. While the bio-oil fraction was the primary product of interest, the dissolved organics in the aqueous phase also represented a significant fraction of the overall products. In order to clarify the presentation of information, the bio-oil and the aqueous fraction were discussed as separate entities. Following the elemental composition of the bio-oil fraction as a function of time-on-stream revealed a clear and linear trend, the magnitude of which was, however, quite limited. Figure 4.7 shows that the bio-oil oxygen content steadily increased over time, whereas the carbon content displayed an opposite trend. The CFP process was carried out at otherwise constant conditions, and therefore the observed change in bio-oil elemental composition indicated that the catalyst was, in fact, undergoing a clear and potentially permanent loss of activity.

Coke formation also exhibited a similar trend as the bio-oil carbon content. While the values that are shown in Figure 4.8 may not immediately strike the reader as being very high, one has to take into account the ratio between the catalyst circulation rate and the biomass feeding rate, which was approximately 7:1 in this experiment. The relatively high catalyst-to-biomass ratio decrees that the amount of biomass converted into coke was far from being insubstantial. As it was discussed in Section 2.2.2, CFP
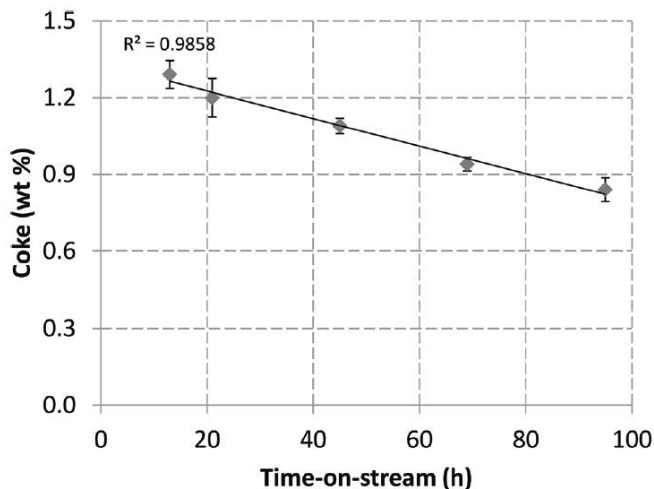
Figure 4.8. HZSM-5 coke content, as determined by thermogravimetric analysis, as a function of time-on-stream in pilot-scale CFP of pine sawdust over HZSM-5 at 520 °C (III).

main reactions are always accompanied by coke formation. Although coke formation is not a desirable phenomenon in itself, it nevertheless, can be used as an indication of catalyst activity. Because of this, coke formation has also been used directly as a performance metric to identify high activity catalysts in a catalyst screening study for biomass CFP [78]; lower overall catalyst activity also resulted in lower coke formation. All in all, the observations which were presented in Figures 4.7 and 4.8 support the notion that the catalyst was indeed gradually losing its activity throughout the course of the experiment.

4.3.2 Properties and composition of liquid products

Although the bio-oil quality was gradually changing over time in terms of its elemental composition, the overall product from the 96 h time period was clearly different compared to bio-oil from conventional TFP. As was to be expected, the yield of organic liquids decreased significantly, whereas the yield of water, gases and char/coke increased. The actual coke yield was estimated as 7-8 wt% based on the results presented in Figure 4.8. The 32 wt% overall yield of organic liquids, which is shown in Table 4.4, already represented a relative decrease of approximately 50 % compared to TFP. In this case, however, more than 40 % of the overall organic liquids were actually recovered in the aqueous phase. This is a clear challenge when considering e.g. the carbon efficiency of the CFP process

Table 4.4. Overall product yields (wt%, dry basis) from catalytic and thermal fast pyrolysis of pine sawdust in the 20 kg/h pilot-scale CFB pyrolysis system. The value inside the parentheses denotes the part of overall organics which was recovered in the bio-oil fraction.

| Yield (wt%, db)	Catalytic	Thermal
Organic liquids	32 (18)	63
Water	19	10
Gases	21	9
Char/coke (by difference)	27	18

and the overall fuel production pathway. Only the bio-oil fraction is seen as an attractive feedstock for catalytic hydrotreating, whereas alternate processing routes would have to be identified and employed for the aqueous phase. In a worst case scenario, subsequent processing of the aqueous phase may actually become a technical and a financial burden. Therefore, the nearly even distribution of organics between the bio-oil and the aqueous phase that was observed in Publication III is far from desirable. Additional measures should be taken to further develop the CFP process in a direction which would potentially help limit the amount of aqueous organics.

Seeing as CFP is essentially a trade-off between product quantity and quality, the observed decrease in the quantity of organic liquids should translate into improved quality. Table 4.5 shows that the physicochemical properties of the CFP bio-oil clearly differed from those of a typical fast pyrolysis bio-oil. Notable changes of the positive kind were observed for water content, elemental composition, heating value and total acid number. In summary, it can be said that the CFP bio-oil was less oxygenated, more hydrophobic and less acidic compared to its thermally produced counterpart. Not all of the observed changes were, however, positive. Due to carryover of catalyst fines, the solids content of the CFP bio-oil was high. Similar values for the overall solids content and the ash content corroborate that inorganic catalyst material, rather than entrained char, was the main culprit behind this. One may expect that the entrained catalyst particles present in the bio-oil can become a source of plugging problems in subsequent upgrading processes, which would typically utilize fixed bed catalytic reactors. The problem of catalyst carryover also highlights the value of hot vapor filtration, which is an efficient solution for eliminating solids from bio-oil, but has yet to be proven viable for continuous long-term operation.

Table 4.5. Physicochemical properties of CFP and TFP bio-oils produced from pine saw-dust in the 20 kg/h CFB pyrolysis unit.

Property	Catalytic	Thermal [72]
Water (wt%)	8.3	23.9
Solids (wt%)	0.76	0.01
Ash (wt%)	0.6	0.03
Carbon (wt%, dab)	72.0	53.4
Hydrogen (wt%, dab)	6.4	6.5
Nitrogen (wt%, dab)	0.02	0.1
Oxygen (wt%, dab)	21.5	40.0
Higher heating value (MJ/kg, dab)	30.4	22.2
Lower heating value (MJ/kg, dab)	28.7	20.1
Kinematic viscosity (cSt, 40 °C)	285	17
Density (kg/dm^3, 15 °C)	1.183	1.206
pH	2.6	2.7
Total acid number (mg KOH/g)	30	71
Carbonyls (mmol/g)	2.8	3.5
Micro carbon residue (wt%)	29.3	20.8
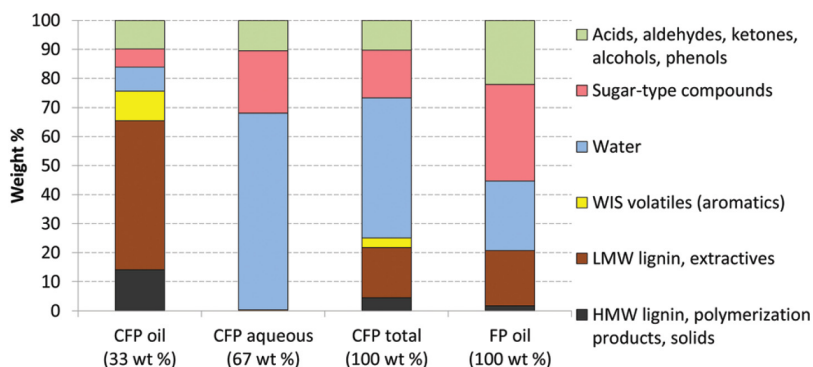
Figure 4.9. Solvent fractionation results for CFP oil, CFP aqueous fraction and a typical TFP oil from pine. Relative amounts of the two product fractions are given inside the parentheses for CFP liquid products (III).

The hydrophobic character of the CFP bio-oil was also reflected in its compositional analysis. Similarly to the bio-oils in Publication II, the organic bio-oil fraction contained mostly water-insoluble compounds. Figure 4.9, which contains the results from the solvent fractionation analysis, also draws attention to the stark difference between the CFP bio-oil and aqueous phase. Less polar water-insoluble compounds had enriched in the bio-oil, whereas the aqueous phase contained most of the water-soluble

polar oxygenates. The difference in the composition of these two product fractions also strongly indicates that different upgrading strategies should be employed to account for the distinct compositional characteristics of each fraction. In addition to the differences in the macro-level composition of the liquid products, the aqueous phase was observed to contain more quantifiable water-soluble organics (see Table 4 in Publication III). In particular, the preferential enrichment of acids and aldehydes/ketones in the aqueous phase was evident. In contrast to this, the concentration of lignin monomers was higher in the CFP bio-oil, which also contained 6.4 wt% of aromatic hydrocarbons.

4.3.3   Catalyst characterization

The properties of the catalyst also changed during the 96 h experimental period. Certain changes already took place during the initial heat-up period of the pyrolysis unit, when biomass was not being fed into the reactor yet. This observation concerned primarily the porous characteristics of the catalyst, which in this case included specific surface area, micropore area and micropore volume. Compared to the fresh catalyst, the values of these parameters decreased substantially during the 2½ day heat-up stage. The decrease was relatively highest for the micropore area and volume, which indicated that the microporous zeolite component of the catalyst was getting partially degraded. This change was also evident in the X-ray diffraction pattern of the catalyst samples, where the used catalyst exhibited changes which are associated with loss of crystallinity and zeolite framework dealumination. On the other hand, this initial heat-up period was somewhat similar to the steaming process that is used for partially deactivating and consequently stabilizing zeolite catalysts prior to use [79, 55]. During the actual pyrolysis part of the experiment, the surface area and pore volume of the catalyst continued to gradually decrease, but at a much slower rate compared to the heat-up period. In addition to the micro-structural changes of the catalyst, physical degradation of the catalyst particles was also observed. Figure 4.10 shows how the original spherical shape of the catalyst particles transformed during the course of the experiment. The catalyst sample which was collected after the initial heat-up period already exhibited signs of slight agglomeration. In the final sample, on the other hand, both agglomeration and fracturing of individual microspheres was clearly evident.

One essential concern in CFP is the potential deposition of inorganic
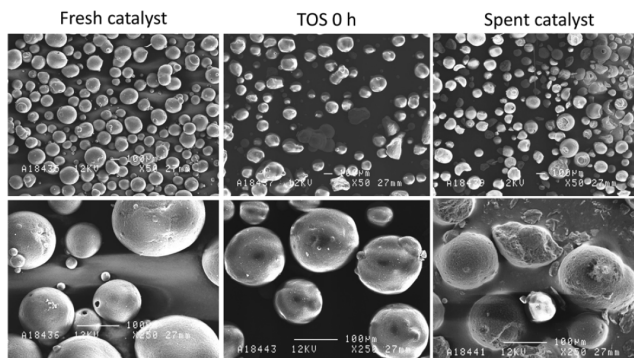
Figure 4.10. Scanning electron microscopy images of the spray-dried HZSM-5 catalyst before the experiment (left), at the beginning of the pyrolysis stage (middle), and after the experiment (right) (III).
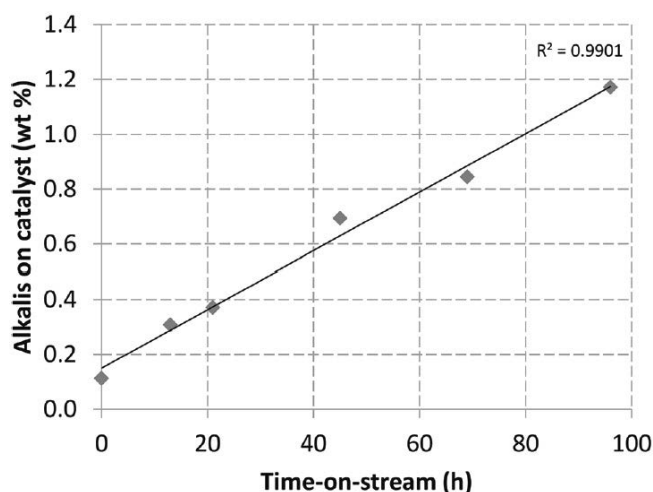
Figure 4.11. Alkali metal content (K, Ca, P, Mg) of the HZSM-5 catalyst as a function of time-on-stream in CFP on pine sawdust (III).

biomass-derived contaminants on the catalyst, and their subsequent effect on its activity. Figure 4.11 clearly shows that the amount of biomass-derived metals increased as a function of time, which correlates with the amount of biomass that has been cumulatively processed over the catalyst. Even when utilizing a low ash feedstock like pine sawdust, the observed rate of metal deposition suggested that operating with a single catalyst batch without continuous catalyst addition/removal could eventually compromise the performance of the catalyst. Because of this, zeolite metal tolerance and the associated catalyst costs are considered as one the main uncertainty parameters for evaluating the technical and economic feasibility of the CFP process [80, 60].

Although the exact mechanisms which are involved in the contamination process still require more elucidation, it is innately clear that introduction of foreign matter, which in the current context means biomass-derived inorganic contaminants, will in all likelihood have a negative effect on the performance of the catalyst. Previous studies [81, 82] concerning the deactivation of zeolite-based deNO$_x$ catalysts have indicated that the deactivating effect of alkaline metals is two-fold. On one hand, the alkalis can interact with the cationic acid sites of the catalyst, thus effectively decreasing the acidity of the catalyst. A correlation between alkali concentration and catalyst acidity was also observed in Publication III. In addition to this, straightforward plugging of catalyst pores has also been suggested. It is, therefore, possible that zeolite deactivation due to contaminant deposition may proceed according to more than one mode of deactivation. Coke deposition on zeolites is known to cause deactivation via three separate modes: partial coverage of active sites, poisoning of active sites and pore blockage [50]. The prevailing deactivation mode typically depends on the overall coke content of the catalyst. Pore blockage, which has the most dramatic effect among the aforementioned three modes, normally happens when the overall coke content is high. Thus, it is possible that biomass-derived contaminants may act in a similar fashion: at low contaminant concentrations individual active sites are affected, but after a certain concentration threshold is passed, pore blockage may also ensue. This pore blockage was clearly evident in a recent patent application by KiOR [83], wherein a zeolitic catalyst sample which had been utilized in a thermocatalytic conversion unit contained contaminant metal oxides with concentrations ranging from 14 wt% all the way up to 28 wt%. At the highest concentration level, the catalyst no longer contained any accessible micropore volume. However, the catalyst could still be rejuvenated by washing it in an acidic solution, which facilitated the dissolution of the metal oxide deposits.

4.3.4   Summary of findings

The observations of Publication III showed that a relatively constant bio-oil quality could be maintained in an extended four day CFP experiment. Due to continuous catalyst regeneration, short-term deactivation that stems from coke formation no longer hindered the performance of the process. However, gradual changes in the properties of the HZSM-5 catalyst indicated that permanent deactivation would in all likelihood set a limit

for the overall lifetime of the catalyst. Although changes in the bio-oil composition were limited during the course of this experiment, a linear increase in the oxygen content suggested that the catalyst was continuously losing its activity. The loss of activity most likely resulted from a combination of factors which included severe regeneration conditions coupled with biomass-derived inorganic contaminants. While the primary product of interest in this study was the carbon-rich hydrophobic bio-oil, the water-soluble organics which were recovered in the aqueous phase also warrant further attention simply due to their significant amount.

4.4 Optimizing the CFP process with the catalyst-to-biomass ratio

4.4.1 Overview of the experiment

One obvious challenge in the CFP product distribution of Publication III was the high amount of water-soluble organics which were recovered in the aqueous phase. In theory, it would be beneficial if these compounds could be further converted into a form which would be preferentially recoverable in the bio-oil, rather than in the aqueous phase. Various model compound studies [84, 85, 86] have shown that water-soluble products from the thermal decomposition of carbohydrates can be converted into aromatic hydrocarbons and olefins. Therefore, the plentiful aqueous phase products of Publication III can be in a way considered as an unconverted resource that would require further valorization. One potential way of further converting this material would be to increase the amount of catalyst that is available for contact with the pyrolysis vapors. In a CFB reactor system, this is possible by manipulating the catalyst-to-biomass (C/B) ratio. By supplying more catalyst, and consequently more active sites to the process, one would expect to improve the conversion of the aqueous phase organics. This approach was pursued in Publication IV, where a commercial hardwood biomass was pyrolyzed over the same partially deactivated HZSM-5 catalyst that had already been utilized in Publication III. The effect of the C/B ratio was evaluated at four different levels while otherwise keeping the process conditions constant.

Increasing the C/B ratio to a certain extent enhanced the catalytic effect that is typically associated with HZSM-5 in biomass CFP. Operating with a higher C/B ratio decreased the overall yield of organic liquids whereas

Table 4.6. Product yields (wt%, dry basis) from catalytic fast pyrolysis of Lignocell over HZSM-5 at 500 °C using different catalyst-to-biomass (C/B) ratios.

C/B ratio (wt/wt)	11	14	17	21
Bio-oil organics (wt%, db)	18	18	17	15
Aqueous phase organics (wt%, db)	6	6	5	5
Reaction water (wt%, db)	24	25	25	25
Gases (wt%, db)	35	35	36	37
Char/coke (wt%, db)	16	16	17	18

the yields of other product fractions increased. However, as it can be seen in Table 4.6, the differences which were observed in the overall product distribution between the different C/B ratios were quite limited. Overall, the ratio between bio-oil and aqueous phase organics was higher compared to results of Publication III, which were obtained in a different reactor system. However, varying the C/B ratio between 11 and 21 did not significantly influence the relative distribution of organics between the two phases. Thus, increasing the catalyst circulation rate was clearly not a sufficient measure by itself to effectively eliminate the aqueous phase organics. The general trend of the products yields is similar to what has been otherwise obtained in the same reactor system [87]. Nevertheless, seeing as the changes brought on by increasing the C/B are quite limited, it is always possible other sources of experimental uncertainty can further influence the results. One potential issue is further deactivation of the catalyst due to e.g. contaminant deposition and thermal effects. Contaminant deposition should in this case remain limited, as the total amount of biomass that was processed in these experiments was only approximately 8 kg, whereas the catalyst inventory was in the range of 10-15 kg. The experiments were carried out using a single catalyst batch, i.e. the catalyst was not changed between experiments. Thus, it is possible that the chronological order of the experiments might also influence the results. The experiments were carried out in the following chronological sequence: 21, 11, 14, 17. Nevertheless, the overall similarity of these results with previously published data concerning the C/B ratio [87, 77] is a strong indication that the variation in the current results is, in fact, caused by operating at different C/B ratios.

The overall product distribution from CFP can also be examined on an elemental basis. The distribution of the main elemental constituents of biomass, i.e. carbon, hydrogen and oxygen can be derived from the over-
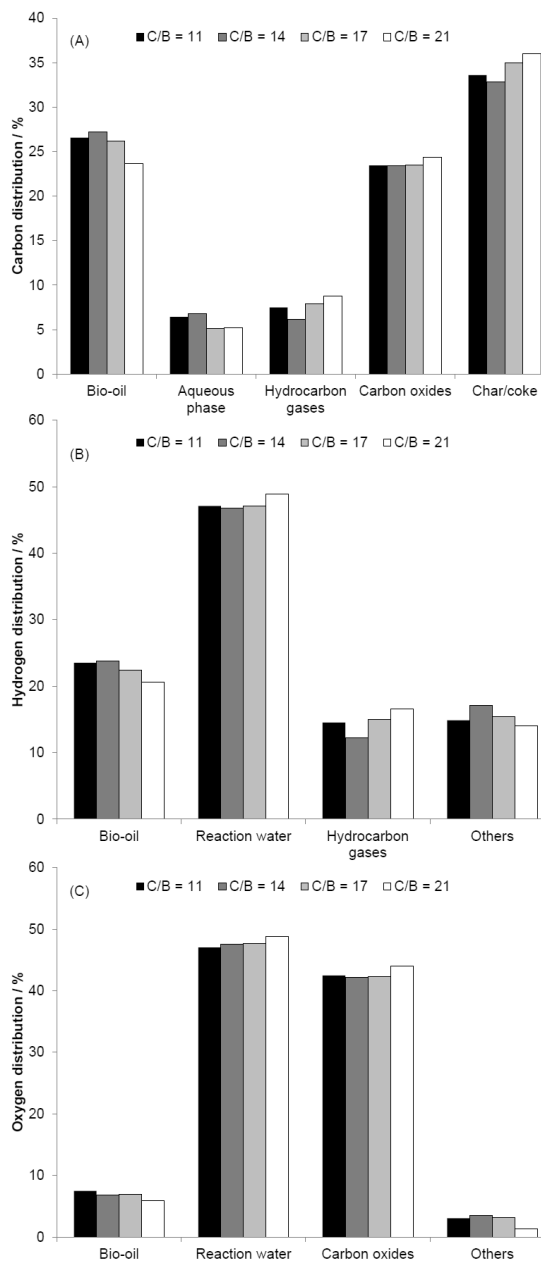
Figure 4.12. Distribution of carbon (A), hydrogen (B) and oxygen (C) in CFP at varying catalyst-to-biomass ratios. In sub-figures (B) and (C), the fraction 'Others' has been determined by difference (IV).

all product distribution coupled with various analytical data. Figure 4.12 shows how these three elements were distributed between liquid, gaseous and solid products at different C/B ratios. The data that is presented in each sub-figure depends on the analytical procedures which were car-

ried for each product fraction. For this reason, aqueous phase organics and char/coke are only included in the carbon distribution. In general, the carbon distribution followed a similar pattern as the overall product distribution of Table 4.6. At higher C/B ratios, less carbon was recovered in the form of organic liquids, whereas the proportion of gases and char/coke increased. The increase of the char/coke fraction should be mainly attributable to higher coke formation, as increasing the catalyst circulation rate would not be expected to influence the initial thermal stage of the CFP process. This situation bears a resemblance to the FCC (fluid catalytic cracking) process, where increasing the catalyst-to-oil ratio typically increases both conversion and coke yield [88]. The noncondensable gases represent another significant product fraction. While a part of these can be recycled back into the CFP process for fluidization purposes [63, 75], there will nevertheless be an excess of gases produced. Combustion is certainly the most straightforward approach, but alternative uses such as hydrogen generation [89] should be considered as well. While the carbon distribution is roughly equivalent to the overall product distribution, the distribution of hydrogen and oxygen clearly reflect the oxygen rejection that takes place during CFP. The hydrogen distribution in Figure 4.12B shows that almost of half of the hydrogen from the biomass was ultimately recovered in the form of water. The importance of these water producing dehydration reactions is also evident in the oxygen distribution of Figure 4.12C, which shows that water and carbon oxides both played a prominent role in the rejection of oxygen. Although approximately 90 % of the oxygen is present in products other than the actual bio-oil, these results still highlight the challenges of CFP that were extensively discussed in a recent review by Venderbosch [90]. The oxygen rejection is achieved at clear the expense of the carbon and the hydrogen. Because of this, these two desirable elements of the original biomass feedstock are distributed between different product types. This presents a clear contrast with the efficiency of TFP, where the majority of the biomass carbon will be contained in the bio-oil.

4.4.2 Effect of the C/B ratio on CFP bio-oil quality

Because of the limited differences which were observed in the CFP product distribution (see Table 4.6), one would expect that certain properties of the bio-oils, such as its elemental composition, would not differ greatly with changing C/B ratio. The bio-oil product analyses, which are dis-

Table 4.7. Physicochemical properties of the CFP bio-oils produced at different catalyst-to-biomass (C/B) ratios over a HZSM-5 catalyst at 500 °C.

C/B ratio (wt/wt)	11	14	17	21
Water (wt%)	6.7	5.7	5.7	5.5
Carbon (wt%, db)	73.3	74.9	74.2	75.1
Hydrogen (wt%, db)	7.2	7.4	7.2	7.4
Oxygen by difference (wt%, db)	19.5	17.7	18.6	17.5
H/C (mol/mol, db)	1.17	1.17	1.15	1.17
O/C (mol/mol, db)	0.20	0.18	0.19	0.17
Higher heating value (MJ/kg, db)	32.3	32.7	32.6	34.4
Lower heating value (MJ/kg, db)	30.6	30.9	30.9	32.6
Kinematic viscosity (cSt, 40 °C)	64	42	60	81
Density (kg/dm^3, 40 °C)	1.123	1.106	1.122	1.125
Total acid number (mg KOH/g)	31	26	25	24
Micro carbon residue (wt%)	19.7	17.3	18.5	20.8

played in Table 4.7, indeed show that in terms of water content, elemental composition and heating value, manipulation of the C/B ratio did not affect the bio-oil properties to a large extent. However, subtle changes which highlight the interdependency of certain bio-oil quality parameters could still be observed. For example, the increasing hydrophobic character of the bio-oils was evident in the relationship between the bio-oil elemental composition and water content, the correlation for which has been presented in Figure 2 of Publication IV.

Among the various characteristics of the bio-oils, viscosities exhibited the largest relative differences. In this instance, the differences cannot be explained by the water content, a factor which is known to affect the viscosity of TFP bio-oils [73]. Therefore, the underlying reason is likely to be differences in the organic composition of the bio-oils, as was also reported in Publication II. Both the absolute and relative differences in bio-oil viscosities varied with temperature. Figure 4.13 shows that the differences which were observed at 40 °C became insubstantial as the temperature was increased to 60 °C. On the other hand, if the bio-oil has to be handled at a temperature of e.g. 20 °C, the differences in viscosity become more pronounced. Interestingly enough, it was the bio-oil which was produced at the highest C/B ratio that exhibited the highest viscosity, and the highest micro carbon residue value. One would have assumed that supplying more catalyst into the process would have enhanced the
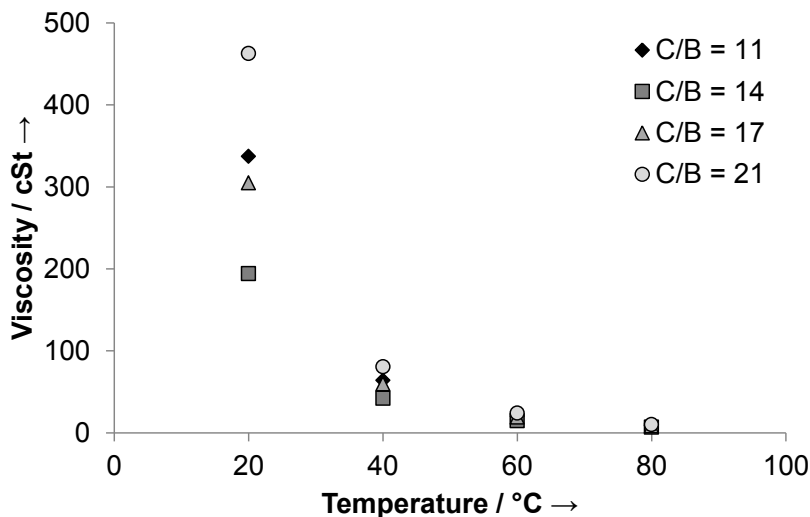
Figure 4.13. Kinematic viscosity of bio-oils produced at different catalyst-to-biomass (C/B) ratios as a function of temperature (IV).

cracking of pyrolysis vapors, thus leading to the formation of a less viscous and more volatile liquid product. However, the current results indicate that at C/B 21, the opposite had actually taken place.

The composition of the bio-oil also changed with variation of the C/B ratio. The composition of the volatile fraction, which was determined using GC-MS, exhibited only limited differences between the different C/B ratios. On a relative basis, all four bio-oils contained mostly molecules with an aromatic structure and limited amounts of carbohydrate decomposition products. The aromatic fraction included single-ring aromatic hydrocarbons, phenols with varying degrees and types of substitution, heavier lignin-derived compounds and polyaromatic hydrocarbons (PAH) with either two or three rings in their structure. Three ring PAH compounds (phenanthrene and pyrene) were, however, only observed at C/B 21. One observable trend in the results was decrease of single-ring aromatic hydrocarbons with increasing C/B ratio. These compounds are a known precursor for coke formation on zeolites [91], and thus it is possible that supplying more acid sites to the CFP process could lead to the further conversion of these desirable products into undesirable PAH compounds and coke.

In addition to the limited changes in the GC-detectable part of bio-oil, differences were also observed in the proportions of low molecular weight (LMW) and high molecular weight (HMW) lignin. As it can be seen in Figure 4.14, all four bio-oils contained more than 60 wt% of water-
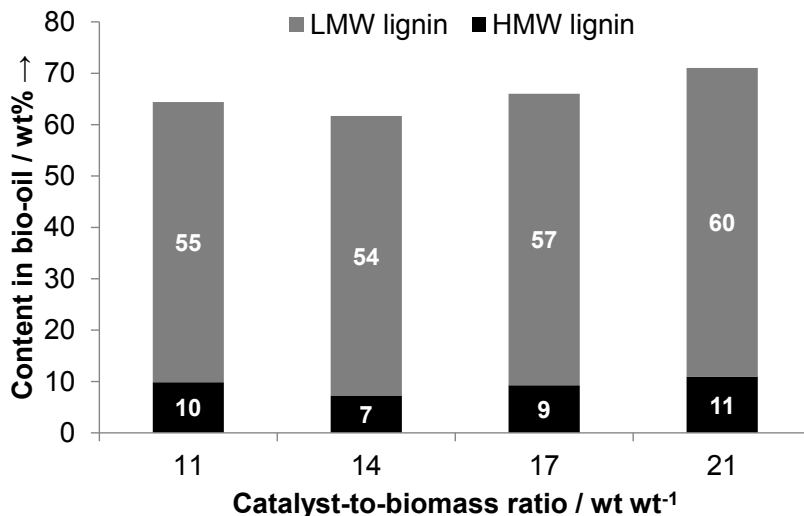
Figure 4.14. Low molecular weight (LMW) and high molecular weight (HMW) lignin content of bio-oils produced from Lignocell over HZSM-5 at 500 °C using different catalyst-to-biomass ratios (IV).

insoluble compounds. This, yet again, emphasizes the hydrophobic character of these bio-oils. Even though the bio-oil is in direct contact with aqueous phase during condensation and product recovery, only limited amounts of water and water-soluble compounds were transferred into the bio-oil. Changes in the HWM lignin content coincided with other observed changes in bio-oil properties; bio-oils with higher HMW lignin content also exhibited higher viscosities and MCR values. The HMW lignin fraction is the heaviest part of fast pyrolysis bio-oils, and it can clearly have a negative influence on certain physicochemical properties.

Apart from the influencing the properties of the fresh bio-oil, the chemical composition also affects the stability and aging characteristics. For TFP bio-oils, the compositional changes that take place during bio-oil aging manifest as an increase in viscosity. This change can be observed either during long-term storage, or alternatively by using an accelerated aging test where the bio-oil is kept at 80 °C for 24 h. For TFP bio-oils, which typically have a low initial viscosity due to their high water content, the relative increase in viscosity during accelerated aging is typically 70 % or more [92, 93]. The CFP bio-oils of Publication IV all presented favorable stability characteristics when subjected to the accelerated aging test. Figure 4.15 shows, that the relative increase in viscosity was 40 % or less, for all four bio-oils. Improved stability of CFP oils has also been reported previously [64, 48], but what exactly determines the stability of
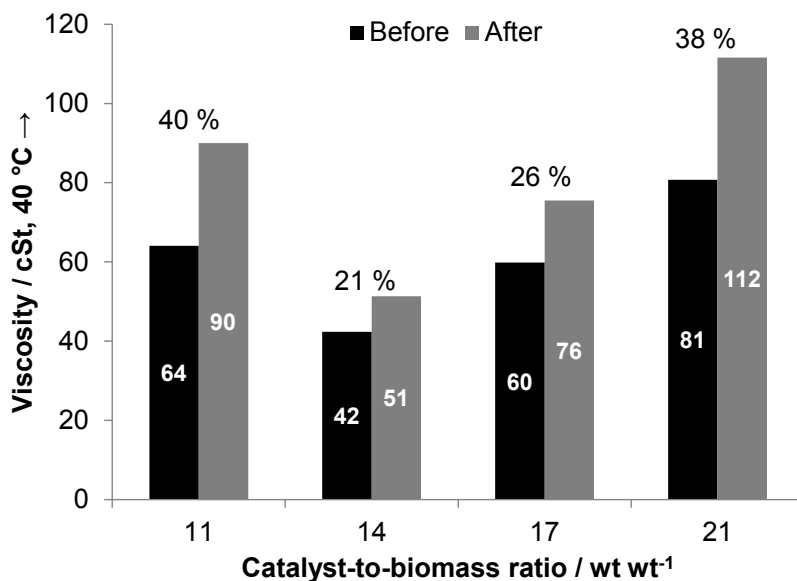
Figure 4.15. Bio-oil kinematic viscosity (cSt, 40 °C) before and after the accelerated aging test (24 h 40 °C), and the corresponding relative viscosity increase (IV).

a given CFP bio-oil is still unclear. Mante and Agblevor [48] presented a correlation between bio-oil storage stability and the relative amount of carbonyl-type carbons in ^{13}C NMR analysis. This approach would be in agreement with what has been previously observed for TFP bio-oils: carbonyl species react during bio-oil aging reactions, and the change in their concentration linearly correlates with physical parameters such as viscosity increase [93] and heat generation [94].

Because of the differences in their composition, it is likely that TFP bio-oils and CFP bio-oils age in a different manner. CFP bio-oils contain primarily water-insoluble compounds, whereas in typical TFP bio-oils this lignin-derived fraction accounts for a much smaller part of the overall oil [95]. It has been suggested that for bio-oils which contain a larger than typical amount of water-insoluble pyrolytic lignin, physical aggregation rather than polymerization would be the main reason behind the aging-related viscosity increase [96]. This conclusion was based on the observation that for aged lignin-rich bio-oils, the viscosity did not correlate with the average molecular weight. This indicated that the increase in viscosity was not caused by the formation of larger molecular structures - a relationship which has normally been valid for fast pyrolysis bio-oils [97]. The aggregation behavior of pyrolytic lignin has also been compared to petroleum asphaltenes [98]. Asphaltenes are the heaviest fraction of

Table 4.8. Properties of the CFP aqueous phase products obtained using different catalyst-to-biomass (C/B) ratios.

C/B ratio (wt/wt)	11	14	17	21
Water (wt%)	83.0	83.7	87.0	87.7
Organics (wt%)	17.0	16.3	13.0	12.3
Carbon (wt%)	8.1	8.6	6.7	6.6
Total acid number (mg KOH/g)	72	69	57	60
Micro carbon residue (wt%, db)	-	-	-	-

petroleum, and therefore the HMW lignin fraction would represent their analogous counterpart in fast pyrolysis bio-oils. Asphaltene concentration and temperature are factors that are known to affect the aggregation process [99, 100]. For the CFP bio-oils of Publication IV, the concentration of the HMW lignin fraction correlated with both the initial viscosity and the subsequent viscosity increase during accelerated aging. This indicated that the heaviest part of the lignin-rich CFP bio-oils also played a role in their aging process.

4.4.3 The challenge of the aqueous phase products

As it was stated earlier, attempting to limit the amount of aqueous phase organics was one of the focal points of this study. Although the yield of aqueous organics decreased slightly with increasing C/B ratio, the aqueous phase products, nevertheless, contained significant amounts of dissolved organics. Table 4.8 shows that the aqueous phase became more dilute with increasing C/B ratio. This result stems from the combined effect of two factors: decreasing yield of aqueous phase organics and increasing yield of water. Based on the TAN values of the aqueous phase, it was clearly more acidic than the actual bio-oil. Acetic acid was the single-most abundant compound that was identified in the aqueous phase, and its concentration ranged from 4.6 to 6.2 wt% (see Table 5 in Publication IV for details). This difference in the acidities of the bio-oil and the aqueous phase highlights the role phase separation in the CFP product recovery. On one hand, the yield of actual recoverable bio-oil decreases as organics are lost into the aqueous phase. Then again, certain water-soluble compounds, which preferentially enrich in the aqueous phase, are responsible for some of the adverse properties that are typically associated with TFP bio-oils. This includes e.g. the highly acidic nature of bio-oils, which stems primarily from the presence of carboxylic acids such acetic acid [101].

The amount of acetic acid that was present in the CFP aqueous phase products also emphasizes the stark difference between different reactor technologies and operational scales. Model compound studies have shown that acetic acid and other bio-oil oxygenates can be converted into aromatic hydrocarbons and olefins over an HZSM-5 catalyst [85, 102, 103]. When operating a fixed bed catalytic reactor, the vapors that are released upon heating/pyrolysis of a solid biomass, a liquid bio-oil or a single model compound are ensured to have good and uniform contact with the catalyst. This also results in rapid coke formation, which is why continuous catalyst regeneration is deemed to be an absolute necessity for CFP. Although CFB reactors fulfill the requirement of continuous catalyst regeneration, the results of Publication IV indicate that conversion of low molecular weight water-soluble oxygenates could still be improved. If one assumes that both thermal and catalytic reactions continue throughout the riser part of the CFB reactor, it is clear that the pyrolysis vapors which are released at the upper parts of the riser will have only a limited contact time with the catalyst. Further increasing the C/B ratio does not appear to be a viable option either, as operation at C/B 21 already affected the bio-oil quality in a negative fashion. Thus, it is clear that alternative valorization strategies would have to be implemented for the aqueous phase products.

One potential approach is to recycle the aqueous phase organics into the primary CFP reactor [104]. This would entail revolatilization of the aqueous phase, which, based on the fairly low micro carbon residue values that were presented in Table 4.8, could be in theory carried out with only limited charring. On the other hand, feeding the entire aqueous phase would introduce substantial amounts of water into the CFP reactor. Vaporizing this water would further increase the energy needs of the pyrolysis process, which is already endothermic to begin with. In general, fast pyrolysis can be operated as an autothermal process: the energy requirements of the pyrolysis process are met by combusting the char and a part of the non-condensable gases. The flow of heat transfer material, i.e. sand or catalyst, is manipulated to achieve the desired reaction temperature for pyrolysis. In Publication III, a C/B ratio of 7 was already adequate for maintaining a temperature of 520 °C for the CFP process. In contrast to this, the high C/B ratios which were reported in Publication IV were only achievable by utilizing a separate catalyst cooler, which made it possible to decouple the C/B ratio and the reactor temperature.

Feeding the aqueous phase into the CFP reactor would increase the overall energy requirement, but this would consequently allow operation at higher C/B ratios without the use of a separate catalyst cooler. Co-feeding steam into the CFP process has also been shown to have a positive effect. Mukarakate et al. [105] reported that the presence of steam in the CFP of pine over HZSM-5 increased the yield of single-ring aromatic hydrocarbons, olefins, and phenolic compounds, while inhibiting the formation of polyaromatic hydrocarbons and coke. Yang et al. [106] presented contrasting findings when they examined the effect of steam in cellulose CFP. They reported that steam caused irreversible changes to the ZSM-5 structure already at 500 °C, and that it also affected the chemistry of the CFP process. Both of these changes reflected negatively in the CFP product distribution, wherein the yield of aromatic hydrocarbons decreased.

4.4.4 Summary of findings

Increasing the C/B ratio did not have a profound effect on the CFP product distribution. The overall yield of organic liquids decreased with increasing C/B ratio, but the relative distribution of organics between the CFP bio-oil and the aqueous phase remained fairly constant. The differences in CFP bio-oil elemental composition were limited as well, whereas larger relative differences were observed for viscosity and MCR values. Overall, the results indicate that increasing the C/B ratio beyond a certain threshold resulted in the formation of heavier bio-oil without a clear improvement in the degree of oxygen removal. In all cases, the aqueous phase organics represented a significant product fraction, which would have to be further processed in an industrial process.

4.5 Further upgrading of CFP bio-oil via FCC co-processing

Even with its lower oxygen content and otherwise improved properties over TFP bio-oils, CFP bio-oil is, nevertheless, still an intermediate product. If the final desired product is hydrocarbons, the CFP bio-oil requires further upgrading. One alternative for this co-processing of bio-oil with petroleum distillates in existing oil refinery processes. These co-processing efforts have mainly focused on the FCC (fluid catalytic cracking) process, which utilizes an acidic zeolite catalyst to crack a heavy hydrocarbon feed such as vacuum gas oil (VGO) primarily into gasoline. The

Table 4.9. Properties of the co-processing experiment feedstocks.

Feedstock	VGO	Dry bio-oil	CFP oil	HDO oil
Water (wt%)	0.6	6.7	8.3	7.4
Carbon (wt%, db)	87.5	56.8	71.5	69.4
Hydrogen (wt%, db)	11.9	6.4	6.4	8.1
Nitrogen (wt%, db)	0.3	0.3	0.0	0.4
Oxygen by difference (wt%, db)	0.3	36.5	22.0	22.0
H/C_{eff} (mol/mol)	1.6	0.4	0.6	0.9
Micro carbon residue (wt%)	0.2	24.8	29.3	14.3

effect of introducing a fast pyrolysis bio-oil into the FCC process depends mainly on two factors: bio-oil concentration and bio-oil composition. Although recent findings [15] indicate that even crude fast pyrolysis bio-oil can be co-processed in a satisfactory manner as long as the concentration is kept low enough (5-10 wt% bio-oil), partial upgrading of the bio-oil prior to co-processing has been shown to have a beneficial effect. While the large majority of the co-processing work has focused on hydrotreated bio-oils, some examples of co-processing CFP bio-oils also exist [88, 107].

In Publication V, the co-processing characteristics of three bio-oils were evaluated in a MAT (micro activity test) reactor as 20 wt% blends with VGO. The main purpose of this was to compare the co-processability of two partially upgraded bio-oils with identical oxygen content, and a third thermally produced fast pyrolysis bio-oil with low water content. The CFP bio-oil that was used in these experiments corresponded to the one reported in Publication III. The other partially upgraded bio-oil was produced via HDO (hydrodeoxygenation) of a wood-based TFP bio-oil. Although the CFP and HDO oils contained the same amount of oxygen, Table 4.9 shows that there were, nevertheless, other clear differences between these feedstocks. The difference in the hydrogen content of these two oils clearly reflects the different chemistries which are involved CFP and HDO. In the former approach, hydrogen is removed from the pyrolysis vapors along with oxygen due to acid-catalyzed dehydration reactions. Although carbon is also rejected in a similar manner as CO, the resulting CFP bio-oils can still be considered as hydrogen deficient. In HDO, on the other hand, hydrogen is incorporated into the molecular structure of the bio-oil organics. These hydrogenation reactions are of course accompanied by actual HDO reactions, where oxygen is removed as water via reactions which involve the externally supplied hydrogen. The elemental composition of
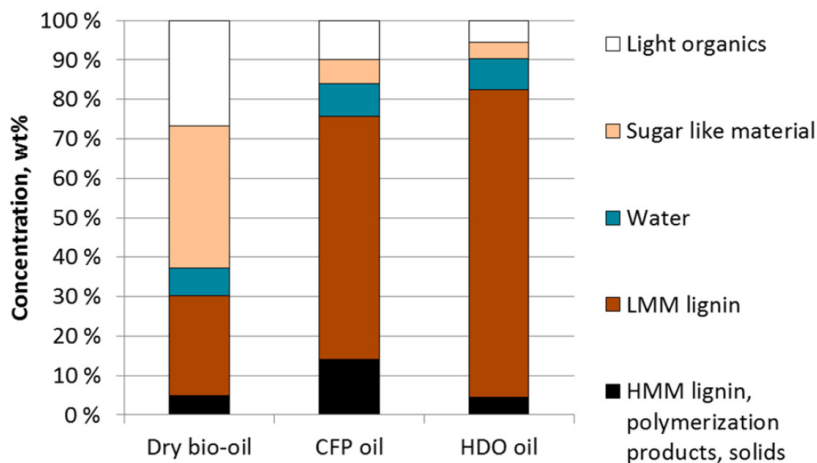
Figure 4.16. Chemical composition of the bio-oils used for co-processing experiments with VGO (V).

a given feedstock or a molecule can also be described using the effective molar hydrogen-to-carbon ratio H/C_{eff}, which is defined as [108]:

$$H/C_{\text{eff}} = \frac{H - 2O}{C}$$

The H/C_{eff} ratio describes how challenging it is to convert a given feedstock into hydrocarbons over a ZSM-5 catalyst. Processing of feedstocks with low H/C_{eff} values results in more coke formation, whereas lower amounts of desirable products are formed [109]. Although Y-zeolite, rather than ZSM-5, is the active component in FCC catalysts, the H/C_{eff} values given in Table 4.9 suggest that the processability of these feedstocks should improve in the order dry bio-oil < CFP oil < HDO oil. The high MCR value also suggests that the CFP bio-oil would be prone to cause fouling of the catalyst.

In addition to the different elemental composition, the two partially upgraded bio-oils also had differences in their chemical composition. As it can be seen in Figure 4.16, both CFP oil, and HDO oil contained mostly water-insoluble compounds. The CFP oil contained clearly more high molecular weight matter, which can partially explain the high MCR value in Table 4.9. Both CFP oil and HDO oil contained various lignin monomers and very few detectable carbohydrate degradation products (see Figure 3 in Publication V). The CFP oil also contained aromatic hydrocarbons, whereas cyclohexanols with varying degrees of substitution were present in the HDO oil. This indicates that the increased hydrogen content of the HDO oil can be accounted to hydrogenation of aromatic structures. In

contrast to these two partially upgraded bio-oils, polar oxygenates comprised more than 60 wt% of the dry bio-oil. Overall, the differences which were observed in the composition of the CFP and HDO oils indicated that the HDO oil should be easier to process over an acid catalyst.

In general, the differences observed in the co-processing of the three bio-oils were quite limited. A general trend that can, however, be seen in Table 4.10 is that more gases and coke were produced in the co-processing experiments compared to processing pure VGO. The overall conversion, which was defined as the summed up yields of dry gas, LPG, gasoline, and coke, remained low in all experiments, which, to a certain extent, limits the general applicability of these results. Nevertheless, some key differences could still be observed in the behavior of the different bio-oils. The difference in the coke yield confirmed the assumptions that were made based on the feedstock analyses. Figure 4.17 shows that the coke yield increased linearly as a function of the H/C_{eff} ratio. A similar correlation could also be attained between the coke yield and the feed MCR value (see Figure 7 in Publication V). Although the oxygen content of fast pyrolysis bio-oils and their upgraded versions is considered as a key quality metric, it is not by itself, an adequate indicator for co-processability over acid catalysts. While less oxygenated than typical fast pyrolysis bio-oils, CFP bio-oils possess a high degree of unsaturation. Aromatic molecules are known intermediates in the formation of coke on acidic zeolite at high reaction temperatures [91]. Therefore, it is quite logical that introducing a primarily aromatic feed such as this CFP bio-oil into the FCC process

Table 4.10. Product yields and conversion from co-processing of dry bio-oil, catalytic fast pyrolysis bio-oil, and hydrotreated bio-oil as 20 wt% blends with vacuum gas oil; T = 482 °C, C/O = 3, WHSV = 6.4 h^{-1}. The conversion is defined as the summed up yields of dry gas, LPG, gasoline, and coke.

		VGO	VGO/dry BO	VGO/CFP oil	VGO/HDO oil
Dry gas (wt%)	H_2, CO_x, C_1-C_2	2	4	3	3
LPG (wt%)	C_3-C_4	8	9	9	9
Gasoline (wt%)	40-221 °C	16	17	19	18
LCO (wt%)	221-370 °C	15	16	17	16
HCO (wt%)	370-425 °C	8	6	6	7
Slurry oil (wt%)	> 425 °C	46	31	32	35
Coke (wt%)		5	10	10	8
Conversion (%)		30	41	40	38
Mass balance (wt%)		100	93	96	96

LPG = liquid petroleum gas, LCO = light cycle oil, HCO = heavy cycle oil
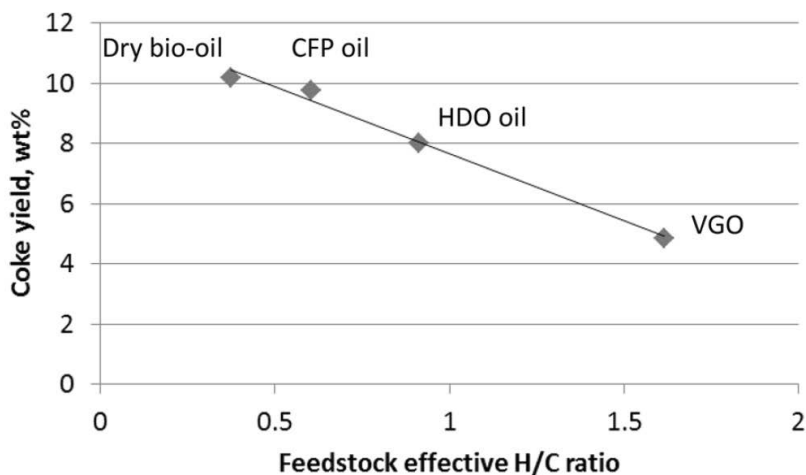
Figure 4.17. Coke yield in FCC co-processing as a function of feedstock undiluted H/C_{eff} ratio (V).

would result in higher coke formation compared to a hydrotreated bio-oil with similar oxygen content. Subjecting the CFP bio-oil to a subsequent acid-catalyzed cracking process is, in a way, comparable to increasing the C/B ratio of the CFP process, as was done in Publication IV. An excessive amount of acid sites coupled with aromatic compounds eventually lead to an eventual decrease in the bio-oil quality.

4.6 Putting the results of this thesis into perspective

4.6.1 How the results of this thesis reflect the story of KiOR

As it was mentioned in the Introduction of this thesis, there was already one major commercial undertaking for catalytic fast pyrolysis of biomass. This was, of course, a reference to the company KiOR, whose foray into the field of advanced lignocellulosic biofuels terminated in less than stellar fashion [21]. The original business model of KiOR entailed the production of CFP biocrude, which would then be subsequently upgraded in existing oil refineries. When the characteristics of the biocrude did not meet specifications of the original refining partners, KiOR had to resort to carrying out the hydrotreating themselves. The resulting drop-in hydrocarbon blendstock was to be supplied to customers.

Recent reports [110, 111, 112] have revealed that the challenges faced by this company were not limited to only technical ones; various manage-

rial issues also seem to have played a prominent part in bringing about the eventual downfall of KiOR. From the perspective of this thesis, it is, however, more pertinent to examine the technical challenges that were involved in this process. The experimental work in this thesis was carried out during a time period when the development work at KiOR was already far underway. While the recent reports also outline some of the major technical challenges, patent publications by KiOR can also provide an enhanced understanding of the issues that the engineers and researchers are trying to solve. When considering the results of this thesis, two substantial challenges that have been observed for CFP are the aqueous phase organics, and permanent catalyst deactivation. Both of these are also themes which appear in KiOR's patent publications. These two are by no means the only technical challenges encountered by KiOR, but from the viewpoint of this thesis, they are the ones which warrant the most attention.

The experimental results which were reported in Publications III and IV clearly showed that in CFP, the aqueous phase organics can represent a considerable part of the overall organic liquid yield. While it is easy to consider this as a direct loss of recoverable bio-oil, one should bear in mind the compositional differences between the bio-oil and the aqueous phase products. Even if it was possible to conveniently recover the dissolved organics, they would not yield similar products as the actual bio-oil in a subsequent upgrading step. Nevertheless, being able to produce added value from the aqueous phase would potentially improve the profitability of the overall CFP process. Examples related to the processing and utilization of the aqueous phase include:

1. Recovery of organics using a solid sorbent material [113]

2. Condensation of water-soluble organics into water-insoluble tar by using a strong mineral acid [114]

3. Recovery of organics using liquid-liquid extraction with a water-insoluble organic solvent and subsequent evaporation of the solvent [115]

4. Regeneration of contaminated CFP catalyst by dissolution of metal oxides [83]

The last item on the list is a curious combination, as it actually attempts to address both issues: aqueous phase product and permanent catalyst

deactivation due to biomass-derived contaminants. At this stage, it is not necessary to start examining the individual merits and shortcoming of each of the aforementioned patent applications. Nevertheless, it is clear that the findings in this thesis coincide with issues which have also been observed at larger scale.

When the work in this thesis originally began, the available literature of CFP to a large extent focused on promoting the beneficial effect of catalyst on bio-oil quality. However, more recently, the limitations and challenges that are involved with this technology have been gaining more attention [90, 60, 61]. In particular, the effect of biomass-derived inorganic contaminants on the catalyst lifetime, and how this affects the overall viability of the CFP process, has been identified as a key issue. This can be countered by constant catalyst removal and addition, as is done in commercial FCC units. However, the rate of catalyst replacement can have a substantial effect on the economics of the process. Numbers from KiOR suggest daily catalyst replacement rates of up to 9 % [112]. A recent techno-economic analysis paper states that with a catalyst cost 6500 USD per metric ton, increasing the daily replacement rate from 2 to 8 % would increase bio-oil production costs by 27 % [80]. The required rate of catalyst replacement would also depend on the overall catalyst inventory of the CFP unit, the contaminant content of the feedstock, and on the extent of contaminant deposition on the catalyst.

Overall, the issue of permanent catalyst deactivation can be seen as a strong incentive for the development and utilization of less expensive catalysts. An added benefit would be if these catalysts were less sensitive than zeolites to biomass-derived inorganic contaminants. One interesting example is red mud, a by-product from the production of aluminium oxide. It has been used as a CFP catalyst [116], and the resulting bio-oil has been subsequently upgraded using single-stage catalytic hydrotreatment [117], an approach that is not viable for thermally produced fast pyrolysis bio-oils.

4.6.2 Examining the yield versus quality interdependency

While various technical details and experimental results from KiOR are available in patent publications, reliable yield data and bio-oil quality characteristics, however, are not. Thus, when it comes to direct comparison of experimental results, journal publications offer the most convenient source of data. As it has been shown in this thesis and various
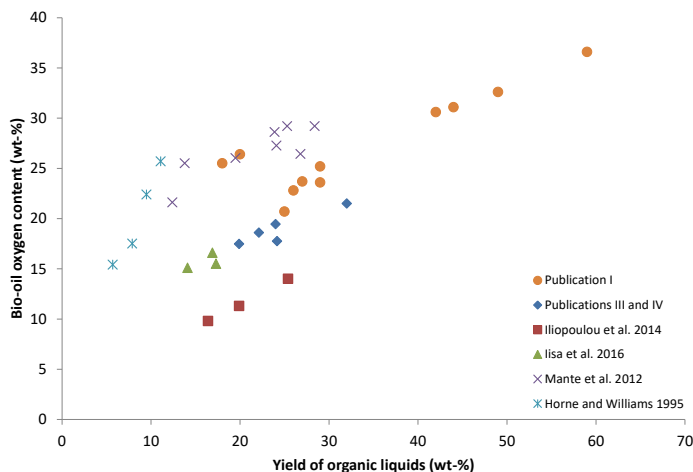
Figure 4.18. Yield of organic liquids / reported yield of bio-oil versus oxygen content of bio-oil; data adapted from Publications I, III and IV, and references [47, 118, 119, 53].

other publications, the use of catalysts affects several different properties of bio-oils. However, seeing as the concept of CFP in its current form essentially revolves around the removal of oxygen, it is fitting to examine how the bio-oils produced in this thesis compare against their counterparts in literature. Figure 4.18 shows that in terms of organics yield and bio-oil oxygen content, the majority of the results in this thesis falls into a similar range as many other studies. One should note that the x-axis of Figure 4.18 represents the overall yield of organic liquids, not only the bio-oil fraction. This approach was selected purely on the basis of enabling easier comparison of results, as in many instances, no differentiation has been made between the yield of bio-oil and aqueous phase organic liquids. The importance of this distinction is not only academic, as it has also been implied that the some of the yield estimates provided by KiOR might have been inflated due to this same reason [111]. This figure also serves a clear reminder of the inherent limitations that acidic zeolites have in removing oxygen from pyrolysis vapors - a further decrease in bio-oil oxygen content is always associated with a consequent decrease in yield. Although there are clear differences between the individual data sources of 4.18, the direction of the overall trend leaves little room for interpretation.

5. Concluding remarks

The results which have been presented in this thesis clearly show that CFP with an acidic HZSM-5 zeolite catalyst can be used for producing partially upgraded bio-oils. Because of the oxygen rejection process that takes place in CFP, the resulting bio-oils are less oxygenated than conventional TFP bio-oils. This shift in the elemental composition is accompanied by an array of other changes in both physical properties and chemical composition of the bio-oil. Although a large part of CFP research revolves around the production of aromatic hydrocarbons, the actual CFP bio-oils which were produced in this thesis were still complex mixtures. One factor that clearly sets CFP bio-oils apart from TFP bio-oils is the increased hydrophobicity of the former. This, coupled with increased water production due to catalytic dehydration reactions, results in the formation of a two-phase liquid product. Thus, in addition to the hydrophobic bio-oil, a separate aqueous phase with dissolved organics is also recovered.

BFB reactors are widely employed for fast pyrolysis research at bench-scale, but their direct usability for CFP is limited due to rapid coke formation and the consequent catalyst deactivation that follows it. Stable long-term operation would necessitate the use of continuous catalyst removal and addition, a functionality that is absent in most BFB reactors which have been designed for research purposes. Alternatively, the activity of the catalyst can be maintained by periodically stopping the biomass feeding and regenerating the catalyst via a oxidative treatment. Such an approach makes it possible to mimic the operational characteristics of a reactor with continuous catalyst regeneration. Although this option is still viable for limited research purposes, it is far from being practical for continuous large-scale operation. Seeing as catalyst deactivation effectively limits the practicality of maintaining constant product quality in BFB reactors operating with a fixed catalyst batch, it stands to rea-

son that a reactor type which can effectively and conveniently negate the effect of coke formation is particularly well suited for biomass CFP.

Carrying out CFP in a CFB reactor with continuous catalyst regeneration made it possible to maintain nearly constant bio-oil quality in terms of elemental composition for a time period of four days. Although reversible deactivation due to coke formation was no longer a key concern, signs of permanent catalyst deactivation were clearly evident. This indicated that subjecting the HZSM-5 catalyst to numerous reaction-regeneration cycles under severe process conditions resulted in both structural changes and deposition of biomass-derived contaminants. Based on these observations, conventional catalysts such as zeolites will have a limited lifetime under CFP conditions. A continuously operated CFP process would therefore require constant catalyst removal and addition, which would result in the formation of an equilibrated catalyst mixture that contains both fresh and aged catalyst.

In addition to permanent catalyst deactivation, another substantial challenge that was observed was the large amount of dissolved organics in the aqueous phase. As such, these organics possess only limited value and usability. Thus, limiting the formation of water-soluble oxygenates within the CFP process itself would in turn simplify the subsequent downstream processing of the liquid products. It was envisioned that supplying more catalyst to the CFP process could enhance the conversion of the oxygenate compounds which would otherwise enrich in the aqueous phase. Ultimately, increasing the C/B ratio in a CFB reactor did not significantly affect the relative distribution of organic liquids between the bio-oil and the aqueous phase. It did, however, have an impact on the overall product distribution as well as on the characteristics of the liquid products. Thus, the C/B ratio is clearly another important variable for controlling tuning the CFP process. One should also bear in mind that the C/B ratio is directly connected to heat balance of the CFB reactor system, and cannot therefore be freely manipulated without catalyst cooling.

While the results of this thesis have managed to provide answers to the research questions that were posed in Section 1.2, it has at the same time generated a new set of questions that would be worthwhile to pursue in the future. One definite knowledge gap concerns the effect of biomass-derived contaminants on the catalyst. This is a clear challenge for in situ CFP in particular, as regeneration of the catalyst in the presence of char exposes the catalyst to the contaminants at elevated temperatures

of 650 to 700 °C. While the effect of this phenomenon could be examined by carrying out extended CFP experiments with a single catalyst batch, it would make more sense to develop methods of artificially deactivating the catalyst. If one considers that catalyst regeneration is the most likely instance for contaminant deposition to take place, then simply combusting char in the presence of the CFP catalyst could serve as a straightforward way of contaminating the catalyst without having to carry out actual CFP experiments.

Although most published studies focus primarily on the bio-oil product, the issue of the aqueous phase products is also an aspect that cannot simply be overlooked. First of all, establishing a reporting convention which clearly differentiates between the yield of recoverable bio-oil and aqueous phase organics would decrease the level of ambiguity when examining CFP product distributions. As it was shown in Publications III and IV, the aqueous phase organics can represent a significant product fraction, and therefore their further processing should be examined in more detail as well.

Very little is also known about the upgrading, and in particular the catalytic hydrotreating of CFP bio-oils. On the path to transportation fuels, the CFP bio-oil is still an intermediate product, and any perceived improvement in its quality has to be ultimately verified through further upgrading experiments. Recent results from CFP bio-oil hydrotreating experiments indicate that this material is indeed less challenging to upgrade compared to TFP bio-oils [120, 121, 117]. Although encouraging results have been obtained even while using single-stage upgrading, a clearer understanding of what actually constitutes a readily upgradable CFP bio-oil is still required.

When considering the different steps which are involved in converting solid biomass into liquid fuels via CFP, the availability of experimental data becomes more sparse as one moves downstream in the overall processing scheme. This, in a sense, also reflects how challenging in practice carrying out different types of experiments is. For the CFP step, publications involving experimental work with analytical pyrolysis or fixed-bed reactors are more common compared to the use of fluidized bed reactors. While the former options can certainly be useful for e.g. studying process fundamentals and screening catalysts, they do have the distinct downside of producing very limited amounts of bio-oil, or in the case of analytical pyrolysis, no bio-oil at all. Whether it is carried out in batch or con-

tinuous reactor systems, further upgrading via hydrotreatment requires larger quantities of bio-oil. This, coupled with the limited bio-oil yield in CFP and the need to address the issue of reversible catalyst deactivation, means that producing bio-oil quantities that can be considered relevant for upgrading is clearly a practical challenge. One should also bear in mind that the actual upgrading of the bio-oil is still a considerable challenge in itself. So far, the overall direction of CFP research has clearly focused on the pyrolysis process itself, whereas knowledge concerning the further upgrading of the products is limited. Since the applicability of the CFP process is to a certain extent based on the premise of better bio-oil upgradability, more research on this particular aspect is clearly warranted.

While it is possible to further optimize the CFP process, there is no avoiding the yield decrease that is associated with oxygen removal. The carbon and hydrogen which are removed from the pyrolysis vapors in the form of carbon oxides and water cannot be reincorporated back into the bio-oil in a realistic way. The bio-oil product contains primarily lignin-derived material along with some aromatic hydrocarbons, whereas carbohydrate degradation products are found in the aqueous phase. All in all, CFP with acidic zeolites can be seen as an approach that lacks a certain finesse - the decrease in the bio-oil yield is ultimately very large compared to the improvement in bio-oil quality. If one considers the primary purpose of pyrolysis to be the production of a liquid intermediate that can be further upgraded into hydrocarbons, there should also be milder options than acidic zeolites for achieving the desired results. Upon hydrotreating of bio-oil, the majority of liquid hydrocarbon products contains ring structures, which originate from lignin. Thus, catalysts which would e.g. depolymerize the lignin fraction into a more readily processable form while avoiding excessive coke formation and extensive decomposition of the carbohydrate fraction would be worth pursuing. This, yet again, raises the question of what to do with the carbohydrate decomposition products. Whether dealing with pyrolysis vapors or already condensed bio-oil, the sheer chemical complexity of these mixtures dictates that a single process or catalyst cannot provide an all-encompassing solution. Thus, the search for technically and economically viable ways of producing transportation fuels via fast pyrolysis still continues.

References

[1] BP Energy Outlook 2035, http://www.bp.com/en/global/corporate/energy-economics/energy-outlook-2035.html, accessed 29 January 2016.

[2] Fortum invests EUR 20 million to build the world's first industrial-scale integrated bio-oil plant, http://www.fortum.com/en/mediaroom/Pages/fortum-invests-eur-20-million-to-build-the-worlds-first-industrial-scale-integrated-bio-oil-plant.aspx (2012), accessed 7 March 2016.

[3] btg-btl: Empyro project, http://www.btg-btl.com/en/company/projects/empyro (2015), accessed 7 March 2016.

[4] Olden days, golden days, and golden gripes, http://www.biofuelsdigest.com/bdigest/2016/01/27/olden-days-golden-days-and-golden-gripes/, accessed 29 January 2016.

[5] Scott, D. S., Piskorz, J., The flash pyrolysis of aspen-poplar wood, *Can. J. Chem. Eng.* **60** (1982) 666–674.

[6] Scott, D. S., Piskorz, J., Radlein, D., Liquid products from the continuous flash pyrolysis of biomass, *Ind. Eng. Chem. Process Des. Dev.* **24** (1985) 581–588.

[7] Lehto, J., Oasmaa, A., Solantausta, Y., Kytö, M., Chiaramonti, D., Review of fuel oil quality and combustion of fast pyrolysis bio-oils from lignocellulosic biomass, *Appl. Energy* **116** (2014) 178 – 190.

[8] Oasmaa, A., Kuoppala, E., Solantausta, Y., Fast pyrolysis of forestry residue. 2. physicochemical composition of product liquid, *Energy Fuels* **17** (2003) 433–443.

[9] Solantausta, Y., Oasmaa, A., Sipilä, K., Lindfors, C., Lehto, J., Autio, J., Jokela, P., Alin, J., Heiskanen, J., Bio-oil Production from Biomass: Steps toward Demonstration, *Energy Fuels* **26** (2012) 233–240.

[10] Elliott, D., Baker, E., Process for upgrading biomass pyrolyzates (1989), US Patent 4,795,841.

[11] Elliott, D. C., Historical Developments in Hydroprocessing Bio-oils, *Energy Fuels* **21** (2007) 1792–1815.

[12] Baldauf, W., Balfanz, U., Rupp, M., Upgrading of flash pyrolysis oil and utilization in refineries, *Biomass Bioenergy* **7** (1994) 237 – 244.

[13] Samolada, M., Baldauf, W., Vasalos, I., Production of a bio-gasoline by upgrading biomass flash pyrolysis liquids via hydrogen processing and catalytic cracking, *Fuel* **77** (1998) 1667 – 1675.

[14] Fogassy, G., Thegarid, N., Schuurman, Y., Mirodatos, C., The fate of bio-carbon in FCC co-processing products, *Green Chem.* **14** (2012) 1367–1371.

[15] de Rezende Pinho, A., de Almeida, M. B., Mendes, F. L., Ximenes, V. L., Casavechia, L. C., Co-processing raw bio-oil and gasoil in an FCC Unit, *Fuel Process. Technol.* **131** (2015) 159 – 166.

[16] Scott, D. S., Piskorz, J., Bergougnou, M. A., Graham, R., Overend, R. P., The role of temperature in the fast pyrolysis of cellulose and wood, *Ind. Eng. Chem. Res.* **27** (1988) 8–15.

[17] Garcia-Perez, M., Wang, X. S., Shen, J., Rhodes, M. J., Tian, F., Lee, W.-J., Wu, H., Li, C.-Z., Fast Pyrolysis of Oil Mallee Woody Biomass: Effect of Temperature on the Yield and Quality of Pyrolysis Products, *Ind. Eng. Chem. Res.* **47** (2008) 1846–1854.

[18] Bartholomew, C. H., Mechanisms of catalyst deactivation, *Appl. Catal., A* **212** (2001) 17–60.

[19] Joly, J.-F., Sanchez, E., Surla, K., Selection of Process and Mode of Operation. in *Deactivation and Regeneration of Zeolite Catalysts*, eds. M. Guisnet, F. Ramôa Ribeiro, Imperial College Press, London 2011, pp. 173–193.

[20] Garcia-Perez, M., Chaala, A., Pakdel, H., Kretschmer, D., Roy, C., Characterization of bio-oils in chemical families, *Biomass Bioenergy* **31** (2007) 222–242.

[21] A biofuel dream gone bad, http://fortune.com/kior-vinod-khosla-cleantech/, accessed 27 January 2016.

[22] Bridgwater, A., Review of fast pyrolysis of biomass and product upgrading, *Biomass Bioenergy* **38** (2012) 68 – 94.

[23] IEA Bioenergy Task 34 for Direct Thermochemical Liquefaction, http://www.pyne.co.uk/, accessed 29 January 2016.

[24] Fahim, M., Al-Sahhaf, T., Elkilani, A., *Fundamentals of Petroleum Refining*, Elsevier Science 2009.

[25] Flagan, R. C., Seinfeld, J. H., *Fundamentals of Air Pollution Engineering*, 1 edition, Prentice-Hall, Inc., Englewood Cliffs, New Jersey 1988, 542 p.

[26] Lappas, A. A., Samolada, M. C., Iatridis, D. K., Voutetakis, S. S., Vasalos, I. A., Biomass pyrolysis in a circulating fluid bed reactor for the production of fuels and chemicals, *Fuel* **81** (2002) 2087 – 2095.

[27] Aho, A., Kumar, N., Eränen, K., Salmi, T., Hupa, M., Murzin, D. Y., Catalytic Pyrolysis of Biomass in a Fluidized Bed Reactor: Influence of the Acidity of H-Beta Zeolite, *Process Saf. Environ. Prot.* **85** (2007) 473 – 480.

[28] Williams, P. T., Horne, P. A., The influence of catalyst type on the composition of upgraded biomass pyrolysis oils, *J. Anal. Appl. Pyrolysis* **31** (1995) 39 – 61.

[29] Diebold, J., Scahill, J., Biomass to gasoline (BTG): Upgrading pyrolysis vapors to aromatic gasoline with zeolite catalysis at atmospheric pressure., *ACS Division of Fuel Chemistry, Preprints* **32** (1987) 297–306.

[30] Agblevor, F. A., Beis, S., Mante, O., Abdoulmoumine, N., Fractional Catalytic Pyrolysis of Hybrid Poplar Wood, *Ind. Eng. Chem. Res.* **49** (2010) 3533–3538.

[31] Zhang, H., Xiao, R., Huang, H., Xiao, G., Comparison of non-catalytic and catalytic fast pyrolysis of corncob in a fluidized bed reactor, *Bioresour. Technol.* **100** (2009) 1428 – 1434.

[32] Chang, C. D., Silvestri, A. J., The conversion of methanol and other O-compounds to hydrocarbons over zeolite catalysts, *J. Catal.* **47** (1977) 249 – 259.

[33] Jae, J., Tompsett, G. A., Foster, A. J., Hammond, K. D., Auerbach, S. M., Lobo, R. F., Huber, G. W., Investigation into the shape selectivity of zeolite catalysts for biomass conversion, *J. Catal.* **279** (2011) 257 – 268.

[34] Mihalcik, D. J., Mullen, C. A., Boateng, A. A., Screening acidic zeolites for catalytic fast pyrolysis of biomass and its components, *J. Anal. Appl. Pyrolysis* **92** (2011) 224 – 232.

[35] Carlson, T., Tompsett, G., Conner, W., Huber, G., Aromatic Production from Catalytic Fast Pyrolysis of Biomass-Derived Feedstocks, *Top. Catal.* **52** (2009) 241–252.

[36] Olsbye, U., Bjørgen, M., Svelle, S., Lillerud, K.-P., Kolboe, S., Mechanistic insight into the methanol-to-hydrocarbons reaction, *Catal. Today* **106** (2005) 108 – 111.

[37] Haw, J. F., Zeolite acid strength and reaction mechanisms in catalysis, *Phys. Chem. Chem. Phys.* **4** (2002) 5431–5441.

[38] Mukarakate, C., Zhang, X., Stanton, A. R., Robichaud, D. J., Ciesielski, P. N., Malhotra, K., Donohoe, B. S., Gjersing, E., Evans, R. J., Heroux, D. S., Richards, R., Iisa, K., Nimlos, M. R., Real-time monitoring of the deactivation of HZSM-5 during upgrading of pine pyrolysis vapors, *Green Chem.* **16** (2014) 1444–1461.

[39] Carlson, T., Jae, J., Huber, G., Mechanistic Insights from Isotopic Studies of Glucose Conversion to Aromatics Over ZSM-5, *ChemCatChem* **1** (2009) 107–110.

[40] Carlson, T. R., Jae, J., Lin, Y.-C., Tompsett, G. A., Huber, G. W., Catalytic fast pyrolysis of glucose with HZSM-5: The combined homogeneous and heterogeneous reactions, *J. Catal.* **270** (2010) 110 – 124.

[41] Zhang, H., Carlson, T. R., Xiao, R., Huber, G. W., Catalytic fast pyrolysis of wood and alcohol mixtures in a fluidized bed reactor, *Green Chem.* **14** (2012) 98–110.

[42] Nowakowski, D., Bridgwater, A., Elliott, D., Meier, D., de Wild, P., Lignin fast pyrolysis: Results from an international collaboration, *J. Anal. Appl. Pyrolysis* **88** (2010) 53 – 72.

[43] Graça, I., Comparot, J.-D., Laforge, S., Magnoux, P., Lopes, J. M., Ribeiro, M. F., Ramôa Ribeiro, F., Influence of Phenol Addition on the H-ZSM-5 Zeolite Catalytic Properties during Methylcyclohexane Transformation, *Energy Fuels* **23** (2009) 4224–4230.

[44] Mullen, C. A., Boateng, A. A., Catalytic pyrolysis-GC/MS of lignin from several sources, *Fuel Process. Technol.* **91** (2010) 1446 – 1458.

[45] Wang, K., Kim, K. H., Brown, R. C., Catalytic pyrolysis of individual components of lignocellulosic biomass, *Green Chem.* **16** (2014) 727–735.

[46] Zhao, Y., Deng, L., Liao, B., Fu, Y., Guo, Q.-X., Aromatics Production via Catalytic Pyrolysis of Pyrolytic Lignins from Bio-Oil, *Energy Fuels* **24** (2010) 5735–5740.

[47] Iliopoulou, E. F., Stefanidis, S., Kalogiannis, K., Psarras, A. C., Delimitis, A., Triantafyllidis, K. S., Lappas, A. A., Pilot-scale validation of Co-ZSM-5 catalyst performance in the catalytic upgrading of biomass pyrolysis vapours, *Green Chem.* **16** (2014) 662–674.

[48] Mante, O. D., Agblevor, F. A., Catalytic pyrolysis for the production of refinery-ready biocrude oils from six different biomass sources, *Green Chem.* **16** (2014) 3364–3377.

[49] Aho, A., Kumar, N., Eränen, K., Salmi, T., Hupa, M., Murzin, D. Y., Catalytic pyrolysis of woody biomass in a fluidized bed reactor: Influence of the zeolite structure, *Fuel* **87** (2008) 2493 – 2501.

[50] Guisnet, M., Costa, L., Ribeiro, F. R., Prevention of zeolite deactivation by coking, *J. Mol. Catal. A: Chem.* **305** (2009) 69 – 83.

[51] Wan, S., Waters, C., Stevens, A., Gumidyala, A., Jentoft, R., Lobban, L., Resasco, D., Mallinson, R., Crossley, S., Decoupling HZSM-5 Catalyst Activity from Deactivation during Upgrading of Pyrolysis Oil Vapors, *ChemSusChem* **8** (2015) 552–559.

[52] Engtrakul, C., Mukarakate, C., Starace, A. K., Magrini, K. A., Rogers, A. K., Yung, M. M., Effect of ZSM-5 acidity on aromatic product selectivity during upgrading of pine pyrolysis vapors, *Catal. Today* .

[53] Horne, P. A., Williams, P. T., The effect of zeolite ZSM-5 catalyst deactivation during the upgrading of biomass-derived pyrolysis vapours, *J. Anal. Appl. Pyrolysis* **34** (1995) 65 – 85.

[54] Mullen, C. A., Boateng, A. A., Mihalcik, D. J., Goldberg, N. M., Catalytic Fast Pyrolysis of White Oak Wood in a Bubbling Fluidized Bed, *Energy Fuels* **25** (2011) 5444–5451.

[55] Cerqueira, H., Caeiro, G., Costa, L., Ribeiro, F. R., Deactivation of FCC catalysts, *J. Mol. Catal. A: Chem.* **292** (2008) 1 – 13.

[56] Escobar, A., Pereira, M., Pimenta, R., Lau, L., Cerqueira, H., Interaction between Ni and V with USHY and rare earth HY zeolite during hydrothermal deactivation, *Appl. Catal., A* **286** (2005) 196–201.

[57] Wise, J., Vietor, D., Provin, T., Capareda, S., Munster, C., Boateng, A., Mineral nutrient recovery from pyrolysis systems, *Environ. Prog. Sustainable Energy* **31** (2012) 251–255.

[58] Mullen, C. A., Boateng, A. A., Accumulation of Inorganic Impurities on HZSM-5 Zeolites during Catalytic Fast Pyrolysis of Switchgrass, *Ind. Eng. Chem. Res.* **52** (2013) 17156–17161.

[59] Yildiz, G., Ronsse, F., Venderbosch, R., van Duren, R., Kersten, S. R., Prins, W., Effect of biomass ash in catalytic fast pyrolysis of pine wood, *Appl. Catal., B* **168-169** (2015) 203–211.

[60] Yildiz, G., Ronsse, F., van Duren, R., Prins, W., Challenges in the design and operation of processes for catalytic fast pyrolysis of woody biomass, *Renewable Sustainable Energy Rev.* **57** (2016) 1596 – 1610.

[61] Stefanidis, S. D., Kalogiannis, K. G., Pilavachi, P. A., Fougret, C. M., Jordan, E., Lappas, A. A., Catalyst hydrothermal deactivation and metal contamination during the in situ catalytic pyrolysis of biomass, *Catal. Sci. Technol.* **6** (2016) 2807–2819.

[62] Wang, K., Zhang, J., Shanks, B. H., Brown, R. C., The deleterious effect of inorganic salts on hydrocarbon yields from catalytic pyrolysis of lignocellulosic biomass and its mitigation, *Appl. Energy* **148** (2015) 115–120.

[63] Mante, O. D., Agblevor, F., Oyama, S., McClung, R., The influence of recycling non-condensable gases in the fractional catalytic pyrolysis of biomass, *Bioresour. Technol.* **111** (2012) 482 – 490.

[64] Agblevor, F. A., Mante, O., Abdoulmoumine, N., McClung, R., Production of Stable Biomass Pyrolysis Oils Using Fractional Catalytic Pyrolysis, *Energy Fuels* **24** (2010) 4087–4089.

[65] Mante, O., Agblevor, F., McClung, R., Fluid catalytic cracking of biomass pyrolysis vapors, *Biomass Conv. Bioref.* **1** (2011) 189–201.

[66] Mante, O. D., Agblevor, F. A., Catalytic conversion of biomass to biosyncrude oil, *Biomass Conv. Bioref.* **1** (2011) 203–215.

[67] Meyers, R., *Handbook of Petroleum Refining Processes*, McGraw-Hill handbooks, McGraw-Hill 2003.

[68] de Miguel Mercader, F., Groeneveld, M., Kersten, S., Way, N., Schaverien, C., Hogendoorn, J., Production of advanced biofuels: Co-processing of upgraded pyrolysis oil in standard refinery units, *Appl. Catal., B* **96** (2010) 57 – 66.

[69] Talmadge, M. S., Baldwin, R. M., Biddy, M. J., McCormick, R. L., Beckham, G. T., Ferguson, G. A., Czernik, S., Magrini-Bair, K. A., Foust, T. D., Metelski, P. D., Hetrick, C., Nimlos, M. R., A perspective on oxygenated species in the refinery integration of pyrolysis oil, *Green Chem.* **16** (2014) 407–453.

[70] Fogassy, G., Thegarid, N., Toussaint, G., van Veen, A. C., Schuurman, Y., Mirodatos, C., Biomass derived feedstock co-processing with vacuum gas oil for second-generation fuel production in FCC units, *Appl. Catal., B* **96** (2010) 476 – 485.

[71] Fogassy, G., Thegarid, N., Schuurman, Y., Mirodatos, C., From biomass to bio-gasoline by FCC co-processing: effect of feed composition and catalyst structure on product quality, *Energy Environ. Sci.* **4** (2011) 5068.

[72] Oasmaa, A., Solantausta, Y., Arpiainen, V., Kuoppala, E., Sipilä, K., Fast Pyrolysis Bio-Oils from Wood and Agricultural Residues, *Energy Fuels* **24** (2010) 1380–1388.

[73] Oasmaa, A., Peacocke, C., VTT Publications 731: Properties and fuel use of biomass-derived fast pyrolysis liquids. A guide, *Technical Report 731*, VTT, Espoo (2010).

[74] Sipilä, K., Kuoppala, E., Fagernäs, L., Oasmaa, A., Characterization of biomass-based flash pyrolysis oils, *Biomass Bioenergy* **14** (1998) 103–113.

[75] Jae, J., Coolman, R., Mountziaris, T., Huber, G. W., Catalytic fast pyrolysis of lignocellulosic biomass in a process development unit with continual catalyst addition and removal, *Chem. Eng. Sci.* **108** (2014) 33 – 46.

[76] Lappas, A. A., Dimitropoulos, V. S., Antonakou, E. V., Voutetakis, S. S., Vasalos, I. A., Design, Construction, and Operation of a Transported Fluid Bed Process Development Unit for Biomass Fast Pyrolysis: Effect of Pyrolysis Temperature, *Ind. Eng. Chem. Res.* **47** (2008) 742–747.

[77] Lappas, A., Kalogiannis, K., Production of an Advanced Bioenergy Carrier (Bio-oil) from Biomass Catalytic Pyrolysis. Effect of Catalyst Deactivation on Bio-oil Yield and Quality, tcbiomass 2013, Chicago, US, http://www.gastechnology.org/tcbiomass/tcb2013/12-Lappas-tcbiomass2013-presentation-Thur.pdf (2013), accessed 7 March 2016.

[78] French, R., Czernik, S., Catalytic pyrolysis of biomass for biofuels production, *Fuel Process. Technol.* **91** (2010) 25 – 32.

[79] Rautiainen, E., Pimenta, R., Ludvig, M., Pouwels, C., Deactivation of ZSM-5 additives in laboratory for realistic testing, *Catal. Today* **140** (2009) 179 – 186.

[80] Vasalos, I. A., Lappas, A. A., Kopalidou, E. P., Kalogiannis, K. G., Biomass catalytic pyrolysis: process design and economic analysis, *WIREs Energy Environ.* **5** (2016) 370–383.

[81] Kern, P., Klimczak, M., Heinzelmann, T., Lucas, M., Claus, P., High-throughput study of the effects of inorganic additives and poisons on NH_3-SCR catalysts. Part II: Fe-zeolite catalysts, *Appl. Catal., B* **95** (2010) 48 – 56.

[82] Putluru, S. S. R., Riisager, A., Fehrmann, R., Alkali resistant Cu/zeolite deNOx catalysts for flue gas cleaning in biomass fired applications, *Appl. Catal., B* **101** (2011) 183 – 188.

[83] Zhou, L., Bryant, A., Ramirez, M. M., May, L., Engelman, R. A., Rainer, B. A. D., Method of rejuvenating biomass conversion chart, KiOR Inc. US Patent Application (2015), US2015004093 AA.

[84] Chen, N. Y., Walsh, D. E., Koenig, L. R., Fluidized-Bed Upgrading of Wood Pyrolysis Liquids and Related Compounds, Fluidized-Bed Upgrading of Wood Pyrolysis Liquids and Related Compounds. in *ACS Symposium Series*, ed. , American Chemical Society (ACS) 1988, pp. 277–289.

[85] Wang, K., Zhang, J., H. Shanks, B., Brown, R. C., Catalytic conversion of carbohydrate-derived oxygenates over HZSM-5 in a tandem micro-reactor system, *Green Chem.* **17** (2015) 557–564.

[86] Cheng, Y.-T., Huber, G. W., Chemistry of Furan Conversion into Aromatics and Olefins over HZSM-5: A Model Biomass Conversion Reaction, *ACS Catal.* **1** (2011) 611–628.

[87] Nicoleit, T., Niebel, A., Funke, A., Lappas, A., Kalogiannis, K., Michailof, C., Iliopoulou, E., D.Iatridis, Fougret, C., Jordan, E., Kusche, S., BioBoost: Final report of WP2 summarizing the optimization of conversion technology processes: Pyrolysis, Catalytic Pyrolysis, Hydrothermal Carbonization, http://www.bioboost.eu/uploads/files/bioboost_d2.6_certh_final_report_wp2_vers1.0-final.pdf (2015), accessed 14 August 2016.

[88] Thegarid, N., Fogassy, G., Schuurman, Y., Mirodatos, C., Stefanidis, S., Iliopoulou, E., Kalogiannis, K., Lappas, A., Second-generation biofuels by co-processing catalytic pyrolysis oil in FCC units, *Appl. Catal., B* **145** (2014) 161–166.

[89] Marker, T. L., Felix, L. G., Linck, M. B., Roberts, M. J., Ortiz-Toral, P., Wangerow, J., Integrated hydropyrolysis and hydroconversion (IH 2®) for the direct production of gasoline and diesel fuels or blending components from biomass, Part 2: continuous testing, *Environ. Prog. Sustainable Energy* **33** (2013) 762–768.

[90] Venderbosch, R. H., A Critical View on Catalytic Pyrolysis of Biomass, *ChemSusChem* **8** (2015) 1306–1316.

[91] Guisnet, M., Magnoux, P., Organic chemistry of coke formation, *Appl. Catal., A* **212** (2001) 83 – 96.

[92] Elliott, D. C., Oasmaa, A., Preto, F., Meier, D., Bridgwater, A. V., Results of the IEA Round Robin on Viscosity and Stability of Fast Pyrolysis Bio-oils, *Energy Fuels* **26** (2012) 3769–3776.

[93] Oasmaa, A., Korhonen, J., Kuoppala, E., An Approach for Stability Measurement of Wood-Based Fast Pyrolysis Bio-Oils, *Energy Fuels* **25** (2011) 3307–3313.

[94] Sundqvist, T., Solantausta, Y., Oasmaa, A., Kokko, L., Paasikallio, V., Heat Generation during the Aging of Wood-Derived Fast-Pyrolysis Bio-oils, *Energy Fuels* .

[95] Oasmaa, A., Sundqvist, T., Kuoppala, E., Garcia-Perez, M., Solantausta, Y., Lindfors, C., Paasikallio, V., Controlling the Phase Stability of Biomass Fast Pyrolysis Bio-oils, *Energy Fuels* **29** (2015) 4373–4381.

[96] Meng, J., Moore, A., Tilotta, D. C., Kelley, S. S., Adhikari, S., Park, S., Thermal and Storage Stability of Bio-Oil from Pyrolysis of Torrefied Wood, *Energy Fuels* **29** (2015) 5117–5126.

[97] Czernik, S., Johnson, D. K., Black, S., Stability of wood fast pyrolysis oil, *Biomass Bioenergy* **7** (1994) 187–192.

[98] Fratini, E., Bonini, M., Oasmaa, A., Solantausta, Y., Teixeira, J., Baglioni, P., SANS Analysis of the Microstructural Evolution during the Aging of Pyrolysis Oils from Biomass, *Langmuir* **22** (2006) 306–312.

[99] Oh, K., Ring, T. A., Deo, M. D., Asphaltene aggregation in organic solvents, *J. Colloid Interface Sci.* **271** (2004) 212 – 219.

[100] Maqbool, T., Srikiratiwong, P., Fogler, H. S., Effect of temperature on the precipitation kinetics of asphaltenes, *Energy Fuels* **25** (2011) 694–700.

[101] Oasmaa, A., Elliott, D. C., Korhonen, J., Acidity of Biomass Fast Pyrolysis Bio-oils, *Energy Fuels* **24** (2010) 6548–6554.

[102] Adjaye, J., Bakhshi, N., Catalytic conversion of a biomass-derived oil to fuels and chemicals I: Model compound studies and reaction pathways, *Biomass Bioenergy* **8** (1995) 131–149.

[103] Gayubo, A. G., Aguayo, A. T., Atutxa, A., Aguado, R., Olazar, M., Bilbao, J., Transformation of Oxygenate Components of Biomass Pyrolysis Oil on a HZSM-5 Zeolite. II. Aldehydes, Ketones, and Acids, *Ind. Eng. Chem. Res.* **43** (2004) 2619–2626.

[104] Mazanec, T., Whiting, J., Fast catalytic pyrolysis with recycle of side products, Anellotech Inc. US Patent Application (2014), US2014027265 AA.

[105] Mukarakate, C., McBrayer, J. D., Evans, T. J., Budhi, S., Robichaud, D. J., Iisa, K., ten Dam, J., Watson, M. J., Baldwin, R. M., Nimlos, M. R., Catalytic fast pyrolysis of biomass: the reactions of water and aromatic intermediates produces phenols, *Green Chem.* **17** (2015) 4217–4227.

[106] Yang, H., Coolman, R. J., Karanjkar, P., Wang, H., Xu, Z., Chen, H., Moutziaris, T. J., Huber, G. W., The effect of steam on the catalytic fast pyrolysis of cellulose, *Green Chem.* **17** (2015) 2912–2923.

[107] Agblevor, F. A., Mante, O., McClung, R., Oyama, S., Co-processing of standard gas oil and biocrude oil to hydrocarbon fuels, *Biomass Bioenergy* **45** (2012) 130 – 137.

[108] Chen, N. Y., Degnan Jr., T. F., Koenig, L. R., Liquid fuel from carbohydrates, *Chemtech* **16** (1986) 506–511.

[109] Zhang, H., Cheng, Y.-T., Vispute, T. P., Xiao, R., Huber, G. W., Catalytic conversion of biomass-derived feedstocks into olefins and aromatics with ZSM-5: the hydrogen to carbon effective ratio, *Energy Environ. Sci.* **4** (2011) 2297–2307.

[110] KiOR: The inside true story of a company gone wrong, http://www.biofuelsdigest.com/bdigest/2016/05/17/kior-the-inside-true-story-of-a-company-gone-wrong/, accessed 13 August 2016.

[111] KiOR: The inside true story of a company gone wrong, Part 2, http://www.biofuelsdigest.com/bdigest/2016/05/18/kior-the-inside-true-story-of-a-company-gone-wrong-part-2/, accessed 13 August 2016.

[112] KiOR: The inside true story of a company gone wrong. Part 3, ?You?ve Cooked the Books?, http://www.biofuelsdigest.com/bdigest/2016/08/03/the-inside-true-story-of-a-company-gone-wrong-part-3-youve-cooked-the-books/, accessed 13 August 2016.

[113] Ramirez-Corredores, M. M., May, L., Paradise, C., Kent, N., Tong, X., Banda, R. M., Roemisch, R., Organics recovery from the aqueous phase of biomass catalytic pyrolysis, and upgrading thereof, KiOR Inc. US Patent Application (2014), US20130306557A1.

[114] Lin, R., Process for recovering organics from wastewater, KiOR Inc. US Patent Application (2014), US20140076821A1.

[115] Moore, B., Sanchez, V., Smith, E., Process for upgrading biomass derived products using liquid-liquid extraction, KiOR Inc. US Patent Application (2013), US20140076821A1.

[116] Yathavan, B. K., Agblevor, F. A., Catalytic Pyrolysis of Pinyon?Juniper Using Red Mud and HZSM-5, *Energy Fuels* **27** (2013) 6858–6865.

[117] Agblevor, F. A., Elliott, D. C., Santosa, D. M., Olarte, M. V., Burton, S. D., Swita, M., Beis, S. H., Christian, K., Sargent, B., Red Mud Catalytic Pyrolysis of Pinyon Juniper and Single-Stage Hydrotreatment of Oils, *Energy Fuels* **Article ASAP**.

[118] Iisa, K., French, R. J., Orton, K. A., Yung, M. M., Johnson, D. K., ten Dam, J., Watson, M. J., Nimlos, M. R., In Situ and ex Situ Catalytic Pyrolysis of Pine in a Bench-Scale Fluidized Bed Reactor System, *Energy Fuels* **30** (2016) 2144–2157.

[119] Mante, O. D., Agblevor, F., Oyama, S., McClung, R., The effect of hydrothermal treatment of FCC catalysts and ZSM-5 additives in catalytic conversion of biomass, *Appl. Catal., A* **445-446** (2012) 312 – 320.

[120] Elliott, D., Santosa, D., Olarte, M., Solantausta, Y., Paasikallio, V., Agblevor, F., Upgrading in situ catalytic pyrolysis bio-oil to liquid hydrocarbons, tcbiomass 2015, Chicago, US, http://www.gastechnology.org/tcbiomass/tcb2015/Elliott_Doug-Presentation-tcbiomass2015.pdf (2015), accessed 7 March 2016.

[121] Gust, S., Upgrading of catalytic pyrolysis oil, BioBoost DSM Workshop, Geleen, NL, http://www.bioboost.eu/uploads/files/06-gust_neste.pdf (2015), accessed 7 March 2016.

Publication I

Publication II

Catalytic Pyrolysis of Forest Thinnings with ZSM-5 Catalysts: Effect of Reaction Temperature on Bio-oil Physical Properties and Chemical Composition

Ville Paasikallio,*,[†] Foster Agblevor,[‡] Anja Oasmaa,[†] Jani Lehto,[†] and Juha Lehtonen[§]

[†]Synfuels, VTT Technical Research Centre of Finland, P. O. Box 1000, 02044 VTT, Finland

[‡]Biological Engineering Department, Utah State University, 4105 Old Main Hall, Logan, Utah 84322, United States

[§]Department of Biotechnology and Chemical Technology, School of Chemical Technology, Aalto University, P. O. Box 16100, 00076 Aalto, Finland

ABSTRACT: In this study, noncatalytic and catalytic fast pyrolysis of forest thinnings was carried out in a bench-scale bubbling fluidized bed reactor using two commercial ZSM-5 catalysts. After the initial comparison experiments at 475 °C, the catalyst which showed a clearly higher activity was further tested at reaction temperatures of 400 and 550 °C. The yield of organic liquids, which was 39 wt % in the noncatalytic experiment, decreased to 14−24 wt % depending on the reaction temperature. Varying the reaction temperature while using the ZSM-5 catalyst also caused significant changes in the elemental composition, viscosity, and pH, as well as the chemical composition of bio-oil. In general, the use of the catalyst resulted in a less viscous bio-oil with an oxygen content as low as 19 wt %. The catalytically produced bio-oil contained less carbohydrate degradation products and more aromatic compounds. Based on the chemical characterization results (^{13}C nuclear magnetic resonance spectroscopy, gas chromatography−flame ionization detector, gas chromatography−mass spectrometry, and solvent fractionation) obtained in this study, a new supplementary procedure for the existing solvent fractionation method was suggested to be used as an initial screening tool for aromatic hydrocarbon content in bio-oil samples. In this procedure, a water-insoluble, dichloromethane-soluble fraction containing low molecular mass lignin compounds and aromatic hydrocarbons is first isolated using solvent fractionation. When the dichloromethane is allowed to evaporate at room temperature, the consequent mass loss of the pyrolysis products exhibits a linear correlation with the content of aromatic hydrocarbons in bio-oil, as quantified by gas chromatographic methods.

■ INTRODUCTION

Fast pyrolysis of biomass is a thermochemical conversion process which produces a liquid product commonly referred to as bio-oil or pyrolysis oil. Bio-oil, which is formed via thermal decomposition reactions of individual biomass components, exhibits many adverse properties such as high viscosity, acidity, chemical instability, and low energy content, which in turn severely limit its usability in stationary and transportation fuel applications.[1,2] Catalytic pyrolysis is seen as one alternative for alleviating the adverse physicochemical properties of bio-oil.[3,4] In catalytic pyrolysis, the chemical nature of the bio-oil is shifted from its typical polar composition closer toward traditional petroleum-derived fuels.[5,6] This change is caused by the oxygen rejecting cracking reactions.[7,8] Catalytic pyrolysis is commonly carried out as an in situ cracking process in bubbling fluidized bed (BFB) reactors,[3,4,6,9] where the vapors released in the primary pyrolysis reactions come into immediate contact with the catalytic heat transfer material, such as ZSM-5,[3,6] fluid catalytic cracking (FCC) catalyst which has Y zeolite as its active component,[10−12] or other zeolite catalysts.[4,13] Oxygen is released from the pyrolysis vapors in the form of H_2O, CO, and CO_2 via dehydration, decarbonylation, and decarboxylation reactions.[7,8] The intermediate product molecules formed in the aforementioned reactions can then react further to form value added products such as aromatic hydrocarbons.[14,15] This opens up new opportunities for the utilization of upgraded bio-oil, one of which is the possibility of coprocessing bio-oil with petroleum-derived feedstocks in a FCC unit.[16−18] Introducing bio-oil into an existing oil refinery process would serve at least two purposes: coprocessing with a hydrocarbon feedstock would help to offset the heavy coking tendency of the hydrogen deficient bio-oil,[19,20] and incorporation of second generation lignocellulose-based biofuels into the existing fuel infrastructure could be achieved without having to build capital-intensive greenfield biorefineries.

Composition and properties of the pyrolysis feedstock affect the product distribution of a fast pyrolysis process. High yields of organic liquids have been correlated with factors such as low ash content, high volatiles content, and high O/C molar ratio in the biomass feedstock. Higher ash content in the biomass leads to increased formation of water and gases, which stems from secondary alkali metal catalyzed vapor-phase reactions.[21] Even though such high-ash materials exhibit properties which by all means cannot be considered optimal for bio-oil production, interest in them, nevertheless, remains strong. Compared to higher quality feedstocks such as wood sawdust, forest and agricultural residues offer benefits in terms of availability and price. In countries such as Finland, where the forest industry has for a long time been a mainstay of the local economy, biomass materials such as forest residue and forest thinning are

of particular interest for bioenergy purposes. Since the development work of integrated fast pyrolysis has taken major steps[22] toward commercialization in recent years, it is conceivable that a large future potential exists for more advanced conversion techniques such as catalytic pyrolysis. It is thus essential that materials, which could be considered as realistic feedstock options for industrial-scale processes, are included in the currently ongoing research efforts.

The selection of a suitable catalyst and process conditions play an important role in determining the overall outcome of a catalytic pyrolysis process. Ever since the early work of Evans and Milne[23] and Diebold and Scahill[24] in 1987, ZSM-5 has been shown to be a suitable catalyst for deoxygenating pyrolysis vapors and for producing aromatic hydrocarbons.[8,25,26] ZSM-5 has a three-dimensional pore structure consisting of 10-membered rings and a pore size of 0.51−0.56 nm. Shape selectivity, which originates from the particular pore size of the ZSM-5 catalysts, has been shown to have a positive influence on the formation of aromatic hydrocarbons.[8,25] Low silica-to-alumina ratios (SAR) and the consequent high acidities are another factor that can enhance the formation of aromatic hydrocarbons. According to Foster et al.,[27] a silica-to-alumina ratio of 30 was the optimal choice for producing aromatic hydrocarbons from glucose. When the SAR was further decreased to 23, the increased density of Brønsted acid sites led to higher coke yields due to bimolecular condensation reactions. In a study by Mihalcik et al.,[8] a ZSM-5 catalyst with SAR = 23 produced the highest amount of hydrocarbons in the catalytic pyrolysis of various lignocellulosic feedstocks. Ma et al.[28] also observed the highest aromatic hydrocarbon yields when pyrolyzing lignin over a ZSM-5 catalyst with SAR = 30.

High catalyst-to-biomass ratios in batch reactors or analogously low weight hourly space velocities (WHSVs) in continuous reactors are another key factor for obtaining high yields of aromatic hydrocarbons. In batch experiments, catalyst-to-biomass ratios of up to 19:1 have been reported.[26,27] French and Czernik[29] stated that choosing such a high catalyst-to-biomass ratio can be used for demonstrating the potential of producing hydrocarbons from biomass and that the ratio would have to be optimized in later stages of process development. Carlson et al.[6] investigated the effect of WHSV on the yield of aromatics and olefins when pyrolyzing pine wood with a ZSM-5 catalyst in a bubbling fluidized bed reactor. Increasing the WHSV from 0.1 to 1.7 h^{-1} decreased the carbon yield of aromatics from 14.0 to 9.7% while the yield of olefins increased from 5.4 to 6.1%. Low WHSV also inhibited the formation of two-ring aromatic compounds such as indene and naphthalene. For conventional fast pyrolysis, vapor residence times of less than 2 s have been considered optimal for maximizing the liquid yield. In contrast to this, examples of catalytic pyrolysis experiments carried out in BFB reactors with vapor residence times of 6.5−10 s can be found in the literature.[6,12,30] While the utilization of small ∼100 μm particulate catalysts may necessitate the use of low fluidization velocities, increasing the vapor residence time can exert a positive influence on the properties of the bio-oil.[12,30] One should still bear in mind that if a catalytic fast pyrolysis process would be carried out in circulating fluidized bed (CFB) reactor, as was done by Lappas et al.,[11] the vapor residence time will be far shorter than 6−10 s.

Reaction temperature is also one of the main parameters which affect the outcome of biomass pyrolysis. While a pyrolysis temperature of approximately 500 °C has conventionally been applied for maximizing liquid production, a

different temperature may be optimal in the presence of a catalyst. In catalytic pyrolysis, maximizing the liquid yield is no longer the overall goal. Rather, the objective is to find a balanced trade-off between the yield of bio-oil and its quality. Thus, the combined thermocatalytic effect and how it influences the composition and properties of bio-oil is of particular interest. Although there are studies which discuss the effect of reaction temperature in biomass catalytic pyrolysis or pyrolysis vapor upgrading,[6,29,31] these studies have typically focused on either physical or chemical characterization of the product bio-oil. Thus, there is a clear need to investigate how reaction temperature in catalytic pyrolysis affects both the chemical composition and the physical properties of bio-oil. This should in turn provide a better understanding of how the chemical composition of bio-oil affects certain physical parameters, e.g., viscosity.

In this work, noncatalytic and catalytic pyrolysis of Finnish forest thinnings was carried out in a bench-scale bubbling fluidized bed reactor using two ZSM-5 catalysts. Initial experiments were conducted using both catalysts and silica sand, and afterwards the more promising catalyst was selected for further experimentation, where the effect of reaction temperature in catalytic pyrolysis was studied. The effects of the catalysts and the reaction temperature were evaluated by examining the product distribution, physical properties, and chemical composition of the product bio-oil.

■ EXPERIMENTAL SECTION

Biomass and Catalyst Characterization. Finnish forest thinnings were used as the feedstock in these experiments. The properties of the feedstock are shown in Table 1. Moisture content

Table 1. Pyrolysis Feedstock Properties

property	value
moisture (wt %, as received)	6.7
carbon (wt %, db)	50.6
hydrogen (wt %, db)	6.1
nitrogen (wt %, db)	0.2
sulfur (wt %, db)	0.02
oxygen (by difference; wt %, db)	41.88
ash (wt %, db)	1.2
volatiles (wt %, db)	81.6
higher heating value (MJ/kg, db)	20.3
lower heating value (MJ/kg, db)	18.9

was determined using a Denver Instrument IR-60 moisture analyzer (Denver Istruments, Bohemia, NY, USA). Elemental composition (CHN) of the dry feedstock was determined using a Elementar vario MAX CHN analyzer (Elementar Analysensysteme GmbH, Hanau, Germany). Oxygen content was calculated by difference (100 wt % − CHNS − ash). Sulfur content was determined using a LECO SC-432 analyzer. Volatiles and ash content were determined using a LECO TGA-601 thermogravimetric analyzer. Heating values were determined with a IKA Werke C 5000 Control calorimeter. Before the experiments, the biomass was ground and sieved to obtain a particle size of under 1 mm. For the noncatalytic experiments, sand with a particle size of 250−425 μm was used as the fluidized bed heat-transfer material. In the catalytic experiments, two ZSM-5 catalysts were used. The first one was a spray dried ZSM-5-based fluid catalytic cracking additive supplied by BASF Catalysts LLC (Iselin, NJ, USA). The particle size of this catalyst was 125−180 μm. The second catalyst was a ZSM-5 zeolite which was supplied as cylindrical extrudates by Süd-Chemie catalysts. The extrudates were ground and sieved to obtain a fraction with a particle size of 125−250 μm. Both catalysts were
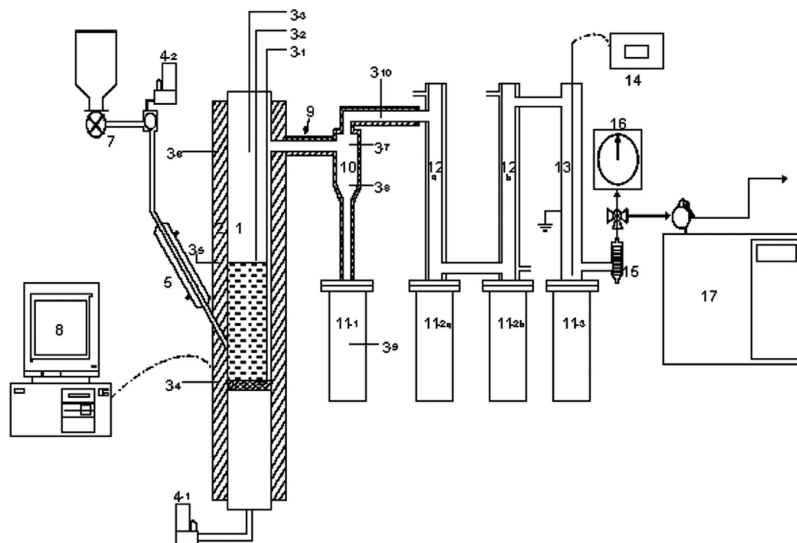
Figure 1. Bench-scale bubbling fluidized bed reactor: (1) fluidized bed, (2) furnace, (3) thermocouple, (4) mass flow controller, (5) jacketed air-cooled feeder tube, (6) hopper, (7) screw feeder, (8) computer, (9) insulated pipeline, (10) hot gas filter, (11) reservoir, (12) condenser, (13) electrostatic precipitator (ESP), (14) AC power supply, (15) filter, (16) flow totalizer, and (17) micro-gas chromatograph.

calcined in a muffle furnace under an air atmosphere. The furnace was heated from room temperature to 500 °C in 1 h, the temperature was maintained at 500 °C for 5 h, and finally the oven was allowed to cool back to room temperature. The specific surface area of the calcined catalysts was measured using nitrogen physisorption. The measurements were carried out with a Micromeritics Tristar surface area analyzer (Micromeritics, Norcross, GA, USA). The surface area was calculated according to the Brunauer–Emmett–Teller (BET) equation. The acidity of the two ZSM-5 catalysts was determined using temperature-programmed desorption of ammonia (NH_3-TPD). The NH_3-TPD spectra of the calcined ZSM-5 samples were recorded using a flow-through microreactor which was equipped with a Balzers GAM-415 quadrupole mass spectrometer. A 400 mg sample of the catalyst was saturated with 1 mL pulses of 5 vol % NH_3 in He at a temperature of 30 °C. After the NH_3 adsorption, the catalyst was flushed in a flow of pure He for 15 min. Temperature-programmed desorption of NH_3 was then carried out by heating the reactor to 650 °C at a rate of 5 °C/min while monitoring mass number 17. The share of weak, medium, and strong acid sites was estimated by fitting least-squares Gaussian curves to the NH_3 desorption curves.

Reactor System and Experimental Procedure. The pyrolysis experiments were conducted in a bench-scale bubbling fluidized bed reactor unit. A schematic picture of the pyrolysis unit is presented in Figure 1. The reactor, which was externally heated with a three-zone electric furnace (Thermcraft, Winston-Salem, NC, USA), had an inner diameter of 50 mm and a length of 500 mm, which included a 140 mm gas preheating zone below a 100 μm porous gas distribution plate. Nitrogen was used as the fluidization gas. The flow of fluidization nitrogen was 10 and 3.5 L min^{-1} for the noncatalytic and catalytic experiments, respectively. Biomass was loaded into a feed hopper, from where it was first conveyed into an entrapment section using a K-Tron volumetric feeder system (K-Tron Process Group, Pitman, NJ, USA). The feeding rate of the biomass was approximately 200 g/h on a dry basis. In the entrapment section, high-velocity nitrogen swept the biomass particles through a sloped feeder tube into the reactor where they were back-mixed with the sand/catalyst. Nitrogen flow through the feed hopper was 8 and 3 L min^{-1} for the noncatalytic and catalytic experiments, respectively. The mass of the catalyst bed was 100 g, which resulted in a weight hourly space velocity of approximately 2 h^{-1}. Depending on the experiment, the temperature of the fluidized

bed was 400–550 °C. A negative temperature gradient was maintained in the axial direction in order to inhibit secondary cracking reactions of the pyrolysis vapors in the upper parts of the reactor. Temperatures of the catalyst bed and the reactor were measured and controlled with three K-type thermocouples. The first thermocouple spanned the entire length of the catalyst bed, the second one was situated above the upper edge of the catalyst bed, and the third one measured the temperature of the pyrolysis vapors and gases exiting the reactor.

Upon exiting the reactor, the pyrolysis vapors and gases were first passed through a hot gas filter, which was maintained at a temperature of 400 °C. The purpose of the hot gas filter was to separate char, ash, and entrained catalyst particles from the product vapors and gases. The hot gas filter was followed by a sequential liquid recovery system, which consisted of two condensers, an electrostatic precipitator (ESP) and a coalescing filter. The condensers were cooled using a 50/50 mixture of ethylene glycol and water. The mixture itself was cooled using an 18-L refrigerated circulating bath (Haake, Karlsruhe, Germany). Temperature of the first condenser was maintained at 10–15 °C, which resulted in efficient condensation of water and light organics. The operating voltage of the ESP was 18–20 kV. After the coalescing filter, the gas flow passed through a flow totalizer, which was followed by a micro-gas chromatograph. The yields of liquid products and char/coke were determined gravimetrically by weighing all components of the system before and after the experiment. The yield of noncondensable gases was determined by difference.

Bio-oil Analyses. All liquid products were analyzed for their water content using volumetric Karl Fisher titration. Water content was determined with a Metrohm 701KF Titrino (Brinkmann Instruments, Inc., NY, USA) and a 703 titration stand using Hydranal Composite 5 reagent. Approximately 0.2–0.3 g of bio-oil was dissolved in methanol prior to the titration. The liquid collected from the ESP, which will be referred to as bio-oil, was further characterized using the following methods. The elemental composition (CHNS) of the bio-oil was determined using a Thermo Scientific Flash 2000 organic elemental analyzer (ThermoFisher Scientific, Cambridge, U.K.). The sample size was 2–4 mg. Oxygen was determined by difference. The pH of the bio-oil was measured using a Mettler Toledo SevenEasy pH meter and probe (Mettler-Toledo GmbH, Switzerland). The bio-oil was mechanically stirred and then allowed to stabilize for 10 min before taking the pH reading. The dynamic viscosity of the bio-oil was
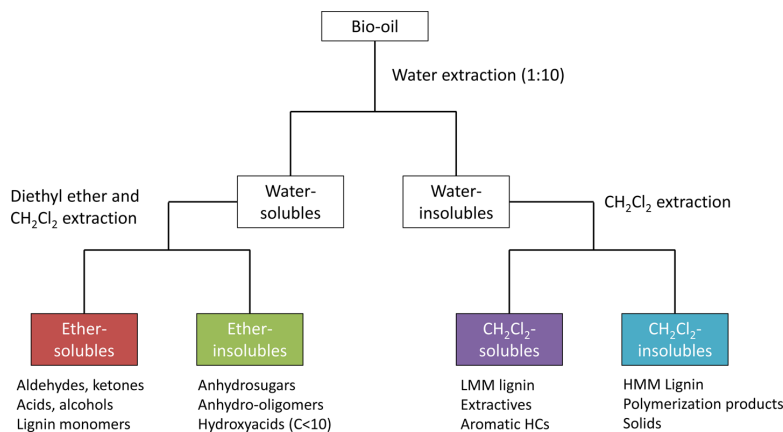
Figure 2. Solvent fractionation scheme for bio-oil chemical characterization (adapted from Oasmaa et al.[32]).
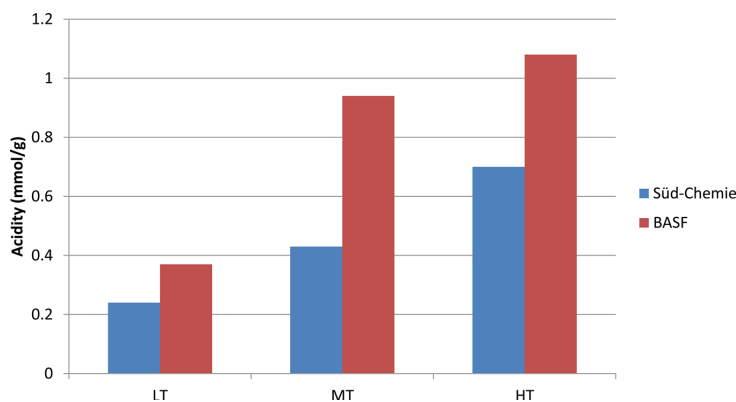

Figure 3. Weak (LT), medium (MT), and strong (HT) acidity (mmol/g) of BASF and Süd-Chemie catalysts.

determined at 40 °C using a Brookfield DV-II+ Pro viscometer (Brookfield Engineering Laboratories, Middleboro, MA, USA) equipped with a Brookfield Thermosel accessory. Viscosity measurements were carried out approximately 3 days after the pyrolysis experiments. The size of the sample was 7 mL, and the shear rate was increased until the bio-oil exhibited Newtonian behavior over a certain shear rate range. A higher heating value of the bio-oil was determined using a IKA C2000 basic bomb calorimeter (IKA Works, Inc., NC, USA). The ^{13}C nuclear magnetic resonance (NMR) spectrum of the bio-oil was recorded using a JEOL 300 MHz NMR spectrometer (JEOL Ltd., Tokyo, Japan) by dissolving approximately 0.5−1.0 g of bio-oil into 0.7 mL of deuterated dimethyl sulfoxide (Sigma-Aldrich, St. Louis, MO, USA). The pulse width was 14.75 μs, the acquisition time 1.57 s, the relaxation delay 2 s, and the number of scans 3000. Analysis of the spectra was carried out using ACD 1D NMR Processor (Advanced Chemistry Development, Inc., Toronto, Canada).

The chemical composition of the bio-oils was also analyzed using a solvent fractionation method,[32] which is presented in Figure 2. The bio-oil was first separated into water-soluble and water-insoluble fractions using liquid−liquid extraction. The water-soluble fraction was then extracted with diethyl ether to produce ether-soluble and ether-insoluble fractions. The water-insoluble fraction was extracted with dichloromethane to produce dichloromethane-soluble and dichloromethane-insoluble fractions, which mostly contain low molecular mass (LMM) and high molecular mass (HMM) lignin, respectively. Two methods based on gas chromatography with flame ionization detector (GC-FID) were used for quantitative analysis of the bio-oil

compounds. The first method was used for quantification of water-soluble oxygenate compounds. Approximately 1 mL of bio-oil was extracted with 10 mL of water which was followed by mixing and centrifugation. The supernatant was then analyzed using an Agilent Technologies 7890A gas chromatograph (Agilent Technologies, Santa Clara, CA, USA), which was equipped with an Agilent 19091 N-136 HP-Innowax column (length, 60 m; inner diameter, 0.25 mm; film thickness, 0.25 μm). The calibration for the quantification was based on model compounds, and *n*-butanol was used as an internal standard. Aromatic hydrocarbons along with some oxygenated aromatics were quantitatively analyzed using an Agilent Technologies 6890 Series GC system (Agilent Technologies, Santa Clara, CA, USA), which was equipped with an Ultra 2 column (length, 23 m; inner diameter, 0.32 mm; film thickness, 0.52 μm). Approximately 1 g of bio-oil was first dissolved in 50 mL of dichloromethane (DCM). The solution was filtered in order to remove any precipitate that formed, after which a 20 mL aliquot was taken and combined with 5 mL of internal standard (dodecane). Calibration curves were determined using model compounds which ranged from benzene to pyrene. Compound identification was carried out using gas chromatography with a mass selective detector (GC-MS). Measurements were performed using a Shimadzu GC17A gas chromatograph (Shimadzu Corp., Kyoto, Japan) equipped with a HP Ultra 1 fused silica capillary column (length, 50 m; inner diameter, 0.32 mm; film thickness, 0.52 μm) and a quadrupole detector.

Gas Analyses. The composition of the noncondensable product gases was analyzed using a Varian CP-490 micro-gas chromatograph

Table 2. Product Distribution (wt %) for Noncatalytic and Catalytic Pyrolysis

	product distribution (wt %) for the given pyrolysis medium and temperature (°C)				
	silica sand	BASF	Süd-Chemie		
	475 °C	475 °C	400 °C	475 °C	550 °C
total liquid product	55 ± 1.5	48 ± 0.01	45 ± 0.3	38 ± 0.5	35 ± 0.3
organic liquids	38 ± 0.5	31 ± 0.9	24 ± 0.6	15 ± 0.9	14 ± 0.6
water	17 ± 1.0	17 ± 0.9	22 ± 0.3	23 ± 0.3	21 ± 0.9
char/coke	19 ± 1.1	20 ± 0.3	25 ± 0.7	20 ± 0.2	18 ± 0.1
gases (by difference)	25 ± 0.4	32 ± 0.2	30 ± 1.0	42 ± 0.3	48 ± 0.2

(micro-GC; Agilent Technologies, Inc., Santa Clara, CA, USA). During the pyrolysis experiments, samples were taken every 7.25 min. The micro-GC was equipped with two channels. The first channel was equipped with a 10 m Molsieve 5 Å (MS) column and the second channel with a 10 m porous polymer (PPU) column. Thermal conductivity detectors were used for quantifying the individual gas components. The micro-gas chromatograph was calibrated using standard gas mixtures comprised of N_2, H_2, CO, CO_2, CH_4, C_2H_6, C_3H_8, C_4H_8, and C_5H_{10}. N_2, H_2, CO, and CH_4 were analyzed using the MS column. The PPU column was used for analyzing the C_2-C_5 hydrocarbons. The carrier gases for the Molsieve and PPU columns were argon and helium, respectively. Temperatures of the columns were 55 and 100 °C for the MS and PPU columns, respectively. The temperature of the injector was 100 °C.

■ **RESULTS AND DISCUSSION**

Catalyst Characterization. The specific surface areas of the two catalysts were 105 and 334 m^2/g for the BASF and Süd-Chemie ZSM-5 catalysts, respectively. The lower specific surface area of the BASF catalyst is most likely due to its lower zeolite content and higher binder content. Because the BASF catalyst is a fluid catalytic cracking additive which was originally designed for use in a CFB reactor, its zeolite content was lower in order to allow for a higher proportion of filler and binder material. This kind of catalyst formulation gives the catalyst sufficient mechanical and thermal stability to withstand the stresses of a fluid catalytic cracking unit. On the other hand, the Süd-Chemie ZSM-5 was supplied as extrudates which are typically designed to be used in fixed bed reactors, where mechanical stress is less severe. The zeolite content can therefore be higher, which consequently results in a higher specific surface area. The results of the NH$_3$-TPD measurements are presented in Figure 3. The acid sites were categorized as either weak (LT = low temperature), medium (MT = medium temperature), or strong (HT = high temperature) based on the desorption temperature of ammonia. The fitting of the least-squares Gaussian curves placed the desorption peaks at temperature ranges of 110−125, 170−185, and 350−380 °C for LT, MT, and HT acid sites, respectively. Based on the NH$_3$-TPD results, it appears that the BASF catalyst was clearly more acidic than the Süd-Chemie catalyst. A BASF patent describing the synthesis of ZSM-5 additives for fluid catalytic cracking mentions the use of reactive alumina as one possible catalyst component.[33] This is also a factor which could contribute toward the overall acidity of the BASF catalyst. Because the specific surface area, and consequently the pore volume, of the BASF catalyst is low, it is possible that these characteristics combined with the high acidity could contribute to rapid deactivation of the catalyst.

Product Yields. The catalyst comparison experiments were carried out using 100 g of sand or catalyst at a temperature of 475 °C. The main purpose of these experiments was to compare the performance of the two ZSM-5 catalysts against

silica sand. In addition to this, the effect of reaction temperature was evaluated by conducting experiments at 400 and 550 °C with the Süd-Chemie ZSM-5 catalyst. The experimental time was 2 h in all experiments. The product distribution for the noncatalytic and catalytic experiments is shown in Table 2 on a moisture free basis. The data show average values with standard deviations from duplicate experiments. The experiment with silica sand yielded only 38 wt % organic liquids, which is less than what would be typically expected[21] for a biomass with a relatively low ash content (1.2 wt %) and a high amount of volatile compounds (81.6 wt %). For comparison purposes, an organic liquid yield of approximately 50 wt % was obtained using the same feedstock in VTT's 20 kg/h circulating fluidized bed reactor (unpublished results). One of the factors that can possibly influence the yield of organic liquids is the use of the hot gas filtration unit for solids separation. It has been reported in the literature that supplementing a cyclone with an additional hot gas filtration unit decreased the yield of organic liquids due to secondary cracking of pyrolysis vapors in the filtration unit.[34,35] A cyclone separator is not as efficient as a hot gas filter; thus, cyclone separated bio-oils can have a higher solids content due to char and entrained catalyst particles. In addition to the effect of the hot gas filter itself, partial condensation of pyrolysis vapors between the hot gas filter and the first condenser caused a slight overestimation of the char yield.

Compared to the noncatalytic reference experiment, the yield of noncondensable gases was higher with the BASF ZSM-5 catalyst. The decrease in the yield of organic liquids was only 7 wt %, which would indicate that the expected change in bio-oil properties will be very limited, as the yield of organic liquids and their oxygen content have been shown to exhibit a relatively linear relationship.[15] In contrast to the BASF catalyst, the Süd-Chemie ZSM-5 catalyst was highly efficient in converting pyrolysis vapors to both gases and water. This indicates that this particular catalyst exhibited significant activity in the removal of oxygen as both water and carbon oxides. With such a drastic decrease in the yield of organic liquids, it can be expected that the bio-oil produced with the Süd-Chemie catalyst will exhibit a clearly lower oxygen content compared to the bio-oils produced using silica sand and the BASF catalyst. Decreasing the reaction temperature to 400 °C with the Süd-Chemie catalyst caused a noticeable change in the product distribution. The yields of organic liquids increased, while the yield of noncondensable gases decreased. Lowering the reaction temperature therefore resulted in less severe cracking of the primary pyrolysis vapors. The yield of water remained roughly the same as at 475 °C. This suggests that decreasing the reaction temperature did not have a large effect on the dehydration reactions, which are one of the primary routes for oxygen removal in catalytic pyrolysis. The 5 wt % increase in the char/coke yield can be attributed to the low reaction temperature, the effect of which has been observed in both

Table 3. Average Product Gas Composition (wt %) on a N$_2$ Free Basis for Noncatalytic and Catalytic Pyrolysis

	gas composition (wt %) for the given pyrolysis medium and temperature (°C)				
	silica sand	BASF	Süd-Chemie		
	475 °C	475 °C	400 °C	475 °C	550 °C
H$_2$	0.2 ± 0.11	0.9 ± 0.06	0.4 ± 0.07	0.7 ± 0.07	0.7 ± 0.07
CO	31.0 ± 1.93	41.4 ± 1.92	43.2 ± 0.91	46.5 ± 0.79	48.9 ± 1.11
CO$_2$	61.5 ± 1.72	46.3 ± 2.41	46.6 ± 0.55	41.9 ± 1.33	35.9 ± 0.50
CH$_4$	2.4 ± 0.12	4.6 ± 0.50	3.4 ± 0.53	3.7 ± 0.21	5.1 ± 0.03
C$_2$–C$_5$	4.9 ± 0.22	6.8 ± 0.05	6.5 ± 0.24	7.2 ± 0.56	9.5 ± 0.51
CO/CO$_2$	0.5 ± 0.05	0.9 ± 0.11	0.9 ± 0.03	1.1 ± 0.05	1.4 ± 0.05
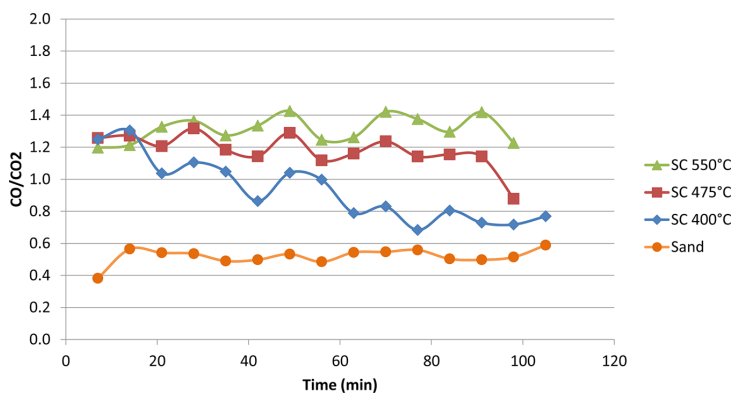
Figure 4. Weight-based CO/CO$_2$ ratio as a function of time for noncatalytic pyrolysis at 475 °C and catalytic pyrolysis at 400, 475, and 550 °C using the Süd-Chemie (SC) catalyst.

Table 4. Physicochemical Properties of Bio-oils from Noncatalytic and Catalytic Pyrolysis

	property value for the given pyrolysis medium, temperature (°C), and time (h)							
	silica sand	BASF		Süd-Chemie				
	475 °C	475 °C		400 °C		475 °C		550 °C
property	0−2 h	0−1 h	1−2 h	0−1 h	1−2 h	0−1 h	1−2 h	0−2 h
water (wt %)	3.7	2.5	2.7	1.4	1.6	0.6	0.9	0.9
carbon (wt %, db)	59.1	62.3	60.8	64.3	65.4	73.6	68.7	68.3
hydrogen (wt %, db)	6.5	6.5	6.5	6.6	6.9	6.8	6.7	6.7
nitrogen (wt %, db)	0.4	0.5	0.5	0.8	0.8	0.5	0.6	0.9
oxygen (wt %, db)	34.0	30.7	32.0	28.3	27.0	19.1	24.0	24.1
H/C (mol/mol)	1.31	1.24	1.30	1.22	1.25	1.10	1.16	1.21
O/C (mol/mol)	0.43	0.37	0.40	0.33	0.31	0.20	0.26	0.30
higher heating value (MJ/kg, db)	25.6	27.2	26.4	28.9	27.7	32.8	31.9	30.1
pH	3.0	3.1	3.2	2.9	2.9	3.2	3.1	3.9
dynamic viscosity (cP, 40 °C)	560	259	345	62	115	-	175	311

noncatalytic and catalytic pyrolysis.[6,31] Increasing the reaction temperature to 550 °C caused a slight decrease in the overall yield of liquid products. The change in the overall liquid products occurred mostly due to a decreased yield of water. The yield of char/coke also decreased, whereas the yield of noncondensable gases increased by 6 wt % when compared to 475 °C.

Gas Analysis. The average composition of the non-condensable product gases is presented in Table 3 on a nitrogen free basis. In the noncatalytic experiment, CO and CO$_2$ made up more than 92 wt % of the product gases, with the amount of CO$_2$ being approximately two times that of CO. On a general level, the use of the catalysts increased the formation of H$_2$, CO, CH$_4$, and C$_2$–C$_5$ hydrocarbons. With the BASF

ZSM-5 catalyst, CO$_2$ was still the most abundant product gas, whereas the Süd-Chemie ZSM-5 catalyst produced more CO than CO$_2$ at 475 and 550 °C. The BASF and Süd-Chemie catalysts respectively produced approximately 1.7 and 2.5 times more CO than what was obtained using silica sand. For CO$_2$, the changes were negligible or very small. This suggests that in terms of carbon oxides, formation of CO is the primary route of oxygen removal for both catalysts. Both catalysts produced similar amounts of CH$_4$ and other light hydrocarbons.

Lowering the reaction temperature caused a slight decrease in the concentration of CO, while the concentration of CO$_2$ increased. Increasing the reaction temperature had an opposite effect, and the CO/CO$_2$ ratio increased at higher operating temperatures. Formation of CH$_4$ and C$_2$–C$_5$ also increased
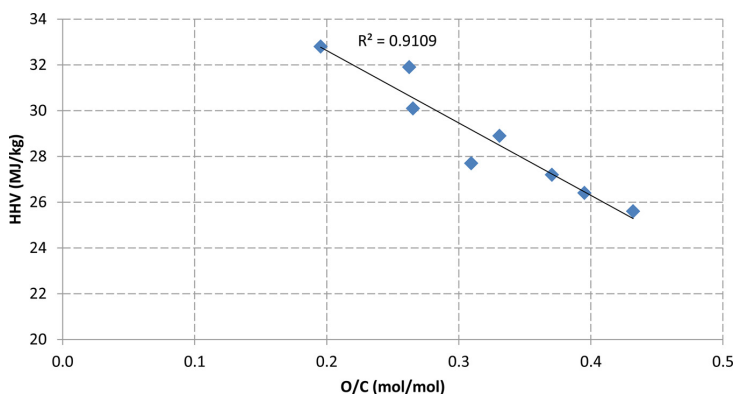
Figure 5. Higher heating value (HHV, MJ/kg) of bio-oils as a function of molar O/C ratio.

when the temperature was 550 °C. The CO/CO_2 ratio has also been used to monitor the activity of zeolite catalysts over time.[3] The CO/CO_2 ratios in these three experiments are presented in Figure 4. Periodic fluctuations in the CO/CO_2 ratio were attributed to cyclic temperature fluctuation in the reactor itself. As shown in Table 3, a higher reaction temperature resulted in a higher average CO/CO_2 ratio. Thus, whenever the temperature in the reactor reached its maximum value, the CO/CO_2 ratio was highest. Some differences could still be observed between the three different reaction temperatures. The experiment at 400 °C was the only one which showed a clear declining trend in the value of the CO/CO_2 ratio as a function of time, whereas with the two higher reaction temperatures the changes appeared to be mostly periodic fluctuation. Furthermore, in the case of 400 °C, the CO/CO_2 ratio value at the end of the experiment was clearly higher than the average value of 0.5 which was obtained using silica sand as the heat-transfer material. Even though signs of catalyst deactivation were evident at 400 °C, these results indicate that even after 2 h of time on stream, the catalyst still retained a significant proportion of its initial activity.

Bio-oil Physicohemical Properties. Physicochemical properties of the bio-oils are shown in Table 4. In the results reported below, the term "bio-oil" refers to the organic liquid product that was collected from the electrostatic precipitator. The analyses were performed for this fraction because it contained the least amount of water but still had properties similar to those of the organic phase from the condenser. The liquid product in the condenser had two phases, a light aqueous phase and a heavier organic phase. For the noncatalytic reference experiment, the bio-oil was collected only at the end of the experiment. For the catalytic experiments, the bio-oil was collected at two separate points: after 1 h time-on-stream and at the end of the experiment. This was done in order to assess the effect of catalyst deactivation on the bio-oil properties. In the 550 °C experiment with the Süd-Chemie catalyst, bio-oil could only be collected at the end of the experiment. The two catalysts used in this study had profoundly different effects on the physicochemical properties of bio-oil produced from forest thinnings. The bio-oil produced using silica sand exhibited characteristics typical for a conventionally produced bio-oil: high oxygen content, low heating value, and high viscosity. The BASF catalyst did not cause a large change in the properties of the bio-oil. The elemental composition, and consequently the

higher heating value, changed very little compared to the noncatalytic experiment. The viscosity of the first hour bio-oil sample did, however, decrease by more than 50% compared to silica sand. The sample that was collected after the second hour of the experiment already had a higher viscosity. This suggests that the catalyst was continuously losing its activity, which was already very limited during the first hour of the experiment. Since the viscosity decrease was not accompanied by a large change in the elemental composition of the bio-oil, it is possible that the change in viscosity occurred through cracking of heavier oligomeric molecules into lighter molecular weight products.

In contrast to the limited activity of the BASF catalyst, the Süd-Chemie catalyst caused significant changes in the properties of the bio-oil at 475 °C. There was a dramatic change in the elemental composition of the bio-oil, with the oxygen content reaching a minimum value of 19 wt %. This change was directly reflected in the higher heating value of the bio-oil, which increased from its reference value of 25.6 MJ/kg to as high as 32.8 MJ/kg. The higher heating value of the bio-oil samples followed a clear trend as a function of the molar O/C ratio, as is shown in Figure 5. The data presented in Figure 5 covers all the bio-oil samples shown in Table 4. When using the Süd-Chemie catalyst, the difference in the oxygen content of the samples collected at different time periods was 3−5 wt %. This shows that even after 1 h time-on-stream, the catalyst was still able to produce a deoxygenated bio-oil with improved fuel characteristics. The change in the elemental composition and the higher heating value of the bio-oil was also accompanied by a lower viscosity. For the experiments which were conducted at 475 °C with the Süd-Chemie catalyst, the amount of bio-oil collected after the first hour was not sufficient to measure the dynamic viscosity. The viscosity of the second hour sample was, however, clearly lower than what was obtained using silica sand or the BASF catalyst. While the viscosity of the first hour sample could not be quantified, visual inspection of the sample did indicate that the viscosity was lower compared to the second hour sample.

Varying the reaction temperature caused some interesting changes in the physical properties of the bio-oil. Reducing the reaction temperature to 400 °C caused the viscosity of the bio-oil to decrease. The viscosity of the sample collected during the first hour was only 62 cP, and even the second hour sample was clearly less viscous than the oil which was obtained at 475 °C.
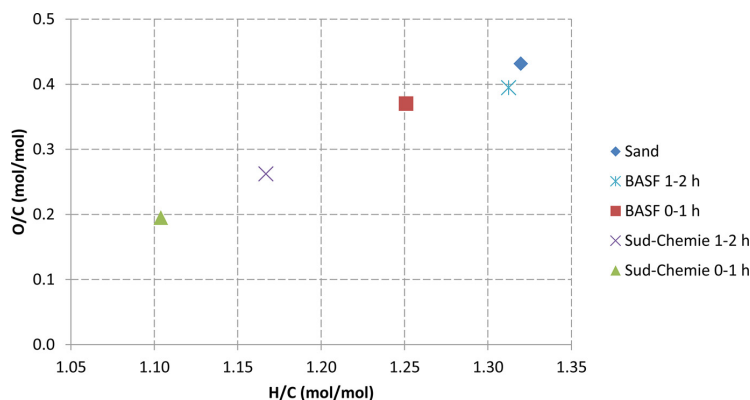
Figure 6. Van Krevelen plot for the bio-oils obtained in noncatalytic and catalytic pyrolysis at 475 °C.

Table 5. Relative Distribution of Carbon (%) in Bio-oils As Determined by ^{13}C NMR Spectroscopy

		carbon distribution (%) for the given pyrolysis medium, temperature (°C), and time (h)							
		sand	BASF		Süd-Chemie				
		475 °C	475 °C		400 °C		475 °C		550 °C
region (ppm)	carbon type	0−2 h	0−1 h	1−2 h	0−1 h	1−2 h	0−1 h	1−2 h	0−2 h
0−54	alkyl carbons	25.1	26.0	25.4	28.0	25.0	17.3	20.8	17.6
55−57	methoxyl	10.5	7.5	8.9	5.7	9.7	2.4	6.2	3.5
60−103	anhydrosugars, alcohols, ethers	23.4	14.2	18.2	3.1	5.2	0.9	3.8	8.8
103−160	aromatics and olefins	34.3	46.2	40.9	58.3	53.4	78.1	66.3	67.6
160−180	carboxylic acids, esters	5.1	4.8	5.2	3.3	4.2	0.9	1.9	1.3
180−220	aldehydes, ketones	1.6	1.4	1.3	1.5	2.5	0.3	0.9	1.2

In contrast to the viscosity change, the oxygen content was higher than at 475 °C. In this case, the decrease in viscosity cannot therefore be explained solely by deoxygenation of the bio-oil. The moisture content, which is known to affect viscosity,[36] of both bio-oils was also very similar. Thus, it seems plausible that lowering the reaction temperature could affect the chemical composition of bio-oil in such a fashion, where the viscosity decreases even though the oxygen content remains relatively high. In this work, when the reaction temperature was increased to 550 °C, no bio-oil could be collected after the first hour of the experiment. The oil that was used for characterization is, therefore, representative of the entire 2 h experimental period. Increasing the temperature to 550 °C caused a clear increase in the viscosity of the bio-oil. The temperature increase did not, however, induce a further decrease in the oxygen content of the bio-oil. The elemental composition was relatively similar to the second hour sample of the 475 °C experiment. The pH of the bio-oil also appeared to increase at higher temperatures. Similar observations about the effect of temperature on bio-oil viscosity and pH were made by Mante et al.[31] when hybrid poplar was pyrolyzed using FCC catalyst.

The overall effect of the catalysts on the elemental composition of bio-oil can be visualized using a Van Krevelen plot, which is shown in Figure 6 for the experiments conducted at 475 °C. In general, a high molar H/C and a low molar O/C ratio are desirable characteristics for a fuel, and conventional hydrocarbon fuels would be situated directly on the x-axis of the Van Krevelen plot. As can be clearly seen from Figure 6, catalytic pyrolysis produces a liquid product which has a lower O/C ratio and a lower H/C ratio compared to bio-oil produced

using conventional fast pyrolysis. The low H/C ratio, which is in part caused by the dehydration reactions taking place in catalytic pyrolysis, signifies the increased proportion of aromatic compounds in the bio-oil. Molecules of this type contain similar amounts of hydrogen and carbon on a molar basis and thus have a low H/C ratio. Previous studies have shown that aromatic and olefinic carbon species can make up almost 70% of the total carbon atoms found in bio-oil which was produced using catalytic pyrolysis.[12,30] This kind of bio-oil could potentially be used as a fuel precursor for applications where high aromatics content is still a desired property, e.g., jet fuel. The Van Krevelen plot also shows the impact of catalyst deactivation on the elemental composition of bio-oil. There was a significant difference in the initial H/C and O/C ratios between the bio-oils produced using the BASF and Süd-Chemie catalysts. A similar phenomenon was, however, observed for both catalysts when comparing the first and second hour bio-oil samples. A clear shift toward the H/C and O/C values of the noncatalytically produced bio-oil took place for both catalysts. For the Süd-Chemie catalyst, the bio-oil collected at the end of experiment was still significantly different than the bio-oil which was produced using silica sand. In the case of the BASF catalyst, the bio-oil collected at the end of the experiment was already very similar compared to the noncatalytic experiment. This is a clear indication that, during the second hour of the experiment, the BASF catalyst had lost a significant part of its deoxygenation activity, which was very limited even during the first hour.

Bio-oil Chemical Composition. *^{13}C NMR Spectrometric Analysis.* The bio-oils produced in these experiments were initially characterized using ^{13}C NMR spectroscopy. The results
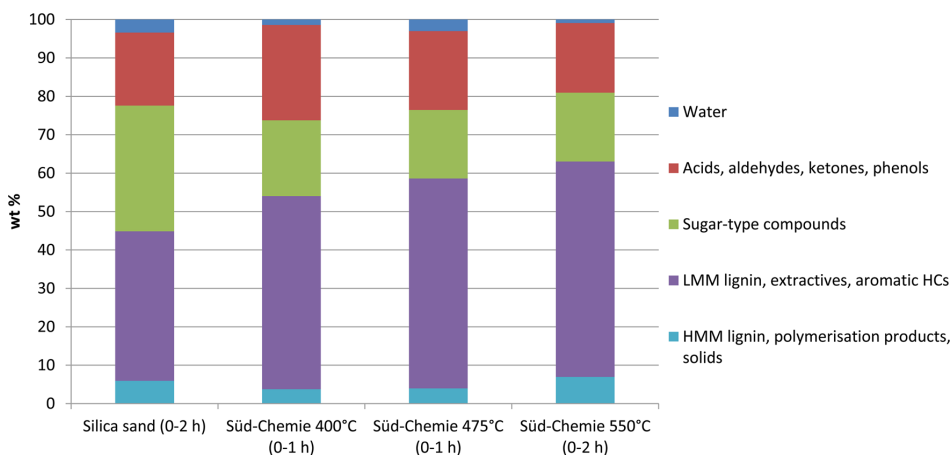
Figure 7. Solvent fractionation of bio-oils produced using silica sand and the Süd-Chemie catalyst.

from the semiquantitative integration of the spectra are shown in Table 5, which shows the distribution of carbon among the different functional groups present in bio-oil. The interpretation of the ^{13}C NMR spectra was carried out as reported by Mante et al.[30] The use of the BASF catalyst caused a very limited change in the chemical composition of the bio-oil. The intensity of the 60−105 ppm region which contains levoglucosan, anhydrosugars, alcohols, and ethers decreased slightly, while the 105−160 ppm region which contains olefins and aromatic compounds showed a small increase. Zeolite-based catalysts have been typically found to be effective in partially eliminating compounds, such as levoglucosan, that are found in the 60−105 ppm region.[3,12] The amount of methoxyl carbon also decreased slightly. These results, however, clearly show that the BASF catalyst was not able to alter the chemical composition of the bio-oil produced from forest thinnings to a large extent. Even though the bio-oil sample was collected after the first hour of the experiment, the physicochemical similarity compared to the bio-oil which was produced using silica sand suggests that the BASF catalyst possessed a very limited initial activity toward deoxygenation reactions, or that the catalyst deactivated very rapidly. Comparing the first and second hour samples, it can be seen that catalyst deactivation led to an increased proportion of oxygenated functionalities. The relative change was clearest for the carbohydrate degradation products and for the methoxyl carbon. The proportion of aromatic compounds decreased due to catalyst deactivation.

The Süd-Chemie catalyst, however, had a significant effect on the chemical composition of the bio-oil which was produced during the first hour of the experiment. At 475 °C, the amount of levoglucosan, acids, and aldehydes/ketones clearly decreased, which was accompanied by a large increase in the amount of aromatic compounds. By combining the results of the ^{13}C NMR spectroscopy with the elemental analysis, it appears that the Süd-Chemie catalyst was especially effective in eliminating highly oxygenated molecules such as levoglucosan, which led to an increase in the proportion of aromatic molecules. A clear decrease in the amount of methoxyl phenols, carboxylic acids, and aldehydes and ketones was also observed. For the second hour sample, the effect of catalyst deactivation could be seen most clearly in the amounts of carbohydrate degradation products, aromatics and methoxylated phenols. Even though

the concentration of carbohydrate degradation products approximately quadrupled compared to the first hour sample, the overall concentration was still very low. The concentration of aromatics also remained high, although there was a clear decrease compared to the first hour sample. Lowering the reaction temperature resulted in the production of less aromatic bio-oil. Lignin is known to form large amounts of char at lower temperatures,[37,38] which can in turn explain the lower amount of aromatic molecules in the bio-oil. This also correlates with the increase in char yield which was observed in this study at 400 °C. Observation of the general carboxylic acid region at 160−180 ppm and aldehyde/ketone region at 180−210 ppm showed that overall conversion of oxygenated functionalities was not as effective at 400 °C as it was at 475 °C. Before discussing the properties of the bio-oil which was produced at 550 °C, it should be once again pointed out that this sample represents the overall organic product which was formed during the 2 h of the experiment. If a separate sample would have been successfully collected after the first hour of the experiment, as was done at 400 and 475 °C, one would expect it to be different than the overall sample presented here. The bio-oil produced at 550 °C was also less aromatic compared to 475 °C. The amount of alkyl carbons was roughly the same, whereas the extent of demethoxylation and carbohydrate degradation product conversion was lower than at 475 °C. The increased concentration of for example levoglucosan can most likely be attributed to catalyst deactivation, since the formation of these kind of oxygenates has been shown to increase over time in catalytic pyrolysis.[29]

Solvent Fractionation and Quantitative GC-FID Analysis of Water-Soluble Organics. In addition to the ^{13}C NMR analysis, the bio-oil samples which were produced using silica sand and the Süd-Chemie ZSM-5 catalyst were characterized using solvent fractionation and gas chromatography. The results of the solvent fractionation analysis are shown in Figure 7. A clear difference could be seen between the bio-oil that was produced using silica sand and the catalytically produced bio-oils. The use of the catalyst led to a decrease in the ether-insoluble fraction, which contains sugar-type compounds. This supports the results which were obtained using ^{13}C NMR spectroscopy, but there were some clear differences between these two methods. Although the ^{13}C NMR results showed a
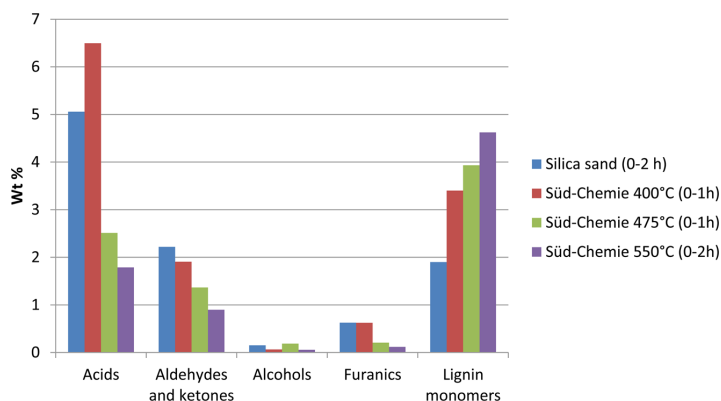
**Figure 8.** Quantitative GC-FID analysis of water-soluble organic compounds in bio-oil.
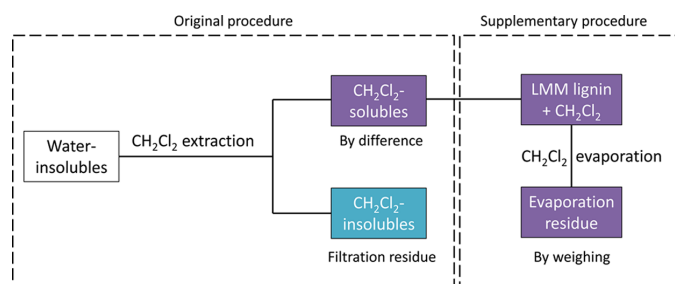
Figure 9. Original and supplementary procedure for quantifying the LMM lignin fraction in VTT's solvent fractionation method.

clear decrease in the amount of carbohydrate degradation products such as levoglucosan, a significant amount of ether-insoluble sugar-type compounds was still detected in the solvent fractionation. Comparing the Süd-Chemie 400 °C bio-oil sample to the silica sand bio-oil sample, a 6 wt % increase in the amount of ether-soluble compounds can be seen. This compound group contains light molecular weight oxygenate molecules, which can have a solubilizing effect on the entire bio-oil matrix. Thus, the increase in these kinds of compounds could be one of the factors which might explain the low viscosity of the 400 °C sample. At higher reaction temperatures, the amount of ether-soluble compounds was lower and the gas yield was higher, which indicates that some of these light oxygenates were converted to gases. This claim was further supported by the results of the GC-FID analysis for the water-soluble part of bio-oil, the results of which are presented in Figure 8. In Figure 8, bio-oil−water-soluble organic compounds were divided into five groups in order to highlight the changes caused by the catalyst and the variation of the reaction temperature. When compared to the noncatalytically produced bio-oil sample, the use of the catalyst at 400 °C caused an increase in the amount of acids, which consisted mainly of acetic acid. Increasing the reaction temperature caused a clear decrease in the concentration of acids in the catalytic experiments. This supports the observed increase in bio-oil pH at higher reaction temperatures. The concentration of aldehydes and ketones decreased in catalytic pyrolysis oils. At higher reaction temperatures, the concentration of furanic compounds decreased, whereas at 400 °C the concentration remained at a level similar to that of the noncatalytic

experiment. The concentration of lignin monomers increased when the catalyst was used, and the highest concentration was observed when the reaction temperature was 550 °C. In general, the use of the catalyst mainly increased the concentration of phenol, cresols, and catechols.

A general trend that could be observed in Figure 7 for all of the catalytically produced bio-oils was the increase in the light molecular mass (LMM) lignin fraction. While this change partly reflected the conversion or elimination of other fractions, any aromatic hydrocarbons which were formed would be quantified as a part of this fraction. This is due to the fact that aromatic hydrocarbons are insoluble in water but soluble in dichloromethane. Other nonpolar molecules would exhibit similar behavior as well. In the second stage of the solvent fractionation scheme, the water-insoluble fraction was extracted with dichloromethane, and the dichloromethane-insoluble residue was filtered and weighed in order to quantify the fraction containing HMM lignin, polymerization products, and solids (Figure 2). In the results which are shown in Figure 7, the amount of LMM lignin was calculated as the difference between the overall water-insoluble fraction and the amount of HMM lignin. In addition to calculating the amount of LMM lignin by difference, evaporation of the dichloromethane solution containing the LMM lignin fraction was carried out at room temperature after the extraction step. The difference in these two procedures is shown in Figure 9. If this LMM lignin fraction consisted of nothing but lignin-derived oligomers, it could be expected that not much of the sample material would be lost in the evaporation of the dichloromethane. Thus, the mass of the evaporation residue should be close to the mass

Table 6. Quantification of the Light Molecular Mass Lignin Fraction by Calculation and Evaporation/Weighing

|	LMM lignin fraction amount for the given pyrolysis medium, temperature (°C), and time (h)			
	silica sand	Süd-Chemie		
	475 °C (0−2 h)	400 °C (0−1 h)	475 °C (0−1 h)	550 °C (0−2 h)
LMM lignin by difference (wt %)	38.9	50.3	54.6	56.1
LMM lignin by evaporation/weighing (wt %)	38.7	47.9	47.6	51.7
difference (wt %)	0.3	2.4	7.0	4.3
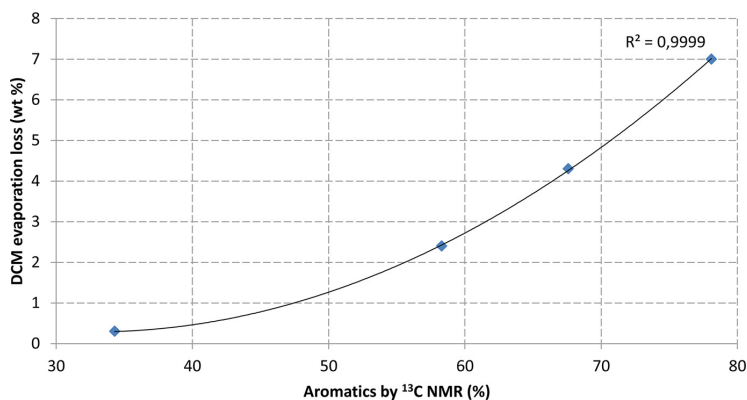
Figure 10. Mass loss in LMM lignin dichloromethane evaporation as a function of ^{13}C NMR aromatics content.
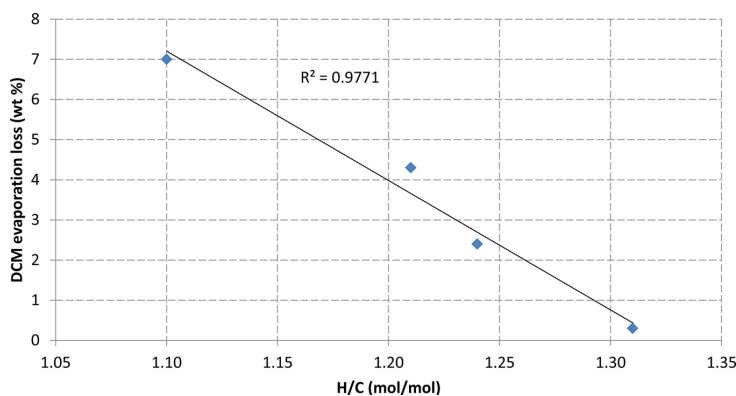
Figure 11. Mass loss in LMM lignin dichloromethane evaporation as a function of bio-oil molar H/C ratio.

that was obtained by difference. However, if this LMM lignin fraction contained aromatic hydrocarbons, some of them could evaporate together with the dichloromethane. The differences in the quantification of LMM lignin are shown in Table 6. Based on these results, it is clear that use of the Süd-Chemie catalyst produced more water-insoluble and dichloromethane-soluble compounds which evaporated together with dichloromethane at room temperature. The extraction and evaporation procedure which was described here is relatively straightforward to perform, and thus it would be interesting if its results could be correlated with a more specific and accurate quantification method. As an example, Figure 10 shows a plot of the mass loss in the evaporation of the LMM lignin dichloromethane solution as a function of aromatics content as determined by ^{13}C NMR. These particular results appear to show a clear correlation, but naturally the usability of such a method would have to be confirmed using a wider array of samples and alternative

analytical techniques. Another factor which could potentially be used as a measure for bio-oil aromaticity is the molar H/C ratio. Figure 11 contains a plot of LMM lignin evaporation mass loss as a function of bio-oil molar H/C ratio. This showed a clear trend between the molar H/C ratio and the dichloromethane evaporation mass loss. Thus, two separate analytical parameters associated with bio-oil aromaticity, i.e., aromatics content by ^{13}C NMR spectroscopy and the molar H/C ratio, both appear to show a correlation with the amount of evaporable compounds in the LMM lignin fraction. The solvent fractionation method that was employed in this study has been a valuable tool for characterizing conventional bio-oils which consist of polar compounds. However, its inability to differentiate between low molecular mass lignin and fully nonpolar compounds limits its effectiveness in the characterization of upgraded pyrolysis products. Thus, further refinement of the present solvent fractionation method with

particular regard to the LMM lignin fraction is a task that could be pursued in the future.

Quantitative GC-FID of Aromatics and GC-MS. In order to measure the amount of aromatic hydrocarbons in the bio-oils, a quantitative GC-FID analysis was carried out using methodology which has been originally developed for the analysis of biomass gasification tars.[39] The results of this analysis are presented in Table 7. The results show that the catalytically

Table 7. Amount (wt %) of Aromatic Hydrocarbons and Oxygenates in Bio-oil Samples with Süd-Chemie Catalyst

	amount (wt %) for the given temperature (°C) and time (h)		
sample	400 °C (0−1 h)	475 °C (0−1 h)	550 °C (0−2 h)
benzene	0.38	0.17	0.10
toluene	0.14	0.33	0.35
ethylbenzene	0.17	0.18	0.14
m- + *p*-xylene	0.27	0.61	0.41
o-xylene	0.09	0.25	0.10
phenol	0.85	1.83	2.60
indene	0.14	0.44	0.42
o-cresol	0.35	0.92	1.02
m- + *p*-cresol	0.65	1.72	1.91
naphthalenes	0.93	1.71	1.61
dibenzofuran	0.06	0.25	0.23
2-methyl-1-naphthol	0.26	0.34	0.15

produced bio-oils contained both single-ring benzene derivatives, naphthalene compounds as well as some oxygenated aromatics such as different phenolic molecules and dibenzofuran. Because the samples for 400 and 475 °C catalytic experiments were collected after 1 h and the sample for 550 °C was collected at the end of the experiment, direct comparison cannot be performed. However, a general trend between the 400 and 475 °C samples is that more aromatic hydrocarbons were produced at 475 °C. This phenomenon can be seen for single-ring and two-ring aromatics. For the catalytic 550 °C sample, it can be seen that the concentration of indene and naphthalenes was similar compared to the catalytic 475 °C sample. For toluene and ethylbenzene, the concentrations were similar at 475 and 550 °C, whereas the concentration of *m*-xylene and *o*-xylene was higher in the 475 °C sample. It has been reported in the literature[6,29] that increasing the reaction

temperature from 500 to 600 °C increased the yield of hydrocarbon products. Thus, it is possible that more aromatic hydrocarbons could have been produced at 550 °C during the first hour of the experiment. However, this should be confirmed in a larger reactor system where more bio-oil could be collected after the first hour of the experiment. Although the overall amount of aromatics was somewhat lower than the mass loss in evaporation of the LMM lignin dichloromethane solution, a correlation could still be observed between these two factors. This is presented in Figure 12, where the evaporation mass loss is shown as a function of concentration of single-ring and two-ring aromatic hydrocarbons. The noncatalytically produced bio-oil contained only trace amounts of aromatic hydrocarbons, and the peaks did not separate as clearly as they did in the catalytic bio-oil samples. Because of this and the fact that this evaporation step is more relevant for catalytically produced bio-oils, the silica sand sample was omitted from Figure 12. Based in Figure 12, it was clear that the observed mass loss in the DCM evaporation step did not show a 1:1 correlation with the concentration of one- and two-ring aromatic hydrocarbons. There was, nevertheless, a clear correlation between the two. Based on this limited number of samples, it appears that this DCM evaporation step could possibly be incorporated into the existing solvent fractionation method as a preliminary screening step for detecting the presence of aromatic hydrocarbons. This method could then be supplemented by a more accurate quantification method such as GC-FID.

In order to confirm the presence of the quantified aromatic molecules, GC-MS analyses were also carried out. The GC-MS spectra for the silica sand and Süd-Chemie 475 °C bio-oils are presented in Figure 13. The dominant compound groups have been emphasized using arches. Example compounds from each group are shown in Table 8. It is clear from Figure 13 that use of the catalyst significantly altered the chemical composition of the bio-oil, as was already determined using other analytical methods. Most carbohydrate degradation products which were detected in the silica sand bio-oil, including levoglucosan, were for the most part absent in the Süd-Chemie 475 °C sample. Syringols remained one of the dominant compounds in both bio-oil samples, but use of the catalyst increased the formation of monomeric phenols and catechols. The GC-MS analysis also confirmed the presence of aromatic hydrocarbon molecules which were detected in the GC-FID quantification. In addition
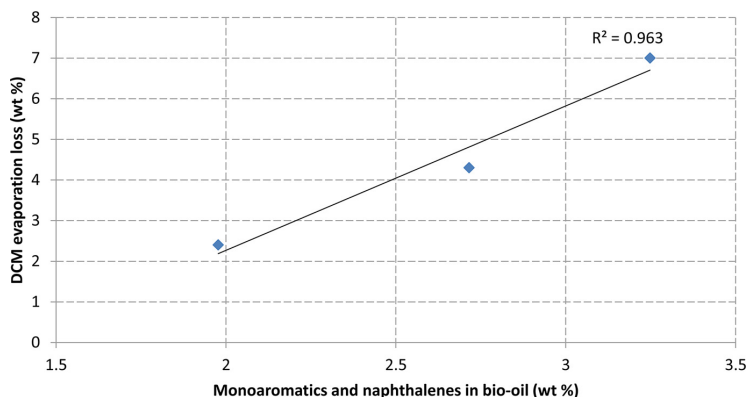

Figure 12. Mass loss in LMM lignin dichloromethane evaporation as a function of single-ring and two-ring aromatic hydrocarbon concentration.
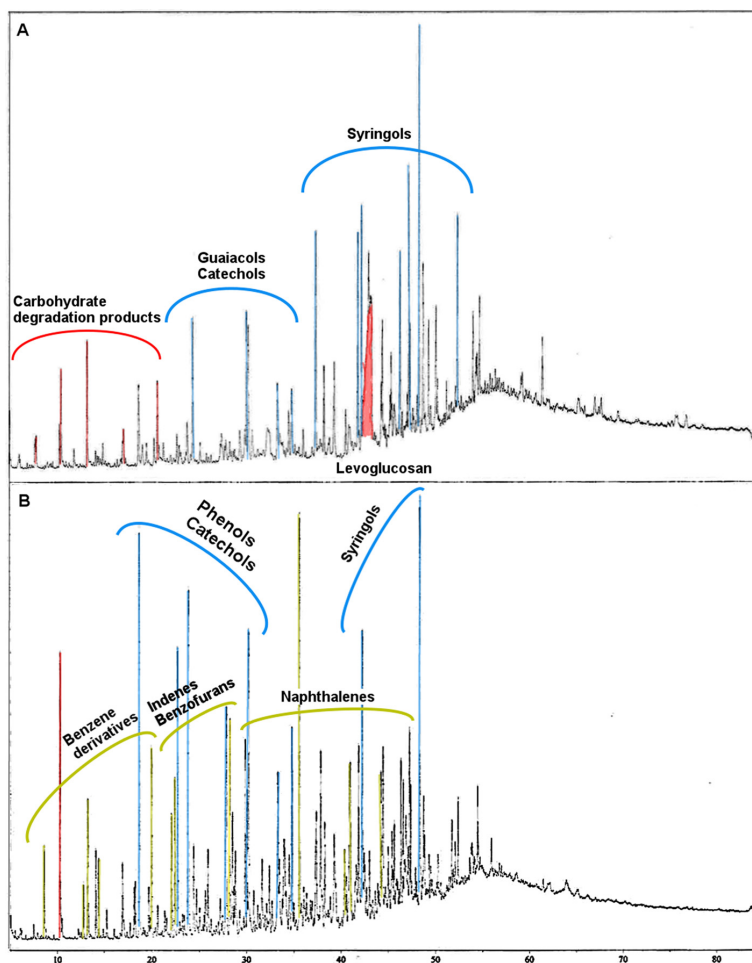
Figure 13. GC-MS spectra of the bio-oils produced at 475 °C using silica sand (A) and Süd-Chemie catalyst (B).

to the quantified compounds, other aromatic molecules such as trimethylbenzene were also detected.

Effect of Bio-oil Chemical Composition on Viscosity. Another important aspect is the effect chemical composition has on bio-oil viscosity. The bio-oil samples in this study all had similar water content, and thus its effect was ruled out as the primary reason for viscosity change. Therefore, the next step was to consider which other compound groups could have a solubilizing effect on the overall bio-oil matrix. According to the present understanding, the compounds contained in ether-soluble fraction, i.e., acids, aldehydes, ketones, and phenols, have a solubilizing effect on bio-oil. Single-ring aromatic hydrocarbons are also known to be good solvents. Thus, it is conceivable that the combined effect of these two compound groups could have a significant effect on bio-oil viscosity. In this case, the previously mentioned dichloromethane evaporation mass loss was used as a measure for compounds which could potentially have a solubilizing effect for the bio-oil. Plotting bio-oil viscosity as a function of the combined amount of ether-soluble compounds and the mass loss of the LMM lignin dichloromethane evaporation yielded the results shown in

Figure 14. Because the dynamic viscosity of the Süd-Chemie 475 °C sample could not be quantified, the number of data points presented in Figure 14 is limited to three. These three points do, however, exhibit a linear correlation. Even combined with the ^{13}C NMR analysis results, physical characteristics such as elemental composition or water content were not enough for explaining the observed changes in bio-oil viscosity. On the other hand, this approach where the amount of different solubilizing compounds is considered as the main factor affecting bio-oil viscosity could offer a logical explanation for the viscosity differences observed in this study.

■ CONCLUSION

Catalytic pyrolysis with an acidic ZSM-5 catalyst was used for producing partially deoxygenated bio-oil from forest thinnings at reaction temperatures of 400−550 °C. Use of the catalyst resulted in a lower yield of organic liquids, whereas more noncondensable gases, water, and coke were produced. Compared to bio-oil produced using silica sand, the catalytically produced bio-oil exhibited a lower oxygen content and improved fuel properties, such as increased heating value and

Table 8. Example Compounds Identified in Bio-oil Using GC-MS
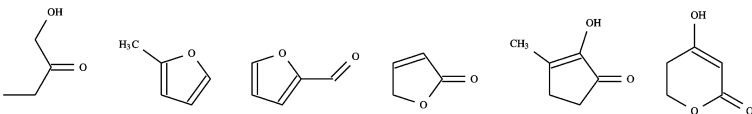
| Carbohydrate degradation products | |
Phenols	
Guaiacols & catechols	
Syringols	
Benzene derivatives	
Indenes & benzofurans	
Naphthalenes	
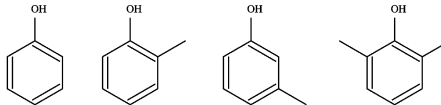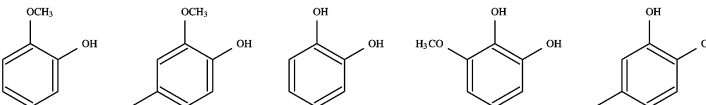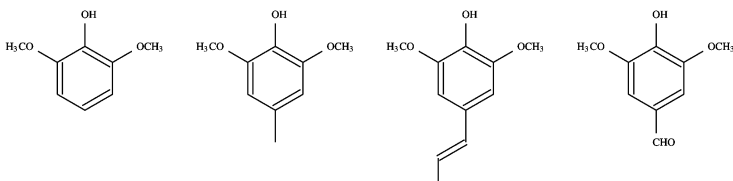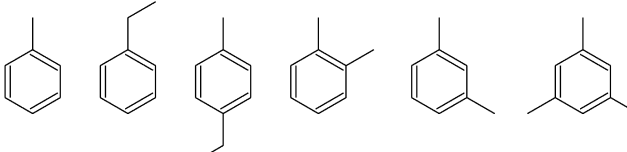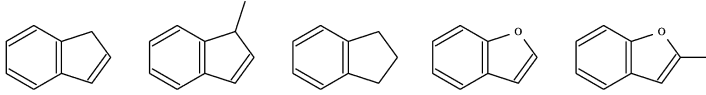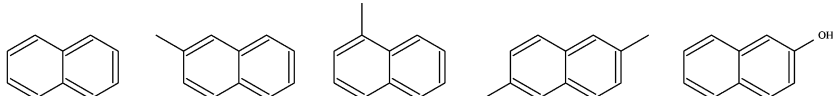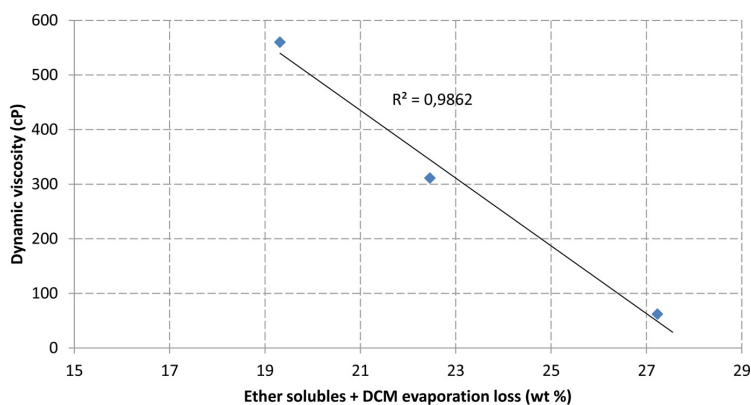
Figure 14. Bio-oil dynamic viscosity at 40 °C as a function of solubilizing compounds amount.

decreased viscosity. These characteristics should improve the usability of catalytically produced bio-oil in various end-use applications such as energy production or further processing to transportation fuels. The catalyst was effective in eliminating carbohydrate-derived oxygenate molecules, which resulted in a more aromatic bio-oil. The catalytically produced bio-oils contained more lignin monomers such as phenol and cresols, as well as some aromatic hydrocarbons such as toluene, xylenes, and naphthalenes. Varying the reaction temperature affected both the product distribution and the physicochemical properties of the bio-oil. Factors such as elemental composition, viscosity, pH, and chemical composition were affected by the reaction temperature. Operating at 400 °C produced a bio-oil with low viscosity but a relatively high oxygen content. Chemical characterization showed that the oil contained a large amount of low molecular weight oxygenate molecules with solvent-like properties. Operating at 550 °C produced a more viscous oil with a higher pH. This oil contained the largest amount of lignin-derived water-insoluble compounds. Solvent fractionation analyses showed that catalytically produced bio-oils contained a varying amount of water-insoluble volatile compounds. A correlation was observed between the amount of water-insoluble volatiles and the amount of aromatic hydrocarbons in bio-oil, as quantified by GC-FID. The existing solvent fractionation method can be supplemented by determining the amount of water-insoluble volatiles as a preliminary screening measure for the presence of aromatic hydrocarbons.

■ **AUTHOR INFORMATION**

Corresponding Author
*E-mail: ville.paasikallio@vtt.fi.

Notes
The authors declare no competing financial interest.

■ **REFERENCES**

(1) Mohan, D.; Pittman, C. U.; Steele, P. H. *Energy Fuels* **2006**, *20*, 848−889.
(2) Oasmaa, A.; Czernik, S. *Energy Fuels* **1999**, *13*, 914−921.
(3) Agblevor, F. A.; Beis, S.; Mante, O.; Abdoulmoumine, N. *Ind. Eng. Chem. Res.* **2010**, *49*, 3533−3538.
(4) Mullen, C. A.; Boateng, A. A.; Mihalcik, D. J.; Goldberg, N. M. *Energy Fuels* **2011**, *25*, 5444−5451.
(5) Carlson, T. R.; Vispute, T. P.; Huber, G. W. *ChemSusChem* **2008**, *1*, 397−400.
(6) Carlson, T. R.; Cheng, Y.-T.; Jae, J.; Huber, G. W. *Energy Environ. Sci.* **2011**, *4*, 145−161.
(7) Carlson, T. R.; Jae, J.; Lin, Y.-C.; Tompsett, G. A.; Huber, G. W. *J. Catal.* **2010**, *270*, 110−124.
(8) Mihalcik, D. J.; Mullen, C. A.; Boateng, A. A. *J. Anal. Appl. Pyrolysis* **2011**, *92*, 224−232.
(9) Agblevor, F. A.; Besler-Guran, S. *Prepr. Symp.—Am. Chem. Soc., Div. Fuel Chem.* **2002**, *47*, 374−375.
(10) Zhang, H.; Xiao, R.; Wang, D.; Zhong, Z.; Song, M.; Pan, Q.; He, G. *Energy Fuels* **2009**, *23*, 6199−6206.
(11) Lappas, A. A.; Samolada, M. C.; Iatridis, D. K.; Voutetakis, S. S.; Vasalos, I. A. *Fuel* **2002**, *81*, 2087−2095.
(12) Mante, O. D.; Agblevor, F.; Oyama, S.; McClung, R. *Appl. Catal., A* **2012**, *445–446*, 312−320.
(13) Aho, A.; Tokarev, A.; Backman, P.; Kumar, N.; Eränen, K.; Hupa, M.; Holmbom, B.; Salmi, T.; Murzin, D. *Top. Catal.* **2011**, *54*, 941−948.
(14) Olazar, M.; Aguado, R.; Bilbao, J.; Barona, A. *AIChE J.* **2000**, *46*, 1025−1033.
(15) Stefanidis, S.; Kalogiannis, K.; Iliopoulou, E.; Lappas, A.; Pilavachi, P. *Bioresour. Technol.* **2011**, *102*, 8261−8267.
(16) de Miguel Mercader, F.; Groeneveld, M.; Kersten, S.; Way, N.; Schaverien, C.; Hogendoorn, J. *Appl. Catal., B* **2010**, *96*, 57−66.
(17) Fogassy, G.; Thegarid, N.; Toussaint, G.; van Veen, A. C.; Schuurman, Y.; Mirodatos, C. *Appl. Catal., B* **2010**, *96*, 476−485.
(18) Agblevor, F. A.; Mante, O.; McClung, R; Oyama, S. *Biomass Bioenergy* **2012**, *45*, 130−137.
(19) Corma, A.; Huber, G. W.; Sauvanaud, L.; O'Connor, P. *J. Catal.* **2007**, *247*, 307−327.
(20) Lappas, A.; Bezergianni, S.; Vasalos, I. *Catal. Today* **2009**, *145*, 55−62.
(21) Oasmaa, A.; Solantausta, Y.; Arpiainen, V.; Kuoppala, E.; Sipilä, K. *Energy Fuels* **2010**, *24*, 1380−1388.
(22) Solantausta, Y.; Oasmaa, A.; Sipilä, K.; Lindfors, C.; Lehto, J.; Autio, J.; Jokela, P.; Alin, J.; Heiskanen, J. *Energy Fuels* **2012**, *26*, 233−240.
(23) Evans, R. J.; Milne, T. A. *Prepr. Pap.—Am. Chem. Soc., Div. Fuel Chem.* **1987**, *32*, 287−296.
(24) Diebold, J.; Scahill, J. *Prepr. Pap.—Am. Chem. Soc., Div. Fuel Chem.* **1987**, *32*, 297−306.
(25) Jae, J.; Tompsett, G. A.; Foster, A. J.; Hammond, K. D.; Auerbach, S. M.; Lobo, R. F.; Huber, G. W. *J. Catal.* **2011**, *279*, 257−268.
(26) Carlson, T.; Tompsett, G.; Conner, W.; Huber, G. *Top. Catal.* **2009**, *52*, 241−252.
(27) Foster, A. J.; Jae, J.; Cheng, Y.-T.; Huber, G. W.; Lobo, R. F. *Appl. Catal., A* **2012**, *423–424*, 154−161.
(28) Ma, Z.; Troussard, E.; van Bokhoven, J. A. *Appl. Catal., A* **2012**, *423–424*, 130−136.
(29) French, R.; Czernik, S. *Fuel Process. Technol.* **2010**, *91*, 25−32.
(30) Mante, O. D.; Agblevor, F.; Oyama, S.; McClung, R. *Bioresour. Technol.* **2012**, *111*, 482−490.
(31) Mante, O. D.; Agblevor, F.; McClung, R. *Fuel* **2013**, *108*, 451−464.
(32) Oasmaa, A.; Kuoppala, E.; Solantausta, Y. *Energy Fuels* **2003**, *17*, 433−443.
(33) Smith, G. M.; Speronello, B. K. ZSM-5 Additive. U.S. Patent 7547653 B2, BASF Catalysts LLC, Jun. 16, 2009.
(34) Pattiya, A.; Suttibak, S. *J. Anal. Appl. Pyrolysis* **2012**, *95*, 227−235.
(35) Kang, B.-S.; Lee, K. H.; Park, H. J.; Park, Y.-K.; Kim, J.-S. *J. Anal. Appl. Pyrolysis* **2006**, *76*, 32−37.
(36) Oasmaa, A.; Peacocke, C. *Properties and fuel use of biomass-derived fast pyrolysis liquids. A guide*, VTT Publications 731; VTT: VTT, Finland, 2010.
(37) Thring, R. W.; Katikaneni, S. P. R.; Bakhshi, N. N. *Fuel Process. Technol.* **2000**, *62*, 17−30.
(38) Zhao, Y.; Deng, L.; Liao, B.; Fu, Y.; Guo, Q.-X. *Energy Fuels* **2010**, *24*, 5735−5740.
(39) Simell, P.; Ståhlberg, P.; Kurkela, E.; Albrecht, J.; Deutsch, S.; Sjöström, K. *Biomass Bioenergy* **2000**, *18*, 19−38.

Publication III

Ville Paasikallio, Christian Lindfors, Eeva Kuoppala, Yrjö Solantausta, Anja Oasmaa, Jani Lehto, Juha Lehtonen. Product quality and catalyst deactivation in a four day catalytic fast pyrolysis production run. *Green Chemistry*, **Volume 16, pages 3549-3559, DOI: 10.1039/c4gc00571f, June 2014.**

Green Chemistry

PAPER

Product quality and catalyst deactivation in a four day catalytic fast pyrolysis production run†

Ville Paasikallio,*[a] Christian Lindfors,[a] Eeva Kuoppala,[a] Yrjö Solantausta,[a] Anja Oasmaa,[a] Jani Lehto[a] and Juha Lehtonen[b]

Catalytic fast pyrolysis of pine sawdust was successfully carried out in VTT's 20 kg h^{-1} Process Development Unit using a spray dried HZSM-5 catalyst. Approximately 250 kg of partially deoxygenated pyrolysis oil was produced over a period of four days. The catalytically produced pyrolysis oil had an average moisture content of 8.3 wt%, and average carbon and oxygen contents of 72.0 and 21.5 wt% on a dry basis, respectively. Approximately 24% of the original biomass carbon was present in the pyrolysis oil, whereas 14% of carbon was in the form of aqueous side products, which totaled approximately 600 kg. The pyrolysis oil contained a high amount of lignin derived water-insoluble material, as well as 6.4 wt% of aromatic hydrocarbons. The majority of the carbohydrate derived products, *i.e.* acids, aldehydes, ketones and sugar-type compounds, were found in the aqueous product fraction. While the quality of pyrolysis oil remained quite stable during the four day experiment, distinct changes were observed in the properties and the behavior of the catalyst. Coke formation was heaviest at the beginning of the experiment, and then subsided over time. Catalyst micropore area and volume also decreased during the experiment. This transformation was accompanied by apparent changes in the crystallinity and the structure of the catalyst. Scanning electron microscope images of the catalyst also revealed clear physical damage to the particles. Biomass alkali metals also deposited on the catalyst, and the spent catalyst contained a total of 1.1 wt% of Ca, K, Mg and P after the experiment. A linear correlation was observed between catalyst alkali metal content and acidity, which indicated that biomass alkalis substituted the proton functionalities of the HZSM-5 acid sites.

1. Introduction

In the recent years, catalytic fast pyrolysis (CFP) of biomass has received a significant amount of attention as a way to produce partially deoxygenated bio-oils.[1–7] This is achieved by replacing the inert heat transfer material that is typically used in fast pyrolysis with a solid catalyst. Zeolites such as ZSM-5, β-zeolite, Y-zeolite and mordenite are among the most commonly used catalytic materials for catalytic pyrolysis.[6,8,9] In catalytic pyrolysis, the organic vapours released in the primary thermal decomposition reactions come into immediate contact with the catalyst. Oxygen is rejected from the pyrolysis vapours in the form of H_2O, CO and CO_2 as dehydration, decarbonylation and decarboxylation reactions take place over the catalyst. The intermediate reaction products formed in this stage can then react further on the acid sites of the catalyst to form higher value products such as aromatic hydrocarbons.[6,10] As the oxygen content of bio-oil decreases, its chemical composition shifts more towards petroleum-derived hydrocarbon fuels. This change can also be seen in the physicochemical properties of the bio-oil, as the use of catalysts enhances the formation of certain types of compound groups while others are diminished.[2,11] Decrease in the concentration of organic acids can result in an increased pH and lower total acid number (TAN).[4,12] Conversion of carbonylic compounds,[3,7] which are a known precursor[13] for the chemical instability of bio-oil, serves to increase the storage stability of bio-oil. Cracking of heavier lignin-derived oligomers into smaller phenolic monomers decreases the average molar mass of bio-oil, and consequently its viscosity. These positive changes in the bio-oil physicochemical characteristics can potentially pave the way for its use in new applications, such as co-processing in existing oil refinery processes.[14,15]

So far, the scale of catalytic pyrolysis experiments presented in open literature has ranged from analytical pyrolysis with a few grams of biomass/catalyst[8,16] to continuous fluidized-bed units with biomass processing capabilities of up to approxi-

[a]*VTT Technical Research Centre of Finland, P.O. Box 1000, 02044 VTT, Finland. E-mail: ville.paasikallio@vtt.fi*

[b]*Department of Biotechnology and Chemical Technology, School of Chemical Technology, Aalto University, P.O. Box 16100, 00076 Aalto, Finland*

†Electronic supplementary information (ESI) available. See DOI: 10.1039/c4gc00571f

mately 2 kg h^{-1}.[4,12] Apart from the results presented by Lappas et al.[1,17] the fluidized-bed reactor units employed in catalytic pyrolysis have been of the bubbling fluidized-bed (BFB) variety.[2–5,9,11,12] In a BFB reactor, the catalyst is in continuous contact with the biomass feedstock, and thus deactivates over time due to coke formation. If a high activity is to be maintained for the catalyst, it is necessary to periodically regenerate the catalyst. The rate of catalyst deactivation depends on the catalyst that is used. This factor also sets the requirements for the regeneration interval of the catalyst. Mullen et al.[4] observed significant differences in product yields and quality when experimenting with five and ten minute regeneration intervals for a β-zeolite related catalyst. In our previous work,[18] we identified that catalyst acidity significantly influenced coke formation over a time period of 30 minutes. Coke formation was heavier on more acidic catalysts, and thus they showed a tendency to deactivate more rapidly. A more acidic catalyst would, therefore, require regeneration on a more frequent basis. Because catalyst deactivation and regeneration is such a critical factor, any industrial-scale catalytic fast pyrolysis process would have to be equipped with online catalyst regeneration capabilities. In a conventional BFB pyrolysis reactor, this will require an additional means of removing deactivated catalyst, while simultaneously supplying regenerated catalyst into the reactor.

In contrast to the somewhat problematic nature of the BFB reactor, a circulating fluidized-bed (CFB) reactor offers more flexible operation especially when it comes to the continuous regeneration of the catalyst. The impact of reversible catalyst deactivation becomes less critical, as the catalyst is in contact with the biomass for merely a few seconds at a time. The catalyst is subsequently transported to the regenerator section, where the coke deposits are combusted along with the char and a part of the non-condensable gases. This provides heat for the pyrolysis process itself while simultaneously regenerating the catalyst. The continuous regeneration of the catalyst removes the need to consider how the activity of the catalyst changes over a time span of minutes, which would be a major concern in a BFB process along with the coking phenomenon associated with catalytic fast pyrolysis. When considering the long term stability of the catalyst, there are various factors that need to be taken into account as the catalyst is subjected to both physical and chemical strains. Operation in a CFB reactor can cause catalyst attrition, and thus high mechanical integrity is a very desired property for the catalyst.[19] Repeated exposure to both pyrolysis conditions and the oxidative atmosphere of the regenerator can also cause changes in catalyst structure. Brønsted acid sites, which are responsible for the strong acidity of zeolites in their proton form, can be lost due to dealumination of the zeolite framework.[20,21] Another potential source for catalyst deactivation are the metals that are found in biomass. While so far only a limited number of studies have discussed this phenomenon,[5,22,23] it has been shown that metals present in the biomass feedstock deposit on the catalyst during catalytic pyrolysis. Mullen and Boateng[23] reported a correlation between the presence of biomass metals on the

HZSM-5 catalyst and its efficiency for producing deoxygenated pyrolysis oil containing aromatic hydrocarbons. Studies in the field of selective catalytic reduction of nitrous oxides have shown that alkali metals, and especially potassium, can decrease the number of Brønsted acid sites.[24,25] While this effect is more pronounced for V_2O_5–WO_3–TiO_2 catalysts, it has also been observed when using Fe and Cu substituted ZSM-5 catalysts.[26,27] One point of interest is, therefore, to see what kind of effect long-term exposure to biomass alkali metals will have on catalyst activity in catalytic pyrolysis of biomass.

Lappas et al. were the first to publish results from catalytic pyrolysis of biomass in a CFB reactor.[1] They used two different catalysts in their experiments: a commercial equilibrium FCC catalyst and a ZSM-5 based FCC additive. At that time, the main difference that was detected in the chemical composition of pyrolysis oil was a clear decrease in the concentration of unidentifiable heavy oxygenates. Similar observations were made using both catalysts. High moisture content (37–67 wt%) affected the physical characterization of the pyrolysis oil from the catalytic experiments, but the pyrolysis oils in question showed e.g. better stability and lower micro carbon residue values compared to the non-catalytically produced reference sample. While a CFB reactor could be considered as the conventional choice for a continuous catalytic pyrolysis process with online catalyst regeneration, other reactor types have also been adopted for research purposes. Yildiz et al.[28] recently published results where they employed an auger-type reactor for catalytic pyrolysis of pine wood. Fresh ZSM-5 catalyst was continuously fed into the auger reactor along with the biomass, and thus the biomass was always pyrolysed in the presence of a fully active catalyst. As a result, the yield of organic liquids decreased from approximately 35 to 15 wt%. Analysis of the bio-oil organic fraction showed significant decreases in the concentrations of e.g. levoglucosan, acetic acid, hydroxyacetaldehyde, furfural and 1-hydroxy-2-propanone. On the other hand, the concentrations of phenolic monomers, single-ring aromatics and naphthalenes and indenes clearly increased with the use of the catalyst. Jae et al.[29] also utilized a similar approach where a ZSM-5 catalyst was continuously added and removed from a BFB reactor in CFP on pine wood. The authors reported a constant yield of aromatic hydrocarbons over a time course of 6 hours. While no online catalyst regeneration was employed in this study, subjecting the catalyst to 30 reaction–regeneration cycles caused the yield of aromatics to decrease from 14.2 to 12.2% (carbon yield). One possible reason for this was a decrease in the Brønsted acidity of the catalyst. Because no changes were observed in the crystallinity of the catalyst, the authors stated mineral impurities in the biomass feedstock could have poisoned the acid sites of the catalyst. Another recent development in the field of pyrolysis reactors was published by Zhang et al.[30] The internally interconnected fluidized bed (IIFB) reactor offers the possibility the operate a catalytic pyrolysis process which incorporates continuous catalyst regeneration together with char combustion. Pyrolysing rice husks in this reactor over a HZSM-5 catalyst resulted in a petrochemical

(aromatics + olefins) yield of up to 20% on a carbon basis. The duration of the experiment was 3 hours. This, along with the fact that little change was observed in the product distribution as a function of time, indicates that the catalyst is able to retain its activity and good petrochemical yields due to the continuous regeneration process. In contrast to this, the authors stated that clear catalyst deactivation could be seen in just 30 minutes when continuous regeneration of the catalyst was not carried out.

While a few examples of using fresh or continuously regenerated catalyst for catalytic pyrolysis exist in open literature, the duration of these experiments has been limited to a few hours. Thorough physicochemical characterization of pyrolysis oil produced in such a fashion has not yet been carried out either. In this study, catalytic pyrolysis of pine sawdust was carried out in a 20 kg h^{-1} circulating fluidized-bed reactor with continuous catalyst regeneration. The product yields and bio-oil properties were compared to results obtained in a non-catalytic experiment conducted with the same feedstock and reactor system. Extensive physical and chemical characterisation of the liquid products was carried out in order to better understand how the presence of a catalyst in a CFB reactor affects the physicochemical properties of pyrolysis oil. In addition to analysing the liquid products, characterization of catalyst samples which were taken before, during and after the experiment was conducted. This was done in order to determine how certain catalyst properties change when the catalyst was subjected to both pyrolysis and regeneration conditions over an extended period of time. To the best of our knowledge, this is the first time when results from biomass catalytic fast pyrolysis with continuous catalyst regeneration are publicly reported from a circulating fluidized bed unit of this size and capacity, and when the overall duration of the experiment reached almost one hundred hours.

2.   Experimental

2.1.   Biomass and catalyst

Pine sawdust was used as the feedstock in the catalytic pyrolysis experiment. The moisture content of the sawdust was 12.0 wt%. The dry biomass contained 0.4 wt% ash, and 51.4 wt%, 5.9 wt% and less than 0.1 wt% of carbon, hydrogen and nitrogen, respectively. Oxygen content, as determined by difference, was 42.2 wt%. Volatiles content was 83.9 wt% and the higher heating value (HHV) 20.4 MJ kg^{-1}. Besides the moisture content, all the aforementioned values are given on a dry basis. Approximately 95 wt% of the sawdust feedstock had a particle size of under 3.15 mm.

A spray dried ZSM-5 catalyst powder (CBV 5524G) was obtained from Zeolyst International. The catalyst was supplied in its ammonium form. Calcination of the catalyst, *i.e.* conversion into its proton form, was carried out in the CFB reactor system during the heat-up phase of the reactor. The SiO_2/Al_2O_3 ratio of the catalyst was 50 and the binder content 50%. Average particle size was 74 μm with 24 vol% of particles being

smaller than 40 μm and 3 vol% larger than 150 μm The bulk density of the catalyst was 0.78 g cm^{-3}. The specific surface area, as reported by the catalyst provider, was 235 m^2 g^{-1}. The catalyst was chosen based on data from preliminary bench-scale experiments.

2.2.   Reactor system

The pyrolysis experiments were carried out using VTT's 20 kg h^{-1} Process Development Unit (PDU) which employs a circulating fluidized-bed reactor. The system has been previously described in *e.g.* ref. 31. The feedstock is fed into the reactor using a screw feeder. The initial amount of catalyst in the system was 120 liters, which corresponded to approximately 94 kilograms. The catalyst to biomass ratio, *i.e.* the ratio of the hourly catalyst circulation rate and biomass feeding rate, was approximately 7 : 1 on a weight basis. The pyrolysis temperature was 520 °C and the fluidization velocity in the reactor was approximately 4 m s^{-1}. Upon exiting the reactor, the product vapour/gas stream passes through two cyclones where the catalyst particles and char are separated. The pyrolysis vapours are condensed in two liquid scrubbers where product pyrolysis oil is used for quenching the pyrolysis vapours. The scrubbers were operated at a temperature of 35 °C. The scrubbers are followed by a secondary condensation system where a highly aqueous liquid product, which will be referred to as condensate, was collected. After the liquid products have condensed, a certain part of the non-condensable gases is recycled to the reactor to be used as the fluidization gas, whereas any excess gas is combusted in the regenerator. Char and catalyst coke deposits are also combusted in the regenerator. The regenerator was operated at a temperature of 650–670 °C.

2.3.   Pyrolysis oil characterization

All the liquid products were analyzed for water content using Karl Fischer titration according to the standard ASTM E 203-96. The analyses were done using a Metrohm 795 KFT Titrino titrator. Elemental composition (CHN) of the pyrolysis oil was determined according to ASTM D 5291 using an Elementar VARIOMAX CHN analyzer. Higher heating value (HHV) was determined according to DIN 51900 using an IKA Werke C 5000 Control calorimeter. The solids content was analysed according to ASTM D7579. Density of the pyrolysis oil was measured according to ASTM D 4052 at 15 °C using an Anton Paar DMA 4500 M digital density meter. Kinematic viscosity was determined at 40 °C according to ASTM D 445. Total acid number (TAN) was determined potentiometrically according to ASTM D664. Micro carbon residue (MCR) of the bio-oil was analyzed according to ASTM D 4530 using an Alcor Micro Carbon Residue Tester. The ash content of the pyrolysis oil was determined by further combusting the micro carbon residue in a muffle furnace at 775 °C. Total organic carbon (TOC) of aqueous liquid products was measured using a Shimadzu TOC-5000A Total Organic Carbon Analyzer.

Several methods were used for characterising the chemical composition of pyrolysis liquids. A general overview for the chemical composition was obtained using the solvent fraction-

ation method,[32] where the pyrolysis oil was first separated into water-soluble and water-insoluble (WIS) fractions using water extraction. The water-soluble fraction was then divided into ether-soluble and ether-insoluble parts. The ether-soluble part contained acids, alcohols, aldehydes, ketones and lignin monomers while the ether-insoluble part contained sugar-type compounds such as anhydrosugars and anhydrooligomers. The water-insoluble fraction, on the other hand, was divided into low molecular weight (LMW) lignin and high molecular weight (HMW) lignin fractions. The LMW lignin fraction is defined as the dichloromethane-soluble part of the water-insoluble fraction. In addition to low molecular weight lignin oligomers, this fraction can also contain extractives and aromatic hydrocarbons. Besides the heaviest lignin oligomers, the HMW lignin fraction contains polymerization products and solids.

The water soluble fraction of pyrolysis liquids was also analyzed using gas chromatography. This was done using an Agilent Technologies 7890 A gas chromatograph equipped with an Agilent 19091 N-136 HP-Innowax column. The length of the column was 60 m, inner diameter was 250 μm and thickness of the liquid phase 0.25 μm. The carrier gas was helium. A flame ionization detector (FID) was used at a temperature of 280 °C. The column oven was first heated to 60 °C using a temperature ramp of 3 °C min⁻¹ and then to 230 °C in 30 minutes. Calibration was carried out using 40 water-soluble model compounds, and n-butanol was used as the internal standard. The list of quantified compounds can be seen in ref. 33. The content of aromatic hydrocarbons along with some oxygenated aromatics in the whole pyrolysis oil was quantitatively analyzed using an Agilent Technologies 6890 Series GC system, which was equipped with an Ultra 2 column (length, 23 m; inner diameter, 0.32 mm; film thickness, 0.52 μm. Calibration curves were determined using model compounds which ranged from benzene to pyrene. Dodecane was used as the internal standard. Compound identification was carried out using gas chromatography with a mass selective detector (GC-MSD). Measurements were performed using a Shimadzu GC17A gas chromatograph equipped with a mass selective quadrupole detector and a HP Ultra 1 fused silica capillary column (length: 50 m, inner diameter: 0.32 mm, film thickness: 0.52 μm.

2.4. Gas analysis

Non-condensable gases were sampled at one hour intervals and analyzed online using a Varian CP-4900 micro gas chromatograph. Three separate columns were used for quantifying the individual gas components. The column types were 5 Å molecular sieve (MS-5), porous polymer (PPU) and alumina (Al₂O₃). The following compounds were quantified: hydrogen (H₂), nitrogen (N₂), methane (CH₄), carbon monoxide (CO), carbon dioxide (CO₂), ethane (C₂H₆), ethene (C₂H₄), 1,2-propadiene (C₃H₄), propane (C₃H₈) and propene (C₃H₆).

2.5. Catalyst characterization

Catalyst samples were taken during the experiment using a sampling system located below the cyclones. Samples were

collected before the catalyst–char mixture was fed into the regenerator. The coke content of the spent catalyst samples was measured using temperature programmed oxidation (TPO) with a LECO TGA-601 thermogravimetric analyzer. The samples were first heated to 100 °C to remove any residual moisture, and then the temperature was ramped up to 815 °C using a heating rate of 10 °C min⁻¹. The samples were held at 815 °C for a minimum of 20 min. The coke content was determined in wt% as 100% – TPO residue of dehumidified sample at 815 °C. The specific surface area, micropore area and micropore volume of the catalysts were determined using N₂ physisorption. The measurements were performed with a Micromeritics Tristar surface area analyser. The specific surface area was determined at P/P₀ 0.05–0.3 using the Brunauer–Emmett–Teller (BET) equation. Micropore area and volume were determined at P/P₀ 0.2–0.5 using the t-plot method where the statistical thickness was calculated using the method of Harkins and Jura. X-ray diffraction (XRD) patterns of the catalysts were recorded with a Philips X'Pert MPD diffractometer using Cu Kα radiation. The samples were scanned for 2θ angles between 5° and 50° with a resolution of 0.02°. Acidity of the catalyst samples was measured using temperature programmed desorption of ammonia NH₃ (NH₃-TPD). The NH₃-TPD spectra of the catalysts were measured using a flow through microreactor equipped with a Balzers GAM-415 quadrupole mass spectrometer. The catalyst sample (400 mg) was saturated with 1 ml pulses of 5 vol% NH₃ in He at a temperature of 30 °C. The catalyst was then flushed in He flow for 15 minutes, after which the temperature was ramped at a rate of 5 °C min⁻¹ to 650 °C while monitoring mass number 17. The potassium (K), phosphorous (P), magnesium (Mg) and calcium (Ca) content of the catalyst samples was measured using inductively coupled plasma atomic emission spectroscopy (ICP-AES). The measurements were carried out using a Perkin-Elmer 7100 DV ICP-AES analyzer coupled with a Varian AA240 atomic absorption spectrometer. The catalyst samples were studied with a scanning electron microscope (SEM) JEOL JSM6400 combined with an energy dispersive X-ray analyser PGT Spirit. Samples of the catalyst particles were mounted on an electrically conductive adhesive. The samples were coated with a thin carbon coating using a Polaron TB500 Carbon Coater. Secondary electrons with an acceleration voltage of 12 kV were used in the imaging.

3. Results and discussion

3.1. Overview of the experiment

The overall duration of the experiment was approximately 4 days. Samples were collected from both scrubbers at one hour intervals and from the condensate at two hour intervals. The average water content of the pyrolysis oil from scrubbers 1 and 2 was approximately 50 and 30 wt%, respectively. After an initial ten hour stabilization phase at the beginning of the experiment, all the liquid products collected from scrubbers 1 and 2 phase separated into an oil fraction (bottom phase)

and an aqueous fraction (top phase). It should be emphasized that phase separation took place even when the water content in scrubber 2 decreased to approximately 20 wt%. This clearly indicates that the chemical composition of the pyrolysis oil had become significantly less polar than what is typically observed for non-catalytically produced oils, which tend to phase separate only when the water content exceeds about 30 wt%.[34] Larger samples of the product liquids were collected from the scrubbers at four hour intervals throughout the experiment. The two-phase products were then separated into oil and aqueous fractions using a separating funnel. The water content of the aqueous fraction typically ranged between 60–70 wt%. The oil fraction was analyzed for its water content and elemental composition. The water content varied between 9–11 wt%. The results of the elemental composition analysis are presented in Fig. 1 on a dry basis. The oxygen content of the oil fraction ranged between 22.4–23.7 wt%. Based on this, it is evident that low oxygen content pyrolysis oil was successfully produced in the 20 kg h^{-1} Process Development Unit over a time course of almost one hundred hours. Another aspect that warrants further attention is the relatively small increase in the oxygen content over time. It clearly indicates that even after almost one hundred hours of time-on-stream, the catalyst still retained a significant part of its initial activity, and could thus efficiently convert part of the primary pyrolysis vapors even at the end of the experiment. Nevertheless, both the carbon and the oxygen content displayed clear trends during the experiment, and it is therefore obvious that some catalyst deactivation did indeed take place. However, because the oxygen content only exhibited a small increase during the course of the entire experiment, all the liquid products were combined to give one overall liquid product. After the combination and the subsequent phase separation, separate organic and aqueous fractions were obtained and subjected to further physicochemical characterization.

In addition to the two-phase product which was collected from the scrubbers, the condensate, which had an overall moisture content of approximately 70–80 wt%, also spontaneously separated into an organic top phase and an aqueous bottom phase. The carbon content of the top phase was high (78.4 wt%, dry basis) and the water content low (2.4 wt%).
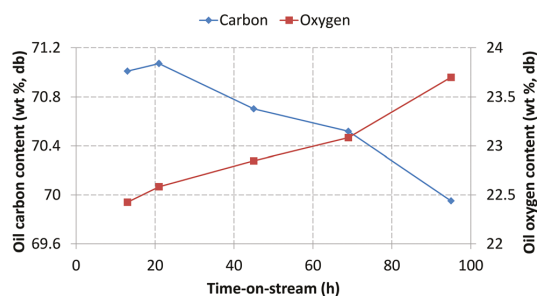

Fig. 1 Oil fraction carbon and oxygen content (wt%, dry basis) as a function of time-on-stream.

GC-MSD analysis of the top phase showed that it contained mostly single-ring aromatic hydrocarbons. The four main compounds were toluene, $m + p$-xylene, ethyl-methylbenzene and ethyl-benzene. In addition to these benzene-derivatives, some indenes and naphthalenes were also identified. Similar aromatic hydrocarbon compounds were also detected in the oil fraction of the scrubber products. The aromatic compounds detected in the condensate top phase are insoluble in water and more volatile than typical lignin derived phenolics, which explains the phase separation and the fact that some aromatic compounds either did not condense, or revolatilized in the scrubbers. Because the top phase of the condensate contained mainly the kind of products which are desirable in catalytic pyrolysis, it was combined with the oil fraction from the scrubbers. It was hypothesized that the addition of these products with solvent characteristics would serve to improve the quality of the overall organic liquid product.

Use of the HZSM-5 catalyst caused clear changes in the pyrolysis product distribution. The product distribution for this experiment and for a typical conventional fast pyrolysis experiment with the same pyrolysis unit and similar biomass feedstock are shown in Table 1. As the yield of char/coke cannot be directly measured in this system, it was determined by difference, $i.e.$ 100% subtracted by the respective yields of organic liquids, pyrolytic water and gases. As it can be seen in Table 1, the use of the catalyst resulted in a significant decrease in the yield of organic liquids. This, and the consequent increase in the yields of pyrolytic water and gases are phenomena typically associated with the use of HZSM-5 catalysts in biomass catalytic pyrolysis. It should, however, be emphasized that not all of the organics were enriched in the oil fraction. Approximately 44 wt% of the overall organics were actually present in the aqueous products, which is something that has to be taken into account when considering the overall efficiency of this process. For the non-condensable gases, the increase in the yield could be mainly attributed to the increased formation of CO (yield 11.5 wt%). This is also typical for catalytic pyrolysis with HZSM-5 catalysts, as the two main routes for oxygen rejection are dehydration and decarbonylation reactions, which produce H_2O and CO, respectively. The average molar CO/CO_2 ratio was 2.9. The CO/CO_2 ratio remained quite stable during the experiment, which was also an indication that the catalyst remained active during the experimental period. Time course gas composition data (see Fig. SM-1 in ESI†) also supports the notion that catalyst deactivation was limited. In addition to the increased CO yield,

Table 1 Product distribution (wt%, dry basis) from catalytic fast pyrolysis (CFP) and conventional fast pyrolysis (FP) of pine sawdust

	CFP pine	FP pine
Total liquid product	51	73
Organic liquids	32	63
Pyrolytic water	19	10
Gases	21	9
Char/coke	27	18

more light hydrocarbons in the C_1–C_3 range were also produced. The overall concentration of N_2 in the gas stream was approximately 50 vol%. Thus, the product gas stream which was recycled back to the reactor to be used as the fluidization gas, contained 50 vol% of pyrolysis product gases with potential reactivity under CFP conditions. The recirculation of non-condensable gases[35] as well as light hydrocarbons, e.g. propene,[5] has been shown to be beneficial in catalytic pyrolysis. The overall N_2 content remained high because continuous purging streams were fed into e.g. the feed hopper and instrumentation ports.

3.2. Characterization of the overall liquid products

The overall liquid products obtained from catalytic fast pyrolysis were collected and combined in the way which is presented in Fig. 2. Three separate liquid products were obtained for characterization: CFP oil (1), CFP aqueous fraction (2) and condensate aqueous fraction (3). The liquid product from both scrubbers was first combined, and then phase separated in order to obtain separate oil and aqueous fractions. The top phase of the condensate was then added into the scrubber oil fraction. This combined product is referred to as 'CFP oil'. Typical fast pyrolysis oil produced from pine sawdust is denoted as 'FP oil'. Characterization of the aqueous fractions is discussed later in the article, where the aqueous fraction obtained from the phase separation of the scrubber products will be referred to as 'CFP aqueous fraction'.

The properties of catalytically produced pyrolysis oil differed greatly compared to typical fast pyrolysis oil. The physicochemical properties of the CFP oil and FP oil are shown in Table 2. When considering the properties of the CFP oil, there are two important factors which contributed towards the formation of the product. First was the catalytic effect of the HZSM-5 catalyst. The reactions it catalyzed included dehydration of the pyrolysis vapors, which in turn led to phase separation of the overall liquid product due to the high water content. As a result of the phase separation, the less polar components enriched in the oil fraction, whereas a larger pro-

Table 2 Physicochemical properties of pyrolysis oils on as received or dry ash-free basis (dab)

Property	CFP oil	FP oil[31]
Water (wt%)	8.3	23.9
Solids (wt%)	0.76	0.01
Ash (wt%)	0.6	0.03
Carbon (wt%, dab)	72.0	53.4
Hydrogen (wt%, dab)	6.4	6.5
Nitrogen (wt%, dab)	0.02	0.1
Oxygen (wt%, dab)	21.5	40.0
Higher heating value (MJ kg^{-1}, dab)	30.4	22.2
Lower heating value (MJ kg^{-1}, dab)	28.7	20.1
Kinematic viscosity (cSt, 40 °C)	285	17
Density (kg dm^{-3}, 15 °C)	1.183	1.206
pH	2.6	2.7
TAN (mg KOH g^{-1})	30	71
Carbonyls (mmol g^{-1})	2.8	3.5
Micro carbon residue (wt%)	29.3	20.8

portion of the polar oxygenates ended up in the aqueous fraction. Thus, the CFP oil exhibited a low water content, a high carbon content and a low oxygen content. The hydrogen content was also low, and the consequently low H/C molar ratio (1.07) suggested that the product would be quite aromatic. The higher heating value was also higher (30.4 MJ kg^{-1}) than that of the pine FP oil (22.2 MJ kg^{-1}), which can be explained by the change in the oil elemental composition. The TAN of CFP oil was distinctly lower compared to FP oil, which suggested that the concentration of the main acidic constituents had decreased significantly. The pH of the CFP oil did not change significantly compared to FP oil.

The CFP aqueous fraction retained a significant proportion of the overall organic liquids which were produced in the CFP of pine. Physicochemical characteristics of the aqueous products are presented in Table 3. When considering the amount of organics in the CFP aqueous fraction, total organic carbon made up approximately 57% of the total organics. This kind of carbon content would be fairly typical for conventional fast pyrolysis oil. This is an indication that the polar oxygenate molecules which are typical products of biomass fast pyrolysis, enriched in the aqueous fraction that was obtained from catalytic fast pyrolysis. For the condensate aqueous fraction, organic carbon made up only 41 wt% of the overall organics, which suggested that the organics present in this fraction would be highly oxygenated compounds. The pH of both aqueous product fractions was below 3, but the TAN was lower than that of typical fast pyrolysis oil. The overall CFP liquid products contained approximately 39% of the biomass carbon.
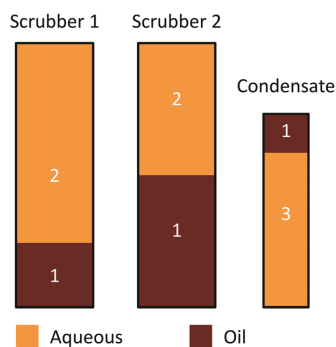

Fig. 2 Conceptual representation of overall liquid product collection from catalytic fast pyrolysis: (1) CFP oil (250 kg); (2) CFP aqueous fraction (520 kg); (3) condensate aqueous fraction (90 kg).

Table 3 Physicochemical properties of CFP aqueous liquid products

Property	CFP aqueous	Condensate aqueous
Water (wt%)	67.7	85.6
Organics (wt%)	32.3	14.4
pH	2.4	2.7
TAN (mg KOH g^{-1})	47	34
TOC (wt%)	18.4	5.9

The carbon yield of the CFP oil was about 24%, whereas the remaining 15% was found in the aqueous product fractions.

The change in the elemental composition of the pyrolysis oil can be further elucidated by using a Van Krevelen plot, which can be seen in Fig. 3. The lignin-derived water-insoluble (WIS) fraction of FP oil, and the whole CFP oil were actually relatively similar in their elemental composition. The WIS fraction of FP oil was, however, almost solid, whereas the CFP oil had a fairly low viscosity for a pyrolysis oil with low water content (8.3 wt%). Without the addition of the condensate aromatic fraction, the viscosity of the CFP oil was higher (437 cSt at 40 °C). The added condensate aromatic fraction constituted 4.4 wt% of the entire CFP oil, but due to its strong solubilizing properties the relative decrease in viscosity was approximately 35%. The amount of water-insoluble material in the CFP oil was high (76 wt%), which was clearly evident in the solvent fractionation of the CFP liquid products, the results of which are presented in Fig. 4. The high WIS content also explains the small difference in the elemental composition of the whole CFP oil and its respective WIS fraction (see Fig. 3). In addition to the LMW and HMW lignin fractions, the CFP oil contained some water-insoluble volatiles which evaporated during the fractionation process. The presence of these WIS volatiles has been previously correlated with aromatic hydrocarbons that have formed in the catalytic pyrolysis process.[36] The amount of

water-soluble oxygenates in the CFP oil was low, whereas the CFP aqueous fraction contained significant amounts of sugar-type compounds and ether-soluble light molecular weight oxygenates. If the CFP oil and aqueous fractions are combined into a single product by means of calculation, almost half of this combined product consists of water. This is due to the high moisture content of the feedstock (12 wt%), and the increased water yield originating from the dehydration reactions. If one considers the composition of the overall organic products on a dry basis (data not shown), it could be observed that the total amount of water-insoluble material increased from 27 to 48 wt%, whereas the amount of water-soluble organics decreased from 73 to 52 wt%. Based on this, it was clear that the yield decrease of organic liquids which was observed in CFP, was accompanied by a change in the overall composition of organic liquid products. While the CFP oil fraction exhibited a low content of water-soluble oxygenates (16 wt %), their significant presence in the aqueous fraction clearly necessitates the development of valorization routes for all liquid product fractions.

GC-MSD analysis of the CFP oil also revealed clear compound level changes compared to typical fast pyrolysis oils (see Fig. SM-2 in ESI†). Alkylated single-ring aromatic hydrocarbons became dominant, whereas typical cellulose and hemicellulose decomposition products had clearly decreased. Lignin monomers ranging from phenol and cresols to bulkier guaiacyl lignin monomers were also detected. Aromatic hydrocarbon structures larger than naphthalene were not detected in the CFP oil. A certain level of catalyst acidity was previously identified as a requirement for the formation three ring poly-aromatic hydrocarbons.[18] The absence of such compounds suggests that this particular HZSM-5 catalyst formulation possessed a suitable level of acidity and acid site density for catalytic fast pyrolysis. Overall, the GC-MSD results further support the results of the elemental analysis and solvent fractionation, which both indicated that the catalytically produced pyrolysis oil was highly aromatic and contained relatively small amounts of carbohydrate-derived thermal decomposition products.

Concentrations of certain typical water-soluble pyrolysis products were clearly lower in CFP oil when compared to FP oil. The results of quantitative GC-FID measurements are presented in Table 4, where the various compounds have been combined together into different chemical groups. The aromatic hydrocarbon content was only determined for the CFP oil. Compared to FP oil, the CFP oil contained less carboxylic acids and clearly less GC-detectable aldehydes and ketones. The decrease in the concentration of carboxylic acids is consistent with the observed decrease in the total acid number of the CFP oil. The changes in the concentrations of alcohols and furanics was not remarkable, whereas the concentration of lignin monomers was higher in the CFP oil. The CFP oil also contained 6.4 wt% of aromatic hydrocarbons. Approximately 2/3 of these were single-ring substituted benzenes, whereas the remaining 1/3 was distributed evenly between indenes and naphthalenes. It appears that the process conditions and the
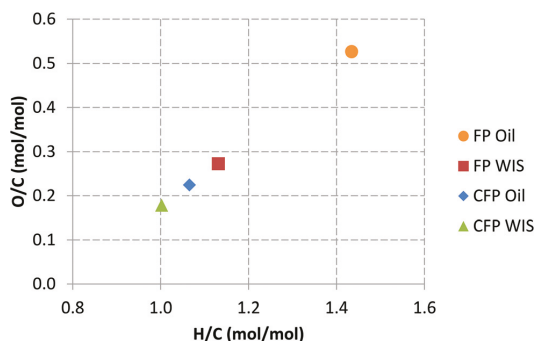

Fig. 3 Van Krevelen plot for pyrolysis oils and their water-insoluble (WIS) fractions produced in fast pyrolysis (FP) and catalytic fast pyrolysis (CFP).
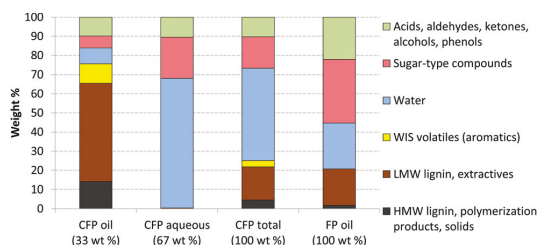

Fig. 4 Solvent fractionation of CFP oil, CFP aqueous fraction and typical FP oil from pine. Relative amounts of product fractions are included for the two phase CFP product.

Table 4 Concentrations (wt%) of different pyrolysis oil compound groups in CFP liquid products and FP oil as quantified by GC-FID. CFP total represents weighted average concentrations from all three CFP liquid product fractions

Sample	CFP oil	CFP aqueous	Condensate aqueous	CFP total	FP oil
Acids	1.8	3.9	2.9	3.2	3.7
Aldehydes and ketones	1.6	3.7	1.5	2.9	10.2
Alcohols	0.2	0.5	0.9	0.5	0.7
Furanics	0.5	0.3	0.2	0.3	1.0
Lignin monomers	3.7	1.0	0.2	1.7	1.7
Benzene derivatives	4.1	—	—	1.2	—
Indenes	1.1	—	—	0.3	—
Naphthalenes	1.1	—	—	0.3	—

catalyst that were employed in this study favoured the formation of the more valuable single-ring aromatics. While aromatic hydrocarbons dominated the GC-MSD analysis (Fig. SM-2 in ESI†), the corresponding quantitative analysis showed that their actual concentration in the pyrolysis oil was still relatively low. For the CFP total product, *i.e.* all three fractions combined, the decrease in the concentration of acids was clearly smaller when compared to FP oil. In fact, low molecular weight aldehydes and ketones were the only oxygenate compound group which exhibited a significant decrease in the total products. This also highlights the fact that the properties and composition of CFP oil were largely affected by the phase separation, and the consequent enrichment of water-soluble organics in the CFP aqueous fraction.

3.3.   Catalyst characterization

Spent catalyst samples, which were withdrawn from the pyrolysis unit during the experiment, showed that the catalyst coke content decreased as a function of time-on-stream. The results are shown in Fig. 5. The declining trend in the catalyst coke content as a function of time-on-stream suggested that the catalyst was losing some of its activity in the course of the experiment. The trend is very similar to what was observed in the carbon content of the pyrolysis oil samples (Fig. 1). The
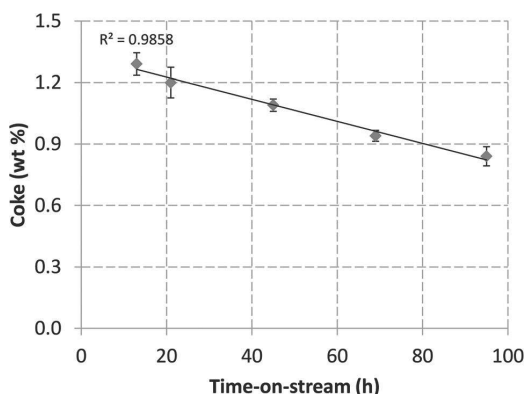
Fig. 5   Catalyst coke content (wt%) as a function of time-on-stream.

decreasing coke content of the catalyst also showed that the temperature and catalyst residence time in the regenerator were both sufficient for effective removal of coke deposits. If the regeneration of the catalyst was not functioning adequately, one would expect to observe an increasing amount of coke on the catalyst. The average coke content of the catalysts was 1.1 wt%. With a biomass feeding rate of 20 kg h^{-1} and a catalyst-to-biomass ratio of 7 : 1, this would correspond to a coke yield of approximately 7–8 wt%. It was previously shown[18] in catalytic fast pyrolysis bench-scale experiments that coke formation with a HZSM-5 catalyst was highest at the beginning of the experiment, *i.e.* when the catalyst still retained a larger proportion of its initial activity. French and Czernik[37] also used coke formation as a metric to identify high activity catalysts in a catalytic pyrolysis screening study. While catalyst deactivation due to coke formation and the potentially permanent catalyst deactivation that has been observed in this study are different phenomena, it is possible that both could decrease the activity of the catalysts *via* a similar mechanism.

Before any further characterization of the spent catalysts, the samples were regenerated in a laboratory muffle furnace for 5 h at 670 °C. The temperature corresponded to the temperature of the regenerator of the pyrolysis unit. The additional regeneration procedure was carried out in order remove the coke from the catalyst, thus eliminating any effect the coke might have had on the properties of the catalyst. It was envisioned that any potential changes in the properties and the structure of the catalyst could be observed with less ambiguity by utilizing an approach such as this. The results from the physisorption of N_2 are reported in Table 5. The results show that the catalyst had already lost a significant part of its specific surface area and micropore volume prior to the start of the experiment, which is represented by the TOS 0 h sample. The actual start of the experiment was preceded by a heat-up period with a duration of approximately two and a half days. During the course of the experiment, the catalyst still continued to lose more of its specific surface area and micropore volume. For the fresh catalyst sample, approximately 80% of the overall specific surface area was contained in the microporous parts of the catalyst. In contrast to this, only 47% of the overall specific surface area was attributable to the micropores for the final catalyst sample (TOS 96 h). The continuous

Table 5 Surface area and micropore volume of fresh, laboratory calcined (4 h at 650 °C) and used catalyst samples from various points of time-on-stream (TOS)

Sample/TOS	BET surface area (m^2 g^{-1})	Micropore area (m^2 g^{-1})	Micropore volume (cm^3 g^{-1})
Fresh catalyst	212	171	0.088
Calcined catalyst	178	125	0.065
0 h	121	76	0.040
13 h	131	67	0.035
21 h	127	62	0.033
45 h	123	60	0.031
69 h	118	56	0.030
96 h	118	55	0.030

decrease which was observed in the micropore area and micropore volume of the catalyst suggested that some degradation of the zeolite structure could have taken place during the experiment. The catalyst sample which was calcined under laboratory conditions (4 h, 650 °C) and not used in the actual experiment, also exhibited a distinct decrease in its specific surface area and micropore volume. This indicates that the properties of the HZSM-5 catalyst are prone to change during the kind of prolonged heating period, which has typically been employed in VTT's fast pyrolysis Process Development Unit.

Compared to the fresh catalyst, the catalyst which was recovered after the experiment exhibited changes in its XRD pattern (see Fig. SM-3 in ESI†). Two distinct peak groups which are associated with the mordenite inverted framework (MFI) structure of the HZSM-5 catalyst could be observed at approximately 8° and 23°. The HZSM-5 structure and the associated XRD pattern can be found on http://www.iza-structure.org/databases/. The intensity of the latter peak group clearly decreased, which has been previously associated with the removal of framework aluminium in the zeolite structure, as well as decrease in crystallinity.[38,39] The intensity of the peak at 23° also exhibited a linear correlation with catalyst micropore area (see Fig. SM-4 in ESI†), which further supports the notion of zeolite structural degradation. The changes in the peak intensities of the zeolite component were accompanied by the disappearance of kaolinite-related peaks (e.g. 12°).[40] In addition to this, crystalline quartz with a main peak at approximately 26.5° was also observed in the spent catalyst sample.[41] Overall, these observations reflect changes in both the zeolite component and the binder material of the catalyst. However, even with the transformation of the catalyst, the quality of the pyrolysis oil which was produced remained quite consistent throughout the experiment.

Alkali metals, which are present in the biomass feedstock in the form of ash, also deposited on the catalyst. As it can be seen in Fig. 6, the alkali metal content of the catalyst, as determined by ICP-AES, increased linearly over time. With an overall catalyst inventory of 94 kg, the metal content of the spent catalyst corresponded to approximately 1.1 kg of biomass derived contaminant metals. Based on the ash content of the pine feedstock, approximately 7.7 kg of ash were fed into the system during the four day experiment. Thus, the 1.1 kg of metals found on the catalyst would equal approximately 14 wt% of the total feedstock ash. While at this point it is too early to speculate whether the metal content of the catalyst would keep increasing linearly, or whether some kind of saturation would eventually be reached, it is clear that the combined reaction and regeneration conditions of the circulating fluidized bed pyrolysis unit resulted in significant deposition of biomass metals on the zeolite catalyst.

While the observed deposition of alkali metals is important in itself, it does not yet explain how these metals affect the properties and ultimately, the activity, of the HZSM-5 catalyst. As it was stated earlier, deposition of alkali metals on the Brønsted acid sites of deNO$_x$ catalysts has been previously observed.[24–27] While in this catalytic fast pyrolysis experiment the changes in the catalyst properties were not limited only to alkali deposition, a clear correlation between catalyst alkali metal content and acidity could, nevertheless, be observed in Fig. 7. As the content of alkali metals on the catalyst increased over time, the overall acidity exhibited a steady decrease as well. Compared to the acidity of the catalyst sample at TOS 0 h (leftmost data point in Fig. 7), the laboratory calcined catalyst sample had a clearly higher acidity (1.0 mmol g^{-1}). Thus, the catalyst had lost a significant part of its initial acidity during the heat-up phase. The relative decrease in acidity was, however, clearly lower during the actual four day catalytic pyrolysis experiment. These observations coincide with the changes previously seen in the surface area and porosity characteristics of the catalyst in Table 5; all parameters exhibited the largest changes before pyrolysis of the biomass was commenced. This would suggest that the HZSM-5 catalyst used in this experiment possessed a certain level of intrinsic thermal instability, which manifested as transformation of
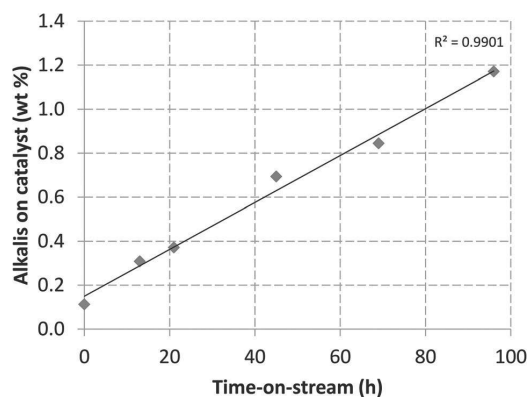

Fig. 6 Alkali metal content (K, Ca, P, Mg) of the catalyst as a function of time-on-stream.
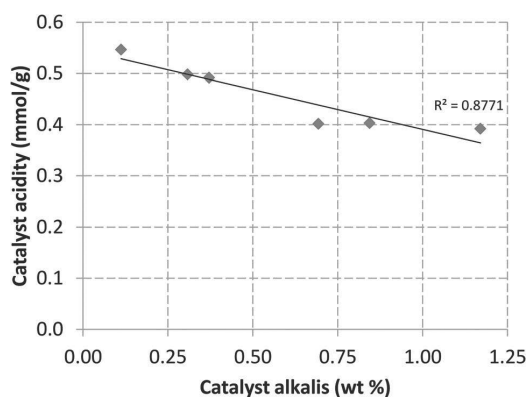

Fig. 7 Catalyst overall acidity (mmol NH$_3$ g^{-1} of catalyst) as a function of catalyst alkali metal content (wt% of K, Ca, P, Mg).

various catalyst properties during the pre-pyrolysis heating period. While the intensity of these so-called transformation phenomena attenuated over time, a clear steady state was not reached during the four day pyrolysis period.

SEM images of the catalyst samples showed that there was clear damage to the catalyst particles during the experiment. As it can be seen in Fig. 8, the fresh catalyst sample consisted mainly of regularly shaped spherical particles with varying sizes. The catalyst at TOS 0 h already showed some signs of wear and agglomeration, but the surfaces of the particles were still mostly intact. The catalyst sample from the end of the experiment was, however, clearly different compared to the other two. While most of the particles still roughly retained their original spherical shape, there were clear signs of damage and changes in the form fractures and particle agglomeration. The spent catalyst sample still contained smaller particles as well, which shows that catalyst fines were not selectively lost in the circulation process. EDS mapping of Si, Al and Ca was also carried out for a single catalyst particle which had a crater-like cavity (Fig. SM-5 in ESI†). The mapping showed that the zeolite metallic constituents, Si and Al, were distributed evenly across the particle surface, including the cavity. Ca, on the other hand, was more concentrated on the original surface of the catalyst particle. While it is not possible to determine when the fracturing of the particle took place, the images suggest that deposition of Ca inside the cavity may have started after the particle was damaged. These results suggest that Ca mainly deposited on the outer surface of the catalyst, instead of entering the catalyst pores.

Based on these observations, one clear focal point for further research would be to investigate the potential changes in catalyst properties on a longer time scale. Even though the oxygen content of the pyrolysis oil produced throughout this experiment remained quite low, it is entirely conceivable that after a long enough period of time-on-stream, the permanently deactivated catalyst would no longer be able to produce pyrolysis oil with the desired quality characteristics. The most obvious method for countering this limitation would be to continuously supply fresh catalyst to the catalytic pyrolysis unit while simultaneously withdrawing spent catalyst from the system. This solution would be analogous to what is routinely

carried out in oil refinery fluid catalytic cracking units. The catalyst that would be withdrawn from the pyrolysis unit would always be a mixture of catalyst fractions with varying degrees of activity. A suitable rate of catalyst replacement would, therefore, have to be determined to reach an operational equilibrium where product quality remains stable.

4. Conclusions

Catalytic fast pyrolysis in a circulating fluidized bed reactor with continuous catalyst regeneration was shown to be a suitable method for producing partially deoxygenated pyrolysis oil over extended time periods. VTT's 20 kg h^{-1} Process Development Unit was successfully operated using a spray dried HZSM-5 catalyst, and approximately 250 kg of pyrolysis oil were produced over an operational time of four days. In addition to the low water (8.3 wt%) low oxygen (21.5 wt%) pyrolysis oil, an aqueous product fraction containing the majority of polar carbohydrate-derived oxygenates was also produced. In order to increase the overall efficiency of the catalytic fast pyrolysis process, separate valorization routes must also be devised for the aqueous product fraction. While most of the oxygenate molecules enriched in the aqueous fraction, the organic fraction of pyrolysis oil contained mostly water-insoluble lignin-derived molecules, which were also supplemented by 6.4 wt% of aromatic hydrocarbons. Properties of the HZSM-5 catalyst changed considerably during the initial pre-pyrolysis heating period, and also to a lesser extent during the four day catalytic pyrolysis experiment. Based on this, it appeared that the properties of the catalyst initially transformed due to thermal instability. After this initial deactivation period, the transformation of the catalyst continued as it was further subjected to both thermal stress and the biomass feedstock. Biomass alkali metals deposited on the catalyst, and a direct correlation was observed between this phenomenon and the acidity of the catalyst. SEM images of the also showed clear signs of physical damage to the particles. Although the elemental composition of the pyrolysis oil remained quite stable during the four day experiment, the observed changes in the catalyst properties clearly indicate that catalyst lifetime will in all likelihood become a crucial factor in future commercial scale catalytic fast pyrolysis units.

Acknowledgements
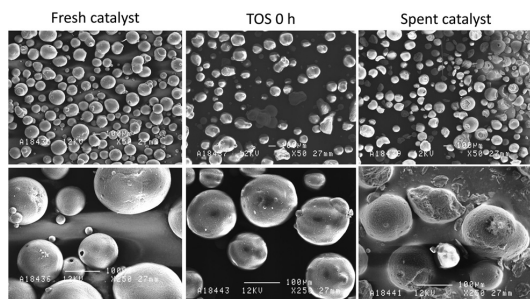
Fig. 8 SEM images of the fresh catalyst, the catalyst at the start of the pyrolysis (TOS 0 h) and the spent catalyst sample.

References

1 A. A. Lappas, M. C. Samolada, D. K. Iatridis, S. S. Voutetakis and I. A. Vasalos, *Fuel*, 2002, **81**, 2087–2095.

2 F. A. Agblevor, S. Beis, O. Mante and N. Abdoulmoumine, *Ind. Eng. Chem. Res.*, 2010, **49**, 3533–3538.

3 H. Zhang, R. Xiao, H. Huang and G. Xiao, *Bioresour. Technol.*, 2009, **100**, 1428–1434.

4 C. A. Mullen, A. A. Boateng, D. J. Mihalcik and N. M. Goldberg, *Energy Fuels*, 2011, **25**, 5444–5451.

5 T. R. Carlson, Y.-T. Cheng, J. Jae and G. W. Huber, *Energy Environ. Sci.*, 2011, **4**, 145–161.

6 D. J. Mihalcik, C. A. Mullen and A. A. Boateng, *J. Anal. Appl. Pyrolysis*, 2011, **92**, 224–232.

7 S. Stefanidis, K. Kalogiannis, E. Iliopoulou, A. Lappas and P. Pilavachi, *Bioresour. Technol.*, 2011, **102**, 8261–8267.

8 T. Carlson, G. Tompsett, W. Conner and G. Huber, *Top. Catal.*, 2009, **52**, 241–252.

9 A. Aho, N. Kumar, K. Eränen, T. Salmi, M. Hupa and D. Y. Murzin, *Fuel*, 2008, **87**, 2493–2501.

10 T. R. Carlson, J. Jae, Y.-C. Lin, G. A. Tompsett and G. W. Huber, *J. Catal.*, 2010, **270**, 110–124.

11 O. Mante, F. Agblevor and R. McClung, *Biomass Convers. Biorefin.*, 2011, **1**, 189–201.

12 F. A. Agblevor, O. Mante, N. Abdoulmoumine and R. McClung, *Energy Fuels*, 2010, **24**, 4087–4089.

13 A. Oasmaa, J. Korhonen and E. Kuoppala, *Energy Fuels*, 2011, **25**, 3307–3313.

14 F. A. Agblevor, O. Mante, R. McClung and S. Oyama, *Biomass Bioenergy*, 2012, **45**, 130–137.

15 F. de Miguel Mercader, M. Groeneveld, S. Kersten, N. Way, C. Schaverien and J. Hogendoorn, *Appl. Catal., B*, 2010, **96**, 57–66.

16 C. Torri, M. Reinikainen, C. Lindfors, D. Fabbri, A. Oasmaa and E. Kuoppala, *J. Anal. Appl. Pyrolysis*, 2010, **88**, 7–13.

17 A. Lappas, S. Bezergianni and I. Vasalos, *Catal. Today*, 2009, **145**, 55–62.

18 V. Paasikallio, C. Lindfors, J. Lehto, A. Oasmaa and M. Reinikainen, *Top. Catal.*, 2013, **56**, 800–812.

19 R. Boerefijn, N. Gudde and M. Ghadiri, *Adv. Powder Technol.*, 2000, **11**, 145–174.

20 C. S. Triantafillidis, A. G. Vlessidis, L. Nalbandian and N. P. Evmiridis, *Microporous Mesoporous Mater.*, 2001, **47**, 369–388.

21 H. Cerqueira, G. Caeiro, L. Costa and F. R. Ribeiro, *J. Mol. Catal. A: Chem.*, 2008, **292**, 1–13.

22 Y.-T. Cheng, J. Jae, J. Shi, W. Fan and G. W. Huber, *Angew. Chem., Int. Ed.*, 2012, **124**, 1416–1419.

23 C. A. Mullen and A. A. Boateng, *Ind. Eng. Chem. Res.*, 2013, **52**, 17156–17161.

24 Y. Zheng, A. D. Jensen and J. E. Johnsson, *Appl. Catal., B*, 2005, **60**, 253–264.

25 J. Chen and R. Yang, *J. Catal.*, 1990, **125**, 411–420.

26 P. Kern, M. Klimczak, T. Heinzelmann, M. Lucas and P. Claus, *Appl. Catal., B*, 2010, **95**, 48–56.

27 S. S. R. Putluru, A. Riisager and R. Fehrmann, *Appl. Catal., B*, 2011, **101**, 183–188.

28 G. Yildiz, M. Pronk, M. Djokic, K. M. van Geem, F. Ronsse, R. van Duren and W. Prins, *J. Anal. Appl. Pyrolysis*, 2013, **103**, 343–351.

29 J. Jae, R. Coolman, T. Mountziaris and G. W. Huber, *Chem. Eng. Sci.*, 2014, **108**, 33–46.

30 H. Zhang, J. Zheng, R. Xiao, D. Shen, B. Jin, G. Xiao and R. Chen, *RSC Adv.*, 2013, **3**, 5769–5774.

31 A. Oasmaa, Y. Solantausta, V. Arpiainen, E. Kuoppala and K. Sipilä, *Energy Fuels*, 2010, **24**, 1380–1388.

32 A. Oasmaa, E. Kuoppala and Y. Solantausta, *Energy Fuels*, 2003, **17**, 433–443.

33 A. Oasmaa and C. Peacocke, VTT Publications 731: Properties and fuel use of biomass-derived fast pyrolysis liquids. A guide, VTT Technical Report 731, 2010.

34 G. Peacocke, P. Russell, J. Jenkins and A. Bridgwater, *Biomass Bioenergy*, 1994, **7**, 169–177.

35 O. D. Mante, F. Agblevor, S. Oyama and R. McClung, *Bioresour. Technol.*, 2012, **111**, 482–490.

36 V. Paasikallio, F. Agblevor, A. Oasmaa, J. Lehto and J. Lehtonen, *Energy Fuels*, 2013, **27**, 7587–7601.

37 R. French and S. Czernik, *Fuel Process. Technol.*, 2010, **91**, 25–32.

38 Y. T. Kim, K.-D. Jung and E. D. Park, *Microporous Mesoporous Mater.*, 2010, **131**, 28–36.

39 C. Ding, X. Wang, X. Guo and S. Zhang, *Catal. Commun.*, 2008, **9**, 487–493.

40 K. G. Bhattacharyya and S. S. Gupta, *Sep. Purif. Technol.*, 2006, **50**, 388–397.

41 Y. Ma, C. Yan, A. Alshameri, X. Qiu, C. Zhou and D. Li, *Adv. Powder Technol.*, 2014, **25**, 495–499.

Publication IV

Ville Paasikallio, Konstantinos Kalogiannis, Angelos Lappas, Jani Lehto, Juha Lehtonen. Catalytic fast pyrolysis: Influencing bio-oil quality with the catalyst-to-biomass ratio. *Energy Technology***, Early View Article, DOI: 10.1002/ente.201600094, July 2016.**

© 2016 Wiley.

Reprinted with permission.

FULL PAPER

Catalytic Fast Pyrolysis: Influencing Bio-Oil Quality with the Catalyst-to-Biomass Ratio

Ville Paasikallio,*[a] Konstantinos Kalogiannis,[b] Angelos Lappas,[b] Jani Lehto,[a] and Juha Lehtonen[a]

In situ catalytic fast pyrolysis can be used to produce partially upgraded bio-oils. This process, however, suffers from rapid catalyst deactivation caused by coke formation, which necessitates the use of continuous catalyst regeneration. This can be achieved by using a circulating fluidized-bed reactor. In such a reactor, one key operational variable is the catalyst-to-biomass (C/B) ratio, which influences the extent of the catalytic reactions that take place. In this study, woody biomass is pyrolyzed in a pilot-scale circulating fluidized-bed reactor system using a HZSM-5 zeolite with varying C/B ratios. The C/B ratio influences the overall product distribution, the elemental distribution, and the characteristics of the liquid products. An increase of the C/B ratio enhances the conversion of pyrolysis vapors but this does not result in a continuous improvement in bio-oil quality. The C/B ratio is, nevertheless, a factor that can be used to optimize the catalytic fast pyrolysis process.

Introduction

Fast pyrolysis of biomass is a well-known thermochemical conversion process that can be used to convert solid biomass into a liquid product commonly referred to as pyrolysis oil or bio-oil.[1] Although this process can achieve a high yield of organic liquids and a significant degree of energy densification compared to the original biomass, the thermal decomposition of the individual biomass constituents results in a very heterogeneous product mixture.[2] The multitude of oxygenated organic functionalities that are present in the bio-oil give it a very challenging set of physicochemical properties,[3,4] which in turn necessitate the use of severe secondary upgrading if the bio-oil is to be converted into, for example, transportation fuels.[5,6] Instead of relying solely on post-pyrolysis upgrading strategies, it is also possible to incorporate a partial upgrading step into the pyrolysis process itself. In fluidized-bed reactors, which are the most commonly used reactor type for fast pyrolysis of biomass, this in situ upgrading can be achieved by replacing the inert heat transfer material with a solid catalyst.[7,8] In the ex situ alternative, the catalytic upgrading of the pyrolysis vapors is performed in a dedicated secondary reactor. The current study, however, focuses on the in situ version of this technology. A shift from a purely thermal process to catalytic fast pyrolysis (CFP) typically improves the quality of the product bio-oil as a result of secondary in situ catalytic upgrading reactions. This positive change occurs, however, at the expense of the bio-oil yield, as typical CFP catalysts produce substantial amounts of non-condensable gases, water, and coke during the upgrading reactions.[9–11]

The most commonly used catalyst for biomass CFP is the zeolite HZSM-5, a shape-selective solid acid catalyst that is able to convert oxygenates into aromatic hydrocarbons.[12,13] However, the highly oxygenated character of the pyrolysis vapors results in a very high coke formation tendency on acidic catalysts.[14,15] As a result HZSM-5 catalysts lose their activity in a rapid but reversible manner upon continuous exposure to pyrolysis vapors.[16,17] The problems caused by rapid coke formation can be circumvented by continuous regeneration of the catalyst. The traditional solution for this is to use a circulating fluidized-bed (CFB) reactor system, which possesses a high degree of similarity to an oil refinery fluid catalytic cracking (FCC) unit. In the CFB reactor, the catalyst spends merely a few seconds in contact with the pyrolysis vapors, after which the coke is combusted in a continuous regenerator unit. Other alternatives, such as the use of a bubbling fluidized-bed (BFB) reactor with continuous catalyst removal and addition, have also been suggested.[18] However, the CFB technology offers better industrial scalability as demonstrated by FCC units and power-generation boilers. Although CFB reactors are effective in dealing with coke, the inorganics present in the pyrolysis feedstock present an additional challenge that is yet to be addressed.[19] It has been shown previously that biomass-derived metals deposit

[a] V. Paasikallio, Dr. J. Lehto, Prof. J. Lehtonen
    Biofuels and Bioenergy
    VTT Technical Research Centre of Finland Ltd
    P.O. Box 1000, 02044 VTT (Finland)
    E-mail: ville.paasikallio@vtt.fi

[b] Dr. K. Kalogiannis, Dr. A. Lappas
    Chemical Process & Energy Resources Institute
    Center for Research and Technology Hellas
    57001 Thessaloniki (Greece)

Supporting Information for this article can be found under http://dx.doi.org/10.1002/ente.201600094.

This publication is part of a Special Issue on "Pyrolysis for Energy Technologies". A link to the issue's Table of Contents will appear here once it is complete.

on the catalyst during in situ CFP, and this deposition has been correlated with, for example, a decrease in catalyst acidity and the extent of bio-oil deoxygenation.[11,20] Various approaches to address this challenging issue are discussed in a recent review by Yildiz et al.[21]

Both of the aforementioned reactor types have their own characteristics that include variables that can be controlled freely. In BFB reactors, the extent of the upgrading reactions can be manipulated by varying the residence time of the pyrolysis vapors in the catalyst bed[18,22] or the space velocity.[8,23] In contrast, CFB reactors have a fairly limited residence time window for pyrolysis vapors because of the need to use high fluidization velocities. CFP process design is discussed in more detail in a recent paper by Vasalos et al.[24] One variable that can be controlled in a CFB reactor is the catalyst-to-biomass (C/B) ratio. In doing so, the amount of catalyst active sites that are available for the pyrolysis vapors as they traverse the length of the riser reactor can be controlled. Thus, operation at higher C/B ratios is expected to increase the extent of the upgrading reactions. Although some studies discuss the effect of the C/B ratio from certain aspects,[25–27] relatively little has been published with regard to the properties and composition of the CFP liquid products obtained using different C/B ratios. It has, nevertheless, been shown that operation at higher C/B ratios in a CFB reactor further decreases the bio-oil yield.[26,27] This change was, however, accompanied by an increase in the extent of deoxygenation, which indicates clearly that the C/B ratio is a parameter that has an impact on the quantity versus quality interdependency that is encountered in CFP. The effect of the C/B ratio also depends on the reactor type that is used, and thus generalizations between different experimental setups should not be drawn hastily. Jae et al.[18] studied the effect of the C/B ratio in a BFB reactor with continuous catalyst addition and removal. As the overall mass of the catalyst bed and biomass feeding rate were kept constant, varying the C/B ratio essentially changed the residence time of the catalyst in the fluidized bed. Thus, at lower C/B ratios, the catalyst has more time to undergo coking and deactivation before it is withdrawn from the reactor. In this instance, the authors concluded that the CFP process should be operated with a C/B ratio that is high enough to minimize the effect of catalyst deactivation. In more idealized systems such as Pyroprobe reactors, experiments are conducted typically at high C/B ratios to ensure that there is a sufficient amount of active catalyst present to convert the pyrolysis vapors.[13] The static conditions of Pyroprobe reactors and other fixed-bed units are not comparable to fluidized-bed reactors, in which both the biomass and catalyst are supplied continuously to the process. This sets the current study and these other fluidized-bed studies[18,20,25–27] clearly apart from work in which the main focus has been to examine how catalyst deactivation in a fixed bed proceeds as a function of accumulated biomass exposure.[16,17]

Although the main product of interest from CFP is bio-oil, increased water production because of acid-catalyzed dehydration reactions results in the formation of a separate aqueous-phase product. The water-soluble organics in this aqueous fraction can represent a significant portion of the overall CFP product slate.[20] The majority of these water-soluble organic molecules fall into compound classes that can be converted into value-added products using HZSM-5 catalysts.[28–30] Thus, rather than obtaining an aqueous fraction with substantial amounts of water-soluble organics and limited valorization potential, one might strive to enhance the conversion of these organics by further optimizing the CFP process. One approach for this is to manipulate the C/B ratio; supplying more catalyst into the process can potentially facilitate the improved conversion of compounds that would otherwise enrich in the aqueous-phase product.

The objective of this study is to examine the effect of the C/B ratio systematically in the in situ catalytic fast pyrolysis of woody biomass. The data presented in this study were generated in a pilot-scale circulating fluidized-bed pyrolysis system using a commercial HZSM-5 catalyst at four different C/B ratios. The effect of the variation of the C/B ratio was evaluated in terms of the overall product distribution, and the composition and properties of different product fractions. Special emphasis was put on the examination of the properties of both the organic and the aqueous liquid products.

Results and Discussion

Catalytic fast pyrolysis product distribution

It has been established in a number of previous studies that the use of HZSM-5 catalysts in fast pyrolysis causes a remarkable decrease in the yield of organic liquids, whereas consequent increases in the yield of water, gases, and coke are generally observed. However, these phenomena are associated typically with positive changes in the quality characteristics of the produced bio-oils. The increased formation of water coupled with changes in the chemical composition of the bio-oil result in the formation of a liquid product with two distinct phases: an organic oil phase, which will be referred to as "CFP bio-oil", and a separate aqueous phase. As a result of this phase separation phenomenon, the overall amount of organic liquids produced in the CFP process is further divided between the aforementioned two fractions. An increased C/B ratio further enhanced the typical effects of the HZSM-5 catalyst (Table 1). The overall yield of organic liquids exhibited a decreasing trend, and more of the biomass feedstock was converted into other product fractions at higher C/B ratios. As the pyrolysis temperature and the fluidization conditions were not varied between the different experiments, one would expect that the initial thermal decomposition of biomass would not be affected by an increase of the C/B ratio. This also relies on an underlying assumption that similar yields of char are obtained under non-catalytic and catalytic operation.[31] Based on this, the increase in the combined char/coke yield should be primarily accountable to increased formation of coke. The variation of the C/B ratio did not cause a significant change of how the organic liquids were divided between the CFP bio-oil and the aqueous

These are not the final page numbers! ↗↗

Table 1. Product yields [dry basis (db)] from CFP with different C/B ratios. The actual mass balances ranged between 96 and 100 wt%, but the values in this table have been normalized to 100%.

Product	Yield [wt%] at C/B ratio			
	11	14	17	21
CFP bio-oil organics	18	18	17	15
aqueous-phase organics	7	6	5	5
reaction water	24	25	25	25
gases	35	35	36	37
char/coke	16	16	17	18

phase. Approximately 75% of the overall organics were in the CFP bio-oil product and 25% remained in the aqueous phase (Table 1).

The overall increase in the yield of gases was fairly limited with the increase of the C/B ratio, and thus the yields of individual gas components did not exhibit significant changes either (Table 1). The yields of individual gas components are shown in Table 2.

Table 2. Yields [wt%, dry basis] of individual gas components from CFP with different C/B ratios.

Gas	Yield [wt%] at C/B ratio			
	11	14	17	21
H_2	0.1	0.1	0.1	0.1
CO	19.1	19.1	19.3	19.9
CO_2	11.9	11.7	11.6	12.2
CH_4	1.2	1.0	1.0	1.2
C_2H_6	0.2	0.2	0.1	0.2
C_2H_4	1.3	1.2	1.1	1.5
C_3H_8	0.1	0.1	0.1	0.1
C_3H_6	1.3	1.2	2.0	2.0
C_4	0.3	0.0	0.3	0.2

Although the overall changes were limited, operation at higher C/B ratios appeared to increase the yield of CO and C_2–C_3 hydrocarbons. The increase in the yield of CO indicates that operation at higher C/B ratios enhanced the overall cracking activity in the CFP process. As the formation of CO is considered to be one of the primary routes of oxygen rejection for HZSM-5 catalysts, this change suggests that slightly less oxygen would be present in the final liquid products. The increasing formation of light alkenes, that is, C_2H_4 and C_3H_6, potentially signifies the further conversion of low-molecular-weight oxygenates. Oxygenates that possess a suitable carbon chain length to produce C_2 and C_3 hydrocarbons through cracking reactions are generally soluble in water. Thus, without cracking and the consequent release of CO, CO_2, and water, molecules such as these would eventually be retained in the aqueous-phase products. In contrast, the initial conversion to alkenes would open up the possibility of further acid-catalyzed aromatization reactions.[28,32]

Properties and composition of the CFP bio-oil

In addition to its effect on the overall product distribution, an increase of the C/B ratio also caused changes in the physicochemical properties and composition of the CFP bio-oils (Table 3).

Table 3. Physicochemical properties of the CFP bio-oils produced at different C/B ratios.

Property	C/B ratio [wt wt^{-1}]			
	11	14	17	21
water content [wt%]	6.7	5.7	5.7	5.5
carbon content [wt%, db]	73.3	74.9	74.2	75.1
hydrogen content [wt%, db]	7.2	7.4	7.2	7.4
oxygen by difference [wt%, db]	19.5	17.7	18.6	17.5
H/C ratio [mol mol^{-1}, db]	1.17	1.17	1.15	1.17
O/C ratio [mol mol^{-1}, db]	0.20	0.18	0.19	0.17
HHV[a] [MJ kg^{-1}, db]	32.3	32.7	32.6	34.4
LHV[b] [MJ kg^{-1}, db]	30.6	30.9	30.9	32.6
kinematic viscosity [cSt, 40°C]	64	42	60	81
density [kg dm^{-3}, 15°C]	1.123	1.106	1.122	1.125
TAN[c] [mg$_{KOH}$ g^{-1}]	31	26	24	24
MCR [wt%]	19.7	17.3	18.5	20.8

[a] Higher heating value. [b] Lower heating value. [c] Total acid number.

Compared to conventional thermal fast pyrolysis bio-oils, the CFP bio-oils have a distinctly lower water content. As the CFP liquid products are recovered initially in a two-phase form, the final water content of the CFP bio-oil is determined by a liquid–liquid equilibrium between the aqueous and oil phases. One essential factor in this equilibrium is the elemental composition of the CFP bio-oil. If the chemical and, consequently, the elemental composition of the bio-oil changes because of the influence of the catalyst, the solubility of water in the bio-oil also changes. This change is illustrated in Figure 1, which shows how CFP bio-oils with lower molar oxygen-to-carbon (O/C) ratios also contained less water. This hydrophobic character of the CFP bio-oils was, therefore, enhanced by operation at higher C/B ratios, which eventually produced bio-oils with a slightly lower oxygen
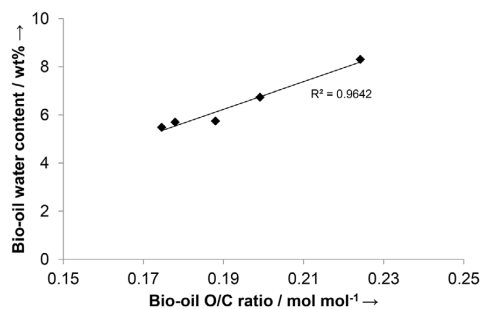

Figure 1. Water content of the CFP bio-oils as a function of the molar oxygen-to-carbon ratio (dry basis); the rightmost point is adapted from Ref. [19].

These are not the final page numbers! ↗↗

content. All of the CFP bio-oils that were produced in this study had clearly lower H/C ratios than typical non-catalytically produced fast pyrolysis bio-oils from woody biomass, which usually exhibit H/C ratios of approximately 1.4–1.5.[4] This represents an increase in the degree of unsaturation, which correlates with the aromatic character of these oils. The overall changes in the elemental composition were also reflected in the heating values of the CFP bio-oils. The dry-basis lower heating values (LHV) were approximately 50% higher than those of conventional fast pyrolysis bio-oils.[4]

Besides the differences in the water content and elemental composition of the CFP bio-oils, certain other physicochemical properties changed as well. The acidity of the CFP bio-oils, which was determined in terms of the total acid number (TAN), decreased with the increasing C/B ratio. This change may well coincide with the decrease in the water content of the bio-oils as this would limit the solubility of water-soluble carboxylic acids in the increasingly hydrophobic bio-oil. The viscosities of these bio-oils were quite low, which would indicate that the bio-oils contained significant amounts of compounds with solvent-like properties, and that the high-molecular-weight lignin compounds have undergone cracking reactions. The viscosity did not, however, decrease continuously with the increasing C/B ratio. Nevertheless, the absolute differences in CFP bio-oil viscosities became rather insubstantial at a temperature of 60 °C (Figure 2). Besides this, the relative differences also decreased as a function of the temperature. For example, at 20 °C, the viscosity of the C/B 21 bio-oil was 138% higher than that of the C/B 14 bio-oil. At 60 °C, the relative difference had decreased to 63%. Nevertheless, if the CFP bio-oils have to be handled at temperatures of 20 °C and below, for example, during storage and transportation, the small differences that were observed in the viscosity at higher temperatures become more pronounced. Similar behavior was also exhibited by the micro-carbon residue (MCR), the value of which increased when using the highest C/B ratio. These observations suggest that increasing the C/B
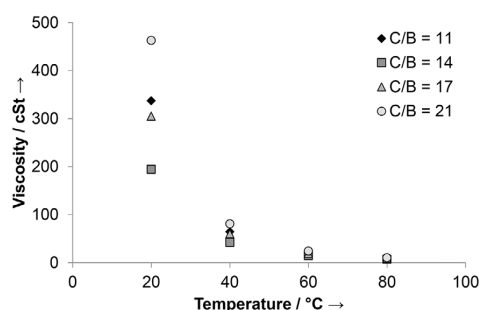

Figure 2. Kinematic viscosity (cSt) of the CFP bio-oils as a function of temperature.

ratio beyond a certain optimal point starts to affect both the viscosity and the volatility of the bio-oil negatively. However, one should bear in mind that the CFP bio-oils produced in this study are ultimately intermediate products that still require further upgrading. Therefore, the quality of the CFP bio-oils would have to be assessed eventually through actual upgrading, that is, catalytic hydrotreating, experiments.

The variation of the C/B ratio caused relatively limited changes in the volatile composition of the CFP bio-oils. The results of the semi-quantitative GC–MS analysis of the CFP bio-oils are shown in Figure 3. These results do not provide absolute quantification of the chemical species and should only be used to compare the relative composition of these particular bio-oils. Overall, the relative composition of these bio-oils was highly aromatic. Consequently, the relative proportion of carbohydrate degradation products was low. One notable change in the composition of the volatile, that is, GC-detectable, part of these bio-oils is the decrease in the relative amount of single-ring aromatic hydrocarbons at higher C/B ratios. Although these compounds are desired products in CFP, they are also known precursors for the formation of polyaromatic coke on acidic zeolites.[33] Thus, it is
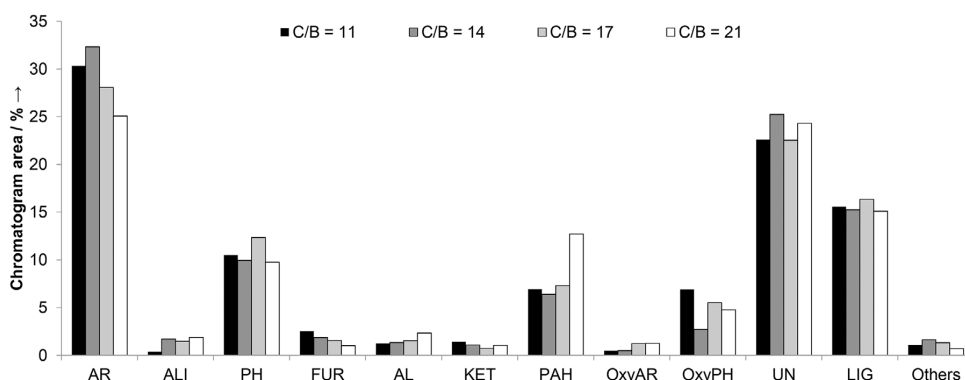

Figure 3. Semi-quantitative GC–MS analysis of the CFP bio-oils produced at different C/B ratios. The bio-oils were divided into the following compositional groups: single-ring aromatic hydrocarbons (AR), aliphatic hydrocarbons (ALI), phenols (PH), furans (FUR), aldehydes (AL), ketones (KET), polyaromatic hydrocarbons (PAH), aromatics with an additional oxygenate functionality (OxyAR), phenols with an additional oxygenate functionality (OxyPH), unidentified compounds (UN), heavy lignin compounds (LIG), and other compounds.

possible that the increase of the C/B ratio, that is, the supply of more acid sites for the CFP process, can lead to the increased formation of both polycyclic aromatic hydrocarbons (PAHs) and coke.

In these experiments, the combined yield of char/coke (see Table 1) indeed increased as a function of the C/B ratio. However, the relative amount of PAHs only increased sharply at the highest C/B ratio. This change coincided with the formation of larger PAH compounds that were not observed at lower C/B ratios. At C/B ratios of 11–17, the largest aromatic hydrocarbon structures consisted of two rings, that is, naphthalene and its derivatives, whereas at the C/B ratio of 21 some traces of phenanthrene and pyrene were detected. This would indicate that a certain threshold for the C/B ratio has to be passed to trigger the formation of three-ring or larger PAHs on this particular HZSM-5 catalyst. Both phenanthrene and pyrene have kinetic diameters that are larger than the pore openings of HZSM-5,[34] which suggests that these compounds would be formed on acid sites located on the external surface of the catalyst. As an increase of the C/B ratio would also increase the number of surface acid sites present in the reactor at a given time, the probability of two-ring aromatic hydrocarbons undergoing further reactions on the catalyst surface may also increase.

In addition to the limited compositional changes in the GC-detectable fraction of the CFP bio-oils, the proportions of low-molecular-weight (LMW) and high-molecular-weight (HMW) lignin fractions varied. This can be seen in the results of the solvent fractionation analysis (Figure 4). Overall, the content of water-insoluble (WIS) heavier compounds in these bio-oil samples follows similar trends to the viscosity and MCR. Both of these parameters exhibit linear correlations with the HMW lignin content (Figures S1 and S2). Based on the differences in the values of the MCR and HMW lignin content, it is clear that the HMW lignin fraction by itself is not the sole source of nonvolatile matter in these bio-oils. Nevertheless, it appears to affect the quality characteristics of these bio-oils directly.
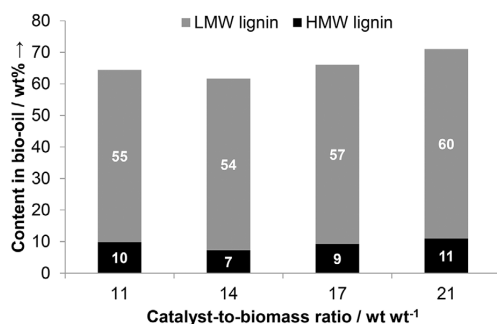
Typically, bio-oils from conventional fast pyrolysis exhibit limited thermal and storage stability. This manifests as either gradual changes in bio-oil properties and composition during prolonged storage periods, or as a more rapid transformation process if the bio-oil is subjected to elevated temperatures. However, the CFP bio-oils produced in this study presented favorable stability characteristics. The relative viscosity increase was 40 % or less after storing the bio-oils at 80 °C for 24 h (Figure 5). For thermal fast pyrolysis bio-oils, which have a much higher initial water content and thus low viscosity, relative viscosity increases of 70 % or more are typical.[35]
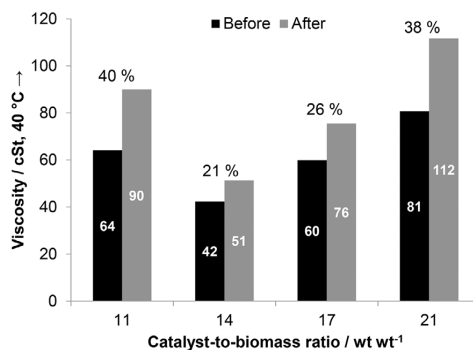
Figure 5. CFP bio-oil viscosities (cSt, 40 °C) before and after the accelerated aging test (24 h at 80 °C) and relative changes in viscosity.

In the current study, both the absolute and the relative increase in viscosity were smallest for the CFP bio-oils that had the lowest initial viscosities. The thermal and storage stability of CFP bio-oils is not a phenomenon that has been researched widely and systematically yet. One aspect that sets these bio-oils apart from conventional thermal fast pyrolysis oils is their composition: the amount of WIS matter in the CFP bio-oils is three times higher than that of typical thermal fast pyrolysis bio-oils.[4] As a result, CFP bio-oils do not age in a similar manner to thermal fast pyrolysis bio-oils. It has been suggested that for fast pyrolysis bio-oils that contain a higher amount of lignin-derived WIS matter, physical aggregation can overcome polymerization as the primary source of viscosity increase.[36] Fratini et al.[37] suggested a similarity in the aggregation behavior of pyrolytic lignins and petroleum asphaltenes. Asphaltene concentration[38,39] and temperature[40] are two of the many factors that affect aggregation. As asphaltenes are the heaviest fraction of petroleum, it stands to reason that the heaviest fraction of bio-oil, that is, the HMW lignin, might play a similar role in the suggested aggregation process. It was already shown that the content of HMW lignin correlated with bio-oil viscosity (Figure S1). In addition, the HMW lignin content of the fresh bio-oil exhibited a linear correlation with the absolute viscosity increase during the accelerated aging test (Figure S3).

Figure 4. Content [wt %] of LMW and HMW lignin in CFP bio-oils produced at different C/B ratios. The LMW lignin fraction may contain aromatic hydrocarbons and extractives, whereas the HMW fraction could also contain polymerization products and solids.

These are not the final page numbers! ↗↗

Characterization of aqueous-phase products

The observed changes in the properties of the primary bio-oil product were also accompanied by changes in the properties of the aqueous-phase products. Although the water content of the CFP bio-oils decreased, an opposing trend was observed for the corresponding aqueous phases. The amount of dissolved organics in the aqueous phase decreased with the increasing C/B ratio (Table 4).

Table 4. Properties of the aqueous-phase products obtained at different C/B ratios.

Property	C/B ratio [wt wt^{-1}]			
	11	14	17	21
water content [wt%]	83.0	83.7	87.0	87.7
organics content [wt%]	17.0	16.3	13.0	12.3
carbon content [wt%]	8.1	8.6	6.7	6.6
TAN [mg$_{KOH}$ g^{-1}]	72	69	57	60
MCR [wt%, db]	7.1	7.4	5.4	8.9

The total acid number, which is more than double that of the bio-oils, indicates that a significant amount of carboxylic acids is still present in the aqueous-phase products. Although the overall amount of dissolved organics is substantially lower (12.3–17.0 vs. 32.3 wt%[20]) than that obtained previously using a fresher version of the same catalyst in another reactor system, the current results indicate clearly that the manipulation of the C/B ratio is not, by itself, an adequate method to eliminate carbon in the aqueous phase completely. Thus, even with increasing process severity, that is, a higher C/B ratio, further valorization options for the acidic aqueous phase must be taken into consideration if the overall CFP product slate is to be exploited. The low MCR values observed for the aqueous-phase products suggest that these aqueous organics would possess a lower tendency towards coke formation than, for example, whole bio-oils. Nevertheless, to develop feasible processing routes for the aqueous phase, one must first attempt to identify which compounds are the most reluctant to undergo conversion over the HZSM-5 catalyst under CFP conditions.

Acetic acid was the most abundant organic compound of all the aqueous-phase products. On average, it accounted for approximately 40 wt% of the organic liquids in the aqueous phase. The concentrations of various water-soluble compounds determined quantitatively from the aqueous-phase products by using GC with flame ionization detection (FID) are shown in Table 5.

Compounds that were included in the GC–FID analysis but had concentrations of less than 0.01 wt% were omitted from Table 5. Although model compound studies[29] have reported high hydrocarbon yields from acetic acid, it appears to be more resistant against conversion on the HZSM-5 catalyst under the current process conditions. As both thermal and catalytic reactions continue throughout the length of the riser reactor that was utilized in this study, it stands to reason

Table 5. Amount (as received) of various water-soluble compounds in the aqueous-phase products. Summed concentrations for four different compound groups are also reported at the bottom of the table in bold text.

Compound	Content [wt%] at C/B ratio			
	11	14	17	21
acetaldehyde	0.12	0.32	0.30	0.06
furan	0.04	0.12	0.07	0.02
acetone	0.21	0.45	0.32	0.14
methanol	0.87	1.08	0.94	0.62
2-butanone	0.09	0.16	0.11	0.05
2-pentanone	0.02	0.02	0.02	0.01
1-hydroxy-2-propanone	0.51	0.47	0.36	0.45
2-hydroxyacetaldehyde	0.47	0.52	0.33	0.53
1-hydroxy-2-butanone	0.01	0.02	0.01	0.01
acetic acid	6.17	5.97	4.59	5.74
furfural	0.03	0.02	0.02	0.02
propanoic acid	0.28	0.26	0.23	0.26
butyric acid	0.01	0.01	0.01	0.01
guaiacol	0.02	0.02	0.02	0.02
2-methylphenol, o-cresol	0.03	0.03	0.04	0.04
phenol	0.14	0.13	0.14	0.19
3-methylphenol, m-cresol	0.02	0.03	0.03	0.04
4-propylphenol	0.01	0.02	0.01	0.01
vanillin	0.01	0.01	0.01	0.01
4-methylcatechol	0.01	0.02	0.02	0.01
aldehydes, ketones	**1.5**	**2.1**	**1.5**	**1.3**
alcohols	**0.9**	**1.1**	**0.9**	**0.6**
acids	**6.5**	**6.2**	**4.8**	**6.0**
lignin monomers	**0.2**	**0.3**	**0.3**	**0.3**

that the primary pyrolysis vapors that are released in the upper parts of the reactor will have substantially less time to undergo secondary catalytic reactions. Thus, one would expect that the complete elimination of aqueous phase organics would be extremely difficult to achieve by using in situ CFP. An increase of the contact time between the pyrolysis vapors and the catalyst by using a longer riser would be one option, but the effect of this would not be limited to just the aqueous organics. The issue of the aqueous phase has also been reflected in some fairly recent patent applications that have suggested, for example, recycling a part of the aqueous phase back into the pyrolysis process[41] and the use of the aqueous phase to remove inorganic contaminant deposits to rejuvenate the spent catalyst.[42]

Overall elemental distribution

By combining the overall product distribution and the analytical results presented previously, it is possible to determine the distribution of the main elemental constituents of biomass, that is, carbon, hydrogen, and oxygen, among the different product fractions of CFP. The results that show how carbon, hydrogen, and oxygen from dry, ash-free biomass are distributed between the liquid, gaseous, and solid products are presented in Figure 6. The information presented in each subfigure depends on which compositional properties were measured directly from each product fraction. Therefore, the char/coke product fraction is only included in the carbon distribution. The char from fast pyrolysis contains hydrogen and oxygen as well,[14] whereas coke that forms on acidic zeolites
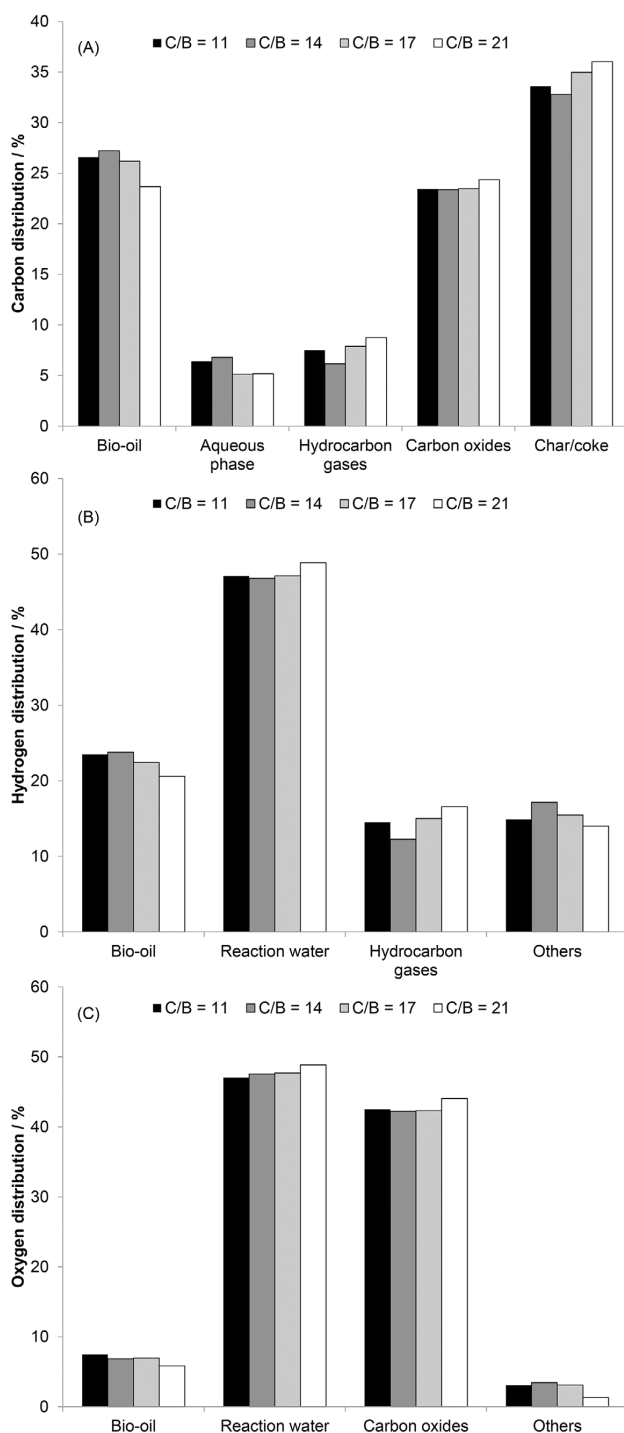
Figure 6. Distribution of (A) carbon, (B) hydrogen, and (C) oxygen from dry, ash-free biomass among the catalytic fast pyrolysis product fractions. In (B) and (C), the fraction "Others" has been determined by difference.

at high temperatures consists of polyaromatic structures.[33] These aspects have not been taken into account in the elemental distribution because of experimental limitations. For the aqueous-phase organic liquids, carbon was the only quantified element.

The typical effect of the HZSM-5 catalyst is also reflected in the carbon distribution presented in Figure 6a. With the increasing C/B ratio, less of the biomass carbon is recovered in the CFP bio-oil and in the aqueous fraction. Consequently, more carbon can be found in the gaseous products and the char/coke fraction. The presence of the catalyst should not affect the primary thermal decomposition of biomass, and thus the increased carbon yield of the char/coke fraction is mainly attributable to an increased amount of catalytic coke. The situation can be considered analogous to FCC, in which an increase of the catalyst-to-oil ratio typically increases both the conversion and coke yield.[43] In addition to the high yield of solid products, carbon oxides were also produced at carbon yields that were roughly equivalent to those of the bio-oil. Although in an industrial CFP process the noncondensable gases would be recycled and used for fluidization,[20,22] applications that are more advanced than the standard combustion option should be considered for the excess CO and hydrocarbon gases. One alternative would be to convert these gases into hydrogen,[44] which could then be utilized in a subsequent upgrading process. Overall, these results highlight some of the challenges of CFP that were discussed in a recent review by Venderbosch.[45] One particular challenge compared to conventional thermal fast pyrolysis is the broader distribution of the biomass carbon between the different product fractions. Although efforts should of course be taken to increase both the quality and quantity of the main bio-oil product, it is clear that process concepts based on CFP should also take into account the efficient utilization of the side products.

The hydrogen yield of the bio-oil fraction followed a similar trend to the carbon yield; slightly less hydrogen was retained in the CFP bio-oil at higher C/B ratios. The overall hydrogen distribution, however, highlights the importance of dehydration reactions in CFP. Almost half of the hydrogen in the biomass was removed in the form of water. The substantial production of water was also reflected directly in the oxygen distribution (Figure 7c). In total, water and carbon oxides accounted for approximately 90% of the oxygen that originates from the original biomass feedstock. Consequently, this means that the CFP bio-oil contained only a limited fraction of the overall oxygen. However, as it has been shown here, this
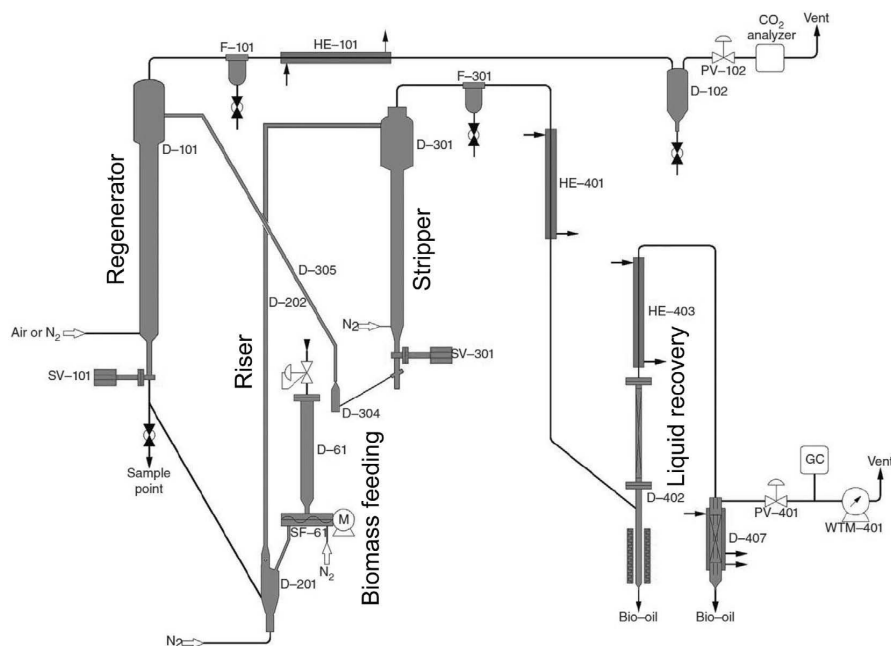
Figure 7. Schematic of the CPERI circulating fluidized-bed reactor system used in these experiments.

transformation is essentially a trade-off: a decreased oxygen content in the bio-oil coincided with decreased bio-oil yields.

Conclusions

The variation of the catalyst-to-biomass (C/B) ratio with a HZSM-5 catalyst resulted in limited changes in the in situ catalytic fast pyrolysis (CFP) product distribution and product properties. Nevertheless, the C/B ratio is still a parameter that can be used to fine-tune the in situ CFP process to a certain extent. The optimal C/B ratio would in all likelihood depend on a number of other factors such as biomass and catalyst type, reactor design, and reaction temperature. Operation at higher C/B ratios enhanced the cracking effects of the catalyst, that is, more gases, water, and coke were produced. Although the overall yield of organic liquids decreased with the increasing C/B ratio, the distribution of organics between the CFP bio-oil and the aqueous phase remained almost constant at approximately 3:1. Acetic acid was the most abundant compound identified within the aqueous-phase products. All the bio-oils produced with four different C/B ratios had a dry-basis oxygen content of less than 20 wt%. Among the various physical properties, viscosity exhibited the largest intersample differences. The bio-oils that had the lowest initial viscosity were also the most stable ones. Both the initial viscosity and absolute viscosity increase during a 24 h thermal treatment at 80 °C could be correlated with the amount of high-molecular-weight lignin compounds in the bio-oils.

Experimental Section

Biomass and catalyst

The biomass used in these experiments was a commercial beech wood feedstock (Lignocel HBS 150–500) with a particle size of 150–500 μm. It is known that the effect of particle size on heat transfer is less critical in CFB than in BFB reactors.[46] It has been shown previously that high liquid yields can be obtained in a BFB reactor with the use of similar particle sizes as in the current study.[47] Thus, the current conditions should be very suitable to observe the effect of other process parameters, that is, the C/B ratio. The properties and characterization methods for the feedstock are described in more detail elsewhere.[26] To summarize, the dry-basis elemental composition of the feedstock was 48.44 wt% carbon, 5.83 wt% hydrogen, and 45.73 wt% oxygen (by difference). The ash content of the biomass was 0.54 wt% (dry basis), and the moisture content was 8.0 wt%.

The catalyst that was used in these experiments was a partially deactivated spray-dried HZSM-5 catalyst (CBV 5524G) from Zeolyst International. The molar SiO_2/Al_2O_3 ratio of the zeolite was 50, and the zeolite content of the catalyst formulation was 50%. The catalyst had been used previously in a 4 day experiment, which, along with the properties of the catalyst itself, was documented previously.[20] In the previous experiment, almost 2 tons of pine sawdust were pyrolyzed in a CFB pyrolyzer with a feeding rate of 20 kg h^{-1}. The pyrolysis was performed at 520 °C, and the continuous regeneration of the catalyst was conducted at 650–670 °C. The overall catalyst inventory was approximately 120 L (95 kg), and the C/B ratio was 7. After this 4 day experiment, the catalyst had a specific surface area of 118 m^2 g^{-1}, a micropore area of 55 m^2 g^{-1}, and a micropore volume of

⫿8⫿

These are not the final page numbers! ↗↗

$0.030 \, cm^3 g^{-1}$. All of these values had decreased throughout the course of the experiment reported previously. The catalyst also contained approximately 1.2 wt% of biomass-derived contaminants (K, Ca, P, Mg).

Pyrolysis unit and experiments

The experiments were conducted in a CFB reactor system situated at the Chemical Process and Energy Resources Institute (CPERI). The reactor system, described in detail elsewhere,[25, 48] is shown in Figure 7. The pyrolysis takes place in a reactor that consists of a mixing zone (D-201) in which the hot catalyst and the biomass first come into contact, and a riser part (D-202) in which the pyrolysis vapors come into intimate contact with the catalyst and cracking reactions take place. The reactor is fluidized using N_2. The catalyst is supplied to the reactor from a bubbling fluidized-bed regenerator (D-101), which is used to combust both the char and the coke that are formed in the pyrolysis reactions. The biomass is fed into the mixing zone from a feed hopper using a screw feeder (SF-61). After they exit the riser, the catalyst and char are separated from the pyrolysis vapors and incondensable gases in a stripper (D-301), in which the separated catalyst is stripped with N_2 to remove any reaction products adsorbed within the pores of the catalyst. The stripped catalyst and the char are conveyed to the regenerator through a liftline (D-305). Any particulate matter that was not separated in the stripper was retained in a hot vapor filtration unit (F-301). After the separation of the solids, the pyrolysis vapors are condensed in a series of two heat exchangers in which the bio-oil vapors are cooled from the reaction temperature, typically around 500 °C, to room temperature. The composition of the noncondensable product gases was monitored by using a continuous gas analyzer (Servomex 1440D), which measures CO and CO_2, and a HP 5890 Series II gas chromatograph equipped with four columns (Precolumn: OV-101; Columns: Porapak N, Molecular Sieve 5Å, and Rt-Qplot 30 m × 0.53 mm I.D.) and two detectors: a thermal conductivity detector (TCD) and a FID. The CO_2 concentration in the regenerator flue gas was also monitored by using a Servomex 1440D online gas analyzer to measure the combined yield of char and coke indirectly. The volumetric flows of both the flue and the product gases were measured by using two wet test meters (WTM).

There are several advantages of the above technology that lead to an optimum bio-oil yield. Besides the type of catalyst, crucial parameters are (1) the design of the mixing zone that assures the very rapid mixing of biomass particles with the hot catalyst particles with high heat transfer rates, (2) the residence time of the pyrolysis vapors in the riser, which should be low (< 2 s) to avoid overcracking, (3) the fast separation of the solid and the vapors in the cyclone type stripper, and (4) the fast quenching of the produced vapors in the heat exchangers to favor a high liquid yield.

For this study, the pyrolysis was performed at 500 °C, and the regenerator was operated at 700 °C. The feeding rate of the biomass was typically 500 g h^{-1}, and approximately 2 kg of biomass was processed in each experiment. Operation at four different C/B ratios (11, 14, 17, 21) was achieved by varying the circulation rate of the catalyst.

Characterization of liquid products

To eliminate the effect of any potential ageing reactions, all liquid products were kept refrigerated after their recovery from the CFP experiments. The water content of the CFP bio-oil and the aqueous phase was determined by Karl Fisher titration (ASTM E203-08). The elemental composition (carbon, hydrogen) was measured by using a LECO-628 CHN elemental analyzer. The oxygen content was determined by difference. The higher heating value of the bio-oil was measured by using a Parr 1261 bomb calorimeter. Bio-oil viscosity was determined by using an Anton Paar SVM3000 Viscometer according to ASTM D7042. MCR was determined according to ASTM D-4530. Total acid number was measured by using a 751 Titrino Metrohm analyzer. The storage/thermal stability of the bio-oil was evaluated from an accelerated aging test, in which the bio-oil is stored at 80 °C for 24 h. The change in bio-oil viscosity was used as the stability indicator.

The composition of the bio-oil was analyzed by using GC–MS by using an Agilent 7890A/5975C GC–MS equipped with a HP-5MS column. Details of the GC–MS method were reported previously.[26] The bio-oil was also analyzed by using a shortened version of the VTT solvent fractionation method[2] to observe changes in the WIS part of the bio-oils. The WIS fraction of the bio-oil was split into dichloromethane-soluble and methanol-soluble fractions. The dichloromethane-soluble fraction is typically LMW lignin, whereas the methanol-soluble fraction contains HMW lignin and polymerization products. For CFP bio-oils, the LMW lignin fraction may also contain aromatic hydrocarbons, as these are insoluble in water but soluble in dichloromethane.

The composition of the aqueous phase was analyzed by using GC (Agilent Technologies 7890 A) coupled with a FID. The analysis entails the quantitative determination of 40 water-soluble compounds by using an Agilent 19091 N-136 HP-Innowax column. The method is described in more detail elsewhere.[20]

Keywords: biofuels · biomass · bio-oil · catalytic fast pyrolysis · zeolites

[1] D. S. Scott, J. Piskorz, *Can. J. Chem. Eng.* **1982**, *60*, 666–674.
[2] A. Oasmaa, E. Kuoppala, Y. Solantausta, *Energy Fuels* **2003**, *17*, 433–443.
[3] A. Oasmaa, S. Czernik, *Energy Fuels* **1999**, *13*, 914–921.
[4] A. Oasmaa, Y. Solantausta, V. Arpiainen, E. Kuoppala, K. Sipilä, *Energy Fuels* **2010**, *24*, 1380–1388.
[5] D. C. Elliott, T. R. Hart, G. G. Neuenschwander, L. J. Rotness, A. H. Zacher, *Environ. Prog. Sustainable Energy* **2009**, *28*, 441–449.
[6] D. C. Elliott, T. R. Hart, G. G. Neuenschwander, L. J. Rotness, M. V. Olarte, A. H. Zacher, Y. Solantausta, *Energy Fuels* **2012**, *26*, 3891–3896.
[7] F. A. Agblevor, S. Beis, O. Mante, N. Abdoulmoumine, *Ind. Eng. Chem. Res.* **2010**, *49*, 3533–3538.

9

These are not the final page numbers! ↗↗

[8] T. R. Carlson, Y.-T. Cheng, J. Jae, G. W. Huber, *Energy Environ. Sci.* **2011**, *4*, 145–161.

[9] H. Zhang, R. Xiao, H. Huang, G. Xiao, *Bioresour. Technol.* **2009**, *100*, 1428–1434.

[10] O. D. Mante, F. Agblevor, S. Oyama, R. McClung, *Appl. Catal. A* **2012**, *445–446*, 312–320.

[11] C. A. Mullen, A. A. Boateng, *Ind. Eng. Chem. Res.* **2013**, *52*, 17156–17161.

[12] C. D. Chang, A. J. Silvestri, *J. Catal.* **1977**, *47*, 249–259.

[13] T. R. Carlson, T. P. Vispute, G. W. Huber, *ChemSusChem* **2008**, *1*, 397–400.

[14] P. A. Horne, P. T. Williams, *J. Anal. Appl. Pyrolysis* **1995**, *34*, 65–85.

[15] H. Zhang, T. R. Carlson, R. Xiao, G. W. Huber, *Green Chem.* **2012**, *14*, 98–110.

[16] C. Mukarakate, X. Zhang, A. R. Stanton, D. J. Robichaud, P. N. Ciesielski, K. Malhotra, B. S. Donohoe, E. Gjersing, R. J. Evans, D. S. Heroux, R. Richards, K. Iisa, M. R. Nimlos, *Green Chem.* **2014**, *16*, 1444–1461.

[17] S. Wan, C. Waters, A. Stevens, A. Gumidyala, R. Jentoft, L. Lobban, D. Resasco, R. Mallinson, S. Crossley, *ChemSusChem* **2015**, *8*, 552–559.

[18] J. Jae, R. Coolman, T. Mountziaris, G. W. Huber, *Chem. Eng. Sci.* **2014**, *108*, 33–46.

[19] G. Yildiz, F. Ronsse, R. Venderbosch, R. van Duren, S. R. A. Kersten, W. Prins, *Appl. Catal. B* **2015**, *168*, 203–211.

[20] V. Paasikallio, C. Lindfors, E. Kuoppala, Y. Solantausta, A. Oasmaa, J. Lehto, J. Lehtonen, *Green Chem.* **2014**, *16*, 3549–3559.

[21] G. Yildiz, F. Ronsse, R. van Duren, W. Prins, *Renewable Sustainable Energy Rev.* **2016**, *57*, 1596–1610.

[22] O. D. Mante, F. Agblevor, S. Oyama, R. McClung, *Bioresour. Technol.* **2012**, *111*, 482–490.

[23] O. D. Mante, F. Agblevor, R. McClung, *Fuel* **2013**, *108*, 451–464.

[24] I. A. Vasalos, A. A. Lappas, E. P. Kopalidou, K. G. Kalogiannis, *WIREs Energy Environment* **2016**, *5*, 370–383.

[25] A. A. Lappas, M. C. Samolada, D. K. Iatridis, S. S. Voutetakis, I. A. Vasalos, *Fuel* **2002**, *81*, 2087–2095.

[26] E. F. Iliopoulou, S. Stefanidis, K. Kalogiannis, A. C. Psarras, A. Delimitis, K. S. Triantafyllidis, A. A. Lappas, *Green Chem.* **2014**, *16*, 662–674.

[27] "Production of an Advanced Bioenergy Carrier (Bio-oil) from Biomass Catalytic Pyrolysis. Effect of Catalyst Deactivation on Bio-oil Yield and Quality": A. A. Lappas, K. Kalogiannis in *tcbiomass2013 The International Conference on Thermochemical Conversion Science* (Chicago), **2013**, http://www.gastechnology.org/tcbiomass/tcb2013/12-Lappas-tcbiomass2013-presentation-Thur.pdf.

[28] T. R. Carlson, J. Jae, Y.-C. Lin, G. A. Tompsett, G. W. Huber, *J. Catal.* **2010**, *270*, 110–124.

[29] K. Wang, J. Zhang, B. H. Shanks, R. C. Brown, *Green Chem.* **2015**, *17*, 557–564.

[30] H. Zhang, Y.-T. Cheng, T. P. Vispute, R. Xiao, G. W. Huber, *Energy Environ. Sci.* **2011**, *4*, 2297–2307.

[31] G. Yildiz, T. Lathouwers, H. E. Toraman, K. M. van Geem, G. B. Marin, F. Ronsse, R. van Duren, S. R. A. Kersten, W. Prins, *Energy Fuels* **2014**, *28*, 4560–4572.

[32] Y.-T. Cheng, G. W. Huber, *Green Chem.* **2012**, *14*, 3114–3125.

[33] M. Guisnet, P. Magnoux, *Appl. Catal. A* **2001**, *212*, 83–96.

[34] J. Jae, G. A. Tompsett, A. J. Foster, K. D. Hammond, S. M. Auerbach, R. F. Lobo, G. W. Huber, *J. Catal.* **2011**, *279*, 257–268.

[35] D. C. Elliott, A. Oasmaa, F. Preto, D. Meier, A. V. Bridgwater, *Energy Fuels* **2012**, *26*, 3769–3776.

[36] J. Meng, A. Moore, D. C. Tilotta, S. S. Kelley, S. Adhikari, S. Park, *Energy Fuels* **2015**, *29*, 5117–5126.

[37] E. Fratini, M. Bonini, A. Oasmaa, Y. Solantausta, J. Teixeira, P. Baglioni, *Langmuir* **2006**, *22*, 306–312.

[38] Y. Liu, E. Y. Sheu, S. Chen, D. Storm, *Fuel* **1995**, *74*, 1352–1356.

[39] K. Oh, T. A. Ring, M. D. Deo, *J. Colloid Interface Sci.* **2004**, *271*, 212–219.

[40] T. Maqbool, P. Srikiratiwong, H. S. Fogler, *Energy Fuels* **2011**, *25*, 694–700.

[41] T. Mazanec, J. Whiting (Anellotech Inc.) US20140027265A1, **2014**.

[42] L. Zhou, A. Bryant, M. M. Ramirez, L. May, R. A. Engelman, B. A. D. Rainer (KiOR Inc.), US20150004093A1, **2015**.

[43] N. Thegarid, G. Fogassy, Y. Schuurman, C. Mirodatos, S. Stefanidis, E. Iliopoulou, K. Kalogiannis, A. Lappas, *Appl. Catal. B* **2014**, *145*, 161–166.

[44] T. L. Marker, L. G. Felix, M. B. Linck, M. J. Roberts, P. Ortiz-Toral, J. Wangerow, *Environ. Prog. Sustainable Energy* **2014**, *33*, 762–768.

[45] R. H. Venderbosch, *ChemSusChem* **2015**, *8*, 1306–1316.

[46] P. Basu, P. K. Nag, *Chem. Eng. Sci.* **1996**, *51*, 1–26.

[47] J. Shen, X.-S. Wang, M. Garcia-Perez, D. Mourant, M. J. Rhodes, C.-Z. Li, *Fuel* **2009**, *88*, 1810–1817.

[48] A. A. Lappas, V. S. Dimitropoulos, E. V. Antonakou, S. S. Voutetakis, I. A. Vasalos, *Ind. Eng. Chem. Res.* **2008**, *47*, 742–747.

Publication V

Co-processing of Dry Bio-oil, Catalytic Pyrolysis Oil, and Hydrotreated Bio-oil in a Micro Activity Test Unit

Christian Lindfors,* Ville Paasikallio, Eeva Kuoppala, Matti Reinikainen, Anja Oasmaa, and Yrjö Solantausta

VTT Technical Research Centre of Finland, Limited, Post Office Box 1000, FI-02044 VTT, Finland

ABSTRACT: Fast pyrolysis technology is currently moving forward to commercialization, and demonstration plants are at the commissioning stage. The quality of bio-oil differs significantly from fossil fuels, and therefore, upgrading technologies are needed to improve the fuel properties of bio-oil. Co-processing of bio-oil in refinery fluid catalytic cracking (FCC) would have many economic advantages compared to other upgrading technologies because no essential modifications to the refinery are needed. However, because of its different chemical composition, the introduction of bio-oil into the FCC unit will introduce uncertainty to the refinery operation. In this paper, co-processing of dry thermal bio-oil, catalytic pyrolysis oil, and hydrotreated bio-oil was compared using a micro activity test (MAT) setup. The experiments show that the bio-oil concentration during co-processing should remain low to avoid high coke formation. Co-processing of dry bio-oil also resulted in a much lower liquid yield compared to catalytic pyrolysis oil and hydrotreated bio-oil. This was probably caused by the higher amount of sugar-like material in the dry bio-oil. The differences between catalytic pyrolysis oil and hydrotreated bio-oil were relatively small, except for the coke formation tendency, which was higher for the more aromatic catalytic pyrolysis oil.

■ INTRODUCTION

Fast pyrolysis is a promising technology for converting solid biomass into liquid fuel. The technology is currently moving forward to commercialization, and demonstration plants are under commission. The quality of bio-oil differs significantly from that of fossil fuels, and for this reason, bio-oil cannot be used for applications requiring complete evaporation before combustion.[1] The first end use for bio-oil has been to replace heavy fuel oil in burners.[2] If the bio-oil is to be used for other applications, upgrading is needed. Catalytic pyrolysis and hydrotreatment of bio-oil are considered to be two technologies with good potential for producing bio-oil with improved fuel properties.[3,4] A high severity hydrotreatment process can be used for converting bio-oil into a practically oxygen-free hydrocarbon fuel. However, one key disadvantage with such complete hydrotreatment is the high hydrogen consumption, which makes the process very expensive.[5]

In an oil refinery, fluid catalytic cracking (FCC) is commonly used for increasing the gasoline yield by decomposing heavy oil feedstocks into lighter fractions. Introducing bio-oil into a FCC unit would have many economic advantages because no essential modifications to the refinery are needed. The bio-oil will, however, introduce uncertainty into existing refinery operation because of its high oxygen content, low hydrogen content, and poor stability and distillability. In an oil refinery, the FCC feed consists mostly of paraffins, olefins, naphtenes, and aromatics.[6,7] Bio-oil, on the other hand, contains highly polar compounds, such as water, carboxylic acids, aldehydes, ketones, furfurals, sugar-like material, and lignin-derived compounds.[8,9] Catalytic cracking of crude bio-oil in a FCC unit is not possible without extensive coking. To reduce the coke formation, co-processing of bio-oil with some hydrocarbon liquid is needed. During co-processing, a shift in oxygen

rejection from decarboxylation to dehydration takes place, which increases the yield of hydrocarbons in the end product.[10]

The coke yield from direct co-processing of crude bio-oil has usually been relatively high, and therefore, Baldauf et al. suggested to use mild hydrodeoxygenation (HDO) to stabilize the bio-oil before feeding it into an FCC unit.[5] Both Samolada et al. and Lappas et al. carried out co-processing experiments with hydrotreated bio-oil. Before co-processing, the hydrotreated bio-oil was distilled into light and heavy fractions. Only the heavy fraction with an oxygen content close to 5 wt % was used for the experiments. Light cycle oil (LCO) and LCO + vacuum gas oil (VGO) were used as co-feed in the experiments. Introduction of the heavy fraction into LCO and LCO + VGO reduced the crackability of the feedstock but increased the gasoline and coke yields. The gasoline from the co-processing contained more saturated naphthenes and aromatics than the gasoline from pure LCO and VGO. Even though the heavy fraction from hydrotreatment contains heavier compounds than LCO and VGO, they contribute mainly to gasoline and coke formation rather than to heavy aromatic compound formation.[11,12]

The higher coke formation and lower cracking rate with bio-oil can be explained by the higher adsorption capability of oxygenates on the acid site of the catalyst compared to hydrocarbons. Most of these oxygenates cannot enter the zeolite pores because of their relatively large size, and therefore, cracking of these molecules will take place outside of the zeolite framework on either the silica–alumina matrix and/or the alumina extra framework deposits. This will lead to enhanced coke formation and pore blocking. Cracking of oxygenates on

the catalyst surface consumes hydrogen from paraffins, which results in olefin production. In the next step, these olefins can together with the cracked bio-oil components enter the zeolite pores and react further into aromatics as well as more coke.[13]

Hydrotreatment of bio-oil to an oxygen content close to 5 wt % requires a lot of hydrogen and is for this reason not economically the best solution. To reduce the costs, de Miguel Mercader et al. tested milder HDO upgrading before FCC. The conclusion from these experiments was that co-processing of a hydrotreated bio-oil with a high oxygen content (28.0 wt % on a dry basis) is still possible without an extreme increase in coke formation. A sufficient upgrading of bio-oil would therefore include only reduction of the highly reactive components/functional groups (olefins, aldehydes, ketones, etc.) that lead to coke formation and prevent successful co-processing.[14]

Besides HDO, catalytic pyrolysis has also been used for the stabilization of bio-oil before co-processing.[15,16] Thegarid et al. compared co-processing of catalytic pyrolysis oil and HDO-upgraded pyrolysis oil in a FCC laboratory-scale unit to assess the advantages and drawbacks of each upgrading strategy. The main difference observed between catalytic pyrolysis oil and the HDO oil was the higher amount of alkyl phenols and aromatics from catalytic pyrolysis oil. This was caused by the heavier composition of catalytic pyrolysis oil containing more lignin polymers and aromatics compared to HDO oil.[16]

In this work, co-processing of dry bio-oil, catalytic pyrolysis oil, and hydrotreated bio-oil was compared using a micro activity test (MAT) setup. Dry bio-oil has a lower water content compared to normal bio-oil and was, therefore, selected for the experiments to be more comparable to catalytic pyrolysis oil and hydrotreated bio-oil. Catalytic pyrolysis and HDO can both be used for producing partially upgraded bio-oils, which differ significantly from conventional fast pyrolysis bio-oils. Although both of these upgrading techniques can be used for producing bio-oils with, e.g., similar oxygen contents, the different types of reactions taking place in each respective route result in end products with different chemical compositions. The main objective of the comparative experiments that were carried out in this study was to determine whether the two partially upgraded bio-oils, which had a very similar oxygen content, would exhibit significant differences under FCC co-processing conditions.

■ EXPERIMENTAL SECTION

Feeds for the MAT Unit. For MAT tests, VGO from Neste Oil was used to simulate FCC feedstock.

Bio-oil with a low water content (dry bio-oil), hydrotreated bio-oil (HDO oil), and catalytic pyrolysis oil (CFP oil) were used as co-feeds in the experiments. Dry bio-oil was produced in the VTT fast pyrolysis process development unit (20 kg/h) by operating the scrubbers at a higher temperature (66 °C). A more detailed description of the equipment can be found elsewhere.[17] Forest thinning was used as raw material in the experiments, and the pyrolysis was carried out at a temperature of 480 °C with a vapor-phase residence time of <1 s. The higher recovery temperature resulted in a product that contained less water, acids, and alcohols compared to normal bio-oil.[18]

CFP oil was produced from pine sawdust in the same process development unit. The details of the production process have been documented in a previous publication.[19] A HZSM-5 catalyst (CBV 5524G) from Zeolyst International was used as the heat-transfer material. The pyrolysis temperature was 520 °C, and the vapor residence time was approximately 1 s. The catalyst/biomass ratio was approximately 7:1 on a weight basis. The recovered catalytic pyrolysis oil phase separated directly after condensation into an oily bottom

phase and an aqueous top phase. For the MAT test, only the oily fraction was used.

HDO oil was produced in a continuous two-stage hydrotreating unit at VTT using a 5 wt % ruthenium on carbon (Ru/C) catalyst from Sigma-Aldrich. Bio-oil produced in the process development unit from forest thinning was used as the raw material (water content of 24.4 wt % and elemental composition calculated on a dry basis: C, 54.6 wt %; H, 6.8 wt %; N, 0.3 wt %; and O, 38 wt %). The hydrotreating temperature was 175 + 300 °C; the pressure was 200 bar; and the weight hourly space velocity (WHSV) was 10 h^{-1}. After the hydrotreatment, a phase-separated product was obtained. For the MAT test, only the oily bottom phase was used.

Experimental Setup and Procedure. A MAT unit was built at VTT to simulate the co-processing of bio-oil in a FCC unit. The MAT technique is an ASTM standard procedure (ASTM D3907), which was developed on the basis of using a fixed bed (4 g of catalyst), operated with a continuous oil feed (1.33 g) for 75 s and at a temperature of 482 °C. The standard method has limited usability for the catalytic cracking of bio-oil, because the recovered amount of liquid product is too small for carrying out in-depth physicochemical characterization.

Because VGO is solid at room temperature (boiling point range: 4% < 425 °C and 96% > 425 °C), heating the MAT feeds to 75 °C and mixing at 20 000 rpm for 5 min was required before the experiments. Mixing was performed with an ULTRA-TURRAX mixer equipped with a S25N-25G homogenization blade. To ensure that the feed entered in the MAT reactor is homogeneous, the VGO and bio-oil blend should stay homogeneous for 10 min. The homogeneity of the VGO and bio-oil blend was checked with microscopy. The definition for homogeneity was homogeneous solution or even distribution of small bio-oil droplets in VGO at room temperature and at 75 °C with no change in microscopic structure during 10 min. The maximum concentration of bio-oil in MAT feed (VGO) to ensure 10 min homogeneity was assessed to be 25 wt % for bio-oil (24.4 wt % water and 38 wt % O on a dry basis).

In VTT's system, 10 g of an equilibrated FCC catalyst is packed into a quartz tube, 14 mm inner diameter and 318 mm length (Figure 1). The tube is heated in an oven at 482 °C under nitrogen flow (30
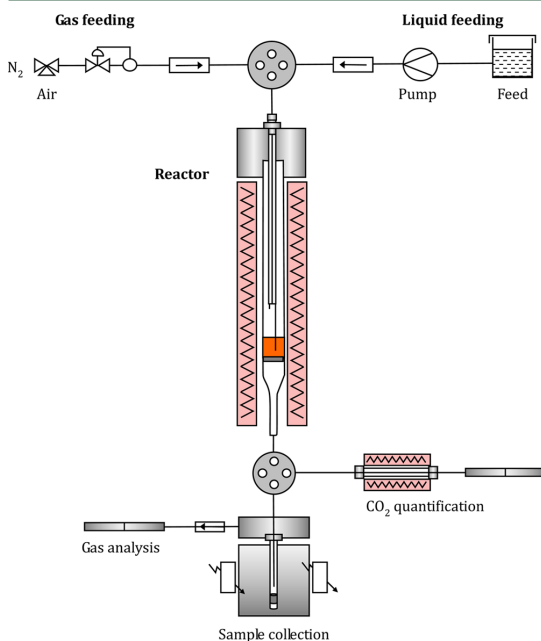

Figure 1. MAT unit used at VTT.

Table 1. Physicochemical Composition of MAT Feedstocks

	standard	VGO	dry bio-oil	CFP oil	HDO oil
water (wt %)	ASTM E203-96	0.6	6.7	8.3	7.4
MCR (%)	ASTM D4530	0.2	24.8	29.3	14.3
HHV (MJ/kg)	DIN 51900	nd	22.1	27.7	29.6
LHV (MJ/kg)	DIN 51900	nd	20.6	26.2	27.8
TAN (mg of KOH/g, VTT)	ASTM D664	nd	85.4	29.8	78.0
carbonyl content (mmol/g)		nd	4.45	2.80	0.92
carbon [wt %, dry matter (dm)]	ASTM D5291	87.5	56.8	71.5	69.4
hydrogen (wt %, dm)	ASTM D5291	11.9	6.4	6.4	8.1
nitrogen (wt %, dm)	ASTM D5291	0.3	0.3	0.0	0.4
oxygen (wt %, dm) (by difference)		0.3	36.5	22.0	22.0

NmL/min) before oil feeding. To obtain enough products for analysis, 10 g of feed was used in each experiment. The feedstock was fed into the reactor in either 1 reaction cycle (1:1 catalyst/oil ratio) or 3 reaction cycles (3.33 g/cycle feed and 3:1 catalyst/oil ratio) with catalyst regeneration between the cycles. The reaction cycle consists of either 360 or 188 s cracking, 30 min stripping under nitrogen (30 NmL/min), and 60 min regeneration at 530 °C with air (80 NmL/min). Liquid products were collected in a cooled liquid trap. During the 3 reaction cycles, all products were collected in the same liquid trap. The gas leaving the trap was collected in gas bags and analyzed with micro gas chromatography (GC) (Agilent 490 series) after the experiments. The FCC catalyst was regenerated by air *in situ*. Carbon monoxide in the effluent gas was catalytically oxidized to carbon dioxide using a copper catalyst. The formed gas was analyzed by micro GC, and the amount of coke on the catalyst was calculated from the CO_2 content.

Analysis of Feedstocks and Products. Physical characterization of pyrolysis oil feeds and MAT products was carried out by employing modified standard methods.[20] The water content was analyzed by Karl Fischer titration using a Metrohm 795 KFT Titrino titrator (ASTM E203). Elemental composition analysis (CHN) was carried out using an Elementar VARIOMAX CHN analyzer (ASTM D5291), and the higher heating value (HHV) was determined using an IKA Werke C 5000 control calorimeter (DIN 51900). The total acid number (TAN) was determined with a 785 DMP Titrino analyzer (ASTM D664), and the micro carbon residue (MCR) was analyzed using an Alcor MCR tester (ASTM D4530). The ash content of the liquid was further determined by combusting the residue from the MCR determination in a muffle furnace at 775 °C.

The chemical composition of the bio-oil feeds was determined with the solvent fractionation scheme.[9,21] In this method, bio-oil is first divided into water-soluble (WS) and water-insoluble (WIS) fractions by water extraction. The WS fraction is further extracted with diethyl ether to ether-soluble (ES) and ether-insoluble (EIS, sugar-like material) fractions. The WIS fraction is extracted with dichloromethane (DCM) to a DCM-soluble fraction containing low-molecular-mass (LMM) lignin and a DCM-insoluble fraction containing high-molecular-mass (HMM) lignin. The LMM fraction contains poorly water-soluble lignin monomers and dimers (MM = 400 Da) and extractives, while the HMM fraction contains powder-like HMM (MM = 1050 Da) lignin-derived material and solids.[9]

MAT feeds and products were also qualitatively analyzed using gas chromatography with a mass selective detector (GC−MSD). Measurements were performed using a Shimadzu GC17A gas chromatograph equipped with a mass selective quadrupole detector. A HP Ultra 1 fused silica capillary column (length, 50 m; inner diameter, 0.32 mm; and film thickness, 0.52 μm) was used. Helium was used as the carrier gas, and the temperature program was 2 min at 50 °C, 3 °C/min to 170 °C, 10 °C/min to 300 °C, and 30 min at 300 °C. Samples were dissolved in DCM and methanol before injection.

Simulated distillation was used to analyze the MAT products. Simulated distillation is a gas chromatographic (GC−FID) method that separates individual hydrocarbon components in order of their boiling points. The result of the simulated distillation provides a mass fraction yield as a function of the boiling point of the hydrocarbon

components of the sample. The chromatographic elution times of the hydrocarbons are calibrated to the atmospheric equivalent boiling point of the paraffin reference material. Simulated distillation was carried out according to ASTM D2887 using a Agilent 125-10 HP gas chromatograph equipped with a nonpolar column (length, 10 m; inner diameter, 0.53 mm; and film thickness, 2.65 μm). This standard covers the boiling range of 55−538 °C, which corresponds to a *n*-alkane chain length of about C_5-C_{44}. Before injection, the samples were diluted with either 100% DCM or a mixture of DCM (60%) and methanol (40%).

Product gases (H_2, O_2, N_2, CO, CO_2, CH_4, and C_2-C_4) were analyzed after the experiments with a micro GC (Agilent 490 series). The gas chromatograph was equipped with a thermal conductivity detector (TCD).

RESULTS AND DISCUSSION

Characterization of Feedstocks. The physicochemical composition of VGO, dry bio-oil, CFP oil, and HDO oil is
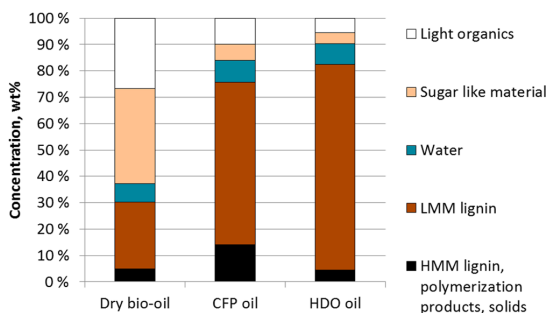

Figure 2. Chemical composition of dry bio-oil, catalytic pyrolysis oil, and hydrotreated oil determined by the solvent fractionation scheme.

presented in Table 1. CFP oil and HDO oil had lower carbonyl contents and lower oxygen contents compared to dry bio-oil. The TAN number was significantly reduced during catalytic pyrolysis, but with HDO oil, the TAN number was almost similar to the dry bio-oil. The high TAN number in HDO oil may depend upon acetic acid, which requires usually more severe conditions for its decomposition. Acetic acid distributes also between the organic and aqueous phases and, for this reason, is not only present in the aqueous phase.[22,23]

The chemical composition of bio-oils was analyzed with the solvent fractionation scheme (Figure 2). The amount of WIS material in the CFP oil and HDO oil was high compared to dry bio-oil, because phase separation had already taken place during the process. In catalytic pyrolysis and HDO, the polarity of the WIS fraction decreases as oxygen is removed from it and
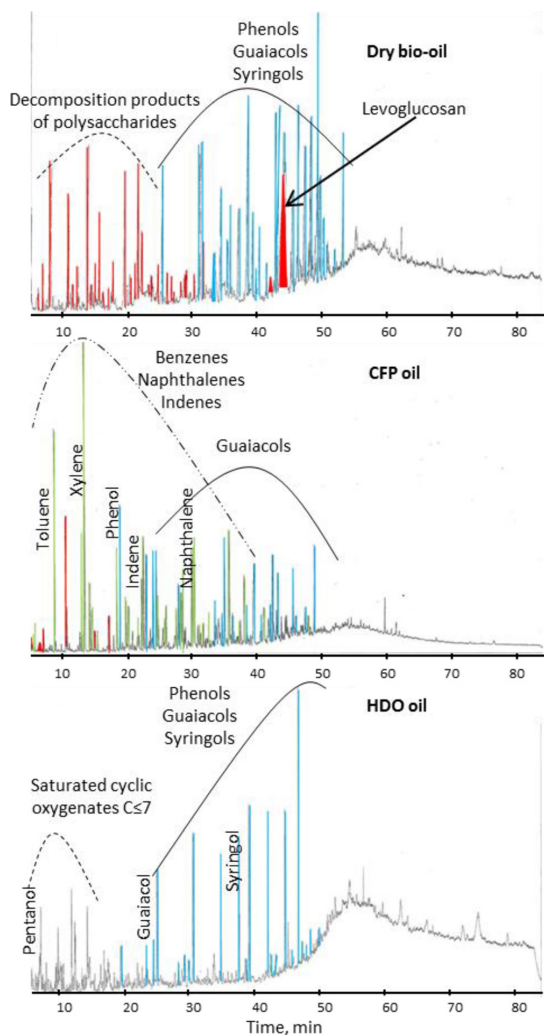
Figure 3. Total ion chromatogram for dry bio-oil, CFP oil, and HDO oil: (red) cellulose and hemicellulose decomposition products, (blue) lignin monomers, and (green) aromatic hydrocarbons.
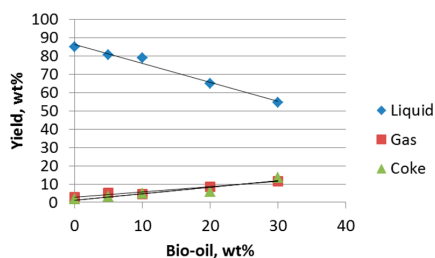

Figure 4. Product yields from MAT tests with different bio-oil and VGO blends.

hydrogen is incorporated into it. The latter change only applies to the HDO process. These transformations also enhance the phase separation, and thus, only limited amounts of WS
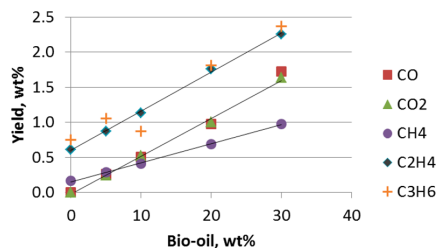

**Figure 5.** Gas component yields from MAT tests with different bio-oil and VGO blends.
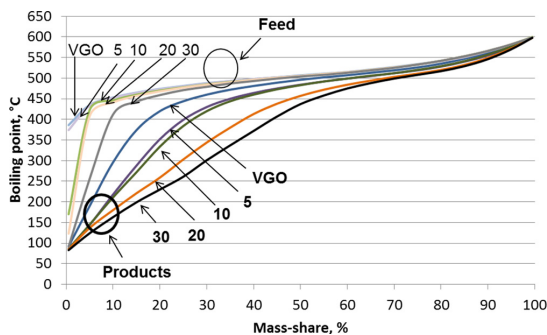
Figure 6. Characterization of the MAT feed and products with different amounts of dry bio-oil (wt %) by simulated distillation.

oxygenates are retained in the oil product. The amount of HMM lignin was higher in the CFP oil compared to the HDO oil. One reason for this is the narrow pore size in the ZSM-5 catalyst, which can hardly crack the heavy lignin polymer fragments during catalytic pyrolysis.[13,16]

The total ion chromatograms (TICs) for dry bio-oil, CFP oil, and HDO oil are presented in Figure 3.

The GC-detectable fraction of the dry bio-oil consisted of typical cellulose, hemicellulose, and lignin decomposition products. For the CFP oil, aromatic hydrocarbons (alkyl benzenes, naphthalenes, and indenes) became dominant in the TIC, but their actual concentration was still only 6.4 wt %. The presence of hydrocarbons in the bio-oil is a factor that is not directly detected in the solvent fractionation analysis. Because of their solubility characteristics, any hydrocarbon compound is classified as LMM lignin instead. Thus, this particular fraction warrants special attention when dealing with upgraded pyrolysis oils. Apart from the aromatic hydrocarbons, typical cellulose and hemicellulose decomposition products had clearly decreased, while lignin monomers were still present. The HDO oil, on the other hand, contained saturated cyclic oxygenates with a carbon number of less than 7 (cyclopentanones, cyclopentanols, cyclohexanones, and cyclohexanols). This indicates that the HDO process resulted in the saturation of the benzene ring backbone of some lignin monomers but not the final deoxygenation of the OH group. Just as aromatic hydrocarbons are absent from the HDO oil, these saturated cyclic oxygenates were not detected in the CFP oil. This can be considered as one of the key differentiating factors between these two upgraded oils. Typical cellulose and hemicellulose decomposition products had also clearly decreased during HDO, while lignin monomers (guaiacol and syringol) were still present.

Table 2. Yield of Different Distillation Ranges for MAT Runs with Increasing Amounts of Pyrolysis Oil in VGO

		VGO	VGO + 5% bio-oil	VGO + 10% bio-oil	VGO + 20% bio-oil	VGO + 30% bio-oil
dry gas (wt %)	H_2, CO, CO_2, and C_1–C_2	1	2	3	5	7
LPG (wt %)	C_3–C_4	2	3	2	4	5
gasoline (wt %)	40–221 °C	11	8	9	10	10
LCO (wt %)	221–370 °C	10	10	10	12	11
heavy cycle oil (wt %)	370–425 °C	6	5	5	5	4
slurry oil (wt %)	>425 °C	58	58	55	38	29
coke		2	3	5	6	14
sum		89	89	89	79	80
conversion (%)	gas + coke + gasoline	16	16	18	24	35

Table 3. Overall Product Distribution and Yields of Different Distillation Ranges for MAT Runs with 20 wt % Dry Bio-oil, Catalytic Pyrolysis Oil, and Hydrotreated Bio-oil in VGO

		VGO	VGO + 20% dry bio-oil	VGO + 20% CFP oil	VGO + 20% HDO oil
liquid (wt %)		85	69	74	76
gas (wt %)		10	14	12	12
coke (wt %)		5	10	10	8
sum		100	93	96	96
dry gas (wt %)	H_2, CO, CO_2, and C_1–C_2	2	4	3	3
LPG (wt %)	C_3–C_4	8	9	9	9
gasoline (wt %)	40–221 °C	16	17	19	18
LCO (wt %)	221–370 °C	15	16	17	16
heavy cycle oil (wt %)	370–425 °C	8	6	6	7
slurry oil (wt %)	>425 °C	46	31	32	35
conversion (%)	gas + coke + gasoline	30	41	40	38
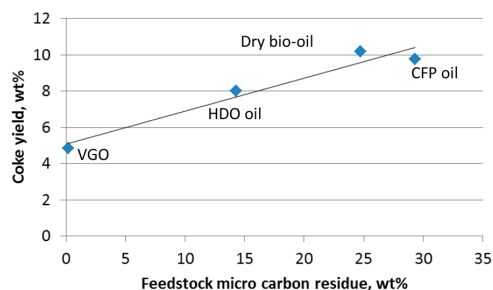
Figure 7. Coke yield as a function of the undiluted feedstock MCR.
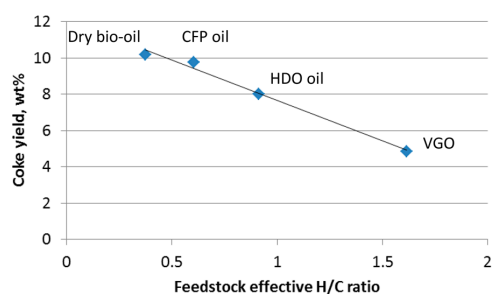
Figure 8. Coke yield as a function of the undiluted feedstock effective H/C ratio.

Validation of the MAT Unit. The repeatability of experiments for the MAT equipment was tested with 10 g of FCC catalyst and 10 g of VGO. The feeding time of VGO was 360 s, and the catalyst/oil ratio was 1:1. The repeatability in four duplicates was good, with a liquid yield of 85 ± 0.2 wt %,

gas yield of 3 ± 0.2 wt %, coke yield of 2 ± 0.2 wt %, and total mass balance closure of 89 ± 0.1 wt %. The loss was caused by products left in the feeding and product pipelines.

Different ratios of dry bio-oil (water content of 6.6 wt %) and VGO blends were also tested in the unit. Good mass balances were obtained only with 5–10 wt % bio-oil concentrations. With higher bio-oil concentrations, coking was a clear problem. The increases in the yield of coke and gases were accompanied by a decrease in the yield of liquid products (Figure 4). Similar results have also been reported in other studies for co-processing of raw bio-oil.[24] This indicates that the bio-oil concentration during co-processing should remain low to obtain the highest advantage of the process.

The product gas contained CO, CO_2, and light hydrocarbons (Figure 5). The gases produced a linear relationship between yield and bio-oil mass share. This confirms also that the bio-oil and VGO blends that fed into the reactor were homogeneous. The increases in the yields of CO and CO_2 can be attributed to oxygen rejection from the bio-oil components. The observed increase in the yield of light olefins could signify the cracking of the lighter components in the bio-oil. The product gas also contained small amounts of hydrogen, the yield of which was significantly reduced when bio-oil was added to the feed.

The liquid products from the MAT tests with different bio-oil and VGO blends were characterized with simulated distillation (Figure 6). Simulated distillation is not calibrated for oxygenated components, and for this reason, only the boiling point curves of the products are comparable to atmospheric distillation. The share of light compounds (<425 °C) increased with an increasing amount of bio-oil in the feed.

Combining the simulated distillation results with the liquid yields, the yields for the different distillation ranges (gasoline, LCO, heavy cycle oil, and slurry oil) were calculated (Table 2). The product gas was also divided into dry gas and liquefied
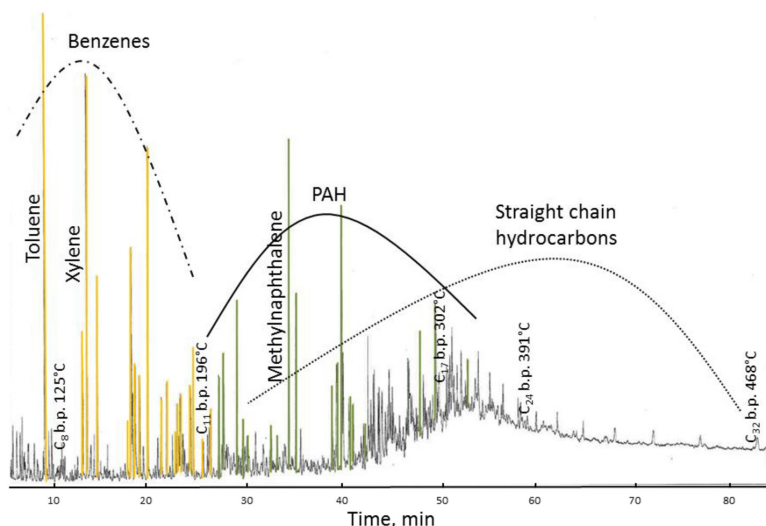
Figure 9. Main chemical compounds identified by GC−MSD in liquid products from co-processing of dry bio-oil: (yellow) benzenes and (green) polyaromatic hydrocarbons (PAHs).
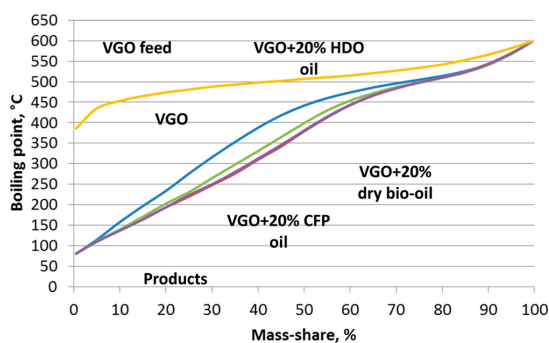

Figure 10. Simulated distillation curves for MAT products.

petroleum gas (LPG) based on its composition. Co-processing of bio-oil with VGO had a very limited effect on the yield of the desired liquid products. Only the yield of slurry oil significantly decreased with an increasing amount of bio-oil. This change was, however, accompanied by a decrease in the overall mass balance closure, and thus, the observed decrease in the yield of slurry oil was potentially influenced by the retention of heavier liquid fractions in the reactor system tubing.

The conversion, which was calculated as the sum of gas, coke, and gasoline yields, was very low in each experiment compared to a commercial FCC unit (70%). One reason for this is the

low catalyst/oil ratio (1:1), which in a commercial FCC unit varies from 4:1 to 10:1. Because of the low conversion, the liquid products from all of these test runs were still very viscous.

Co-processing of Dry Bio-oil, Catalytic Pyrolysis Oil, and Hydrotreated Oil. Co-feeding of dry bio-oil, catalytic pyrolysis oil, and hydrotreated oil was also compared in the unit. A total of 10 g of catalyst was used in all of these experiments, and a total of 10 g of oil was fed into the reactor in 3 cycles with regeneration between the cycles (catalyst/oil ratio was 3:1). To observe clear differences between the three bio-oil feedstocks, the amount of dry bio-oil, catalytic pyrolysis oil, and hydrotreated oil was set as 20% in each experiment.

The product yields are presented in Table 3. Co-processing of partly upgraded bio-oils resulted in a higher liquid yield compared to dry bio-oil. Although the overall conversion still remained fairly low, certain differences were observed between the different feedstocks. Overall, the differences in the product distribution between CFP oil and HDO oil were very small. CFP oil produced slightly more gasoline compared to HDO oil. Similar results have also been reported earlier.[16] One potential reason for this is the aromatic hydrocarbons in the CFP feed, which were probably directly transferred into the gasoline fraction. The lowest coke yield was observed when co-processing the HDO oil. In contrast to this, both the dry bio-oil and the CFP oil eventually resulted in similar coke yields. The observed difference in the coke yields for the two partially upgraded bio-oils is a clear indication that a simple metric, such as oxygen content, cannot be used as the sole

Table 4. Physicochemical Composition for MAT Products

	VGO	VGO + 20% dry bio-oil	VGO + 20% CFP oil	VGO + 20% HDO oil
water (wt %)	0.1	7.1	3.5	2.8
MCR (%)	1.4	2.6	2.1	2.15
ash (wt %)	0	0.2	0	0.2
carbon (wt %, dm)	83.8	85.5	83.1	82.6
hydrogen (wt %, dm)	10.8	10.2	10.1	10.1
nitrogen (wt %, dm)	0.3	0.3	0.2	0.2

criterion for evaluating the co-processability of different bio-oil feedstocks. The coke formation tendency of FCC feeds can be measured by the MCR and effective hydrogen index. The MCR is a measure of carbonaceous material left in a hydrocarbon fraction after all of the volatile components are vaporized in the absence of air.[7] The effective hydrogen index is defined from the molar composition of a particular compound or mixture as $H/C_{eff} = (H - 2O)/C$ (in the absence of nitrogen and sulfur), and it reflects the net oxygen removal (dry oil) via water production. For bio-oil, the hydrogen index is <1, while for hydrocarbons, it is usually >1. Compounds with an effective hydrogen index of <1 are difficult to upgrade to premium products over ZSM-5 catalysts because of rapid catalyst deactivation.[10] Both the MCR and effective hydrocarbon index of the feedstocks formed a linear correlation with the coke yields (Figures 7 and 8). The high coke yield with dry bio-oil was partly caused by the sugar-like material (Figure 2) in the oil. The difference in the coke yield between HDO oil and CFP oil can be attributed to their different chemical compositions, which is also reflected in the results shown in Figures 7 and 8. The CFP oil contained clearly more HMM lignin, which is a highly probable precursor for coke formation or direct fouling of the catalyst. The higher concentration of HMM lignin also contributed toward the limited volatility of the CFP oil, which was one of the reasons for the high MCR value. The difference in the chemistries of these two upgrading routes was also highlighted by the different H/C_{eff} values. Catalytic pyrolysis increased the aromaticity and, consequently, the level of unsaturation in the bio-oil, which resulted in a low H/C_{eff} value and a higher coke yield. In contrast to this, the HDO process decreased the oxygen content of the bio-oil while simultaneously boosting its hydrogen content. This change, which was also evident in the GC–MSD analysis (Figure 3), resulted in the saturation of many ring structures, thus making the bio-oil less prone toward coking.

The chemical compounds present in the liquid products from co-processing of dry bio-oil, catalytic pyrolysis oil, and hydrotreated oil were almost identical to the product from VGO. The main compounds identified by GC–MSD were alkyl benzenes, naphthalenes, and straight-chain hydrocarbons (Figure 9). No oxygen-containing compounds were detected in the total ion chromatogram. The simulated distillation curves were also very similar for dry bio-oil, CFP oil, and HDO oil (Figure 10). The products (boiling < 400 °C) from co-processing contained more aromatics and straight-chain hydrocarbons compared to VGO. The physicochemical composition of the MAT products is presented in Table 4. Catalytic cracking resulted in water formation, when oxygen was removed by dehydration reactions. Water formation increased with the oxygen content in the feed and was, therefore, highest for the dry bio-oil. This phenomenon shows a similar trend to the increased CO and CO_2 yields in Figure 5. As more oxygen was fed into the process, the yields of products, which are associated with the main oxygen rejection pathways for acid catalysts, increased. The elemental composition for all products calculated on a dry basis was very similar.

CONCLUSION

Co-processing of dry and upgraded bio-oil with VGO was tested in a MAT unit. Co-processing of dry bio-oil was first tested with VGO in different ratios. Good mass balances were obtained only with low bio-oil concentrations. At higher bio-oil concentrations, coking was a problem. This indicates that the

bio-oil concentration should be low during co-processing. The product gas from VGO cracking contained small amounts of hydrogen, but this hydrogen was already consumed, when small amounts of bio-oil was co-processed. Higher amounts of bio-oil in the feed resulted in a lighter product containing more aromatics compared to VGO.

Co-processing of dry bio-oil, CFP oil, and HDO oil was also compared in the unit. The amount of bio-oil was 20 wt % in each experiment. CFP oil and HDO oil resulted in a higher liquid yield compared to dry bio-oil. The coke yield was lowest for HDO oil. The high coke yield with dry bio-oil was partly caused by the sugar-like material in the oil. The lower coke yield for HDO oil compared to CFP oil was caused by its lighter chemical composition, less HMM lignin, lower MCR value, and higher hydrogen/carbon ratio. The chemical composition of the liquid product from co-processing of dry bio-oil, CFP oil, and HDO oil was almost identical.

AUTHOR INFORMATION

Corresponding Author

*Telephone: +358-20-722-111. E-mail: christian.lindfors@vtt.fi.

Notes

The authors declare no competing financial interest.

REFERENCES

(1) Czernik, S.; Bridgwater, A. V. Overview of applications of biomass fast pyrolysis oil. *Energy Fuels* 2004, 18, 590–598.

(2) Solantausta, Y.; Oasmaa, A.; Sipilä, K.; Lindfors, C.; Lehto, J.; Autio; Jokela, P.; Alin, J.; Heiskanen, J. Bio-oil production from biomass: Steps toward demonstration. *Energy Fuels* 2012, 26, 233–240.

(3) Elliott, D. C. Historical developments in hydroprocessing bio-oils. *Energy Fuels* 2007, 21, 1792–1815.

(4) Lappas, A.; Samolada, M.; Iatridis, D.; Voutetakis, S.; Vasalos, I. Biomass pyrolysis in a circulating fluid bed reactor for the production of fuels and chemicals. *Fuel* 2002, 81, 2087–2095.

(5) Baldauf, W.; Balfanz, U.; Rupp, M. Upgrading of flash pyrolysis oil and utilization in refineries. *Biomass Bioenergy* 1994, 7, 237–244.

(6) Talmadge, M.; Baldwin, R.; Biddy, M.; McCormick, R.; Beckham, G.; Ferguson, G.; Czernik, S.; Magrini-Bair, K.; Foust, T.; Metelski, P.; Hetrick, C.; Nimlos, M. A perspective on oxygenated species in the refinery integration of pyrolysis oil. *Green Chem.* 2014, 16, 407–453.

(7) Sadeghbeigi, R. *Fluid Catalytic Cracking Handbook*, 3rd ed.; Elsevier: Amsterdam, Netherlands, 2012.

(8) Bridgwater, A.; Czernik, S.; Piskorz, J. The status of biomass fast pyrolysis. In *Fast Pyrolysis of Biomass*; CPL Press: Newbury, U.K., 2002, Vol. 2, pp 1–19.

(9) Oasmaa, A.; Kuoppala, E.; Solantausta, Y. Fast pyrolysis of forestry residue. 2. Physicochemical composition of product liquid. *Energy Fuels* 2003, 17, 433–443.

(10) Chen, N.; Walsh, D.; Koenig, L. Fluidized bed upgrading of wood pyrolysis liquids and related compounds. In *Pyrolysis Oils from Biomass*; Soltes, E. J., Milne, T. A., Eds.; American Chemical Society (ACS): Washington, D.C., 1988; ACS Symposium Series, Vol. 376, Chapter 24, pp 277–289

(11) Samolada, M.; Baldauf, W.; Vasalos, I. Production of a bio-gasoline by upgrading biomass flash pyrolysis liquids via hydrogen processing and catalytic cracking. *Fuel* **1998**, *77*, 1667−1675.

(12) Lappas, A.; Bezergianni, S.; Vasalos, I. Production of biofuels via co-processing in conventional refining process. *Catal. Today* **2009**, *145*, 55−62.

(13) Fogassy, G.; Thegarid, N.; Schuurman, Y.; Mirodatos, C. From biomass to bio-gasoline by FCC co-processing: effect of feed composition and catalyst structure on product quality. *Energy Environ. Sci.* **2011**, *4*, 5068−5076.

(14) de Miguel Mercader, F.; Groeneveld, M.; Kersten, S.; Way, N.; Schaverien, C.; Hogendoorn, J. Production of advanced biofuels: Co-processing of upgraded pyrolysis oil in standard refinery units. *Appl. Catal., B* **2010**, *96*, 57−66.

(15) Agblevor, F.; Mante, O.; McClung, R.; Oyama, S. Co-processing of standard gas oil and biocrude oil to hydrocarbon fuels. *Biomass Bioenergy* **2012**, *45*, 130−137.

(16) Thegarid, N.; Fogassy, G.; Schuurman, Y.; Mirodatos, C.; Stefanidis, S.; Iliopoulou, E.; Kalogiannis, K.; Lappas, A. Second-generation biofuels by co-processing catalytic pyrolysis oil in FCC units. *Appl. Catal., B* **2014**, *145*, 161−166.

(17) Solantausta, Y.; Oasmaa, A.; Sipilä, K.; Lindfors, C.; Lehto, J.; Autio, J.; Jokela, P.; Alin, J.; Heiskanen, J. Bio-oil production from biomass: Steps towards demonstration. *Energy Fuels* **2010**, *26*, 233−240.

(18) Lindfors, C.; Kuoppala, E.; Oasmaa, A.; Solantausta, Y.; Arpiainen, V. Fractionation of bio-oil. *Energy Fuels* **2014**, *28*, 5785−5791.

(19) Paasikallio, V.; Lindfors, C.; Kuoppala, E.; Solantausta, Y.; Oasmaa, A.; Lehto, J.; Lehtonen, J. Product quality and catalyst deactivation in a four day catalytic fast pyrolysis production run. *Green Chem.* **2014**, *16*, 3549−3559.

(20) Oasmaa, A.; Peacocke, C. Properties and fuel use of biomass derived fast pyrolysis liquids. *VTT Publ.* **2010**, *731*, 1−71.

(21) Sipilä, K.; Kuoppala, E.; Fagernäs, L.; Oasmaa, A. Character-ization of biomass-based flash pyrolysis oils. *Biomass Bioenergy* **1998**, *14*, 103−113.

(22) Elliott, D.; Hart, T. Catalytic hydroprocessing of chemical models for bio-oil. *Energy Fuels* **2009**, *23*, 631−637.

(23) Oasmaa, A.; Kuoppala, E.; Ardiyanti, A.; Venderbosch, R.; Heeres, H. Characterization of hydrotreated fast pyrolysis liquids. *Energy Fuels* **2010**, *24*, 5264−5272.

(24) de Rezende Pinho, A.; de Almeida, M.; Mendes, F.; Ximenes, V.; Casavechia, L. Co-processing raw bio-oil and gasoil in an FCC unit. *Fuel Process. Technol.* **2015**, *131*, 159−166.

Aalto-DD 227/2016

VTT SCIENCE 137

BUSINESS +
ECONOMY

ART +
DESIGN +
ARCHITECTURE

SCIENCE +
TECHNOLOGY

CROSSOVER

DOCTORAL
DISSERTATIONS